BIOLOGIA

STUDIA
UNIVERSITATIS BABEŞ-BOLYAI
BIOLOGIA

1 / 2024
January – June

STUDIA
UNIVERSITATIS BABEŞ-BOLYAI

BIOLOGIA

1

SUMAR – CONTENT – SOMMAIRE – INHALT

REGULAR ARTICLES

ABSTRACTS OF THE BIOTA CONFERENCE, MAY 17-18, 2024, FACULTY OF BIOLOGY AND GEOLOGY, BABEŞ-BOLYAI UNIVERSITY, CLUJ-NAPOCA, ROMANIA

All authors are responsible for submitting manuscripts in comprehensible US or UK English and ensuring scientific accuracy.

Original picture on front cover: The diaphonization technique performed on chicken (*Gallus gallus*) embryo in order to highlight structures that are closely linked to phylogenetic evolution © Leonard Calistru

Designing a multi-epitope candidate vaccine against SARS-CoV-2 through *in silico* approach for producing in plant systems

Fatemeh Goudarziasl[1], Fatemeh Kheiri[2], Azam Rahbar[3],
Reza Mohammadhassan[3✉], Javad Mohammadi-Asl[4], Arsalan Jalili[5,6],
Melika Hajkazemian[7]

[1]Department of Biochemistry, Faculty of Biological Science, University of Mazandaran, Mazandaran, Iran; [2]Department of Biotechnology, Faculty of Biological Sciences, Alzahra University, Tehran, Iran; [3]Amino Techno Gene Private Virtual Lab (NGO), Tehran, Iran; [4]Noorgene Genetic & Clinical Laboratory, Molecular Research Center, Ahvaz, Iran; [5]Department of Stem Cells and Developmental Biology, Cell Science Research Center, Royan Institute for Stem Cell Biology and Technology, ACER, Tehran, Iran; [6]Parvaz Research Ideas Supporter Institute, Tehran, Iran; [7]Department of Molecular Biosciences, Wenner-Gren Institute, Stockholm University, Stockholm, Sweden;
✉*Corresponding author, E-mail: rezarmhreza22@gmail.com*

Abstract. The COVID-19 is considered as a type of severe acute respiratory syndrome (SARS-CoV-2). The current pandemic causes a vital destruction in international social and economic systems. Current available vaccines involve entire viruses; however, peptide-based vaccines could be also beneficial. In the present study, a computationally candidate vaccine was designed against SARS-CoV-2. Surface glycoproteins (E, M, and S proteins) and N protein amino acid sequences were analyzed to predict high score of the B and T cell epitopes as antigenic proteins of the virus. High score epitopes, and the B subunit of *Vibrio cholerae* toxin, as an adjuvant put together by appropriate linkers to construct a multi-epitope candidate vaccine. Bioinformatics tools were used to predict the secondary, tertiary structure and physicochemical properties, such as aliphatic index, theoretical pH, molecular weight, and estimated half-life of the multi-epitope candidate vaccine. The interaction of candidate vaccine with TLR2 and TLR4 was computationally evaluated by molecular docking. Finally, the codon optimization and the secondary structure of mRNA were calculated, and

in silico cloning was performed into plant expression vector by SnapGENE. This designed candidate vaccine along with the computational results requires laboratory evaluations to be confirmed as a candidate vaccine against SARS-COV-2 infection.

Keywords: COVID-19, SARS-CoV-2, in silico, Multi-epitope candidate vaccine, Plant systems.

Introduction

Since late 2019, the prevalence of the COVID-19, as a viral infection caused by a novel coronavirus called SARS-CoV-2, has been a vital concern for human society due to severe acute respiratory syndrome caused by the virus and rapid worldwide outbreak. Elders, pregnant women, and individuals suffering an underlying disease such as diabetes and immune deficiency could be less resistant against COVID-19 (Huang *et al.*, 2020; Zhou *et al.*, 2020). The virus can be transmitted among people by respiratory droplets and through faecal-oral route (Dibner, 2021). The droplets can be in different sizes from <5 μm to >5-10 μm (Boopathi *et al.*, 2020). There is a wide range, from mild to serve, of symptoms for COVID-19. Symptoms can appear 2-14 days after the virus infects cells. The symptoms of COVID-19 include fever, cough, chills, shortness of breath or difficult breathing, fatigue, headache, sore throat, nausea or vomiting, and diarrhea (Nokhostin *et al.*, 2020).

Coronavirus is an enveloped non-segmented virus containing a positive-single-strain RNA. The genome of the virus is about 26 to 32 Kbp as one of the most extended viral RNAs (Fehr and Perlman, 2015). There are four genotypes and serotypes of coronavirus to classify as α, β, γ, and δ. Novel coronavirus-19 belongs to the β-coronavirus genus (Lim *et al.*, 2016; Rahbaran, 2021). COVID-19 is the third detected viral infection caused by Coronaviridae family. Previously, severe acute respiratory syndrome (SARS) and middle east respiratory syndrome (MERS) diseases have been identified and studied, respectively, as the first and second viral infections caused by species of the β-coronavirus genus (Amanat and Krammer, 2020; Yoshimoto, 2020). However, the outbreak of the viral infection needs to be control by the immunization. There are recently 6 novel vaccines immunizing individuals against SARS-CoV-2, including Moderna, Johnson and Johnson (made in the USA), Pfizer-Biontech (made by cooperation of US and Germany), Astera-Zeneka (made by cooperation of UK and Sweden), Sinopharm (made in China), and Sputnik V (made by Russia) (Zheng *et al.*, 2022).

As an *in silico* approach, immunoinformatics contains various reliable and precise tools to analyze the new candidate vaccines. In this strategy, the conserved and effective epitopes, including the smallest part of the antigen's protective activity, were used to design a new vaccine instead of using the whole antigen. The advantages of this approach include low-cost production and a more specific design of the subunit vaccine. This strategy can be recommended to manage many epidemics and even pandemics such as COVID-19 (Miles *et al.*, 2019; Shey *et al.*, 2019; Mohammadhassan *et al.*, 2020). It has been demonstrated that the *in silico* designed vaccines against various infections can positively affect cellular and humoral immunity (Liu and Chen, 2004, Cong *et al.*, 2008, Hajissa *et al.*, 2019). In the present study, a candidate multi-epitope vaccine against SARS-CoV-2 was designed and investigated by *in silico* tools regarding high score B and T cell epitopes of the structural proteins.

Materials & Methods

Protein selection for preparing multi-epitope protein

The protein database in NCBI (https://www.ncbi.nlm.nih.gov/protein) was used to access the sequences of the E protein (accession number = QHD43418.1), M protein (accession number = QHD43419.1), S protein (accession number = QHD43416.1) and N protein (accession number = QHD43423.2) of SARS-CoV-2, as FASTA format for further analysis.

Predicting linear B-cell epitopes

BpiPred (http://www.cbs.dtu.dk/services/BepiPred), ABCpred (http://crdd.osdd.net/raghava/abcpred), and SVMTrip (http://sysbio.unl.edu/SVMTriP) were employed for linear B-cell epitopes prediction. Moreover, VaxiJen v.2.0 (http://www.ddg-pharmfac.net/vaxijen/VaxiJen/VaxiJen.html), ToxinPred (http://crdd.osdd.net/raghava/toxinpred), AllerTOP v.2.0 (https://www.ddg-pharmfac.net/AllerTOP) and PepCalc (https://pepcalc.com) were respectively used to evaluate antigenicity, toxicity, allergenicity, and solubility of the high score predicted linear B-cell epitopes.

Predicting T-cell epitopes

The Immune Epitope Database server (IEBD) was utilized to predict MHC class I epitopes regarding 9 mer HLA reference alleles. T-cell epitope prediction was performed on S, E, N, and M proteins. High-score epitopes (regarding percentile rank and inhibitory concentration (IC50)) were evaluated in the aspect of antigenicity, toxicity, hydrophobicity, allergenicity, and immunogenicity

by VaxiJen v.2.0, ToxinPred**,** Peptide 2.0, AllerTOP v.2.0, immune epitope (http://tools.immuneepitope.org/mhci/result) servers, respectively. To predict MHC class II epitopes, we also used the IEDB server (which was employed (http://tools.iedb.org/mhcii/) regarding IEDB recommended 2.22 method and 15 mer total HLA reference alleles. Epitopes with low percentile rank and NetMHCIIpan IC50 (nM) were selected, then analyzed by VaxiJen v.2.0, ToxinPred**,** Peptide 2.0 (https://www.peptide2.com), and AllerTOP v.2.0 to identify their antigenicity, toxicity, hydrophobicity, allergenicity, and immunogenicity, respectively.

Gamma interferon production

To identify regions with the potential gamma interferon production stimulation in the candidate multi-epitope vaccine, we used the IFNepitope server (http://crdd.osdd.net/raghava/ifnepitope) by hybrid approaches.

Multi-epitope subunit vaccine design

Nontoxic and non-allergenic high score epitopes with proper antigenicity and solubility were linked together with the aid of appropriate linkers to construct a multi-epitope vaccine structure. The B-cell and the T-cell epitopes were respectively bound GPGPG and the KK linkers. To better stimulate the immune system by final construction, nontoxic cholera subunit B (CTB) was used as an adjuvant and linked by EAAAK linker. The final construction was screened for antigenicity by VaxiJen v 2.0 and ANTIGENpro (http://scratch. proteomics.ics.uci.edu), respectively. AllerTOP v. 2.0 was used for the evaluation of allergenicity. For probable trans-membrane regions and signal peptide, the sequence of the multi-epitopes candidate vaccine was checked by the TMHMM v.2.0 server (http://www.cbs.dtu.dk/services/TMHMM) and TargetP 5.0 (http://www.cbs.dtu.dk/services/SignalP/index.php), respectively.

Physicochemical properties

The physicochemical properties were evaluated by Expasy ProtParam tool (https://web.expasy.org/protparam). This server computes parameters such as amino acid composition, molecular weight, in-vitro and in-vivo half-life, theoretical isoelectric point (pI), aliphatic index, grand average of hydropathicity (GRAVY), and instability index. The aliphatic index explains the thermo-stability of the query protein.

Secondary and tertiary structure prediction

I-TASSER server (https://zhanggroup.org/I-TASSER/) was employed for the prediction of Tertiary structure. This server is an online tool for annotating structure-based function and predicting automated protein structure (Yang and Zhang, 2015).

Refinement and validation of tertiary structure

ModRefiner server (https://zhanggroup.org/ModRefiner/) was used for refining and modeling protein structure prediction, and then Prosa-web (https://prosa.services.came.sbg.ac.at/prosa.php), and Rampage server (https://zlab.umassmed.edu/bu/rama/) were respectively employed for the structural validation.

Molecular docking

The HDock online server (https://cluspro.bu.edu) was used for docking the refined candidate vaccine construction by TLR4. For this purpose, the PDB structures of TLR 4 (PDB ID: 3FXI) were provided from the RCSB PDB server (https://www.rcsb.org/). As a receptor, this PDB structure, along with its ligand, which is our refined constructed protein, were given to the HDock server (http://hdock.phys.hust.edu.cn/).

Molecular dynamic simulation

iMOD server (https://imods.iqfr.csic.es/) was used to explain the stability of the candidate vaccine-TLR2/TLR4 complexes and perform molecular dynamics and RMSD calculations.

Predicting codon optimization and mRNA secondary structure

The synthetic construct was codon optimization for expression in the desired prokaryote (*E. coli*) and eukaryote (plants) host by different online software (IDT DNA, optimizer, cool, Jcat, and Genscript). The amino acid sequence of the candidate vaccine along with the codon usage table was subjected to OPTIMIZER (http://genomes.urv.es/OPTIMIZER/). The optimized DNA was submitted to GENScript and some features such as GC content, Codon Adaption Index (CAI), and Codon Frequency Distribution (CFD) were evaluated. For predicting the mRNA secondary structure, the optimized DNA sequence was submitted to the RNAfold server (http://rna.tbi.univie.ac.at/cgi-bin/RNAWebSuite/RNAfold.cgi). SnapGENE was also used for the insertion of our construct into the PBI121 vector.

Results

Linear B-cell epitopes prediction

Full-length S and N proteins were subjected to ABCpred, SVMTrip, and BepiPred, separately. Regarding these servers, 110 epitopes were predicted. High score epitopes from each server were analyzed from the aspects of antigenicity, toxicity, allergenicity, and solubility by VaxiJen v.2.0, ToxinPred, AllerTOP v.2.0, and PepCalc, respectively. Finally, among 13 non-allergic and nontoxic epitopes with proper antigenicity and solubility, 4 epitopes with IFNepitope positive were selected to participate in the multi-epitope candidate vaccine. Final selected Linear B-cell epitopes which fulfilled all the criteria for non-allergenicity, antigenicity, non-toxicity, and could also induce the IFN-γ immune response (Tab. 1).

T-cell epitopes prediction

Epitopes with low percentile rank and IC50 have a high affinity with MHCs. Consequently, antigenic, nontoxic, hydrophobic, and non-allergen epitopes with low percentile rank and IC50 were selected and participated in the multi-epitope candidate vaccine (Tab. 2).

Table 1. Linear B-cell epitopes prediction

EPITOPE	Protein name	Start position	Predicted score
QQQQGQTVTKKSAAEASKKP	N protein	239	1.000
RRGPEQTQGNFGDQELIRQG	N protein	276	0.865
HGKEDLKFPRGQGVPI	N protein	59	0.87
TRRIRGGDGKMKDLSP	N protein	91	0.94

Table 2. T-cell epitopes prediction

Epitope	PR name	Start position	MHC binding
VIGFLFLTW	M protein	23	MHC-I
KLIFLWLLW	M protein	50	MHC-I
TLACFVLAA	M protein	61	MHC-I
ACFVLAAVY	M protein	63	MHC-I

Epitope	PR name	Start position	MHC binding
FVLAAVYRI	M protein	65	MHC-I
IAIAMACLV	M protein	80	MHC-I
SELVIGAVI	M protein	136	MHC-I
LVIGAVILR	M protein	138	MHC-I
YYKLGASQR	M protein	178	MHC-I
RYRIGNYKL	M protein	198	MHC-I
LPFNDGVYF	S protein	84	MHC-I
GVYFASTEK	S protein	89	MHC-I
TLDSKTQSL	S protein	109	MHC-I
YYHKNNKSW	S protein	144	MHC-I
FEYVSQPFL	S protein	168	MHC-I
KIYSKHTPI	S protein	202	MHC-I
WTAGAAAYY	S protein	258	MHC-I
YYVGYLQPR	S protein	265	MHC-I
KSNLKPFER	S protein	458	MHC-I
PYRVVVLSF	S protein	507	MHC-I
QLTPTWRVY	S protein	628	MHC-I
SPRRARSVA	S protein	680	MHC-I
LGAENSVAY	S protein	699	MHC-I
IAIPTNFTI	S protein	712	MHC-I
IPTNFTISV	S protein	714	MHC-I
FTISVTTEI	S protein	718	MHC-I
LLFNKVTLA	S protein	821	MHC-I
HWFVTQRNF	S protein	1101	MHC-I
VLKGVKLHY	S protein	1264	MHC-I
QIGYYRRATRRIRGG	N protein	83	MHC-II
IGYYRRATRRIRGGD	N protein	84	MHC-II
DAALALLLLDRLNQL	N protein	216	MHC-II

Epitope	PR name	Start position	MHC binding
AALALLLLDRLNQLE	N protein	217	MHC-II
ALALLLLDRLNQLES	N protein	218	MHC-II
QIAQFAPSASAFFGM	N protein	303	MHC-II
AQFAPSASAFFGMSR	N protein	305	MHC-II

Antigenicity and allergenicity prediction, physicochemical properties

The final multi-epitope candidate vaccine comprises 568 amino acids and consists of three domains, including CTB as adjuvant, linear B-cell epitopes, and T-cell epitopes. Also, for protein purification and identification, a 6xHis tag was added at the C-terminal of the multi-epitope construction (Fig. 1). The antigenicity of the whole multi-epitope structure was calculated to be 0.6633. Furthermore, the results of the AllerTOP server revealed that our protein is non-allergen. Molecular weight and theoretical isoelectric point were 64.48 and 10.39 kDa, respectively. The estimated half-life was 0.8 hours for mammalian reticulocytes, 10 min in yeast, > 10 hours for *E.coli*, and 8 hours for plant. The instability index, aliphatic index, and GRAVY were 31.87, 79.89, and -0.5, respectively. According to these results, our protein is classified as stable, thermostable, and soluble protein. Connecting selected epitopes by appropriate linkers may form a signal peptide or transmembrane regions in the constructed structure. According to this possibility, the amino acid sequence of the multi-epitope candidate vaccine was checked by TMHMM v.2.0 and TargetP 5.0 online servers. Results did not show any signal-peptide or trans-membrane region in the protein construction.
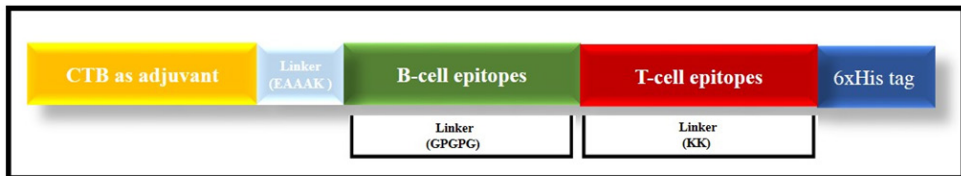
Figure1. The scheme of the final multi-epitope vaccine peptide. The 568-amino acid long peptide sequence containing adjuvant (yellow) at both N terminal was linked with the multi-epitope sequence through an EAAAK linker. HTL epitopes and B-cell epitopes are linked using GPGPG linkers (green) while the CTL epitopes are linked with KK linkers (red).

Secondary and tertiary structure modelling, refinement, and validation

Psipred analyzed secondary structure prediction. The result showed that 44.0, 16.0, and 40.0 of the total 568 amino acids were organized in alpha helix, extended strand, and random coil, respectively.

I-TASSER web server was employed to predict five tertiary 3D structures of the designed vaccine, according to ten threading templates, with Z score values (1.10–2.78) and confidence score (C-score) values (-0.75 to -4.01). Usually, the C score series is from−5 to 2, with high scores representing high sureness. All models refined by ModRefiner. The loop and energy were respectively refined and minimized to achieve the high quality of the predicted structure. The refined structures were exposed to the Ramachandran plot analysis using the RAMPAGE web server.
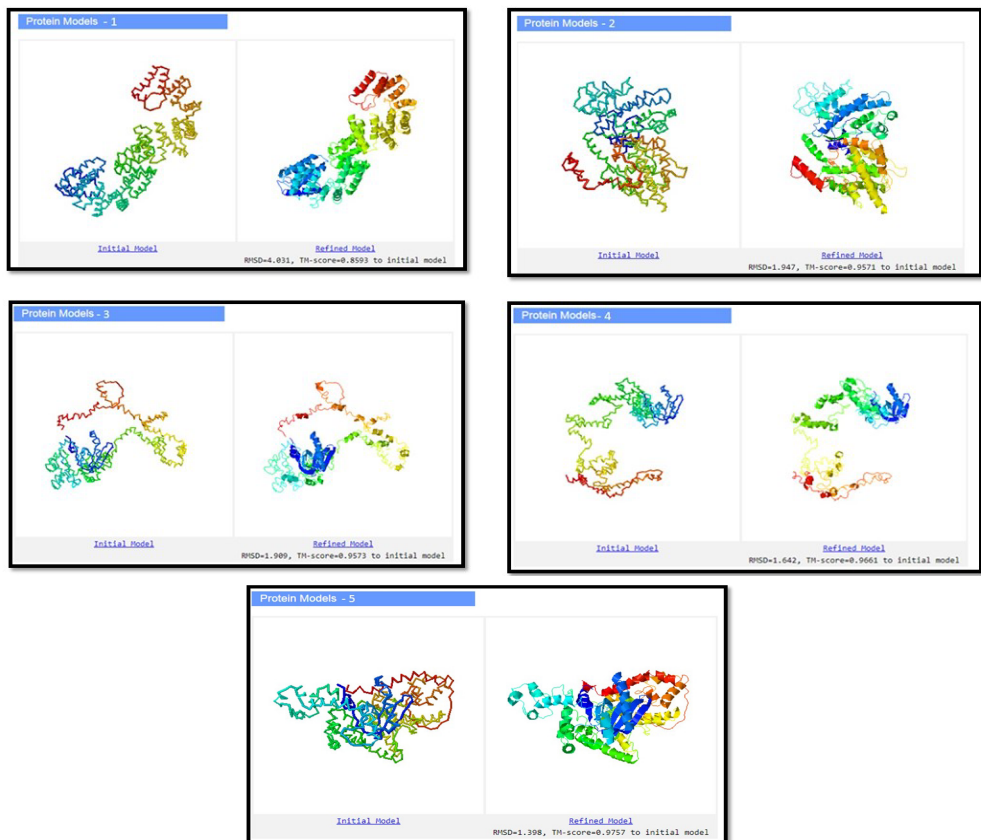
Figure 2. Protein 3D modeling and refining. I-TASSER server was used to provide the 3D model of a multi-epitope vaccine by following homology modeling (left). The protein was refined by the ModRefiner server of a refined 3D structure (right).

Between the 5 models generated by this server, model 5 (Fig. 2) was considered as the best model. For validation of the refined tertiary structures, PROSA-web, VADAR-web, and Rampage servers were utilized. PROSA-web calculated the Z-core of -7.34 for the best tertiary structure (Fig. 3a). This number indicates the tertiary structure of our multi-epitope candidate vaccine is outside the range of the scores that are determined for native proteins of similar size. The quality factor was calculated by the PROSA-web server (Fig. 3b), and the analysis of the Ramachandran plot with the Rampage server indicated that 92.38% of residues were arranged in favored regions, 6.01% of residues in additional allowed regions, 1.6% of residues in disallowed regions (Fig. 3c). This model was selected for an additional study.
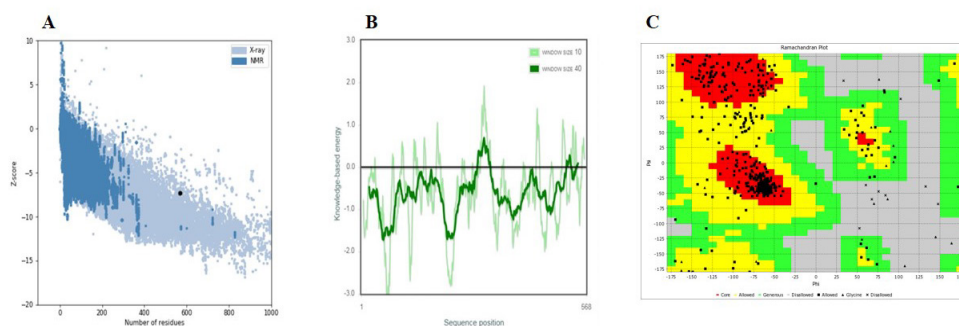
Figure 3. Protein validation. (A) ProSA-web, with a Z score of–7.34. (B) ProSA-web with quality input model graph (positive score is related to areas of the input structure that have low quality. In this model more than 90% of the input structure are in high areas). (C) Ramachandran plot analysis showing 92.38% in favored, 6.0% in allowed, and 1.6% in disallowed regions of protein residues.

Docking

Ten models were promoted for the structure of the designed candidate vaccine with TLR 4. According to the lowest energy scores (-291.56 kJ.mol^{-1}), model 5 was selected for the TLR4-candidate vaccine complex as the best-docked complex (Fig. 4).

Molecular dynamic simulation of the candidate vaccine-receptor complex

The deformability of each residue in the candidate vaccine-TLR4 complexes is very low. Therefore, the stability of complex structures is high. Atomic fluctuations of both complexes also have a minor deviation in the B-factor plot. Consequently, the interaction between vaccine and receptors is strong (Fig. 5).
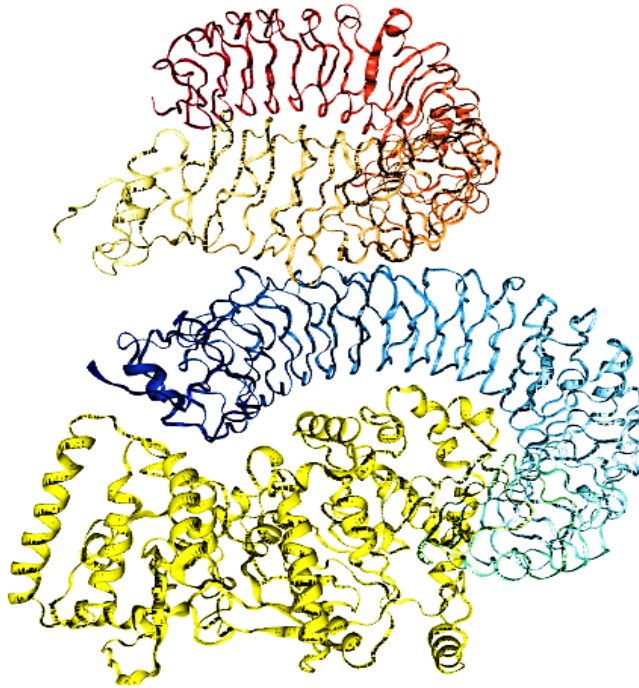
Figure 4. The results of best model molecular docking of vaccine construct (yellow) and TLR-4 (red and blue). The lowest energy score of this complex model is -291.56 kcal.mol^{-1}, indicating good binding affinity.

F. GOUDARZIASL, F. KHEIRI, A. RAHBAR, R. MOHAMMADHASSAN,
J. MOHAMMADI-ASL, A. JALILI, M. HAJKAZEMIAN
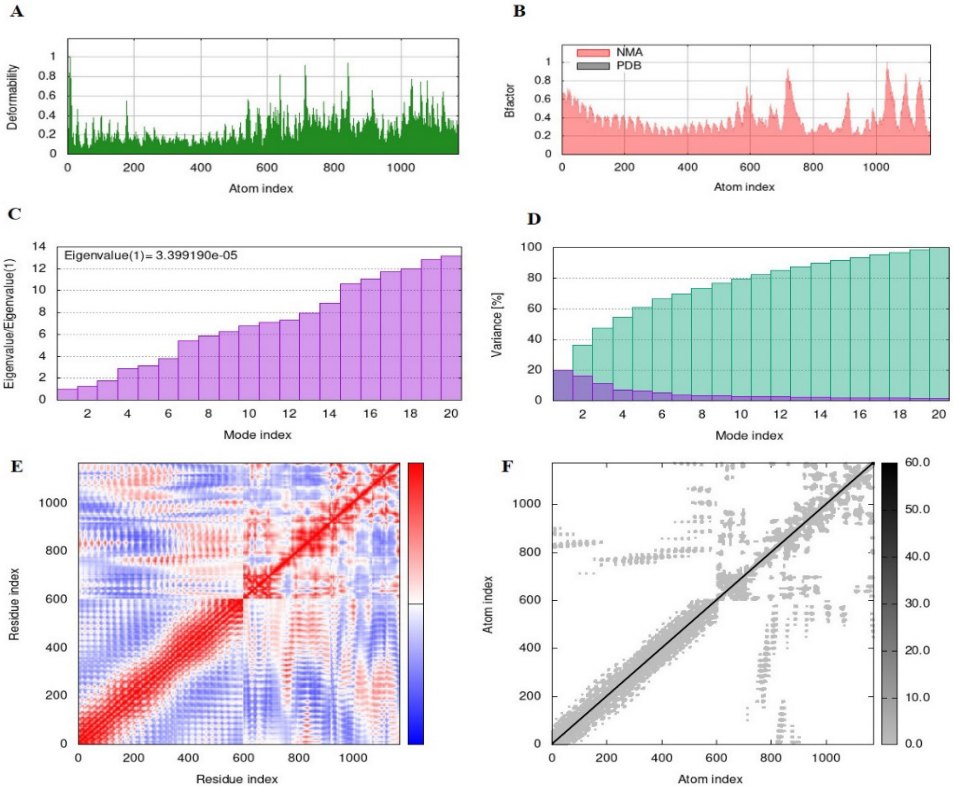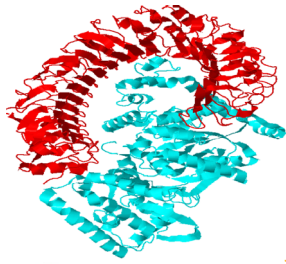
Figure 5. The results of simulating vaccine construct and TLR-4 docked complex via molecular dynamics. (A) Deformability. The deformability simulation of main-chain, the hinges as the regions with high deformability. (B) B-factor values were calculated by normal mode analysis, quantifying the uncertainty of each atom. (C) Eigenvalues; showing the energy required to deform the structure. (D) Variance. The covariance matrix between pairs of residues (white: uncorrelated, red: correlated, blue: anti-correlated). (Red color indicates individual variances and green color indicates cumulative variances), (E) co-variance map (correlated (red), uncorrelated (white) or anti-correlated (blue) motions) and (F) The elastic network model which is suggesting atom-spring connections. The springs with darker gray elastic network are more rigid.

Codon optimization of the vaccine construction and the secondary structure prediction of the mRNA

After optimization, the length of the optimized DNA sequence of the candidate vaccine was 1704 nucleotides for plant-based system. CAI of the optimized nucleotide sequence was 1.00; a number of > 0.8 is considered suitable for expression in a host, and a lower number indicates that your gene may be expressed poorly. The optimal percentage range of GC content was 31.9%. The optimal GC content should be from 30% to 70%. The 20% value of CFD was obtained for our sequence. A value of >30% for CFD may reduce the transcriptional and translational efficiency. The optimal secondary structure of mRNA was predicted with a minimum free energy of -332.97 kcal.mol^{-1}. Finally, the *SacI* and *XbaI* restriction sites were introduced to the N and C-terminals of the sequence, respectively, and this construction was inserted in the PBI121 vector (Fig. 6).
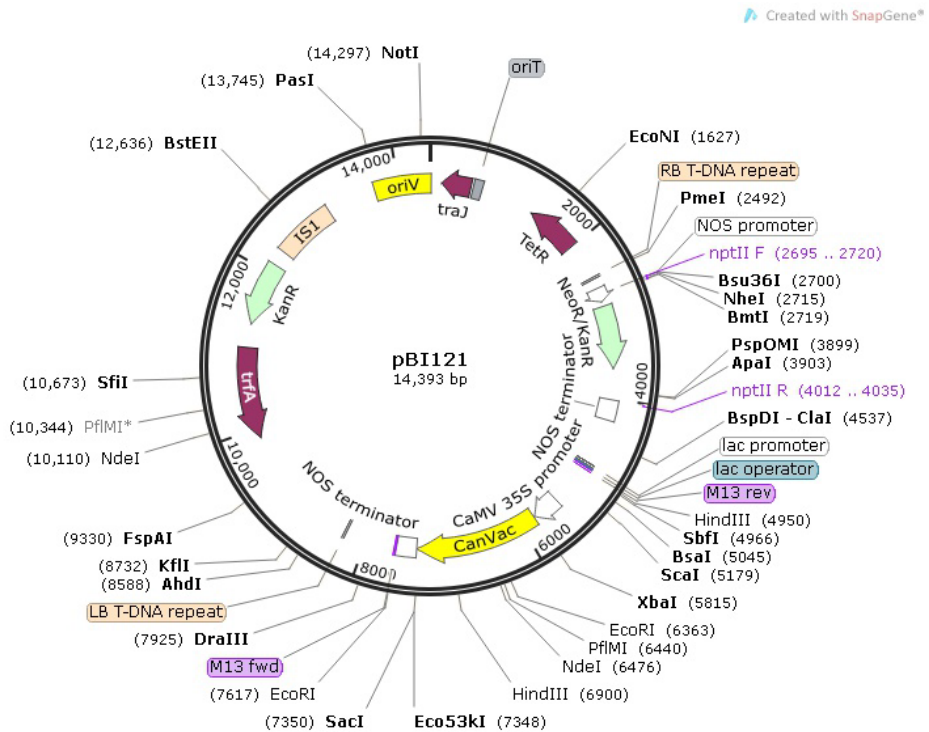
Figure 6. *in silico* cloning of the designed candidate vaccine. The yellow long region represents the codon-optimized candidate vaccine (CanVac) inserted into the pBI121 as an effective plant expression vector.

Discussion

Vaccination could be an appropriate option to manage COVID-19 prevalence (Le *et al.*, 2020). Currently, two vaccines against COVID-19, produced by Moderna and Pfizer, are approved by Food and Drug Administration (FDA). Pfizer and Moderna require to store at -80 and -20, respectively (Dyer, 2020). Recent advances in computational biology and bioinformatics tools facilitate accurate identification of the immunogenic components, such as multi-epitope vaccines (Kaur *et al.*, 2020). Inactive or weak pathogens are not used in multi-epitope vaccines. They are time-saving, cost-effective, and cross-protective (María *et al.*, 2017).

According to the available data, SARS-CoV-2 infects cellular and humoral systems (Grifoni *et al.*, 2020). T-cell response against spike protein of the SARS-CoV-2 has been significant. There is a high correlation between IgG and IgA antibody titers in patients (Shrotri *et al.*, 2021; Braun *et al.*, 2020; van Elslande *et al.*, 2020). Besides, antibodies against N and S proteins have been detected in seropositive patients (Apasov & Sitkovsky, 2005). At the start of the infection, the virus binds to the host cell by the interaction of the ACE receptor and S protein; therefore, this protein is a primary target for neutralizing antibodies (Grifoni *et al.*, 2020). In this study, several computational tools were used to design the multi-epitope vaccine against SARS-CoV-2. According to the reports, the prediction of linear B-cell epitopes was performed on the sequences of S and N proteins. Some characteristics such as High epitope score, good solubility, antigenic, nontoxic, and non-allergen were considered to select suitable B-linear epitopes. On the other hand, M, E, S, and N protein sequences were used for T-cell epitope prediction. Predicted T-cell epitopes were also filtered according to high epitope score, high hydrophobicity, antigenicity, non-toxicity, and non-allergenicity. T-cells are the main components of the adaptive immune system and have a central role in cell-mediated immunity (Apasov & Sitkovsky, 2005). They control antibody responses, activation of innate immune cells, and lysis of infected cells (Suárez-Fueyo *et al.*, 2019). In human and animal models, most of the T-cell epitopes presented by MHC complexes were derived from structural proteins of the coronavirus (Shah *et al.*, 2020). Therefore, in this study, the prediction of CTL and HTL epitopes was performed on structural proteins.

To construct a multi-epitope vaccine, selected B-cell epitopes are adjoined together with GPGPG linkers and T-cell epitopes with KK linkers. GPGPG and KK linkers as flexible spacers help the folding of the protein and increase the accessibility of the immune system to B-cell and T-cells epitopes (Dong *et al.*, 2020). Cholera toxin subunit B (CTB) was added by EAAAK linker as an adjuvant at the N-terminal of the chimeric construction. Generally, subunit vaccines alone have

weak efficiency in stimulating the immune system. Therefore, adjuvants are used in combination with this type of vaccine (Christensen, 2016). The High potential of CTB in the activation of dendritic cells, helper T-cells, and IFN-γ secretion makes it a proper choice to use as a mucosal adjuvant in vaccines (Antonio-Herrera *et al*., 2018; Wiedinger *et al*., 2017). The Fusion of CTB at the N-terminal of a chimeric vaccine creates an opportunity for CTB to form a pentameric structure, consequently binds better to GM1-gangliosids (Lichtenstein & Höcker, 2018). EAAAK linker is a rigid spacer between the CTB domain from others and also can form an alpha-helix structure (Caparco *et al*., 2022). Analysis by AllerTOP and Vaxijen servers revealed that our design candidate vaccine was non-allergen and antigenic. ProtParam analysis showed the molecular weight of the construction was 64.48 kD and instability index was 31.87, which classify designed candidate vaccine in the stable proteins. If a protein's instability index is less than 40, this protein is predicted as a stable protein (Walker, 2005). According to the results of the ProtParam analysis, the half-life of the candidate vaccine was evaluated 0.8 h (mammalian reticulocytes, *in vitro*), >10 min (yeast, *in vitro*), >10 h (*Escherichia coli*, *in vivo*), and 8 h (Plant, *in vitro*). GRAVY index of the candidate vaccine was -0.5. A negative GRAVY score indicates the polarity nature of a protein and effective interaction with water. Consequently, negative GRAVY score reflects the solubility of a protein. The aliphatic index of our construction (aliphatic index =79.89) reflected the thermostability of the protein (Annunziato, & Costantino, 2020). The structural validation was performed by ProSA-web, ERRAT and PRECHECK online servers. Z-score (-7.34), calculated by ProSA-web server, indicates the overall quality for the tertiary structure of the input protein is outside the range of scores of the native proteins with similar size, which determined their structures by NMR and X-ray crystallography experiments (Kar *et al*., 2020). Ramachandran plot developed by PRECHECK server indicated that 92.38% of residues were arranged in favored regions, 6.01% of residues in additional allowed regions, and 1.6% of residues in disallowed regions. These factors validate the quality of our protein structure.

In the body, strong binding of the vaccine products with immune receptors leads to immunological responses (Sheik Amamuddy *et al*., 2020). TLRs are conserved membrane receptors recognizing pathogen-associated molecular patterns, such as bacterial and fungal patterns, and nucleic acids. Also, TLRs play the central role in the initiation of cellular innate immune responses (Zaheer *et al*., 2020; Eisenbarth *et al*., 2019; Smith *et al*., 2019). TLR2 and TLR4 are present on the surface of the cells and are triggered by viral structural and non-structural proteins (Athari, 2019). COVID-19 and SARS have similar clinical symptoms (Huang *et al*., 2020); therefore, the mechanism of pathogenesis of SARS-CoV-2 may be similar to SARS-CoV (Zheng *et al*., 2021). Some studies on SARS-CoV-2 infection suggested that TLR2 and TLR4 have a significant role in immune

responses (van der Donk *et al.*, 2022). For example, Yao *et al.* (2022) indicated that in the infection of SARS-CoV-2, after 24 hours, the expression of TLR4 is upregulated in monocytes. Khan *et al.* (2021) demonstrated that mice with deficient TLR4 are more susceptible to SARS-CoV-2 infection than wild-type mice.

In our study, the binding affinity (ΔG value) of the docked complex was -332.97 kcal.mol^{-1}. A negative sign in ΔG value indicates interaction is thermostatically possible and it can happen in nature (Kakkanas *et al.*, 2022).

A T-cell epitope can stimulate the cellular immune system when represented on the cell surface and detected by TCRs of T-cells (Siebenmorgen & Zacharias, 2020). MHC molecules bind to peptide fragments derived from a pathogen and expose them to immune system components (Reynisson *et al.*, 2020). Therefore, the strong binding of T-cell epitopes with MHCs can be the key feature in the stimulation of cellular immunity (Peters *et al.*, 2020).

Low deviation in deformability and B-factor plots showed vaccine- receptor has acceptable stability. The Eigenvalue indicated the vaccine- TLR4 complex is stable. Finally, the codon adaption and in silico cloning were performed by the OPTIMER server and SnapGENE, respectively. The optimized DNA had a good amount of GC content (31.9%) and CAI value (1.00), which indicates that the DNA sequence has an exact amount of favorable codons; therefore, it is likely to be expressed in a plant.

Mammalian cell culture and microbial fermentation systems are extensively used to produce recombinant proteins commercially (Rahbaran *et al.*, 2021). But there can be found many benefits for molecular farming, using plants to produce recombinant proteins (Mohammadhassan and Asadishad, 2023). The costs of pharmaceutical recombinant proteins, for instance, are significantly lower than other systems, because plants can widely cultivated in greenhouses and farm without any specific facilities such as bioreactors and fementors (Chung *et al.*, 2022; Bhat *et al.*, 2022). In contrast to bacterial systems, plants are capable of producing pharmaceutical medicinal proteins that require post-translational modifications such as glycosylation and aggregation of different subunits, because, plant cells, same as mammalian cells, have intracellular eukaryotic membrane systems, which enables the post-translational modifications (Margolin *et al.*, 2020a; Ratre *et al.*, 2023). At contarary to animal system which can transmits and causes zoonotic diseases (Fallahi and Mohammadhassan, 2020), there is no common disease between humans and plants (Bhat *et al.*, 2022). An an example, Margolin *et al.* (2020b) could produce high level of recombinant SARS-CoV-2 spike protein, as a vaccine, in *Nicotiana benthamiana*.

The most widely used plant expression vector for introducing and expressing recombinant proteins in plants is the pBI121 vector. According to several publications, pBI121 was employed in 40% of the 180 papers on Agrobacterium-mediated transformations (Mohammadhassan *et al.*, 2014).

Other factors for pBI121 adoption include its simplicity, the ability to replace the target gene instead of the GUS gene, and the suitable expression of the transferred gene via *CaMV* 35S as an effective promoter (Mohammadhassan *et al.*, 2018).

Conclusions

According to the COVID-19 prevalence, the development of other vaccines against the disease is necessary to increase the production capacity of the vaccine and the diversity of vaccines. Computational approach can be employed to create an effective vaccine in lesser time. Therefore in this study, we used bioinformatics tools to design a multi-epitope vaccine against SARS-CoV-2. The designed vaccine consists of HTL, CTL, and linear B-cell epitopes of E, M, N, and S proteins of the virus. The results showed the designed vaccine was antigenic and immunogenic. Molecular docking of the three-dimensional structural model of the vaccine with TLR2/TLR4 indicated the designed vaccine could stimulate the innate immune system. Molecular docking of the HTL and CTL epitopes with their respective MHCs showed the selected epitopes had an acceptable interaction with MHCs. As a result, cellular immunity is more likely to develop. However, bioinformatics results suggest that the designed vaccine may stimulate immunity, but laboratory tests are necessary for final confirmation.

References

Annunziato, G., & Costantino, G. (2020). Antimicrobial peptides (AMPs): a patent review (2015–2020). *Exp Opin Thera Patents, 30*(12), 931-947. Doi: 10.1080/13543776.2020.1851679.

Antonio-Herrera, L., Badillo-Godinez, O., Medina-Contreras, O., Tepale-Segura, A., García-Lozano, A., Gutierrez-Xicotencatl, L. Soldevila, G., Esquivel-Guadarrama, F.R., Idoyaga, J. and Bonifaz, L.C. (2018). The nontoxic cholera B subunit is a potent adjuvant for intradermal DC-targeted vaccination. *Front Immunol, 9*, 2212-2228. Doi: 10.3389/fimmu.2018.02212.

Amanat, F. & Krammer, F. (2020). SARS-CoV-2 vaccines: status report. *Immunity, 52*(4), 583-589. Doi: 10.1016/j.immuni.2020.03.007.

Apasov, S.G., & Sitkovsky, M.V. (2005). T cell-mediated immunity. In: *Principles of Immunopharmacology*, Nijkamp FP, Parnham MJ. (ed.), *Springer*, Singapore, pp. 19-28. Doi: 10.1007/978-3-030-10811-3.

Athari, S.S. (2019). Targeting cell signaling in allergic asthma. *Signal Transduct Target Ther, 4*(1), 1-19. Doi: 10.1038/s41392-019-0079-0.

Bhat, K.A., Tariq, L., Ayaz, A., Manzoor, M., Zargar, S.M., & Shah, A.A. (2022). Molecular farming: sustainable manufacturing of vaccines, antibodies, and other therapeutic substances. In: Metabolic engineering in plants*, Springer Nature*, Singapore, pp. 239-261. Doi: 10.1007/978-981-16-7262-0_10.

Boopathi, S., Poma, A.B. & Kolandaivel, P. (2020). Novel 2019 coronavirus structure, mechanism of action, antiviral drug promises and rule out against its treatment. *J Biomol Struct Dyn, 39*(9), 3409-3418. Doi: 10.1080/07391102.2020.1758788.

Braun, J., Loyal, L., Frentsch, M., Wendisch, D., Georg, P., Kurth, F., Hippenstiel, S., Dingeldey, M., Kruse, B., Fauchere, F. & Baysal, E. (2020). SARS-CoV-2-reactive T cells in healthy donors and patients with COVID-19. *Nature, 587*(7833), 270-274. Doi: 10.1038/s41586-020-2598-9.

Caparco, A.A., Dautel, D.R., & Champion, J.A. (2022). Protein mediated enzyme immobilization. *Small, 18*(19), 2106425. Doi: 10.1002/smll.202106425.

Christensen, D. (2016). Vaccine adjuvants: why and how. *Hum Vaccines Immunother*, *12*(10), 2709-2711. Doi: 10.1080%2F21645515.2016.1219003.

Chung, Y.H., Church, D., Koellhoffer, E.C., Osota, E., Shukla, S., Rybicki, E.P., & Steinmetz, N. F. (2022). Integrating plant molecular farming and materials research for next-generation vaccines. *Nat Rev Mater*, *7*(5), 372-388. Doi: 10.1038/s41578-021-00399-5.

Cong, H., Gu, Q.M., Yin, H.E., Wang, J.W., Zhao, Q.L., Zhou, H.Y., Li, Y. & Zhang, J.Q. (2008). Multi-epitope DNA vaccine linked to the A2/B subunit of cholera toxin protect mice against *Toxoplasma gondii. Vaccine, 26*(31), 3913-3921.
Doi: 10.1016/j.vaccine.2008.04.046.

Dibner, J. (2021). Fecal-oral transmission of COVID-19: could hypochlorhydria play a role? *J Med Virol*, *93*(1), 166-167. Doi: 10.1002%2Fjmv.26265.

Dong, R., Chu, Z., Yu, F. & Zha, Y. (2020). Contriving multi-epitope subunit of vaccine for COVID-19: immunoinformatics approaches. *Front Immunol, 11*, 1784-1802. Doi: 10.3389/fimmu.2020.01784.

Dyer, O. (2020). Covid-19: many poor countries will see almost no vaccine next year, aid groups warn. *BMJ Br Med J, 371*, 1-2. Doi: 10.1136/bmj.m4809.

Eisenbarth, S.C. (2019). Dendritic cell subsets in T cell programming: location dictates function. *Nat Rev Immunol, 19*(2), 89-103. Doi: 10.1038%2Fs41577-018-0088-1.

Fallahi S, & Mohammadhassan R. (2020). A review of pharmaceutical recombinant proteins and gene transformation approaches in transgenic poultry. *J Trop Life Sci, 10*(2), 163-173. Doi: 10.11594/jtls.10.02.09.

Fehr, A.R. & Perlman, S. (2015). Coronaviruses, an overview of their replication and pathogenesis, In: Coronaviruses methods in molecular biology, Maier, H., Bickerton, E. & Britton, P. (ed.), *Springer*, Singapore, pp. 1-23. Doi: 10.1007%2F978-1-4939-2438-7_1.

Grifoni, A., Weiskopf, D., Ramirez, S.I., Mateus, J., Dan, J.M., Moderbacher, C.R., Rawlings, S.A., Sutherland, A., Premkumar, L., Jadi, R.S. & Marrama, D. (2020). Targets of T cell responses to SARS-CoV-2 coronavirus in humans with COVID-19 disease and unexposed individuals. *Cell, 181*(7), 1489-1501. Doi: 10.1016/j.cell.2020.05.015.

Hajissa, K., Zakaria, R., Suppian, R. & Mohamed, Z. (2019). Epitope-based vaccine as a universal vaccination strategy against *Toxoplasma gonidii* infection: a mini-review. *J Adv Vet Anim Res, 6*(2), 174–182. Doi: 10.5455%2Fjavar.2019.f329.

Huang, C., Wang, Y., Li, X., Ren, L., Zhao, J., Hu, Y., Zhang, L., Fan, G., Xu, J., Gu, X. & Cheng, Z. (2020) Clinical features of patients infected with 2019 novel coronavirus in Wuhan, China. *Lancet, 395*(10223), 497-506. Doi: 10.1016/S0140-6736(20)30183-5.

Kakkanas, A., Karamichali, E., Koufogeorgou, E.I., Kotsakis, S.D., Georgopoulou, U., & Foka, P. (2022). Targeting the YXXΦ motifs of the SARS coronaviruses 1 and 2 ORF3a peptides by in silico analysis to predict novel virus—host interactions. *Biomolecules, 12*(8), 1052. Doi: 10.3390/biom12081052.

Kar, T., Narsaria, U., Basak, S., Deb, D., Castiglione, F., Mueller, D.M. & Srivastava, A.P. (2020). A candidate multi-epitope vaccine against SARS-CoV-2. *Sci Rep, 10*(1), 1-24. Doi: 10.1038/s41598-020-67749-1.

Kaur, R., Arora, N., Jamakhani, M.A., Malik, S., Kumar, P., Anjum, F., Tripathi, S., Mishra, A. & Prasad, A. (2020). Development of multi-epitope chimeric vaccine against *Taenia solium* by exploring its proteome: an in silico approach. *Expert Rev Vaccines, 19*(1), 105-114. Doi: 10.1080/14760584.2019.1711057.

Khan, S., Shafiei, M. S., Longoria, C., Schoggins, J. W., Savani, R. C., & Zaki, H. (2021). SARS-CoV-2 spike protein induces inflammation via TLR2-dependent activation of the NF-κB pathway. *Elife, 10*, e68563. Doi: 10.7554/eLife.68563.

Le, T.T., Andreadakis, Z., Kumar, A., Román, R.G., Tollefsen, S., Saville, M., & Mayhew, S. (2020). The COVID-19 vaccine development landscape. *Nat Rev Drug Discov, 19*(5), 305-306. Doi: 10.1038/d41573-020-00073-5.

Lichtenstein, B. R., & Höcker, B. (2018). Engineering an AB5 protein carrier. *Sci Rep, 8*(1), 1-11. Doi: 10.1038/s41598-018-30910-y.

Lim, Y.X., Ng, Y.L., Tam, J.P. & Liu, D.X. (2016). Human coronaviruses: a review of virus–host interactions. *Diseases, 4*(3), 26-54. Doi: 10.3390/diseases4030026.

Liu, Z. & Chen, Y.H. (2004). Design and construction of a recombinant epitope-peptide gene as a universal epitope-vaccine strategy. *J Immunol Methods, 285*(1), 93-97. Doi: 10.1016/j.jim.2003.10.018.

Margolin, E., Crispin, M., Meyers, A., Chapman, R., & Rybicki, E.P. (2020a). A roadmap for the molecular farming of viral glycoprotein vaccines: engineering glycosylation and glycosylation-directed folding. *Front Plant Sci*, *11*, 609207. Doi: 10.3389/fpls.2020.609207.

Margolin, E., Verbeek, M., Meyers, A., Chapman, R., Williamson, A.L., & Rybicki, E.P. (2020b). Calreticulin co-expression supports high level production of a recombinant SARS-CoV-2 spike mimetic in *Nicotiana benthamiana*. *BioRxiv*, 2020-06. Doi: 10.1101/2020.06.14.150458.

María, R.R., Arturo, C.J., Alicia, J.A., Paulina, M.G. & Gerardo, A.O. (2017). The impact of bioinformatics on vaccine design and development, In: Vaccines, Afrin, F., Hemeg, H. & Ozbak, H. (eds.), *IntechOpen*, London, pp. 3-6.
Doi: 10.5772/intechopen.69273.

Miles, S., Portela, M., Cyrklaff, M., Ancarola, M.E., Frischknecht, F., Durán, R., Dematteis, S. & Mourglia-Ettlin, G. (2019). Combining proteomics and bioinformatics to explore novel tegumental antigens as vaccine candidates against *Echinococcus granulosus* infection. *J Cell Biochem, 120*(9), 15320-36. Doi: 10.1002/jcb.28799.

Mohammadhassan, R., & Asadishad, T. (2023). Using in silico tools to analyze the 5' untranslated regions of the alcohol dehydrogenase gene from *Arabidopsis thaliana* and Omega Sequence. *Makara J Sci, 27*(4), 8. Doi: 10.7454/mss.v27i4.1472.

Mohammadhassan, R., Fallahi, S. & Mohammadalipour, Z. (2020). ADMET and pharmaceutical activity analysis of caffeic acid diversities by in silico tools. *Lett Appl NanoBioSci, 9*(1), 840-8. Doi: 10.33263/LIANBS91.840848.

Mohammadhassan, R., Esfahani, K. & Kashefi, B. (2018). Constructional and functional evaluation of two new plant expression vectors—pBI121 gus-6 and pBI121 5+1. *Banat J Biotechnol*, *9*(17), 60-68. Doi: 10.7904/2068–4738–IX(17)–60.

Mohammadhassan. R., Kashefi, B. & Delcheh, K.S. (2014). *Agrobacterium*-based vectors: a review. *Int J Farm All Sci, 3*(9), 1002-1008. http://ijfas.com/wp-content/uploads/2014/10/1002-1008.pdf.

Nokhostin, F., Dargahi MalAmir, M., Tutunchi, S., & Rezaeeyan, H. (2020). Evaluation of prognostic/diagnostic value of Hematological markers in the detection of inflammation in coronavirus disease: a review study. *J Adv Med Biomed Res*, *28*(128), 171-174. Doi: 10.30699/jambs.28.128.171.

Peters, B., Nielsen, M., & Sette, A. (2020). T cell epitope predictions. *Annu Rev Immunol, 38*, 123-145. Doi: 10.1146/annurev-immunol-082119-124838.

Rahbaran, M., Razeghian, E., Maashi, M.S., Jalil, A.T., Widjaja, G., Thangavelu, L., & Jarahian, M. (2021). Cloning and embryo splitting in mammalians: brief history, methods, and achievements. *Stem Cells Int*, *2021*, 1-11.
Doi: 10.1155/2021/2347506.

Rahbaran, M. (2021). Pregnancy and Covid-19: a brief review. 1st National Conference in Health, Social sciences and Humanities focusing on COVID19. *Tbilisi*, Georgia. https://b2n.ir/360005637.

Ratre, Y.K., Mehta, A., Shinde, S., Sinha, V., Soni, V.K., Sonkar, S.C., & Vishvakarma, N.K. (2023). Molecular farming and anticancer vaccine: current opportunities and openings. In*: Microbial bioreactors for industrial molecules, Singh S.P. & Upadhyay, S.K. (eds), *Wiley*, Hoboken, pp. 355-373. Doi: 10.1002/9781119874096.ch17.

Reynisson, B., Alvarez, B., Paul, S., Peters, B., & Nielsen, M. (2020). NetMHCpan-4.1 and NetMHCIIpan-4.0: improved predictions of MHC antigen presentation by concurrent motif deconvolution and integration of MS MHC eluted ligand data. *Nuc Acids Res, 48*(W1), W449-W454. Doi: 10.1093%2Fnar%2Fgkaa379.

Shah, V.K., Firmal, P., Alam, A., Ganguly, D. & Chattopadhyay, S. (2020). Overview of immune response during SARS-CoV-2 infection: lessons from the past. *Front Immunol, 11*, 1949-66. Doi: 10.3389/fimmu.2020.01949.

Shrotri, M., van Schalkwyk, M.C., Post, N., Eddy, D., Huntley, C., Leeman, D., Rigby, S., Williams, S.V., Bermingham, W.H., Kellam, P. & Maher, J. (2021). T cell response to SARS-CoV-2 infection in humans: a systematic review. *PloS one, 16*(1), e0245532. Doi: 10.1371/journal.pone.0245532.

Sheik Amamuddy, O., Veldman, W., Manyumwa, C., Khairallah, A., Agajanian, S., Oluyemi, O., Verkhivker, G.M. & Tastan Bishop, Ö. (2020). Integrated computational approaches and tools for allosteric drug discovery. *Int J Mol Sci, 21*(3), 847. Doi: 10.3390/ijms21030847.

Shey, R.A., Ghogomu, S.M., Esoh, K.K., Nebangwa, N.D., Shintouo, C.M., Nongley, N.F., Asa, B.F., Ngale, F.N., Vanhamme, L. & Souopgui, J. (2019). In-silico design of a multi-epitope vaccine candidate against onchocerciasis and related filarial diseases. *Sci Rep, 9*(1), 4409. Doi: 10.1038/s41598-019-40833-x.

Siebenmorgen, T., & Zacharias, M. (2020). Computational prediction of protein–protein binding affinities. *Wiley Interdiscip Rev: Computat Mol Sci, 10*(3), e1448.

Smith, K.G., Kamdar, A.A. & Stark, J.M. (2019). Lung defenses: intrinsic, innate, and adaptive. In: Kendig's disorders of the respiratory tract in children, Wilmott, R.W., Li, A., Sly, P., Bush, A., Deterding, R. & Ratjen, F. (eds.), *Elsevier*, Amsterdam, pp. 120-133. Doi: 10.1016/C2015-0-01292-8.

Suárez-Fueyo, A., Crispín, J.C. & Tsokos, G.C. (2019). T cells. In: Dubois' lupus erythematosus and related syndromes, Wallace, D.J. & Hahn, B.H. (eds.), *Elsevier*, Amsterdam, pp. 116-124. Doi: 10.1016/C2010-0-66018-4.

van der Donk, L.E., Eder, J., van Hamme, J.L., Brouwer, P.J., Brinkkemper, M., van Nuenen, A.C., van Gils, M.J., Sanders, R.W., Kootstra, N.A., Bermejo-Jambrina, M. & Geijtenbeek, T.B. (2022). SARS-CoV-2 infection activates dendritic cells via cytosolic receptors rather than extracellular TLRs. *European J Immunol, 52*(4), 646-655. Doi: 10.1002/eji.202149656.

van Elslande, J., Decru, B., Jonckheere, S., van Wijngaerden, E., Houben, E., Vandecandelaere, P., Indevuyst, C., Depypere, M., Desmet, S., André, E. & van Ranst, M. (2020). Antibody response against SARS-CoV-2 spike protein and nucleoprotein evaluated by four automated immunoassays and three ELISAs. *Clin Microbiol Infect, 26*(11), e1-7. Doi: 10.1016/j.cmi.2020.07.038.

Walker, J.M. (2005). The proteomics protocols handbook, *Springer*, New York. Doi: 10.1385/1592598900.

Wiedinger, K., Pinho, D. & Bitsaktsis, C. (2017). Utilization of cholera toxin B as a mucosal adjuvant elicits antibody-mediated protection against *S. pneumoniae* infection in mice. *Ther Adv Vaccines, 5*(1), 15-24. Doi: 10.1177/2051013617691041.

Yang, J. & Zhang, Y. (2015). I-TASSER server: new development for protein structure and function predictions. *Nucleic Acids Res, 43*(W1), W174-81. Doi: 10.1093/nar/gkv342.

Yao, Y., Subedi, K., Liu, T., Khalasawi, N., Pretto-Kernahan, C.D., Wotring, J.W., Wang, J., Yin, C., Jiang, A., Fu, C. & Dimitrion, P. (2022). Surface translocation of ACE2 and TMPRSS2 upon TLR4/7/8 activation is required for SARS-CoV-2 infection in circulating monocytes. *Cell Discov, 8*(1), 89. Doi: 10.1038/s41421-022-00453-8.

Yoshimoto, FK. (2020). The proteins of severe acute respiratory syndrome coronavirus-2 (SARS CoV-2 or n-COV19), the cause of COVID-19. *Protein J, 39*(3), 198-216. Doi: 10.1007/s10930-020-09901-4.

Zaheer, T., Waseem, M., Waqar, W., Dar, H.A., Shehroz, M., Naz, K., Ishaq, Z., Ahmad, T., Ullah, N., Bakhtiar, S.M. & Muhammad, S.A. (2020). Anti-COVID-19 multi-epitope vaccine designs employing global viral genome sequences. *Peer J, 8*, e9541. Doi: 10.7717/peerj.9541.

Zheng, C., Shao, W., Chen, X., Zhang, B., Wang, G., & Zhang, W. (2022). Real-world effectiveness of COVID-19 vaccines: a literature review and meta-analysis. *Int J Infect Dis, 114*, 252-260. Doi: 10.1016/j.ijid.2021.11.009.

Zheng, M., Karki, R., Williams, E.P., Yang, D., Fitzpatrick, E., Vogel, P., Jonsson, C.B. & Kanneganti, T.D. (2021). TLR2 senses the SARS-CoV-2 envelope protein to produce inflammatory cytokines. *Nat Immunol, 22*(7), 829-838. Doi: 10.1038/s41590-021-00937-x.

Zhou, P., Yang, X.L., Wang, X.G., Hu, B., Zhang, L., Zhang, W., Si, H.R., Zhu, Y., Li, B., Huang, C.L. & Chen, H.D. (2020). A pneumonia outbreak associated with a new coronavirus of probable bat origin. *Nature, 579*(7798), 270-273. Doi: 10.1038/s41586-020-2012-7.

Induction of oxidative stress in a variety of durum wheat (*Triticum durum* Desf) exposed to recommended doses of pesticides

Djamila Hafsi[1], Ibtissem Sbartai[1] ✉ and Hana Sbartai[1]

[1] *Cellular Toxicology Laboratory, Faculty of Sciences, Badji-Mokhtar University, Annaba, Algeria*
✉ **Corresponding author, E-mail:** *ibsbartai@gmail.com*

Abstract. The objective of this study was to assess the toxicity of two pesticides (Prosaro® XRT and Decis® EC 25) widely used in the agricultural region of El-Tarf located in northeastern Algeria, as well as their combinations on a variety of durum wheat "*Triticum durum* Desf". The toxicity of these products was evaluated using physiological (chlorophyll) and biochemical parameters (proteins, glutathione, catalase activity and glutathione S-transferase, acetylcholine esterase, lipoxygenase). The recommended dose and its double were tested individually and in combination for this. It should be noted that the protocol used and the initial concentrations selected are the same as those used in the field. After D7 and D14 of exposure, all dosages were administered. The results obtained revealed a decrease in chlorophyll contents and Glutathione levels as well as an induction of total proteins and the differents enzymatic activity (catalase, glutathione S-transferase, lipooxygenase) and this for the two root and leaf compartments. Thus, it turns out that the concentrations used in open fields are not harmful to the plant but generate free radicals which are taken care of by the latter's defense system, thus allowing it to tolerate these stress conditions.

Keywords: toxicity, pesticides, *Triticum durum*, oxydative stress, stress biomarkers.

Introduction

The use of pesticides worldwide has increased dramatically coinciding with changes in agricultural practices and intensive farming (Konstantinou *et al.*, 2006). However, these chemical products are not without drawbacks, in particular by their toxic effects for non-target organisms such as beneficial insects, the contamination of soils and waterways, the pollution of groundwater as well as by their harmful effect on human health (Mebdoua *et al.,* 2017). Indeed, fungicides and insecticides are the most effective means of combating major diseases and pests of cultivated plants, which are necessary in maintaining or even increasing agricultural yields. However, most of these molecules are highly toxic and difficult to biodegrade. Their massive and repeated use can have harmful consequences for all components of the environment (Hafez *et al.,* 2020).

Application of chemical fungicides has been considered the primary method of protecting crops from many diseases due to their convenience and low cost (Xiao *et al.,* 2006). Although the effects of the latter are confirmed in controlling diseases and increasing crop yields, their toxic effects on crop plants have not been well studied, on the other hand, some studies have shown that they can affect plant respiration (Untiedt *et al.,* 2001), the synthesis of secondary metabolites (Mohamed *et al.,* 2017), the synthesis of plant hormones (Zhang *et al.,* 2020), chlorophyll synthesis and degradation and photosynthesis (Petit *et al.,* 2008). Similarly, insecticides have been shown to cause oxidative stress in plant cells, affecting various metabolic activities and plant growth components (Toscano *et al.,* 1982; Jones *et al.,* 1986). Several authors have demonstrated that pesticides in general induce oxidative stress in different species due to the production of reactive oxygen species (ROS) (Amamra *et al.,* 2014; Saillenfait *et al.,* 2015; Ferfar *et al.,* 2016; Sbartai and Sbartai, 2021; Belaid and Sbartai, 2021). To repair the damage induced by these ROS, plants have developed a complicated method of antioxidant enzyme system (superoxide dismutase (SOD), catalase (CAT), glutathione reductase (GR) and ascorbate peroxidase (APX)), which can effectively maintain redox homeostasis in plant cells by removing excess ROS (Apel *et al.,* 2004).

Algeria is ranked among the countries that use a large amount of pesticides and their use continues to increase in many areas. Thus about 400 phytosanitary products are approved, of which about forty varieties are widely used by farmers (Bordjiba *et al.,* 2009). Among them are pyrethroids, which are a class of insecticide that has recently appeared to replace organophosphates and organochlorines (Horton *et al.,* 2011; Saillenfait *et al.,* 2015). The latter have a higher toxicity thanks to their lipophilic nature allowing them to accumulate in fatty tissues. They are also able to produce ROS during their metabolism, thus altering the

integrity and the function of the cell and its organelles, particularly the mitochondria which produces more ROS likely to generate an imbalance in the redox status causing a respiratory disturbance see even apoptosis or necrosis (Ambolet-camoit *et al.,* 2012; Hossain *et al.,* 2014). Deltamethrin is frequently used in our region to protect cereal crops against pests, it is considered among the most toxic pyrethroids (TianhuiJiaoa *et al.,* 2021). Indeed, the frequent use of this molecule increases the risk of contamination in humans through the inhalation of suspended particles as well as through food (Saillenfait *et al.,* 2015). Following this accumulation, it results in a disruption in the sodium channels of the axons thus causing irritation of the upper tract, dizziness, vomiting and paresthesia (Wolansky and Tornero-Vélez, 2013). At the same time, and among the most used fungicides, we find the triazoles, which have been a well-known family for thirty years now, having an action that is both preventive and to a certain extent curative. At the systemic level, the toxic effects of triazoles lead to hormonal imbalance (Yang *et al.,* 2014), nitrogen imbalance, lower germination rates, impaired root growth and development (Serra *et al.,* 2013, 2015) and the appearance of chromosomal abnormalities (Wandscheer *et al.,* 2017).

Countless studies have reported the toxic effects of these xenobiotics and more particularly tebuconazole and prothioconazole on the defense mechanism of different species such as tomato, wheat, sweet potato and soybean (Nagajothi and Jeyakumar, 2016; Maruthaiya Arivalagan and Ramamurthy Somasundaram, 2017; Shishatskaya *et al.,* 2018; Mohsin *et al.,* 2021; Wang *et al.,* 2023). Thus, the objective of this study consisted in the evaluation of the toxicity of two pesticides Prosaro® (tebuconazole + prothioconazole) and Decis® (deltamethrine), frequently used in agriculture, as well as their combinations, at the recommended doses in open fields, in a variety of durum wheat (*Triticum durum*). Toxicity was monitored through the monitoring of certain stress biomarkers in order to confirm whether these doses are really not harmful and do not affect this plant and thus highlight the capacity of the latter to tolerate the stress conditions represented by our pesticides.

Materials and methods

Biological material

The biological material used in our work was a variety of durum wheat: *Triticum durum* Desf. The variety chosen is Siméto (Italian variety) from the Algerian Inter-professional Office of Cereals (O.A.I.C.) of El Hadjar-Annaba. It is an early variety with average productivity, it is recommended in semi-arid and intermediate arid zones, resistant to rain and drought and tolerates cold.

Chemical material

Two pesticides (Prosaro® XRT and Decis® EC 25) commonly used in the agricultural region of El-TARF in northeastern Algeria were used for this study. Prosaro® XRT is a triazole drug that combines the effects of two active ingredients: prothioconazole and tebuconazole at equal concentration ($125gL^{-1}$). It is a fungicide known for its high efficiency, versatility, and persistence against various cereal diseases. Decis® EC 25 (deltamethrin), a pyrethroid insecticide, is used as an insecticide and snake repellent due to its neurotoxic properties.

Experimental protocol

The wheat seeds used were first disinfected (1mL of 10V hydrogen peroxide with 9mL of distilled water) for 5 min then rinsed thoroughly with distilled water. To facilitate and accelerate germination, the seeds are put in distilled water in the refrigerator for 24 hours (vernalisation). The seeds were then sown in cells filled with a sand / compost mixture (2 volumes of sand / 1 volume of compost) at the rate of 3 seeds for each cell. It should be noted that the bottom of the cells is lined with a layer of gravel to ensure drainage. Watering was carried out twice a week at the rate of 20mL of distilled water per cell until the development of the seedlings. At the same time, the medium was enriched with nutrients thanks to a nutrient solution (Hoshang, 1988) added every 15 days for the various trials. The treatment with the different concentrations of Prosaro® and Decis® alone as well as their combinations (Prosaro®/Decis®) was carried out after 4 weeks from sowing at the 2-3 leaf stage. Regarding the combined treatment, the protocol followed in vitro is identical to that used in the field where it was a question of applying the Prosaro® first and then the deltamethrin at an interval of one month. Concerning the concentrations, we have chose those used by the farmers as well as the double of these. For Prosaro® XRT, the dose used is 0.8 L h^{-1} (P1: 0.66mg kg^{-1} of dry soil) and its double (P2: 1.33mg kg^{-1} of dry soil), for Decis® EC25 1L/h (D1: 0.83mg kg^{-1} of dry soil) and its double (D2: 1.66mg kg^{-1} of dry soil). As for the combined treatment, we used: P1/D1 and P2/D2. All assays were performed after 7 and 14 days of treatment.

Studied parameters

Chlorophyll assay

The extraction of chlorophylls was carried out according to the method of (Holden, 1975), which consisted of macerating the plant in acetone. The samples were treated as follows: 1g of the leaves of the plant cut into small pieces and ground with 20ml of 80% acetone and approximately 100mg of calcium

bicarbonate ($CaCo_3$). After total grinding, the solution is then filtered and put in black boxes to avoid the oxidation of chlorophylls by light. The reading is done at the two wavelengths 645nm and 663nm, after calibrating the device with the 80% acetone control solution.

Total protein content

Total protein content was determined using Bradford's (1976) method, which employs Coomassie Brilliant Blue (G250) as a reagent and Bovine Serum Albumin (BSA 1mg ml^{-1}) as a reference standard for a calibration of spectrophotometer at a wavelength 595nm.

Glutathione levels (GSH)

The GSH level was measured using the Weckberker and Cori (1988) method. The optical density of 2-nitro-5-mercapturic acid was measured due to the reduction of 5,5'-dithiol-2-nitrobenzoic acid (Ellman's reagent or DTNB) by glutathione's (-SH) groups. After 5 min of rest, absorbance readings at 412nm were taken for color stabilization against a blank where the 500µL of the supernatant are replaced by 500µL of distilled water.

Monitoring of catalase activity (CAT)

The method of Cakmak and Horst (1991) was used to calculate CAT. For a final volume of 3mL, the reaction mixture contains: 100µL of the crude enzymatic extract, 50µL of H_2O_2 at 0.1% and 2850µL of phosphate buffer (50 mM, pH 7.2). The decrease in absorbance is recorded for one minute for a wavelength of 240nm. The calibration of the device is done in the absence of the enzymatic extract. The reaction is triggered by the addition of H_2O_2.

Monitoring of glutathione S-transferase activity (GST)

GST determination was carried out according to the method of Habig *et al.,* (1974). The enzyme source represented the fraction obtained after homogenization and centrifugation of leaves and roots. A 200µL aliquot of the supernatant was mixed with 1.2mL phosphate buffer containing 1 mM CDNB (0.1 M, pH 6). At a wavelength of 340nm, absorbance readings were taken every minute for 5 min.

Monitoring of lipoxygenase activity (LOX)

The method of Axelrod *et al.,* (1981) was used to monitor lipoxygenase activity. The leaves and roots were ground in the presence of an extraction buffer composed of 50 mM phosphate buffer (KH_2PO_4/K_2HPO_4; pH 7), 5 mM cysteine

and 10 mM EDTA. The homogenate obtained was centrifuged at 14000 g for 20 min and the supernatant was recovered for the LOX activity assay. The reaction medium, with a final volume equal to 1mL, is composed of 0.16% tween-20 (v/v), 0.2 M glycine buffer (pH 10.0), 100 mM linoleic acid and the enzymatic extract. This activity was determined by measuring the absorbance of the hydroperoxides at 234nm.

Statistical analysis

The results obtained were statistically analyzed using Minitab software (Version 14.0). Datawere represented by the mean plus or minus the standard deviation (m±SD). We used two-way analysis of variance (ANOVA) to evaluate differences related to the effects of two independent variables (concentration and time) on a dependent variable (parameter). P≤0.05 was established as a significant difference.

Results

Effects of different treatments on chlorophyll level

According to the table below (Tab. 1), we have noted a slight variation in the level of chlorophyll **a** in the leaves treated for 7 days by the low concentrations of two pesticides P1, D1 (21.20; 19.17) compared to the control leaves (21.71), while this same rate decreases significantly (p≤.0.05) for the leaves treated by the rest of the concentrations of Prosaro® and Decis® (P2, D2, P1/D1 et P2/D2).

However, the significant decrease (p≤0.05) in the level of chlorophyll **b** is recorded according to the exposure time and the different treatments compared to the control leaves except for Prosaro® P1 (18.39) where this decrease is very low compared to the controls (19.80). As for the values of chlorophyll (**a+b**) recorded after 7 days of exposure, they follow the same direction as for chl**a** and chl **b** with a reduction of almost half for the combined treatment Prosaro®/Decis® (P2/D2) with a value of (23.51) compared to controls (41.51). After 14 days of exposure, there is a significant decrease in chl **a, b, a+b** in the leaves treated at the different concentrations where the lowest levels are recorded for the highest doses of the combined treatment P2/D2. Regarding the **a/b** ratio, there is a significant increase as a function of time and of the concentrations of the different treatments. it is 1.09 in the controls and reaches the value of 1.26 in the leaves treated after 7 days at the Posaro®/Decis® concentrations. After 14 days of exposure, this ratio is at most P2/D2 (1.33), D2 (1.32) and P2 (1.28).

Table 1. Variation in chlorophyll level in weat leaves treated with different concentrations. Standard deviations are obtained from averages corresponding to three replicates ± SE and significant differences were established according to a two-way ANOVA (P≤ 0.05).

Concentrations (mg kg^{-1} dry soil)	Chl a		Chl b		Chla+b		Chl a/b	
	7 days	14 days	7 days	14 days	7 days	14 days	7 days	14 days
Control	21.71± 0.012	22.01± 0.315	19.80± 0.037	19.75± 1.028	41.51± 0.717	41.76± 0.201	1.09± 0.011	1.11± 0.208
P1	21.20± 0.109	20.13± 0.221	18.39± 0.146	16.71± 0.116	39.59± 0.632	36.84± 0.056	1.15± 0.105	1.20± 0.017
P2	18.50± 0.168	15.52± 0.511	15.43± 0.098	12.06± 1.03	33.93± 0.391	27.58± 1.031	1.19± 0.028	1.28± 0.005
D1	19.17± 0.092	16.94± 0.122	15.49± 0.136	13.45± 0.255	34.66± 0.088	30.39± 0.975	1.23± 0.033	1.25± 0.230
D2	15.57± 0.157	13.33± 0.116	12.92± 0.471	10.06± 0.521	28.49± 0.111	23.39± 1.012	1.20± 0.098	1.32± 0.102
P1/D1	16.84± 0.09	13.97± 0.344	13.58± 0.160	11.04± 0.219	30.42± 0.320	25.01± 0.058	1.23± 0.066	1.26± 0.154
P2/D2	13.13± 0.118	10.74± 0.608	10.38± 0.032	8.07± 0.014	23.51± 0.084	18.81± 0.167	1.26± 0.103	1.33± 0.083

Effect of different treatment on the level of total proteins

According to our results (Fig. 1a, 1b), we have observed a significant increase (p ≤0.05) in protein contents in wheat leaves (a) as a function of time and concentrations used, compared to the controls. The most marked values were reported after 7 days for the highest concentration of D2 (9.92 µg mg^{-1} of FM) and for the combination P2/D2 (13.99 µg mg^{-1} of FM) compared to control values (5.96 µg mg^{-1} of FM). Similarly, after 14 days where the highest protein levels were reported at D2 (13.63 µg mg^{-1} of FM) which is twice the control (6.72 µg mg^{-1} of FM) and the combination P2/D2 (17.23 µg mg^{-1} FM) which is almost three times the control (6.72 µg mg^{-1} FM).

The same observations were retained for the quantity of protein in wheat roots which increases significantly (p ≤0.05) as a function of time and the concentrations used of the two pesticides. This quantity reaches its maximum after 14 days with a value of 7.54 µg mg^{-1} FM at P2/D2 which is almost double the value recorded in control roots (3.55 µg mg^{-1} FM).

(a)   (b)
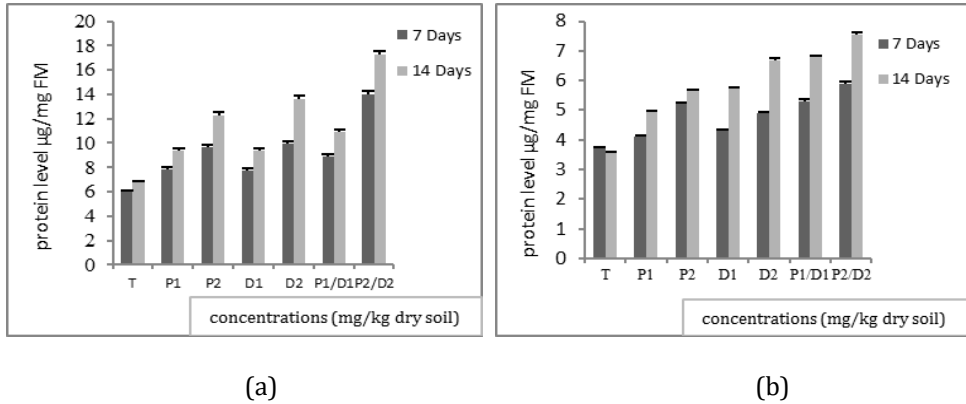
Figure 1. Effect of different treatments on the variation of total protein level in leaves (a) and roots (b) of wheat . Significant differences were established according to a two-way ANOVA (P≤0.05).

Effects of different treatments on glutathione level (GSH)

According to (Fig. 2a, 2b), a significant decrease (p≤0.05) in the GSH level was recorded as a function of the time of exposure of wheat leaves and roots to different concentrations of the two pesticides as well as the combined treatment compared to the control. After 7 days of exposure, the greatest reduction (56%) in the level of GSH was recorded in the leaves treated with combination P2/D2 (0.059 µmol mg^{-1} of Prot) compared to the control value (0.135 µmol/mg of Prot). Similarly for the GSH levels recorded after 14 days where 66% reduction was noted for the combination P2/D2 (0.047 µmol mg^{-1} of Prot) compared to the control leaves (0.137 µmol mg^{-1} of Prot). It should be noted that after 14 days of exposure a strong reduction was also noted in wheat leaves treated with highest concentration of D2 (0.049 µmol mg^{-1} of Prot) which is almost equivalent to the values found for combination P2/D2. In the roots, the lowest content (0.016 µmol mg^{-1} of Prot) was reported for P2/D2 after 14 days of exposure compared to the control roots (0.063 µmol mg^{-1} of proteins), i.e. a reduction of 75%.

(a)   (b)
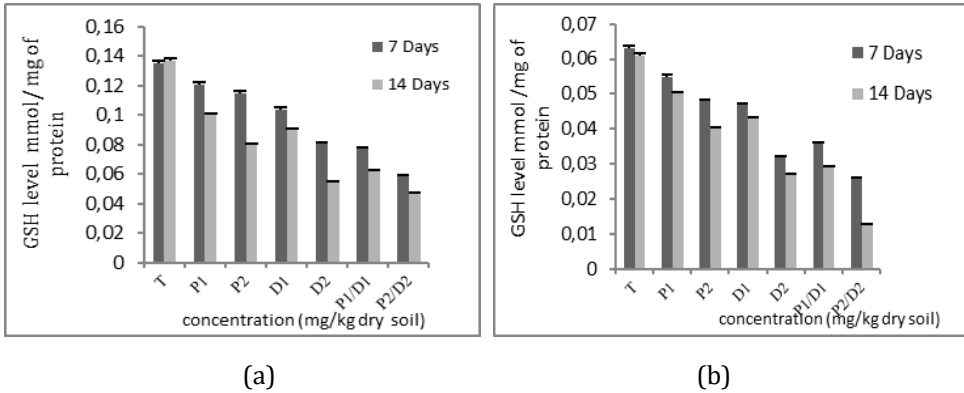
Figure 2. Effect of different treatments on the variation ofGSH level in leaves (a)
and roots (b) of wheat. Significant differences were established according
to a two-way ANOVA (P≤0.05).

Effects of different treatments on glutathione S-transferase activity (GST)

According to (Fig. 3a, 3b), we have noted a significant induction (p≤0.05) of GST activity as a function of time and the concentrations of the different treatments compared to the control leaves and roots. Indeed, GST activity was at its maximum in the leaves (0.045 and 0.065 µmol min^{-1} mg^{-1} of Prot) after 14 days of treatment for D2 and combination (P2/D2) compared to controls (0.019 µmol min^{-1} mg^{-1} of Prot). The same observations were recorded in wheat roots but it should be noted that the values recorded in the leaves were higher than those recorded in the roots.

(a)   (b)
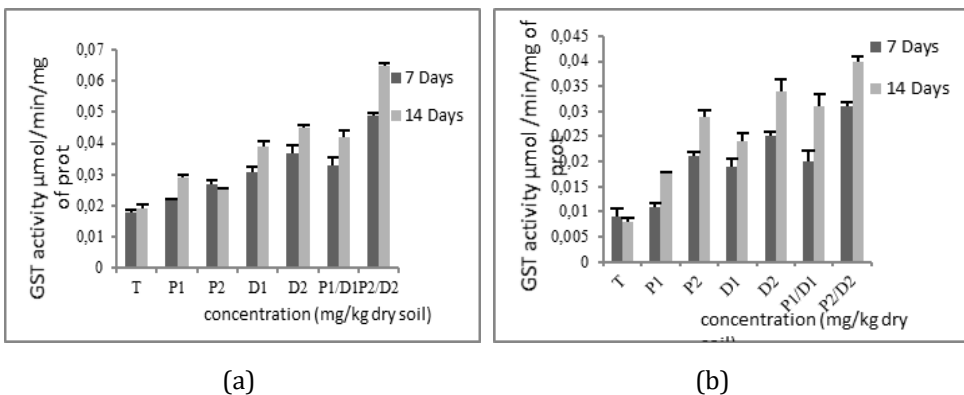
Figure 3. Effect of different treatments on the variation of GST activity in leaves (a)
and roots (b) of wheat. Significant differences were established according
to a two-way ANOVA (P≤0.05).

41

Effects of different treatments on catalase activity (CAT)

According to the results mentioned in (Fig. 4a, 4b), we have observed a significant increase (p≤0.05) in CAT activity as a function of exposure time and increasing concentrations compared to control leaves and roots.

| (a) | (b) |
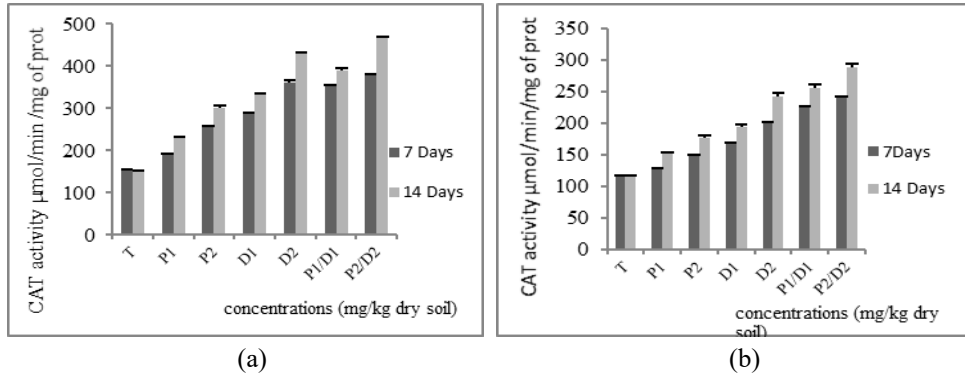
Figure 4. Effect of different treatments on the variation of CAT activity in leaves (a) and roots (b) of wheat. Significant differences were established according to a two-way ANOVA (P≤0.05).

After 7 and 14 days of exposure, the maximum values recorded in the leaves were reported for concentrations D2, P1/D1 and P2/D2 compared to the control values (150 µmol min^{-1} mg^{-1} Prot; 149.8 µmol min^{-1} mg^{-1} of Prot). In the roots, the maximum value was recorded after 14 days of exposure to the combination P2/D2 (288 µmol^{-1} min^{-1} mg^{-1} of Prot) compared to the control values (115 µmol min^{-1} mg^{-1} of Prot).

Effects of different treatments on lipoxygénase activity (LOX)

According to the figure below (Fig. 5a, 5b), wehave observed a significant increase (P≤0.05) in LOX activity as a function of the exposure time of the wheat leaves to the increasing concentrations of the different treatments compared to the controls. However, this activity was more stimulated after 14 days than after 7 days of exposure with maximum values reported for the high concentrations of the different treatments P2, D2, P2/D2 (250 µmol mg^{-1} of Prot; 295 µmol mg^{-1} of Prot and 390 µmol mg^{-1} of Prot) compared to control values which are equivalent to 171 µmol mg^{-1} of Prot.

In the roots, a significant increase (p≤0.05) in this activity was observed as a function of time and the concentrations of the different treatments where the maximum values were recorded after 14 days at the combination P2/D2 (381 µmol mg^{-1} of Prot) which represent three times the control value (134 µmol mg^{-1} of Prot).

(a)   (b)
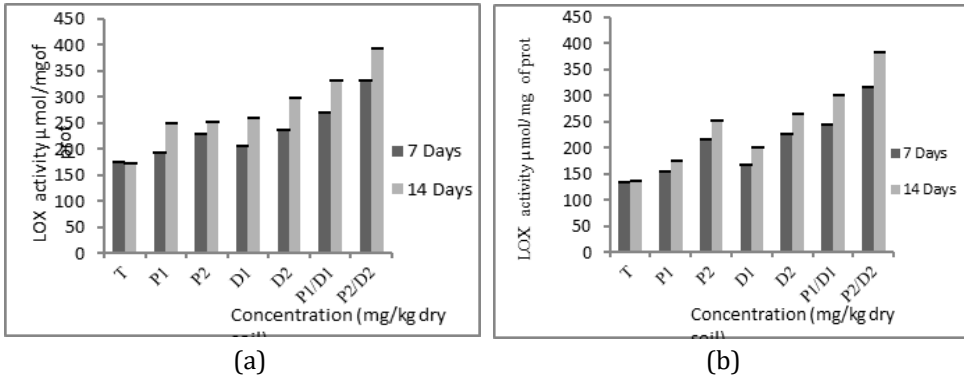
Figure 5. Effect of different treatments on the variation of LOX activity in leaves (a) and roots (b) of wheat. Significant differences were established according to a two-way ANOVA (P≤0.05).

Discussion

The impact of different treatments (Prosaro®, Decis®, Prosaro®/Decis®) on *Triticum durum* was evaluated using a biological approach at different scales of a cellular organization by examining the variations of several physiological and biochemical parameters. In our work we first tested the level of chlorophyll which is considered an excellent biomarker of plant toxicity knowing that there is a strong correlation between cell densities and photosynthetic fluorescence parameters in environmental pollution (Dewez *et al.,* 2007). Our results clearly show a decrease in leaf chlorophyll levels. This decrease can be attributed to the inhibition of its biosynthesis and photo-destruction of pesticides by reducing the formation of aminolevulinic acid (ALA) as a precursor of plant porphyrin essential for photosynthesis. Many studies have reported the negative effect of pesticides on chlorophyll levels in wheat leaves exposed to fungicides (Artea, Punch and Paclobutrazol) and herbicides (Cossack and Sékator) (Berova *et al.,* 2002; Ferfar *et al.,* 2016). Similarly, Liu *et al.,* (2021) showed that foliar exposure of common wheat (*Triticum aestivum* L) to difenoconazole induced a reduction in chlorophyll contents leading to a reduction in photosynthesis and the subsequent inhibition of plant growth.

At the same time, we focused on the response and regulation of the wheat defense system to these two xenobiotics. Indeed, the proportional increase in the total protein level observed as a function of increasing concentrations of the two pesticides as well as combinations in wheat leaves and roots tells us about the stress state of the plant. Gardés-Albert *et al.*, (2003) link this increase to the

fact that the plant seeks to protect its morpho-physiological integrity in response to damage induced by xenobiotics. In other words, protein accumulation is a molecular stress tolerance strategy that is directly linked to overproduction of ROS (Mishra et *al.*, 2006). Thus, oxidative damage can be reduced by activation of the antioxidant defense system to eliminate these ROS (Pompeu *et al.,* 2017; Arfaoui *et al.,* 2018) hence the induction of total proteins. Indeed, to deal with the generation of ROS, plants reinforce their antioxidant action of the enzymatic and non-enzymatic defense system (Hasanuzzaman *et al.,* 2020). Thus, the decrease in GSH recorded in both leaf and root compartments of wheat supports the hypothesis of the induction of the plant's defense system to allow it to tolerate this state of stress. GSH, a non-enzymatic antioxidant, is a low molecular weight thiol involved in a wide range of metabolic processes and constitutes an important plant defense system against environmental stresses, including pesticides (Hossain *et al.,* 2012). GSH is the substrate of GPx which is involved in the elimination of H_2O_2 (Lu, 2013, Mailloux *et al.,* 2014). The recycling of GSSG in GSH is catalyzed by glutathione reductase (GR) using NADPH as an electron donor. NADPH is indispensable for GSH recycling by GR and high GSH levels can lead to reducing stress. NAD(P)H and GSH are reducing equivalents essential for the response to oxidative stress. Paradoxically, excessive accumulation of cellular NAD(P)H and/or GSH leads to reductive stress and cellular dysfunction. In addition, it is also involved in the modulation of cellular redox signaling, in the regulation of proliferation and cell death as well as in the detoxification of xenobiotics and their metabolites (Fratelli *et al.,* 2005; Lu, 2013; Aquilano *et al.,* 2014).

This decrease could be explained by the fact that GSH could establish a direct bond with pesticides or their metabolites (Galaris *et al.,* 2002). This glutathione-pesticide interaction takes place thanks to the intervention of GST which allows this conjugation during phase II of metabolism (Belaid and Sbartai, 2021), this is confirmed by our results which indicate an induction of GST in the presence of pesticides tested. Indeed, GST is a multifunctional phase II enzyme which plays an essential role in the conjugation of electrophilic compounds (phase I metabolites) and catalyzes the conjugation of GSH with substances of an endogenous or exogenous nature. The increase in GST activity indicates both a high concentration of xenobiotics present in the environment and the induction of oxidative stress following the increasing production of ROS (Bhagat *et al.*, 2016). This production of ROS can be favored by the installed reductive stress which has been proposed according to certain researchers as an inducer of oxidative stress depending on the redox couples in which these ROS are engaged (Shen *et al.,* 2005; Yan *et al.,* 2014; Korge *et al.,* 2015; Xiao *et al.,* 2019). Much like oxidative stress, reductive stress also impairs cellular functions (Handy and Loscalzo, 2016).

However, and in the case of deltamethrin, tebuconazole and prothioconazole, metabolism occurs by hydroxylation, oxidation or hydrolysis reactions resulting in different metabolites followed by conjugation to glucuronic acid or sulfate (Ruzo *et al.*, 1979; IPCS, 1990) and not to GSH, which implies that GST is not involved in this biotransformation.Thus, the increase in GST could therefore be explained by the fact that it is also involved in the transport and elimination of reactive compounds that perform other antioxidant functions (Sies, 1993; Livingstone, 2003) such as CAT, GSH and SOD and also in the defense against oxidative damage to lipids and DNA induced by peroxide products (Van der Oost *et al.*, 2003). However, it was noted that at the end of treatment, GSH expression seems to be very sensitive to xenobiotics where it is strongly declined at high concentrations (D2, P2/D2) compared to controls but which are almost equivalent thus suggesting that Decis® (deltamethrin) alone has the same effect as the combined treatment (Prosaro®/Decis®) at these concentrations probably due to an antagonistic effect between the two pesticides. On the other hand, we recorded the induction of CAT activity with the different treatments, which testifies to the state of oxidative stress par excellence. The latter is an important enzyme in the defense system (antioxidant). It catalyzes, extremely quickly, the disproportionation of oxygen peroxide (H_2O_2) into oxygen and water, thus protecting cells from oxidative effects. The change in CAT activity is explained by cellular damage caused by exposure to contaminants (Shi *et al.,* 2011). Our results are in agreement with those obtained by Ferfar *et al.,* (2016) who demonstrated an increase in CAT activity in two varieties of wheat (Simeto and Cirta) exposed to two sulfonylurea herbicides, in leaves and roots of wheat "*Triticum aestivum* L". Similarly, the results of Belahcene *et al.,* (2015) which highlight the influence of oxidative stress caused by a systemic herbicide Cossack on the CAT activity of three varieties of durum wheat (Sersou, Carioca and Wersenis) where a variability very important genotypic was noted resulting from the response of each variety towards the applied stress.

Finally, the increase in LOX activity observed during our study could be due to the peroxidation of linoleic and linolenic acids. The formation of oxidation derivatives in the lipid bilayer, such as 4-hydroxy-2-nonenal, malondialdehyde or phytoprostanes, leads to disturbances in the micro-architecture of membranes, alters their permeability and can act with amine functions, lipids, proteins and DNA, as well as with the thiol functions of proteins.Indeed, these lipid peroxidation products are reactive electrophilic species (RES) which can bind covalently to proteins and thus damage them (Farmer *et al.*, 2007). Lipid peroxidation by forming aldehydes leads to the destruction of structures, inhibits cellular functions and potentially accelerates cell senescence (Reich and Amundson, 1985; Dann and Pell, 1989).

Conclusions

The results obtained in this study clearly revealed the toxicity of the pesticides (Prosaro®/Decis®) used on *Triticum durum* even at regulatory concentrations. Indeed, the application of pesticides (fungicide and insecticide) directly to durum wheat causes disturbances at the foliar level and indirectly a negative effect on the chlorophyll and GSH content as well as an accumulation of total proteins and an induction of enzymatic activities (CAT, GST and LOX). These physiological and biochemical results thus suggest the establishment of a defense mechanism in order to neutralize the free radicals generated by the stress applied to this variety of wheat. In conclusion, the regulatory doses disturb the plant but the latter manages to overcome this stress, on the other hand the high concentrations clearly affect the leaves and roots of wheat. Thus, Decis® (deltamethrin) alone appears more toxic than Prosaro® (prothioconazole/ tebuconazole) and has the same effect as the combined treatment (Prosaro®/ Decis®). All of this information could help us formulate countermeasures to reduce the risk of pesticide contamination in agricultural production.

References

Amamra, R., Djebar, M. R., Grara, N., Moumeni, O., Otmani, H., Alayat, A., & Berrebbah, H. (2015). Cypermethrin-induces oxidative stress to the freshwater Ciliate model: *Paramecium tetraurelia. Annu. Res. Rev. Biol*, *5*(5), 385-399. Doi:10.9734/ARRB/2015/10852.

Ambolet-Camoit A., Kim M.J., Leblanc A., & Aggerbeck M. (2012)**.** Les pollutants organiques persistants : implication dans l'obésité et le syndrome métabolique. *Cah. de Nutr. et de Diet*, *47*(4), 183- 192.

Apel, K., & Hirt, H. (2004). Reactive oxygen species: Metabolism, oxidative stress, and signal transduction. *Annu. Rev. Plant Biol*, *55*, 373–399. Doi: 10.1146/annurev.arplant.55.031903.141701

Aquilano, K., Baldelli, S., & Ciriolo, MR. (2014). Glutathione: new roles in redox signaling for an old antioxidant. *Front Pharmacol,* 5, 196.

Arfaoui, A., El Hadrami, A., & Daayf, F. (2018) Pre-treatment of soybean plants with calcium stimulates ROS responses and mitigates infection by *Sclerotinia sclerotiorum*. *Plant Physiol. Biochem, 122*, 121–128. Doi: 10.1016/j.plaphy.2017.11.014

Arivalagan, M., & Somasundaram, R. (2017). Alteration of photosynthetic pigments and antioxidant systems in tomato under drought with Tebuconazole and Hexaconazole applications. *J. Sci. Agric*, *1*, 146. 10.25081/jsa. 2017.v1.52.

Axelrod, B. (1981). Lipoxygenase from soybeans. *Methods Enzymol*, *71*, 441-451.

Belaid, C., & Sbartai, I. (2021). Assessing the effects of Thiram to oxidative stress responses in a freshwater bioindicator cladoceran (*Daphnia magna*). *Chemosphere*, *268*, 128808. Doi:10.1016/j.chemosphere.2020.128808.

Belahcene, N., Mouaissia, W., Zenati, N., & Djebar, M.R. (2015). Study of the effect of oxidative stress caused by a systemic herbicide cossack on durum wheat (*Triticum durum* Desf.)," *Int. j. of Innov. and Sci. Res*, *14*(1), 104–111.

Berova, M., Zlatev, Z., & Stoeva, N. (2002). Effect of Paclobutrazol on wheat seedlings under low temperature stress. *Bulg. J. Plant Physiol*, *28*(1-2), 75-84.

Bhagat, J., Ingole, B. S., & Singh, N. (2016). Glutathione S-transferase, catalase, superoxide dismutase, glutathione peroxidase, and lipid peroxidation as biomarkers of oxidative stress in snails: A review. *Invertebr. Surviv. J*, *13*(1), 336-349. Doi:10.25431/1824-307X/isj.v13i1.336-349.

Bordjiba, O., & Ketif, A. (2009). Effet de trois pesticides (Hexaconazole, Bromuconazole et Fluazifop-p-butyl) sur quelques métabolites physio-biochimiques du blé dur: *Triticum durum*. Desf. *European* J. Sci. Res, *36*(2), 260-268.

Bradford, M.M., (1976). A rapid and sensitive method for the quantitation of microgram; quantities of protein utilizing the principle of protein-dye binding. *Anal Biochem*, *72*, 248-254.

Cakmak, I., & Horst, W. J. (1991). Effect of aluminium on lipid peroxidation, superoxide dismutase, catalase and peroxidase activities in root tips of soybean (*Glycine max*). *Physiol. Plant, 83*, 463-468.

Dann, M. and Pell, E. (1989). Decline of activity and quantity of rand quantity of ribulose bisphosphate carboxylase oxygenase and net photosynthesis in ozone-treated potato foliage. *Plant Physiol., 91*, 427-432. http: //::dx.doi.org/10.1104/pp.91.1.427.

Dewez, T., Rohmer, J., & Closset, L. (2007). Laser survey and mechanical modeling of chalky sea cliff collapse in Normandy, France, in Mc Innes R., Jakeways J., Fairbanks H. et Mathie E., (eds), Landslide and climate change, *Taylor and Francis*, London, pp. 281-288.

Farmer, E. E., & Davoine, C. (2007). Reactive electrophile species. *Curr. Opin. Plant Biol*, *10*(4), 380-386.

Ferfar M., Meksem-Amara, L., Grara, N., Meksem, N., Benamara, & M., Djebar, M.R. (2016). Phytotoxic effects of a sulfonylurea herbicide on two varieties of durum wheat (Triticum durumDesf). *Int. J. Pharm. Res. Allied Sci*, *5*(4), 159-168.

Fratelli, M., Goodwin, L.O., Orom, U.A., Lombardi, S., Tonelli, R., Mengozzi, & M., Ghezzi, P. (2005). Gene expression profiling reveals a signaling role of 47lutathione in redox regulation. *Proc Natl Acad Sci U S A*, *102*, 13998-4003.

Galaris, D., & Evangelou, A. (2002). The role of oxidative stress in mechanisms of metal-induced carcinogenesis. *Crit. Rev. Oncol. Hematol*, *42*(1), 93-103.

Gardès-Albert, M., Bonnefont-Rousselot, D., Abedinzadeh, Z., & Jore, D. (2003). Espèces réactives de l'oxygène. *L'Act. Chim*, *6*, 91-96.

Habig, W.H., Pabst, M.J., & Jakoby, W.B. (1974). Glutathione-S-transferase: the first enzymatic step in mercapturic acid formation. *J. Biol. Chem, 249*, 7130-7139. Doi:10.1016/S0021-9258(19)42083-8.

Hafez, Y., Attia, K., Alamery, S., Ghazy, A., Al-Doss, A., Ibrahim, E., Rashwan, E. El-Maghraby, L., Awad, A., & Abdelaal, K. (2020). Beneficial effects of biochar and chitosan on antioxidative capacity, osmolytes accumulation, and anatomical characters of water-stressed barley plants. *Agronomy*, *10*, 630.

Handy, D.E., & Loscalzo, J. (2016). Responses to reductive stress in the cardiovascular system. *Free Radic Biol Med*, *109*, 114-124. Doi: 10.1016/j.freeradbiomed.2016.12.006.

Hasanuzzaman, M., Bhuyan, M.H.M.B., Zulfiqar, F., Raza, A., Mohsin, S.M., Mahmud, J.A., Fujita, M., & Fotopoulos, V. (2020). Reactive oxygen species and antioxidant defense in plants under abiotic stress: revisiting the crucial role of a universal defense regulator. *Antioxidants 9*, 681. https://doi.org/10.3390/antiox9080681.

Holden, M. (1975). Chlorophylls I, chemistry and biochemistry of plant pigments. 2éme edition. T.W. Goodwin. *Academic press Edition*. New York., 1-37.

Horton, M. K., Jacobson, J. B., McKelvey, W., Holmes, D., Fincher, B., Quantano, A., & Whyatt, R. M. (2011). Characterization of residential pest control products used in inner city communities in New York City. *J Expo Sci Environ Epidemiol*, *21*(3), 291–301. Doi: 10.1038/jes.2010.18.

Hossain, M.A., Piyatida, P., Da Silva, J.A.T., & Fujita, M., (2012). Molecular mechanism of heavy metal toxicity and tolerance in plants: central role of glutathione in detoxification of reactive oxygen species and methylglyoxal and in heavy metal chelation. *J. Bot* 872875. Doi:10.1155/2012/872875.

Hossain, M. M., Suzuki, T., Jason, R., Richardson, R. J., & Kobayashi, H. (2014). Acute Effects of Pyrethroids on Serotonin Release in the Striatum of Awake Rats: An In Vivo Microdialysis Study. *Biochem Mol Toxicol*, 27(2): 150–156. Doi: 10.1002/jbt.21450.

IPCS INCHEM (1990). Deltamethrin. EHC 97. WHO. Consultable sur le site www.inchem.org/docu- ments/ehc/ehc/ehc97.htm/

Jones, J. B., Pohronezny, K. L., Stall, R. E., & Jones, J. P. (1986). Survival of Xanthomonas campestris pv. vesicatoria in Florida on tomato crop residue, weeds, seeds, and volunteer tomato plants. *Phytopathology*, *76*(4), 430-434.

Konstantinou, I., Hela, D., & Albanis, T. (2006). The status of pesticide pollution in surface waters (rivers and lakes) of Greece. Part I. Review on occurrence and levels. *Environ. Pollut*, *141*, 555–570. Doi: 10.1016/j.envpol.2005.07.024.

Korge, P., Calmettes, G., & Weiss, J.N. (2015). Increased reactive oxygen species production during reductive stress: The roles of mitochondrial glutathione and thioredoxin reductases. *Biochim Biophys Acta 1847*: 514-25.

Liu, R., Li, J., Zhang, L., Feng, T., Zhang, Z., & Zhang, B. (2021). Fungicide difenoconazole induced biochemical and developmental toxicity in wheat (*Triticum aestivum L.*). *Plants*, *10*(11), 2304. Doi: 10.3390/plants10112304.

Livingstone D.R. (2003). Oxidative stress in aquatic organisms in relation to pollution and aquaculture. *Rev Med Vet.*, *154*, 427–430.

Lu SC. (2013). Glutathione synthesis. *Biochim Biophys Acta* 1830: 3143-53.

Mailloux, R.J., Jin, X., & Willmore, W.G. (2014). Redox regulation of mitochondrial function with emphasis on cysteine oxidation reactions. *Redox Biol 2*, 123-39.

Mebdoua, S., Lazali, M., Ounane, S. M., Tellah, S., Nabi, F., & Ounane, G. (2017). Evaluation of pesticide residues in fruits and vegetables from Algeria. *Food Addit & Contam: Part B*, *10*(2), 91-98. Doi: 10.1080/19393210.2016.1278047.

Mishra, S.; Srivastava, S.; Tripathi, R.D.; Govindarajan, R.; Kuriakose, S.V., & Prasad, M.N.V**.** (2006). Phytochelatin synthesis and response of antioxidants during cadmium stress in *Bacopa monnieri* L. *Plant Physiol. Biochem.*, *44*, 25-37. Doi: 10.1016/j.plaphy.2006.01.007.

Mohamed, H.I., & Akladious, S.A. (2017). Changes in antioxidants potential, secondary metabolites and plant hormones induced by different fungicides treatment in cotton plants. *Pestic. Biochem. Physiol*. *142*, 117–122.

Nagajothi, R., & Jeykumar, P. (2016). Foliar application of trifloxystrobin in combination with tebuconazole enhances antioxidant defense system and yield in tomato (*lycopersicon esculentum* mill). *The Biosean. 11*(4), 2615-2619*.

Petit, A.N., Fontaine, F., Clément, C., & Vaillant-Gaveau, N. (2008). Photosynthesis Limitations of Grapevine after Treatment with the Fungicide Fludioxonil. *J. Agric. Food Chem*. *56*, 6761–6767. Doi: 10.1021/jf800919u.

Pompeu, G.B, Vilhena M.B, Gratao, P.L, Carvalho, R.F., Rossi, M.L., Martinelli, A.P., & Azevedo, R.A., (2017). Abscisic acid-deficient sit tomato mutant responses to cadmium-induced stress. *Protoplasma 254*, 771–783. Doi: 10.1007/s00709-016-0989-4.

Reich, P. B., & Amundson, R. G. (1985). Ambient levels of ozone reduce net photosynthesis in tree and crop species. *Science*, *230*(4725), 566-570.

Ruzo, L. O., Engel, J. L., & Casida, J. E. (1979). Decamethrin metabolites from oxidative, hydrolytic and conjugative reactions in mice. *J. Agric. Food Chem*, *27*(4), 725-731.

Saillenfait, A.M., Ndiaye D., & Sabaté J.P., (2015). Pyrethroids: Exposure and health effects – An update. *Int J Hyg Environ. Health, 218*, 281-292.

Mohsin, Sayed. Mohammad., Hasanuzzaman M., Parvin K., Morokuma M., & Fujita M. (2021). Effect of tebuconazole and trifloxystrobin on *Ceratocystis fimbriata* to control black rot of sweet potato: processes of reactive oxygen species generation and antioxidant defense responses. *World J. Microbiol. Biotechnol*. *37*(9), 148. Doi: 10.1007/s11274-021-03111-5.

Sbartai, I., &, Sbartai, H. (2020). Antioxidant activities and lipid peroxidation in the freshwater bioindicator *Paramecium sp*. exposed to hydrazine carboxylate (Bifenazate). *Egypt. J. Aquat. Biol. Fish*, *25*(1), 257-268. https://dx.doi.org/10.21608/ejabf.2021.156670.

Serra, A.A., Couée, I., Renault, D., Gouesbet, G., & Sulmon, C. (2015). Metabolic profiling of *Lolium perenne* shows functional integration of metabolic responses to diverse subtoxic conditions of chemical stress. *J Exp Bot*. *66*(7), 1801-16. Doi: 10.1093/jxb/eru518.

Serra, A.A., Nuttens, A., Larvor, V., Renault, D., Couée, I., Sulmon, C., & Gouesbet, G. (2013). Low environmentally relevant levels of bioactive xenobiotics and associated degradation products cause cryptic perturbations of metabolism and molecular stress responses in *Arabidopsis thaliana*. *J Exp Bot*. *64*(10), 2753-66. Doi: 10.1093/jxb/ert119.

Shen, D., Dalton, T.P., Nebert, D.W., & Shertzer, H.G. (2005). Glutathione redox state regulates mitochondrial reactive oxygen production. *J Biol Chem*, *280*, 25305-12.

Shi, J. J., & Sun, W. (2011). Effect of benzotriazole as corrosion inhibitor for reinforcing steel in cement mortar. *Acta Physico-Chimica Sinica*, *27*(6), 1457-1466.

Shishatskaya E, Menzyanova N, Zhila N, Prudnikova S, Volova T, & Thomas S. (2018). Toxic effects of the fungicide tebuconazole on the root system of *Fusarium*-infected wheat plants. *Plant Physiol Biochem*. *132*, 400-407. Doi: 10.1016/j.plaphy.2018.09.025.

Sies H. (1993). Strategies of antioxidant defenses. *Eur J Bio-chem*., *215*, 213–219. Doi:10.1111/j.1432-1033.1993.tb18025.x.

TianhuiJiao, M.d., Mehedi, H., Jiaji, Zhu., Shujat, A., Waqas, A., Jingjing W., Changxin, L.V, Quansheng, Chen, & Huanhuan Li, (2021)**.** Quantification of deltamethrin residues in wheat by Ag@ZnO NFs-based surface-enhanced Raman spectroscopy coupling chemometric models. *Food Chem, 337*, 127652. Doi:10.1016/j.foodchem.2020.127652.

Toscano, N. C., Sances, F. V., Johnson, M. W., & LaPre, L. F. (1982). Effect of various pesticides on lettuce physiology and yield. *J. Econ. Entomol*, *75*(4), 738-741.

Untiedt, R., & Blanke, M. (2001). Effects of fruit thinning agents on apple tree canopy photosynthesis and dark respiration. *Plant Growth Regul*. *35*, 1–9.

Van der Oost, R., Beyer, J., & Vermeulen, N. P. (2003). Fish bioaccumulation and biomarkers in environmental risk assessment: a review. *Environ. Toxicol. Pharmacol*, *13*(2), 57-149. Doi:10.1016/S1382-6689(02)00126-6.

Wandscheer, A. C., Marchesan, E., Santos, S., Zanella, R., Silva, M. F., Londero, G. P., & Donato, G. (2017). Richness and density of aquatic benthic macroinvertebrates after exposure to fungicides and insecticides in rice paddy fields. *Anais da Academia Brasileira de Ciências*, *89*, 355-369. Doi: 10.1590/0001-3765201720160574.

Wang, Y., Ren, Y., Ning, X., Li, G., & Sang, N. (2023). Environmental exposure to triazole fungicide causes left-right asymmetry defects and contributes to abnormal heart development in zebrafish embryos by activating PPARγ-coupled Wnt/β-catenin signaling pathway. *Sci Total Environ*, *859*, 160286. Doi: 10.1016/j.scitotenv.2022.160286.

Weckbecker, G., & Cory, J. G. (1988). Ribonucleotide reductase activity and growth of glutathione depleted mouse leukemia L1210 cells in vitro. *Cancer Lett*, *40*(3), 257-264. Doi:10.1016/0304-3835(88)90084-5.

Wolansky, M. J., & Tornero-Velez, R. (2013). Critical consideration of the multiplicity of experimental and organismic determinants of pyrethroid neurotoxicity: A proof of concept. *J. Toxicol. Environ. Health, Part B*, *16*(8), 453-490. Doi: 10.1080/10937404.2013.853607.

Xiao, N., Jing B., Ge F., & Liu X, (2006). The fate of herbicide acetochlor and its toxicity to *Eisenia fetida* under laboratory conditions. *Chemosphere* 62, 1366-1373. Doi: 10.1016/j.chemosphere.2005.07.043.

Xiao, W., & Loscalzo, J, (2019). Metabolic Responses to Reductive Stress. *Antioxidants and Redox Signaling*, *32*(18), 1330–1347. Doi: 10.1089/ars.2019.7803

Yan, L.J. (2014). Pathogenesis of chronic hyperglycemia: from reductive stress to oxidative stress. *J Diabetes Res,* 137919.

Yang, J. M., Zhu, C. Z., Tang, X. Y., & Shi, M. (2014). Rhodium (II)-Catalyzed Intramolecular Annulation of 1-Sulfonyl-1, 2, 3-Triazoles with Pyrrole and Indole Rings: Facile Synthesis of N-Bridgehead Azepine Skeletons. *Angew. Chem. Int. Ed*, *53*(20), 5142-5146. Doi: 10.1002/anie.201400881.

Zhang, C., Wang, Q., Zhang, B., Zhang, F., Liu, P., Zhou, S., & Liu, X. (2020). Hormonal and enzymatic responses of maize seedlings to chilling stress as affected by triazoles seed treatments. *Plant Physiol Biochem*. *148*, 220-227. Doi: 10.1016/j.plaphy.2020.01.017.

Potential innovations from the application of beneficial soil microbes to promote sustainable crop production

Chinenyenwa Fortune Chukwuneme[1], Ayansina Segun Ayangbenro[2], Vittori Venturi[3,4], Bernard R. Glick[5] and Olubukola Oluranti Babalola[2]✉

[1]Cell Biology and Regeneration Unit, Department of Natural Sciences, Faculty of Applied and Computer Sciences, Vaal University of Technology, Vanderbijlpark, 1900, Gauteng, South Africa; [2]Food Security and Safety Focus Area, Faculty of Natural and Agricultural Sciences, North-West University, Private Bag, X2046, Mmabatho 2735, South Africa; [3]International Centre for Genetic Engineering and Biotechnology, Trieste, Italy; [4]African Genome Center, University Mohammed VI Polytechnic (UM6P), Ben Guerir, Morocco; [5]Department of Biology, University of Waterloo, Waterloo, ON N2L 3G1, Canada
✉***Corresponding author, E-mail:*** *Olubukola.babalola@nwu.ac.za*

Abstract. Crop productivity may be significantly inhibited by factors, such as increased temperature, soil erosion, pathogen and pest attacks, and drought and salt stresses, mostly resulting from global climate change. However, microorganisms that are found in the rhizosphere can aid in the mobilization of essential soil nutrients, facilitate plant growth, and reduce abiotic and biotic stresses of plants. Soil microbes accomplish these beneficial functions via several mechanisms. Here, an elaborate description of the molecular mechanisms of plant growth-promotion by soil microbes and the potential of these organisms to be used as biofertilizers and biopesticides to improve plant health is provided. In addition, the possible revolution that could be realized by the synergism of these beneficial microbes with nanotechnology is discussed. While the use of biofertilizers to enhance plant growth has been demonstrated to be a beneficial phenomenon, this approach has often failed to yield the desired result in field applications. However, identifying microbial species with beneficial attributes and combining them with nanotechnology tools like nanoencapsulation and biosensors could lead to the formulation of important agriproducts (nanobiopesticides and nanobiofertilizers) that will ensure sustained

delivery of the agriproducts and facilitate early detection and proper management of plant pests and diseases. It is anticipated that precision farming will improve agricultural sustainability by increasing crop production for the steadily increasing world population.

Introduction

The world population continues to increase with predictions that it will reach 8 billion by 2025 and up to 9 billion by 2050, requiring a large increase in food production to meet the nutritional demand of the growing population (Mc-Carthy *et al.*, 2018; Meybeck *et al.*, 2018; Tripathi *et al.*, 2019). Modern agriculture is challenged with inadequate/insufficient supply of nutrients for plant growth, insects and pest attacks, and drought and salt stresses. Another important issue affecting agricultural productivity is soil erosion in which nutrients from topsoil are washed into deeper soil layers. Also, the contamination of soils by heavy metals and chemicals from the excessive use of synthetic fertilizers, which eventually end up in water bodies, makes it difficult to access good drinking water (Mc-Carthy *et al.*, 2018; Osman, 2018). Ironically, in an effort to increase agricultural productivity, farmers have resorted to the excessive use of synthetic fertilizers to boost the nutrient composition of soils (Shabbir *et al.*, 2019).

To ensure the maintenance of sustainable agriculture, an increase in crop productivity is necessary. This can be achieved by the provision of0 essential nutrients, including nitrogen (N), phosphorus (P), and potassium (K) in the soil for plant use. Furthermore, certain traits like better nutritional value, drought and salt tolerance, disease resistance, and heavy metal resistance are required by food crops to boost their productivity. Sustainable agriculture is achievable because certain soil microbial communities, often known as plant growth-promoting microbes (PGPM), assist plants in making the afore-mentioned attributes available for plant use. The consequences of using soil microbial biomass are an increase in water use efficiency as well as the nutrient uptake capacity of plants (Schütz *et al.*, 2018). These microbial communities colonize the plant rhizosphere and favor plant growth. They are also essential in the improvement of plant growth, health, and yield without contaminating the environment (Odelade & Babalola, 2019).

The past few decades have seen the application and commercialization of some plant growth-promoting bacteria (PGPB) strains, including those of *Bacillus*, *Streptomyces*, *Pseudomonas*, *Klebsiella*, *Serratia*, *Azotobacter*, *Enterobacter*, *Variovorax,* and *Azospirillum* as biofertilizers (Alori & Babalola, 2018; Reed *et al*., 2013). Certain fungi, including arbuscular mycorrhizal fungi (AMF), *Trichoderma* (*T. viride*, *T. harzianum*, *T. polysporum*, and *T. koningii*), *Aspergillus niger, A. fumigatus, Saccharomyces* sp. and algae (microalgae) have also been used as biofertilizers for improvement in crop growth (Abbey *et al*., 2019; Kamal *et al*., 2018; Win *et al*., 2018). Despite this progress, their universal application in the agricultural sector represents only a very small fraction of agricultural practice because of the inconsistency in the growth of plants following inoculation with PGPM (Mącik *et al*., 2020). To effectively enhance plant growth, PGPM must be environmentally friendly, exhibit high rhizosphere competence, interact well with other rhizosphere microbes, and tolerate environmental conditions like oxidizing agents, UV radiation, and heat (Alori & Babalola, 2018; Babalola, 2010). To facilitate a large increase in agricultural yield and food production PGPM possessing the above-mentioned qualities are greatly needed.

Recent advancements in PGPM formulations have incorporated technologies such as biosensors and nanoencapsulation, which are essential for developing biofertilizers and biopesticides (Gouda *et al*., 2018). The incorporation of microbes with plant growth-promoting traits and nanotechnology in the development of new formulations of biofertilizers can both promote crop productivity and enhance agricultural sustainability. This review discussed the various strategies employed by PGPM to enhance plant growth, improve soil fertility, and control agricultural pests. It also explored the innovative agricultural products that nanobiotechnology can introduce, which will increase crop production and promote agricultural sustainability in a changing climate.

Importance of soil microbes on plant growth and health

The rhizosphere microbiome, defined as the entire genome of the microbial communities in the roots surrounding soils, performs important roles in plants including facilitating the production of metabolites, uptake of nutrients, as well as tolerance to both abiotic and biotic stresses (Chukwuneme *et al*., 2020). Plants living within an ecosystem exist as colonies, rather than as individual entities. They live along with the plant microbiota (bacteria, fungi, viruses, protists, nematodes), working together to influence plant growth and productivity (Glick & Gamalero, 2021). The current methods of culturing microbes have only been able to culture about 1% of microorganisms in the soil, thereby underestimating

the microbial diversity of rhizosphere and soil microbiomes (Devi & Soni, 2020). The rhizosphere microbiome is composed of beneficial microorganisms, including the free-living bacteria that facilitate plant growth known as plant growth-promoting bacteria, the nitrogen fixers, biocontrol agents, and the mycorrhizal fungi (Ajilogba et al., 2013; Gouda et al., 2018). This microbial habitat is also inhabited by microbes that exert deleterious effects on plant growth, i.e., pathogenic microbes (Orozco-Mosqueda et al., 2018). The use of modern sequencing technologies has expedited the identification of a large number of soil microbes, most importantly, bacteria dwelling in the rhizosphere plant microbiome (Mohanram & Kumar, 2019). The rhizosphere microbiome is dominated by Proteobacteria, Firmicutes, Bacteroidetes, Acidobacteria, Actinobacteria, Planctomycetes, Chloroflexi, Verrucomicrobia, Cyanobacteria, Gemmatimonadetes, Ascomycota, Basidiomycota, Glomeromycota and ectomycorrhizal fungi (Trivedi et al., 2020). The interactions between plant roots and the rhizosphere microbes enable plants to cope with environmental disturbances by identifying and reacting to external stimuli, leading to specific modifications in plant growth and development (Mohanram & Kumar, 2019). Plant health is highly reliant on the ecological services of microbes that act in association with the plant, which includes protecting the plant against disease pathogens, tolerance to environmental stresses and biofertilization.

Soil microbiome aiding in plant nutrient acquisition

In recent studies, nitrogen-fixing free-living rhizospheric and endophytic microbes of the genera *Azotobacter*, *Azospirillum*, *Achromobacter*, *Bradyrhizobium*, *Pseudomonas*, *Burkholderia*, *Bacillus*, Mycorrhizal fungi, *Trichoderma*, and *Aspergillus* have shown positive effects on crops by increasing above and below ground biomasses (Abbey et al., 2019; Igiehon & Babalola, 2018a; Igiehon & Babalola, 2018b; Kamal et al., 2018). The soil microbiome also consists of several microbes that aid in the solubilization of inorganic phosphates for plant use (Babalola, 2010). These microbes include those from the bacterial genera *Aerobacter*, *Alcaligenes*, *Pseudomonas*, and *Bacillus* and those from the fungi genera *Fusarium*, *Penicillium*, *Chaetomium*, *Aspergillus*, and *Cephalosporium* (Moharana et al., 2018). In the soil, inorganic phosphates are often complexed with metal ions including Fe^{3+}, Al^{3+}, and Ca^{2+} and can be solubilized into hydroxyl ions (OH^-) or organic acids released by phosphate solubilizing bacteria (Etesami et al., 2021; Mohanram & Kumar, 2019). Phosphate solubilizing microbes often secrete various phosphatase enzymes that aid in mineralizing organic P from the soil. In addition, they secrete protons and organic acid anions like malate, citrate, and oxalate that assists in solubilizing inorganic P (Moharana et al., 2018).

Rijavec and Lapanje (2016) proposed that hydrogen cyanide (HCN) increases the availability of P indirectly by metal chelation.

Some microbes in the rhizosphere microbiome with sequestrating capabilities participate in the uptake of trace elements like zinc (Zn) and Fe, whose low concentration in the soil may result in a decrease in crop yields (Kumar *et al.*, 2017). An abundance of Fe exists in the soil. However, the majority of this nutrient occurs in forms that are not readily accessible to plants. Rhizosphere bacteria like *Plantibacter*, *Streptomyces*, *Pseudomonas*, *Curtobacterium,* and *Stenotrophomonas* have been shown to mobilize Zn by acidifying the medium through the production of gluconic acid (Costerousse *et al.*, 2018). Their roles also include the release of organic acid anions known as siderophores that chelate and transport ferric ion (Fe^{3+}) to plant cell surfaces, where they are reduced to ferrous ion (Fe^{2+}) (Sabur, 2019). Siderophores also act to deprive pathogenic microbes of Fe, thereby curtailing their growth (Babalola, 2010). Some common microbial siderophores include pyoverdine, achromobactin, citrate, ferrioxamines, pyochelin, enterobactin, ferrichromes, and yersiniabactin (Aznar & Dellagi, 2015). The promotion of iron nutrition through siderophores has been successful in dicotyledonous and gramineous plant species by fluorescent Pseudomonads (Orr & Nelson, 2018). It has also been shown that certain Zn mobilizing bacterial strains increase the uptake of Zn by plants, and as a consequence increase the yields of many crops like wheat, soybean (Bhatt & Maheshwari, 2020), and rice (Vaid *et al.*, 2020). The mechanisms used by these bacteria in the mobilization of Zn in the root microbiome of plants are not especially clear. However, their mode of action is analogous to the phosphate solubilizing microbes and Fe mobilizers, which include the use of organic acids and chelating agents.

Plant growth-promoting microbes can reduce the inorganic fertilizer requirement of various plants by facilitating nutrient acquisition. The study of Ye *et al.* (2020) demonstrated that 75% of inorganic fertilizer application combined with bioorganic fertilizer increased the yields of tomato plants to the same extent as those plants treated with 100% inorganic fertilizer application. In another study, soil nutrient status and the growth of wheat plants were improved by the combined application of bacterial consortia with 75% of the (previously determined) optimal amount of chemical fertilizer (Wang *et al.*, 2020). The results showed that inoculation of wheat plants with bacterial consortia resulted in increased N, P, and K contents by 97.7, 96.4, and 42.1%, respectively. According to the authors, plant height, fresh and dry weight, tiller counts, and N, P, and K contents of soils were the same in the treatment with combined PGPB and 75% fertilizer and that with 100% fertilizer treatment.

Similarly, the combination of nitrogen-fixing and phosphate-solubilizing bacterial strains with a half dose of urea (nitrogen) and di-ammonium phosphate (DAP, phosphorus) fertilizers enhanced the growth and yield of *Brassica juncea* plants (Maheshwari *et al.*, 2010). Also, the addition of urea and DAP granules with a mixture of *Bacillus* sp. KAP6 slurry and compost improved the nutrient use efficiency (NUE), photosynthetic rate, growth, and yield of wheat (Ahmad *et al.*, 2017). Moreover, the nutritional quality of organic fertilizers, such as farmyard manure and composts, can be improved by inoculation with beneficial microbial strains. For instance, the application of an integrated organo-mineral fertilizer composed of farmyard manure and compost, inoculated with a microbial consortium consisting of several phosphorus-solubilizing bacteria, i.e., *Azotobacter*, and *Rhizobium* sp., in soybean and fenugreek fields resulted in increased nutrient content, yield, and biomass of the plants (Biswas & Anusuya, 2014). The combined application of biogas slurry, humic acid, arbuscular mycorrhizal fungi (AMF), *B. ciculans*, and *Azotobacter chrocoocum* on maize seeds resulted in increased growth, yield, and nutrient uptake of the plants as well as increased microbial activity by improving the levels of mycorrhizal colonization, increasing the dehydrogenase and phosphatase enzymes, and bacterial count (Gao *et al.*, 2020).

Plant productivity enhancement is another function of the rhizosphere microbiome. The organisms in the plant rhizosphere help to decompose organic matter, which eventually results in a positive increment in soil fertility. Some bacterial species, including *Cellulomonas* sp., *Sporocytophaga* sp., *Pseudomonas* sp., *Streptomyces* sp., *Cytophaga* sp., and *Chryseobacterium gleum*, can degrade plant biomass and, as a result, release nutrients for plants to absorb (Ahmed *et al.*, 2018). Thus, rhizosphere microbes can facilitate plant growth even in soils with inadequate nutrients.

Signaling events in the plant microbiome

Soil microbiome and production of plant hormones

The major drivers in the regulation of plant growth and development are phytohormones, which also participate in molecular signaling in reaction to abiotic conditions that either curtail plant growth or develop into poisonous substances when uncontrolled (Caddell *et al.*, 2019). Several microbes have been recognized to release hormones for uptake by plant roots. Several other groups have been manipulated in such a way as to maintain hormonal balance in plants for growth promotion and stress response. Many PGPM are capable of producing auxins that strongly promote root architecture and growth (Duca *et al.*, 2014; Kour *et al.*, 2019; Subrahmanyam *et al.*, 2020). Indole-3-acetic acid (IAA) is

the most widely used and studied auxin produced by PGPM (Afzal *et al.*, 2015). The role played by external IAA depends on the levels of internal IAA in plants. Therefore, when the IAA concentration in plants is high, the application of microbial IAA may cause positive, negative, or even neutral effects on plant growth (Wenz *et al.*, 2019). In a study, auxin-producing PGPB were reported to induce transcriptional changes in defense, hormone biosynthesis, and genes that were related to the cell wall of the plant (Kandaswamy *et al.*, 2019). These organisms have also been reported to induce longer roots (Tsukanova *et al.*, 2017), increase root weight, and reduce stomatal density and size (Llorente *et al.*, 2016). They also aid in the activation of genes involved in auxin response that enhance plant growth (Ruzzi & Aroca, 2015).

Moreover, in salt affected soils, the application of halotolerant PGPM typically give a much improved stimulatory effect, because they produce higher IAA under salinity conditions to significantly facilitate the growth of plants (Zhao *et al.*, 2016). Furthermore, Fukami *et al.* (2018) showed that through leaf spraying of hormonal mixtures of bacterial cultures of *A. brasilense* maize growth could be improved. A study by Zhou *et al.* (2017) demonstrated that the microbial strains *Planococcus rifietoensis*, *Micrococcus yunnanensis*, and *Variovorax paradoxus*, with multiple PGP capabilities isolated from halophytes planted in high salt environments, improved the tolerance of sugar beet plants exposed to salt stress by improving the plant photosynthetic capability, seed germination, and biomass. The inoculation of halotolerant IAA-producing bacterial strains, *Brachybacterium saurashtrense* strain JG-06, *Brevibacterium casei* strain JG-08, and *Haererohalobacter* strain JG-11 from *Salicornia brachiata* improved *Arachis hypogaea* growth under salt stress by increasing root and shoot length, dry root and shoot weight, total biomass, and plant height (Zhou *et al.*, 2017). The results of these experiments indicated the presence of reduced proline and soluble sugar contents as well as enhanced amino acid, auxin, and total protein content in inoculated *Arachis hypogaea* plants compared to uninoculated plants under salt stressed conditions (Zhou *et al.*, 2017).

Several PGPM have been reported to produce the phytohormones, gibberellins, and cytokinins (Backer *et al.*, 2018; Gupta *et al.*, 2015), even though their mechanisms of production and synthesis are still poorly understood (Frankenberger Jr & Arshad, 2020). Plant growth-promoting microbes can support the production of large amounts of gibberellins, resulting in improved shoot growth in plants (Gouda *et al.*, 2018). These hormones can alter the architecture of plant roots by interacting with auxins (Gouda *et al.*, 2018). The production of root exudates by plants could also be a result of cytokinin production by PGPM, which significantly increases the plant-associated microbial communities (Olanrewaju *et al.*, 2019).

Another plant hormone whose level is modulated by PGPM is ethylene. This hormone is gaseous, often active at concentrations of about 0.05 ml per liter. This stress hormone is often activated when plants are exposed to either abiotic or biotic stress. Ethylene buildup as a consequence of stress may either contribute to an increase in plant tolerance to stress (low levels of ethylene) or aggravate the stress reaction symptoms and aging in plants (high levels of ethylene) (Backer *et al.*, 2018). The function of ethylene production by PGPM has been examined in both stressed and unstressed environments, while most of the studies have reported the stimulation of plant growth to a greater extent under stressed conditions, such as salt stress and water deficit (Forni *et al.*, 2017; Gepstein & Glick, 2013; Rubin *et al.*, 2017). Some PGPM in the plant rhizosphere produce the enzyme, 1-aminocyclopropane-1-carboxylase (ACC) deaminase, which decreases the production of ethylene in plants (Bakka & Challabathula, 2020; Glick *et al.*, 2007). Numerous studies have reported improved tolerance to abiotic and biotic stresses by inoculating plants with ACC deaminase producing PGPM. This group of microorganisms helps to regulate plant ethylene levels, so as not to get to the levels where they become unfavorable to plant growth (Afridi *et al.*, 2019; Khan *et al.*, 2020).

Soil microbes and the production of volatile organic compounds (VOCs) and secondary metabolites

Some plant-associate microorganisms produce various secondary metabolites and VOCs that can increase plant growth and their ability to withstand stress. For example, polyamines are essential for modifying the physiological properties of plants and providing defense against environmental stressors. The bacterium, *B. megaterium* BOFC15 releases the polyamine spermidine, which causes the production of polyamine in the plant *Arabidopsis*, bringing about an increase in biomass production, higher photosynthetic capacity, and a change in the root architecture. The results obtained showed that the addition of polyethylene glycol (PEG) induced water-deficit conditions, the inoculated plants displayed greater tolerance to drought stress and abscisic acid (ABA) content (Zhou *et al.*, 2016). Hydrogen cyanide production by some PGPM facilitates the control of pathogenic microbes in the rhizosphere (Suresh & Abraham, 2019). The production of VOCs by PGPM may enhance plant growth by increasing shoot biomass and improving stress resistance in plants (Etesami, 2020).

Soil microbes and quorum sensing (QS) molecules

Often, the interactions in the plant rhizosphere occur when plants communicate with microbes in the form of signals to recruit beneficial organisms for their growth and maintenance. In this regard, the plants release roots exudates

consisting of a carbon source, which only the microbes of interest can recognize and respond to. The secretion of root exudates in the plant rhizosphere enables the plant to have control over its inhabiting microbes (Berendsen *et al.*, 2012). Also, the tunable and diverse nature of the chemical composition of plant root exudates help plants to select and recruit the microbes they desire. Quorum sensing (QS), also known as auto-inducers is a form of inter- and intra-species signaling in the rhizosphere that allows soil microbes to communicate and interact with one another by the detection, production, and release of chemical signals (Bukhat *et al.*, 2020; Seneviratne *et al.*, 2017).

Cell to cell communication via QS occurs when PGPM colonize plant roots after receiving a cognate signal. This interaction is subsequently accompanied by alteration of gene expression due to the density of the microbial communities (Helman & Chernin, 2015; Hong *et al.*, 2012). The QS signals control several microbial phenotypes including rhizosphere competence, virulence, the production of secondary metabolites and hydrolytic enzymes, conjugation, biofilm formation, adhesion, motility, coordination of microbial activities in the rhizosphere, and microbial population density (An *et al.*, 2014; Chu *et al.*, 2011).

Recently, plants have started to respond to QS signal molecules used by soil microbes. Plant growth can be enhanced as a result of the release of QS signal molecules, which alters both plants immune responses as well as hormone profiles (Hartmann *et al.*, 2014). One of the key signaling molecules used for communication among microbes for QS are the *N*-Acyl homoserine lactones (AHLs). Many soil organisms have been reported to produce and respond to QS signaling molecules including those from the bacterial genera: *Pseudomonas, Bacillus, Burkholderia, Ochrobacterium, Ralstonia, Erwinia,* and *Serratia* (Imran *et al.*, 2014; Li *et al.*, 2015). Studies have reported the roles of AHLs in promoting the growth of plant species including *Hordeum vulgare, Vigna radiata, Medicago truncatula,* and *Arabidopsis thaliana*. In these plant species, AHLs were reported to have enhanced the formation of root hairs and adventitious roots, root branching, number of nodules, and lateral root hair primordia, and also induced lateral root growth and elongation of roots (Chagas *et al.*, 2018; Ortíz-Castro *et al.*, 2009; Ortiz-Castro & López-Bucio, 2019; Rosier *et al.*, 2018). Furthermore, AHLs may increase a plant's ability to obtain water and nutrients from soil by improving transpiration rates and stomatal conductance (Ortíz-Castro *et al.*, 2009). *N*-Acyl homoserine lactones also regulate gene expression responsible for stress response, regulation of metabolism, the development of roots, balancing of hormones, stimulation of plant defense, and activation of host symbiotic interactions (Ali *et al.*, 2016; Hassan *et al.*, 2016; Imran *et al.*, 2014; Schikora *et al.*, 2016). Another important type of QS signaling molecule is the diffusible-signal factor (DSF; also known as cis2 unsaturated fatty acids) that is produced by

certain Gram-negative bacteria including *Burkholderia* sp. and *Stenotrophomona smaltophilia* (Ryan *et al.*, 2015). Antibiotics are also important QS signaling molecules produced by bacteria that may play significant roles in inter and intra-species signaling at very low and non-inhibitory concentrations (Andersson & Hughes, 2014). The various mechanisms of plant growth enhancement by PGPM are illustrated in Fig. 1.

Improvement of stress tolerance by PGPM

Conventional means of imparting stress tolerance in plants including genetic engineering and breeding have major drawbacks. For instance, the process of breeding requires the allocation of huge capital and time. On the other hand, the issue of public acceptance in some countries (especially in Europe) limits the process of genetic engineering. This has resulted in increased importance in the role played by beneficial microbes in the management of plant stress as well as in the development of climate-resilient agriculture.
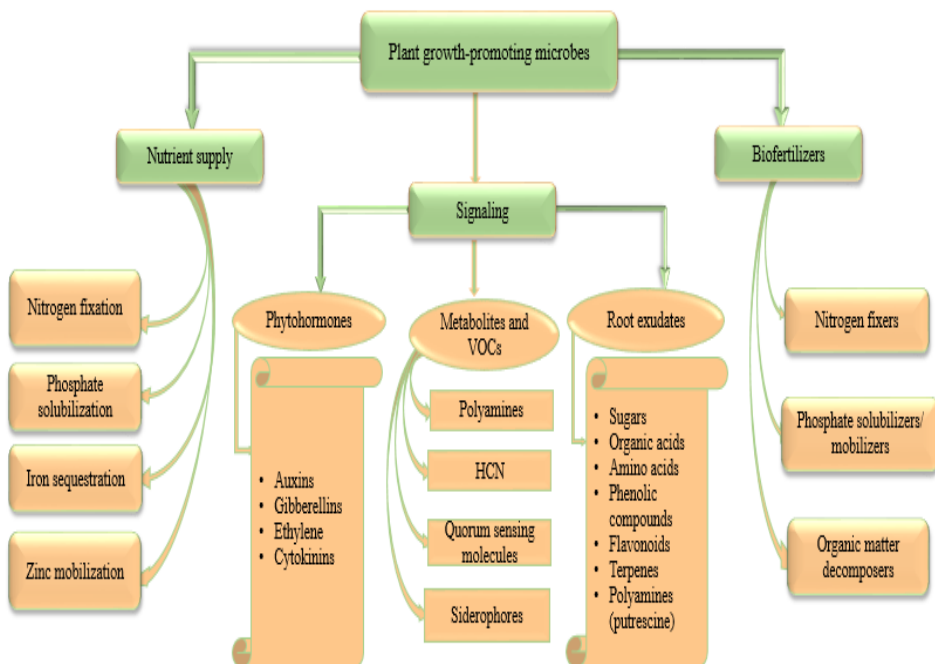
Figure 1. Mechanisms of growth enhancement by plant growth-promoting microbes.

Abiotic stress responses in the rhizosphere microbiome

The potential of soil microbes to mitigate abiotic stressor of plants have been highlighted in many studies. Prudent *et al.* (2015) reported that the use of the small peptide bacteriocin thuricin 17 produced by the bacterium *B. thuringiensis* NEB17 on soybean plants under drought-stressed conditions led to an adjustment in the root structures, increased biomass of the plant's roots and nodules, total nitrogen content, root ABA, and root length. The findings of Chukwuneme *et al.* (2020) on drought tolerance confirmed an improvement in plant dry root and shoot weights, root and shoot length, number of leaves, and the chlorophyll contents of plants inoculated with *S. pseudovenezuelae* and *A. arilaitensis* compared to uninoculated plants. Plants can also cope with flooding stress through the help of beneficial microbes. The ACC deaminase producing *Streptomyces* sp. GMKU 336 inoculated in mung bean (*Vigna radiata*) plant led to increases in plant height, biomass, adventitious roots, leaf area, chlorophyll content, leaf color, and also decreased the plant ethylene level under conditions of flood (Jaemsaeng *et al.*, 2018). Moreover, salt stress in plants can be managed by the activity of ACC deaminase (Cheng *et al.*, 2007; Mayak *et al.*, 2004). Under *in vitro* and greenhouse conditions, the ACC deaminase producing *Bacillus* strains, *Bacillus safensis* NBRI 12 M*, B. subtilis* NBRI 33 N, and *B. subtilis* NBRI 28B enhanced tolerance to salt stress by decreasing the level of stress ethylene in maize plants (Misra & Chauhan, 2020).

Host immunity and protection of plants from pathogens

Many soil microbes have biocontrol effects on plants protecting them from pathogen attacks. They do this by competing for space and nutrients and by producing hydrolytic enzymes or antibiotics (Glick, 2020; Verma *et al.*, 2019). These microbes produce antimicrobial metabolites, such as butyrolactones, ammonia, olygomycin A, pyoluterin, phenazine-1-carboxylic acid (PCA), pyrrolnitrin, etc. (Mohanram & Kumar, 2019; Patel *et al.*, 2020). In a study by Meyer *et al.* (2016), it was found that *P. fluorescens* suppressed the soil pathogens *Fusarium oxysporum* and *Meloidogyne incognita* by producing the antibiotic 2,4,-diacetylphloroglucinol (DAPG). Several rhizosphere microbes with biocontrol ability produce multiple antibiotics with differing magnitudes of antimicrobial activity. Fluorescent *Pseudomonas* strains isolated from plant roots, identified as *Pseudomonas protegens* and *P. chlororaphis*, exhibited the presence of multiple antibiotics biosynthetic genes (Someya *et al.*, 2020). From the above-mentioned study, 4 antibiotic genes were observed in *P. protegens,* including genes encoding hydrogen cyanide (HCN), pyoluteorin, pyrrolnitrin, and 2,4-diacetylphloroglucinol whereas, 3 antibiotic genes, including those encoding pyrrolnitrin, HCN, and

phenazine, were found in *Pseudomonas chlororaphis*. These bacterial strains observed to have antibiotics biosynthesis genes also exhibited antimicrobial activity against the fungal pathogen *Rhizoctonia solani* that caused damping-off disease in cabbage plants. The spray application of chitinase and β-1-3-glucanse-producing microbial consortia (*Penicillium* sp. *B. subtilis* and *B. velezensis*) around the rhizosphere of banana plantlets under greenhouse conditions resulted in 60% reduction in disease severity of both *Alternaria* sp. and *F. oxysporum* (Win *et al*., 2021).

An experiment with different *B. amyloliquefaciens* strains showed an increase in the production of fengycins and iturins (both antimicrobial lipopeptides) as a response mechanism to the plant pathogens, *Botrytis cinerea* and *F. oxysporum* (Cawoy *et al*., 2015). The production, *in situ,* of secondary metabolites by *B. amyloliquefaciens* FZB42 in the lettuce rhizosphere revealed the presence of the lipopolypetides surfactin, bacillomycin D, and fengycin that acted against *Rhizoctania solani* (Chowdhury *et al*., 2015)*.* The study reported an increased production of bacillomycin and surfactin by the bacterium in the presence of *R. solani,* which was attributed to the effect of antibiosis and the recognition of the FZB42 response to fungal attack. In addition, some rhizosphere bacteria known as bacterial iron chelators are capable of restricting the growth of pathogenic microbes by sequestering the available iron in the soil, thereby making iron less available to pathogenic microbes*.* Zhu *et al*. (2020) reported that the siderophore-producing *B. substilis* IBCBF-4 significantly controlled the proliferation of the fungal infection, *Fusarium wilt* of watermelon plants, caused by the pathogen *F. oxysporum*.

Certain microorganisms are capable of reducing diseases in plants by the activation of a resistance mechanism known as microbial-mediated induced systemic resistance (ISR). These microbes can protect plants from pathogenic attacks by triggering molecular and biochemical defense responses inside the plant (Khan *et al*., 2019). The elicitation of ISR by PGPM is capable of activating the genes associated with pathogenesis, which are controlled by phytohormone signaling pathways as well as proteins that attack plant pathogens (NA *et al*., 2020; Wilkinson *et al*., 2019). Microbe-associated molecular elicitors and signal compounds from bacteria, including chitin oligomers, have been reported to regulate the induction of ISR in plants. The cell-surface factors of pathogens like the O-antigen of lipopolysaccharides and flagellins trigger ISR while the analogs of jasmonic and salicylic acids are responsible for triggering ethylene to stimulate non-expresser pathogenesis-related gene 1 (NPR1) that controls systemic acquired resistance (SAR) in plants (Nadarajah, 2017). A graphical representation of the different methods of stress tolerance in plants facilitated by PGPR is shown in Fig. 2.
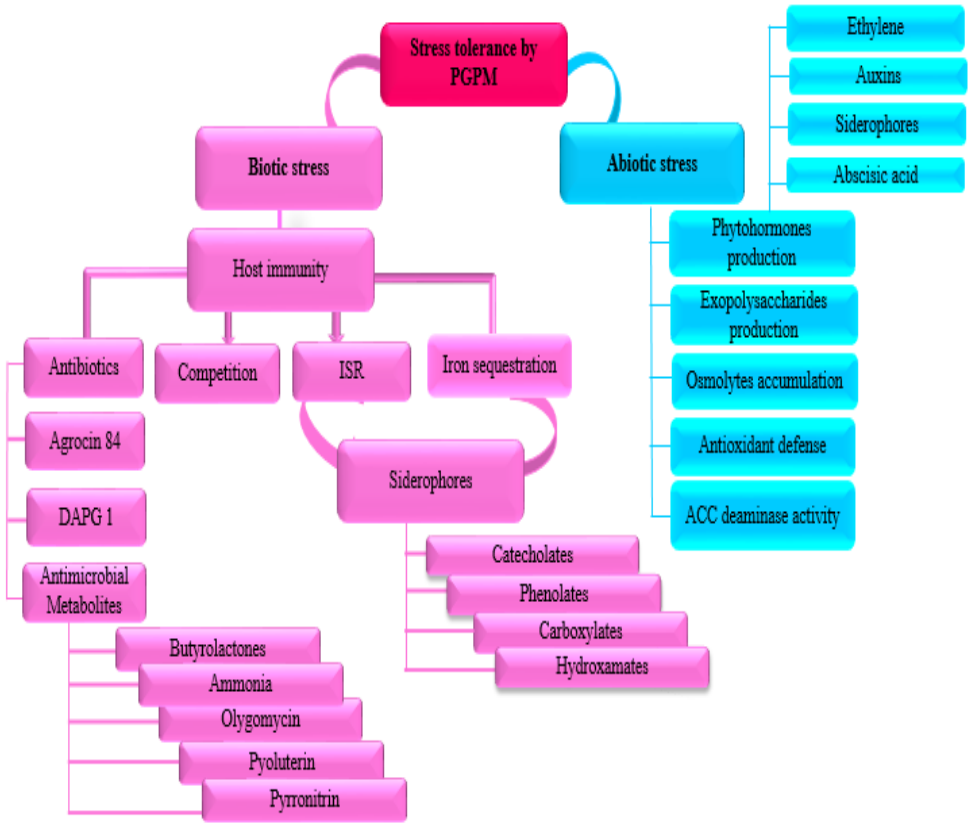
Figure 2. Methods of plant stress tolerance by plant growth-promoting microbes.

Precision agriculture by incorporating PGPM and nanotechnology

Although significant progress has been made in agricultural sector in recent decades, the sector continues to face multiple challenges regarding food crop production sufficient for the constantly increasing world population. Climate change has contributed to a decrease in agricultural products due to increased evapotranspiration rates, temperatures, rainfall intensity, drought, and spread of plant diseases. Plant growth-promoting microbes has successfully been applied as inoculants to boost crop production. However, effective crop improvement by PGPM is determined by factors, such as weather conditions, climate, soil characteristics, and microbial activities in bulk soils (Mukherjee,

63

2019). Moreover, the effectiveness of PGPM in promoting plant growth can be limited by disease infestation, weeds, and herbicide application. Recent advancements in agriculture have involved the development and use of modern technologies, such as biosensors, nanomaterials, and nanofertilizers. Nanotchnology has achieved great success in various scientifc fields, including chemistry, material sciences, physics, medicine, and pharmacy. Considering these achievements, nanotechnology has the potential to improve agriculture and aid in the realization of precision agriculture. Therefore, integrating PGPM with nanotechnolgoy can help to achieve a greater agricultural productivity and address some of the most persistent challenges facing agriculture.

Nanotechnology in biofertilizers production

Success in the application of biofertilizers in agriculture depends on how they were prepared, the method used in the application process, and the storage system used (Duhan *et al.*, 2017). The major pitfall of fertilizers of microbial origins is inconsistency in their performances when applied to different fields, whereas, factors such as sensitivity to temperature, short shelf-life, storage, and dehydration can dramatically affect the field performance of biofertilizers. The use of polymeric nanoparticles as coats on prepared biofertilizers to produce biofertilizer formulations that are desiccation-resistant has been reported (Eleni & Krokida, 2017). An example is a water-in-oil emulsion, a method that is used to disperse and distribute microbes in liquid formulations to the intended sites (Acharya & Pal, 2020). This method helps microbes that dehydrate easily and thereby aids in the improvement of cell viability. Upon application of the polymeric coated nanoparticles, the core ingredient (biofertilizer) is slowly released into the targeted sites (soils) without the contents being inactivated.

Gold and silver nanoparticles may be effective in enhancing the growth of horticultural crops such as peas and legumes (Zulfiqar *et al.*, 2019). Under *in vitro* conditions, these nanoparticles, in combination with natural biofertilizers like *Paenibacillus elgi, P. fluorescens, and Bacillus subtilis,* have been successfully used to promote plant growth. The advantage of nanobiofertilizers over other fertilizers is that they are needed in very low amounts and are relatively inexpensive. For instance, a liter of nanobiofertilizer is sufficient for application on several hectares of crop grown lands. When the effects of gold nanoparticles on PGPB, including *P. putida, P. elgii, P. fluorescens,* and *B. subtilis* were examined, the findings revealed a significant increase in plant growth for *P. elgii, P. fluorescens,* and *B. subtilis,* while no impact was observed for *P. putida* (Shukla *et al.*, 2015)*.*

Improving plant-microbe interactions through nanotechnology

As discussed, quorum sensing molecules released by various soil microbes play important roles in plant health by aiding in the alleviation of plant stresses, stimulating plant defense systems, and producing antibiotics. Quorum sensing microbes or the molecules that they produce may be very useful resources in agriculture e.g., to formulate and commercialize products from QS signal molecules that stimulate plant growth or to commercialize the microbes that produce QS signal molecules for use in agriculture. The processes that could be adopted for the identification of these molecules have previously been described (Antar *et al.*, 2021; Gray & Smith, 2005). However, it is important that further research be conducted to determine whether the use of microbes that produce these signals will be better for applications in fields or the direct use of the signal molecules. If the signal molecules are used directly, then the problem of inoculum viability is eliminated. On the other hand, the application of microbes that produce these signals will ensure the long-lasting secretion of these molecules in the environment compared to when the signal molecules were used (Antar *et al.*, 2021). To ensure the persistence of signal molecules applied in soils for plant growth enhancement, signal molecules could be encapsulated to allow their slow release into the environment. It is also important to optimize the concentration of QS signal molecules during product formulation. When larger concentrations of genistein were applied to soybean, improved growth and nodulation were observed in the plants while the stress of suboptimal root zone temperatures was minimal (Zhang & Smith, 1995).

Nanobiotechnology for controlling insect pests of plants

Nanotechnology is a promising tool for the control and management of insect pests of crop plants. Das *et al.* (2019) studied the effects of zinc oxide, aluminum oxide, and titanium dioxide nanoparticles application in the management of rice weevil (*Sitophilus oryzae*). Iron nanoparticles developed using extracts from *Eucalyptus* plant displayed antifeedant activity against diamondback moth (*Plutella xylostella*), indicating that the *Eucalyptus* plant extract acted in synergy with the iron nanoparticles (Chhipa & Kaushik, 2015). *Bacillus thuringiensis* synthesized ZnO nanoparticles (*Bt*-ZnO) acted against pulse beetles (*Callosobruchus maculatus*) and reduced their hatchability and productiveness. *Bt*-ZnO also decreased the activities of the gut digestive enzymes of this pest including the glutathione S-transferase, α-amylase, α-glucosidase, and cysteine protease (Malaikozhundan *et al.*, 2017). Nanoparticles prepared with a cell-free supernatant from *Photorhabdus luminescens* were used against the cotton insect pests, *Aphis gossypii* and *Tetranychus macfarlanei*.

Results revealed a lower 50% lethal concentration (LC_{50}) of the cell-free supernatant nanoparticle than the normal cell-free supernatant (Kulkarni *et al.*, 2017). The effectiveness of the formulation was attributed to the multistage process involved in the preparation of the nanoparticles, indicating that the methods of delivery of nanoparticles is a vital factor that should be considered when formulating the products. Nanoencapsulation of biopesticides protects the active substances against unfavorable environmental conditions while ensuring a targeted and controlled release of the substances to the target pests (Rodríguez *et al.*, 2016). Unlike conventional agrochemicals, nanoencapsulation of pesticides enables the chemicals to be properly absorbed by plants because they are gradually and continuously released into the soil, and because their effect on pests is more long-lasting and persistent (Djiwanti & Kaushik, 2019; Duhan *et al.*, 2017; Eleni & Krokida, 2017). Therefore, nanobiotechnology presents an innovative system of controlling insect pests, providing an opportunity for increased plant production.

Bioherbicide production through nanotechnology

The major threat facing agricultural production, which substantially reduces crop production, are weeds. Weed pests compete with crop plants for available nutrients. Traditional methods of controlling weeds have been effective; however, the challenges of their use in agriculture include huge time consumption, soil pollution, reduction in soil fertility, and destruction of cultivated plants. The application of a specific herbicide for a long time causes the weed to develop resistance to that particular herbicide. In addition, damages are inflicted on succeeding crops due to continuous and prolonged use of herbicides, which leaves residues in soil. Recently, an ecofriendly approach of weed control, involving the use of microbes or other biotic agents to decrease the impact, reproductive capability, vigor, and density of weeds in an agricultural environment has emerged (Kremer, 2019). The products resulting from this approach, known as bioherbicides (for biocontrol of weeds) is effective in the control and suppression of economically important and persistent weeds. Bioherbicides also efficiently control herbicide-resistant weeds resulting from long-term use of conventional herbicides on plants (Abbas *et al.*, 2018; Hershenhorn *et al.*, 2016). The main constraint towards successful commercialization of bioherbicides is ensuring that the appropriate formulation is available and the method of application is convenient enough to allow a uniform distribution of the biological agent at the targeted site (Hershenhorn *et al.*, 2016).

The control of weeds using nanotechnology is still at its early stage of development. Here, we employ ideas from other studies on nanoformulations to suggest the possibilities of applying nanotechnology in the development of bioherbicides. Viruses are naturally occurring nanoparticles with an outer and a core coating. The size of the viral protein coats of DNA or RNA plant viruses ranges from 10 – 1000 nm, making them suitable as vectors for transmitting substances that are disease-inducible in weeds (Pérez-de-Luque & Hermosín, 2013). The tobacco mild green mosaic virus (TMGMV) is an example of a bioherbicide that was patented for use in the biological control of perennial pasture weed, tropical soda apple (*Solanum viarum*) in the United States (Charudattan & Hiebert, 2007). This virus is extremely effective and could serve as a template for the discovery and formulation of similar biological agents (Charudattan, 2010).

The use of microbial metabolites and other biological products to develop effective bioherbicides has become the focus of researchers in search of alternative means of weed control for sustainable agriculture (Duke *et al.*, 2014; Radhakrishnan *et al.*, 2018). The development of resistance in weeds previously exposed to herbicides could be overcome by the use of microbial metabolites (Duke *et al.*, 2014). However, only a few microbial metabolites are currently being studied for their potential as biochemical bioherbicides. The future development of biochemically formulated bioherbicides needs to mimic the currently developed nanoformulations that enhance the slow or controlled release of agrochemicals into target weeds. Biochemically formulated nanobioherbicides could increase biocontrol because nanoparticles have a large surface area, therefore, only a small quantity of bioherbicide will be needed. This will reduce costs, as a smaller package will contain a higher concentration of the bioherbicide (Pallavi *et al.*, 2017). The small nature of the particles reduces to a large extent, their susceptibility to environmental conditions, such as UV radiation, heat, and desiccation resulting from application, delivery, and storage (Kremer, 2019). The effectiveness of the metabolites of *Photorhabdus luminescens*, an endosymbiotic bacterium that colonizes the parasitic nematode *Heterorhabditis indica*, which acts against arthropod pests of crops, was improved using nanotechnology (Kulkarni *et al.*, 2017). The formulation was prepared using a cell-free supernatant of the bacterium cultures and mixed with gum arabic, which served as a binder. The formulated product was sprayed onto target insects, resulting in a rapid and high rate of death of the pests due to the greater penetration power of the particle that carries the toxins into the insects (Kulkarni *et al.*, 2017). The foliar application of *F. oxysporum* metabolites coated with chitosan nanoparticles on the weed, *Ninidam theenjan* resulted in leaf necrosis, indicating the possibility of the nanobioformulation to effectively control agricultural economically

important weeds (Namasivayam *et al.*, 2015). Notwithstanding the above-mentioned preliminary results, it is important that additional studies be conducted to demonstrate the efficacy of this formulation in field conditions.

Microencapsulation of biological agents, which assures the intactness of the natural phytotoxic metabolites of microbes with herbicidal attributes (Rojas-Sánchez *et al.*, 2022), is promising for potentially effective nanobioherbicides. The nanocapsules are usually organic polymers, in the form of shells carrying the bioherbicide, which open to release their contents under specific conditions such as a change in pH (Pérez-de-Luque & Hermosín, 2013). The encapsulation of biopesticides is an attractive approach for controlling agricultural pests because it makes them efficient, stable, and safe to use (Nuruzzaman *et al.*, 2016). This approach could also be adapted for the formulation of biological agents that can be applied on agricultural weeds. The successful use of nanobiotechnology has the potential to dramatically alter the area of agricultural pest management including the management of agricultural weeds.

Production of biofungicides using nanotechnology

Most of the losses in agricultural production result from fungal attacks on crop plants. Globally, approximately $45 billion in crop productivity is lost yearly due to pathogenic fungi (Fernandez Acero *et al.*, 2011). However, an increase in agricultural production may be achieved if plant pathogenic fungi are effectively managed (Fisher *et al.*, 2012). While several fungicides are commercially available, their application impacts negatively on plants. Fungicides may inhibit photosynthesis, which decreases plant growth and yield (Geetha, 2019; Petit *et al.*, 2012). Also, conventional fungicides form residues, cause the development of resistance by pathogens, and several health problems to man, animals, plants, and microbial communities (Aguilar-Marcelino *et al.*, 2021; Panth *et al.*, 2020). Nanobiotechnology has helped to increase the nutrient-use efficiency of plants through the application of nanoformulations of fertilizers and overcoming the barriers in yield and nutritional quality of plants (Abd-Elsalam *et al.*, 2019). Besides the use of OMICs tool in understanding the mechanisms of host-parasite interactions, nanobiotechnology can assist in investigating and managing diseases and plant pests. The antifungal activities of nanobiofungicides towards many pathogenic fungi have been tested (Ingle *et al.*, 2014; Singh *et al.*, 2015; Yadav *et al.*, 2015). It is expected that, in the near future, the production of nanobiofungicides, with better solubility, specificity, and stable dispersal, will be available for the control of plant diseases. Silver nanoparticles (AgNPs) have potentially significant impact in their use in agriculture (Krishnaraj *et al.*, 2012). The control of *B. sorokiniana* infection that causes spot blotch disease in wheat was investigated using biosynthesized AgNPs. The study, which was conducted both *in vitro* and,

in a greenhouse, revealed strong antifungal activity against *B. sorokiniana* and its infection on the wheat plant. The antifungal activity of biosynthesized AgNPs from a cell-free extract of *Penicillium chrysogenum* was also tested against *Trichophyton rubrum*, which resulted in a large antifungal effect against the pathogen (Pereira *et al.*, 2014). Another study investigated the biocontrol of *Sclerotium rolfsii,* the cause of collar rot of chickpea, by AgNPs synthesized from pelleted *Stenotrophomonas* sp. BHU-S7. In this case, it was reported that the biosynthesized AgNPs exhibited inhibitory effects on the pathogenic propagules by reducing their germination and eliminating their ability to cause disease in the plant (Mishra *et al.*, 2017; Mishra *et al.*, 2014). Sustainable agriculture requires a reduced use of agrochemicals to ensure environmental safety. Nanobiofungicides have shown their ability to be used in the control of plant diseases, enhancement of plant growth, and antifungal activity. For optimum performance, nanobiofungicides can be encapsulated to ensure better penetration and a slow and sustained release of the active ingredients. This technology can provide an efficient, cheap, and ecofriendly means of controlling agricultural pests and ensures less environmental contamination and safe handling.

Benefits of nanobiotechnology in the production of agricultural products

The use of nanoformulations ensures a slow and controlled release of phytotoxic metabolites or the microbes attached to a non-carrier into the target pests. This system reduces the loss of the active ingredients in the formulation by ensuring they stay within the roots or aerial parts of the plant (Fadiji *et al.*, 2022b). The non-carrier will also protect the formulated agriproduct from degradation (Hershenhorn *et al.*, 2016). The mode of delivery of the products helps to ensure environmental safety by reducing environmental toxicity. The products obtained are soluble, highly specific, and stable in dispersal.

The use of nanobiosensors in agriculture

The development of smart biosensors that detect the presence of nutrients and contaminants can greatly affect precision farming. Precision farming uses highly efficient global positioning systems (GPS), computers, and remote sensing devices to identify the nature and locations of problems, measure environmental conditions of a certain location, and use resources with maximum efficiency (Gouda *et al.*, 2018). This type of farming has a long-sought objective of reducing the input of fertilizers, herbicides, and pesticides while improving crop yields through the observation of environmental variables and the application of directed action (Bhattacharyya *et al.*, 2016).

In agriculture, nanobiosensors can be used to detect a range of agricultural inputs like fertilizers, pesticides, herbicides, and soil characteristics including pH and moisture content. They inhance sustainable agriculture because an increase in agricultural productivity can be achieved with biosensors. Smart biosensors as a key component of precision farming ensure better management of fertilizers, reduce the cost of inputs, and are ecofriendly, therefore improving productivity. Through precision farming, smart application systems based on nanosensors can aid in the management of raw materials such as nutrients, agrochemicals, and water (Anjum & Pradhan, 2018; Duhan *et al.*, 2017; Fadiji *et al.*, 2022b). For increments in crop productivity, monitoring of agricultural contaminants, and assessing their impacts on plant health, metal oxide nanoparticles such as the electrochemically controlled single-walled carbon nanotubes (SWCNTs) can be used (Deshpande, 2019). Nanosensors can be applied to spot the incidence of plant pathogens as well as the level of soil nutrients (Kaushal & Wani, 2017). The use of nanobiosensors in agriculture and food industries enables prompt, real time, and site-specific sensing of pathogens in plants and food products, real time crop monitoring, and predicting the field and environmental conditions, thus ensuring food safety (Singhal & Rana, 2019).
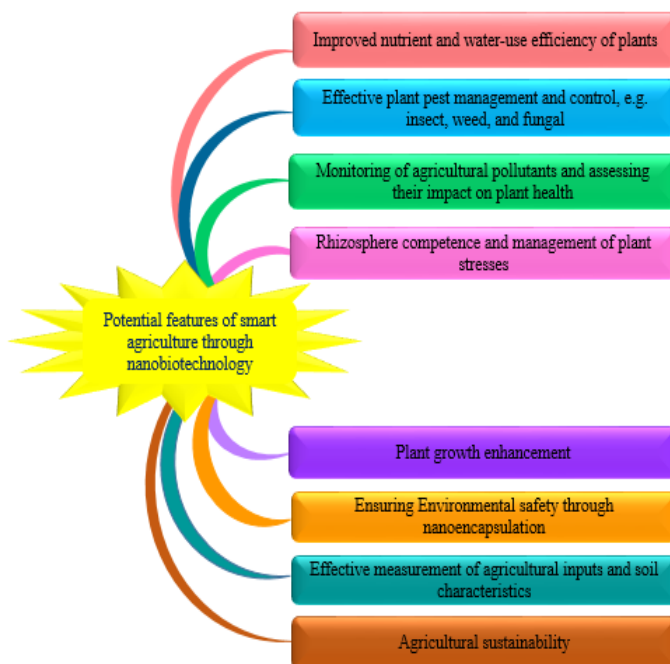
Figure 3. Potential benefits of the application of nanobiotechnology in agriculture.

Nanosensors, such as quantum dots (QDs), are used to sense the presence of pathogens. For instance, the sensor, based on fluorescence resonance energy transfer, can sense a disease affecting lime known as witches' broom, caused by *Candidatus Phytoplasma aurantifolia* (*Ca. P. aurantifolia*). The developed immunosensor exhibited 100% sensitivity and specificity with a detection limit of 5 ca of *P. aurantofolia* per μL (Rad *et al.*, 2012). Several microorganisms have been successfully used to synthesize cadmium quantum dots (Yadav *et al.*, 2015). *Fusarium oxysporum* in combination with tritellurium dichloride (Te_3Cl_2) and cadmium dichloride ($CdCl_2$) was used in the biosynthesis of fluorescent cadmium telluride (CdTe) quantum dots (Alghuthaymi *et al.*, 2015). The presence of deltamethrin in vegetable and fruit samples was detected using the biosensors, highly fluorescent silica nanospheres embedded with CdTe, and water-soluble CdTe quantum dots (Arora, 2018; Ojha *et al.*, 2018). Fig. 3 shows the different features of nanobiotechnology in agriculture.

Major concerns about the use of nanotechnology in agriculture

Although the combination of nanotechnology and plant growth-promoting microbes present a promising approach to curb the growth of many economically important weeds, extensive research needs to be performed to determine host specificity and to ascertain how compatible these nanoparticles are with other microbial agents. Some nanoparticles could have detrimental effects on soil microbial processes and communities (Eivazi *et al.*, 2018), therefore, before considering the adoption of this approach, it is necessary to determine the activity of nanoparticles in the food chain and the environment.

Impacts of nanotechnology on microbial diversity

Microbial communities can serve as models to ascertain the environmental impacts of nanoparticles. Therefore, determining the effects of nanoparticles on the diversity of soil microbial communities is essential. Using different quantitative and qualitative parameters such as metabolic fingerprinting, fatty acid methyl ester analyses, and colony forming units, the short-term effects of gold, silica, copper, and palladium nanoparticles on soil microbial communities were evaluated and it was found that the influence of the nanoparticles on microbial diversity was statistically insignificant (Shah & Belozerova, 2009). Simonin and Richaume (2015) reported that organic nanoparticles including carbon nanotubes and fullerenes exhibited lower toxicity at >250 mg/kg of soil to microbial communities compared to metal and metal oxide nanoparticles

whose toxicity level was 1 mg/kg of soil. The effect of silver sulfide nanoparticles on soil microbiota, particularly those that take part in nitrification processes, was evaluated using metagenomics (Doolette *et al.*, 2016). In this study, a combination of methods including 16S rRNA amplicon sequencing, quantitative PCR, and bacterial sensitivity distribution were used, and a different method to determine the toxicity thresholds of silver nanoparticles on specific members of a microbial community was suggested. One limitation of the study was soil specificity, implying that the method needs to be standardized for each soil type.

In another study, a decline was observed in bacterial communities involved in the fixation of atmospheric nitrogen and the oxidation of methane after these communities were exposed to zinc oxide (ZnO) and titanium oxide (TiO_2) nanoparticles. However, the nanoparticles reacted positively with the bacterial taxa involved in the breakdown of biopolymers and organic contaminants (Ge *et al.*, 2012). Maruyama *et al.* (2016) reported that herbicides, such as imazapyr and imazapic, encapsulated with chitosan/tripolyphosphate (Ch/Tpp) and alginate/chitosan (Alg/Ch), affect bacterial diversity. The study revealed that the microbial profiles of soils treated with encapsulated nanoparticles were different from those treated with only herbicides. The effect of encapsulated and non-encapsulated herbicides on bacterial communities was ascertained using bacterial genes involved in nitrogen cycling viz., nitrification, denitrification, and nitrogen fixation. Encapsulation with Alg/Ch increased the proportion of bacteria that contain nitrate reductase genes, while increases in the proportion of nitrogen-fixing bacteria were observed in Ch/Tpp encapsulated treatments due to the presence of nitrogenase reductase genes.

The mechanism of interaction between soil microbes and nanoparticles involves the direct absorption of nanoparticles by microbes where the nanoparticles immediately penetrate the microbial cells, affecting cytoplasm conductivity when the nanoparticle size is ~50 nm (Samanta & Mandal, 2017; Singh *et al.*, 2019). Most metal and metal oxide nanoparticles exhibit antimicrobial activity through mechanisms such as accumulation of ROS, formation of pores in microbial cell membranes, DNA damage, endocytosis, release of metal ions, membrane attachment and cell growth inhibition (Abd-Elsalam *et al.*, 2019; Singh *et al.*, 2019). The interaction of nanoparticles with microbial diversity may interfere with the mechanisms of plant nutrition in several ways. However, studies have demonstrated a positive interaction between carbon nanotubes and the communities of microarthropods beneath turf grass (Bai *et al.*, 2017). In this study, the effect of three types of carbon nanomaterials namely, carbon nanotubes (CNTs), graphene, and graphene oxide on soil microarthropod communities was studied, with the results suggesting that carbon nanoparticles increased all soil microarthropods.

Recommendation and prospects

Developing novel PGPB strains capable of being used as biofertilizers, biopesticides, and biofungicides is possible by genetic manipulation of such strains (Gouda *et al*., 2018). The process of improving agricultural productivity with soil microorganisms can be a cost-effective, environmentally friendly, and sustainable tool that both increases plant productivity and manages stresses in plants. Nanotechnology and nano-based products are currently used to improve agricultural productivity in several countries including China, France, the United States, Germany, Switzerland, South Korea, and Japan (Gouda *et al*., 2018; Mukherjee *et al*., 2019). In sub-Saharan Africa, this technology is still very new and its use is limited to very few crops, partly due to lack of awareness of this technology by farmers or lack of support from the government. Therefore, increasing efforts towards commercializing nanobioproducts, ensuring their availability at affordable prices, and enabling easy access to farmers should be encouraged. In this way, farmers will embrace and incorporate the technology into agricultural practice for the purpose of improving plant growth, crop yield, and ensuring agricultural sustainability.

Agglomeration, the tendency of grouping together to form large particles is a major issue that raises serious concerns that may result from the use of nanoparticles. In producing nanoparticles, post-synthetic methods, including the use of surface modifiers and chemicals are used to inhibit particle aggregation. Such practices can negatively impact the toxicity and safety of the nanomaterial (Hegde *et al*., 2016), which makes it imperative to perform ecotoxicity studies to ascertain the effect of edaphic factors on the bioavailability as well as the natural mechanisms of nanoparticle uptake. There is also a need to assess the impact of engineered nanomaterials in agriculture (Fadiji *et al*., 2022a), as the human abdomen is its end destination. Increased bioaccumulation of nanoparticles in the food chain may be detrimental to the environment (Gardea-Torresdey *et al*., 2014; Ma *et al*., 2018). The most important task is determining the right concentration at which engineered nanoparticles can be applied without inflicting harm and to ascertain at what concentrations they can become toxic to plants, the environment, and man. Nanoparticles applied to the soil can interact with soil microbial communities, thereby affecting the soil ecosystem, the sequestration of carbon, and soil microbial dynamics. Other functions in the soil, including mycorrhizal associations, organic matter decomposition, and the transformation of nitrogen can also be affected due to the application of engineered nanoparticles on soils. However, published literature on the interaction of nanoparticles with soil microbiota and transmission of nanoparticles from plants to man is limited. Therefore, additional knowledge is needed on the interaction

of plant microbiomes with nanoparticles as well as the safety of food and agricultural products that originate from plants grown in soils where nano-based products were applied.

Conclusion

The practice of agriculture has been an important aspect of human lives for thousands of years as it provides a means of sustenance to humankind. However, the exploitation of global resources by human activities has severely reduced agricultural productivity, resulting in a search for better ways to improve agricultural yields to satisfy the increasing human demand for food. Plant growth-promoting microbes have been shown to be effective in improving plant growth by providing nutrients, acting as biofertilizers, biopesticides, controlling pathogenic attacks on plants, and recycling of nutrients. They have also played major roles in managing and controlling abiotic stresses like drought, high salt, pesticide and heavy metal pollution, cold, and flooding. For decades, farmers have relied heavily on the use of chemical-based fertilizers and pesticides that have resulted in the distribution of chemicals that are ultimately detrimental to human lives. These chemicals are not just poisonous upon consumption by humans but often exhibit adverse effects on soil microorganisms and the environment (Baweja *et al.*, 2020). The modifications resulting from the spread of these chemicals can change the present plant-microbe interactions existing in the soil by modifying the biogeochemical cycles as well as microbial biology. A crucial step towards the development of sustainable agriculture that will aid the improvement of soil fertility, crop productivity, balanced nutrient cycling, and plant stress tolerance would be through the application of modern tools and practices that incorporate PGPM. Signal compounds, such as phytohormones (auxins, cytokinins, and gibberellins), quorum sensing molecules (including AHLs, DSFs, antibiotics, pheromones, peptides, tyrosol, and γ-butyrolactone) and various secondary metabolites may improve plant growth and health by ensuring the availability of nutrients and their acquisition by plants, decreasing the effects of abiotic stresses, as well as suppressing certain plant biotic stresses. Moreover, selecting the appropriate microbes for plant growth enhancement and the incorporation of technologies that bring together the applications of nanotechnology, biotechnology, and agro-biotechnology facilitate the development of novel products with potential to increase production in agriculture. Certain soil microbes can produce QS signal molecules that improve plant growth and yield, and so could play significant roles in marginal land reclamation and sustainable agriculture, especially now that agricultural land is expected to be lost as a result of the growing global

urbanization. In addition, the use of nanobiosensors in agriculture could encourage innovative farming practices, as they aid in the management of nutrients, water, and fertilizers. They also control plant stresses (biotic and abiotic) and detect the presence of pollutants in the soil. However, the commercialization of nano-derived products for agricultural use requires a thorough assessment of its impacts on soil, microbial community, plants, and human endeavors to prevent any unwanted side effects.

References

Abbas, T., Zahir, Z.A., Naveed, M., & Kremer, R.J. (2018). Limitations of existing weed control practices necessitate development of alternative techniques based on biological approaches. *Adv. Agron*, 147, 239-280.

Abbey, L., Abbey, J., Leke-Aladekoba, A., Iheshiulo, E.M.A., & Ijenyo, M.(2019). Biopesticides and biofertilizers: types, production, benefits, and utilization, In: Byproducts from agriculture and fisheries: adding value for food, feed, pharma, and fuels, Simpson, B. K., Aryee, A.N.A., Toldrá, F. (eds.), *John Wiley & Sons*, pp. 479-500.

Abd-Elsalam, K.A., Al-Dhabaan, F.A., Alghuthaymi, M., Njobeh, P.B., & Almoammar, H. (2019). Nanobiofungicides: Present concept and future perspectives in fungal control. In: Nano-biopesticides today and future perspectives, Koul, O. (ed), *Academic Press*, pp. 315-351.

Acharya, A., & Pal, P.K. (2020). Agriculture nanotechnology: translating research outcome to field applications by influencing environmental sustainability. *NanoImpact*, 19, 100232.

Afridi, M.S., Mahmood, T., Salam, A., Mukhtar, T., Mehmood, S., Ali, J., Khatoon, Z., Bibi, M., Javed, M.T., & Sultan, T. (2019). Induction of tolerance to salinity in wheat genotypes by plant growth promoting endophytes: Involvement of ACC deaminase and antioxidant enzymes. *Plant Physiol. Biochem*, 139, 569-577.

Afzal, I., Shinwari, Z.K., & Iqrar, I. (2015). Selective isolation and characterization of agriculturally beneficial endophytic bacteria from wild hemp using canola. *Pak. J. Bot*, 47(5), 1999-2008.

Aguilar-Marcelino, L., Al-Ani, L.K.T., de Freitas Soares, F.E., Moreira, A.L.E., Téllez-Téllez, M., Castañeda-Ramírez, G.S., de Lourdes Acosta-Urdapilleta, M., Díaz-Godínez, G., & Pineda-Alegría, J.A. (2021). Formation, resistance, and pathogenicity of fungal biofilms: Current trends and future challenges. In: Recent trends in mycological research, Yadav, A.N. (ed.) *Springer*, Cham, pp. 411-438.

Ahmad, S., Imran, M., Hussain, S., Mahmood, S., Hussain, A., & Hasnain, M. (2017). Bacterial impregnation of mineral fertilizers improves yield and nutrient use efficiency of wheat. *J. Sci. Food Agric*, 97(11), 3685-3690.

Ahmed, S., Rahman, S., Hasan, M., Paul, N., & Sajib, A.A. (2018). Microbial degradation of lignocellulosic biomass: discovery of novel natural lignocellulolytic bacteria. *BioTechnologia*, 99(2), 137-146.

Ajilogba, C.F., Babalola, O.O., & Ahmad, F. (2013). Antagonistic effects of *Bacillus* species in biocontrol of tomato *Fusarium* wilt. *Stud. Ethno-Med*, 7(3), 205-216.

Alghuthaymi, M.A., Almoammar, H., Rai, M., Said-Galiev, E., Abd-Elsalam, K.A. (2015). Myconanoparticles: synthesis and their role in phytopathogens management. *Biotechnol. Biotechnol. Equip*, 29(2), 221-236.

Ali, A., Hameed, S., Imran, A., Iqbal, M., Iqbal, J., & Oresnik, I.J. (2016). Functional characterization of a soybean growth stimulator *Bradyrhizobium* sp. strain SR-6 showing acylhomoserine lactone production. *FEMS Microbiol. Ecol*, 92(9), fiw115.

Alori, E.T., & Babalola, O.O. (2018). Microbial inoculants for improve crop quality and human health. *Front. Microbiol*, 9, 2213.

An, J.H., Goo, E., Kim, H., Seo, Y.-S., & Hwang, I. (2014). Bacterial quorum sensing and metabolic slowing in a cooperative population. *Proc. Natl. Acad. Sci*, 111(41), 14912-14917.

Andersson, D.I., & Hughes, D. (2014). Microbiological effects of sublethal levels of antibiotics. *Nat. Rev. Microbiol*, 12(7), 465-478.

Anjum, M., & Pradhan, S.N. (2018). Application of nanotechnology in precision farming: A review. *Int. J. Chem. Stud*, 6(5), 755-760.

Antar, M., Gopal, P., Msimbira, L.A., Naamala, J., Nazari, M., Overbeek, W., Backer, R., & Smith, D.L. (2021). Inter-organismal signaling in the rhizosphere. In: Rhizosphere biology: interactions between microbes and plants, Gupta, V. V. S. R., Sharma, A. K. (eds.), *Springer*, Singapore, pp. 255-293.

Arora, K. (2018). Advances in nano based biosensors for food and agriculture. In: Nanotechnology, food security and water treatment, Gothandam, K., Ranjan, S., Dasgupta, N., Ramalingam, C., Lichtfouse, E. (eds), *Springer*, Cham, pp. 1-52.

Aznar, A., & Dellagi, A. 2015. New insights into the role of siderophores as triggers of plant immunity: what can we learn from animals? *J. Exp. Bot*, 66(11), 3001-3010.

Babalola, O.O. (2010). Beneficial bacteria of agricultural importance. *Biotechnol. Lett*, 32(11), 1559-1570.

Backer, R., Rokem, J.S., Ilangumaran, G., Lamont, J., Praslickova, D., Ricci, E., Subramanian, S., & Smith, D.L. (2018). Plant growth-promoting rhizobacteria: context, mechanisms of action, and roadmap to commercialization of biostimulants for sustainable agriculture. *Front. Plant Sci*, 9, 1473.

Bai, X., Zhao, S., & Duo, L. (2017). Impacts of carbon nanomaterials on the diversity of microarthropods in turfgrass soil. *Sci. Rep*, 7(1), 1-6.

Bakka, K., & Challabathula, D. (2020). Amelioration of salt stress tolerance in plants by plant growth-promoting rhizobacteria: insights from "omics" approaches. In: Plant microbe symbiosis, Varma, A., Tripathi, S., Prasad, R. (eds), *Springer*, Cham, pp. 303-330.

Baweja, P., Kumar, S., & Kumar, G. (2020). Fertilizers and pesticides: their impact on soil health and environment. in: Soil Health, Giri, B., Varma, A. (eds), *Springer*, Cham, pp. 265-285.

Berendsen, R.L., Pieterse, C.M., & Bakker, P.A.(2012). The rhizosphere microbiome and plant health. *Trends Plant Sci*, 17(8), 478-486.

Bhatt, K., Maheshwari, D.K. (2020). Zinc solubilizing bacteria (*Bacillus megaterium*) with multifarious plant growth promoting activities alleviates growth in *Capsicum annuum* L. *3 Biotech*, 10(2), 36.

Bhattacharyya, A., Duraisamy, P., Govindarajan, M., Buhroo, A.A., & Prasad, R. (2016). Nano-biofungicides: emerging trend in insect pest control. In: Advances and Applications through Fungal Nanobiotechnology, Prasad, R. (ed), *Springer*, Cham, pp. 307-319.

Biswas, S., & Anusuya, D. (2014). Effect of bioinoculants and organic manure (phosphocompost) on growth, yield and nutrient uptake of *Trigonella foenum-graecum* L. (Fenugreek). *Int. J. Sci. Res*, 3, 38-41.

Bukhat, S., Imran, A., Javaid, S., Shahid, M., Majeed, A., & Naqqash, T. (2020). Communication of plants with microbial world: Exploring the regulatory networks for PGPR mediated defense signaling. *Microbiol. Res*, 238, 126486.

Caddell, D.F., Deng, S., & Coleman-Derr, D. (2019). Role of the plant root microbiome in abiotic stress tolerance. In: Seed Endophytes, Verma, S., White, Jr, J. (eds), *Springer*, Cham, pp. 273-311.

Cawoy, H., Debois, D., Franzil, L., De Pauw, E., Thonart, P., & Ongena, M. (2015). Lipopeptides as main ingredients for inhibition of fungal phytopathogens by *Bacillus subtilis/amyloliquefaciens. Microb. Biotechnol*, 8(2), 281-295.

Chagas, F.O., de Cassia Pessotti, R., Caraballo-Rodriguez, A.M., & Pupo, M.T. (2018). Chemical signaling involved in plant–microbe interactions. *Chem. Soc. Rev*, 47(5), 1652-1704.

Charudattan, R. (2010). A reflection on my research in weed biological control: using what we have learned for future applications. *Weed Technol*, 24(2), 208-217.

Charudattan, R., & Hiebert, E. (2007). A plant virus as a bioherbicide for tropical soda apple, *Solanum viarum. Outlooks Pest Manag*, 18(4), 167.

Cheng, Z., Park, E., & Glick, B.R. (2007). 1-Aminocyclopropane-1-carboxylate deaminase from *Pseudomonas putida* UW4 facilitates the growth of canola in the presence of salt. *Can. J. Microbiol*, 53(7), 912-918.

Chhipa, H., & Kaushik, N. (2015). Development of nano-bio-pesticide using Iron and Eucalyptus plant extract and their application in pest management. *Conference Proceeding of Symposium on Recent Advances in Biotechnology for Food and Fuel*, TERI, New Delhi. pp. 19-20.

Chowdhury, S.P., Uhl, J., Grosch, R., Alquéres, S., Pittroff, S., Dietel, K., Schmitt-Kopplin, P., Borriss, R., & Hartmann, A. (2015). Cyclic lipopeptides of *Bacillus amyloliquefaciens* subsp. *plantarum* colonizing the lettuce rhizosphere enhance plant defense responses toward the bottom rot pathogen *Rhizoctonia solani. Mol. Plant-Microbe Interact*, 28(9), 984-995.

Chu, W., Jiang, Y., Yongwang, L., & Zhu, W. (2011). Role of the quorum-sensing system in biofilm formation and virulence of *Aeromonas hydrophila. Afr. J. Microbiol. Res*, 5(32), 5819-5825.

Chukwuneme, C.F., Babalola, O.O., Kutu, F.R., & Ojuederie, O.B. (2020). Characterization of actinomycetes isolates for plant growth promoting traits and their effects on drought tolerance in maize. *J. Plant Interact*, 15(1), 93-105.

Costerousse, B., Schönholzer-Mauclaire, L., Frossard, E., & Thonar, C. (2018). Identification of heterotrophic zinc mobilization processes among bacterial strains isolated from wheat rhizosphere (*Triticum aestivum* L.). *Appl. Environ. Microbiol,* 84(1), e01715-17.

Das, S., Yadav, A., & Debnath, N. (2019). Entomotoxic efficacy of aluminium oxide, titanium dioxide and zinc oxide nanoparticles against *Sitophilus oryzae* (L.): A comparative analysis. *J. Stored Prod. Res*, 83, 92-96.

Deshpande, M.V. (2019). Nanobiopesticide perspectives for protection and nutrition of plants. In: Nano-biopesticides today and future perspectives, Koul, O. (ed), *Academic Press*, pp. 47-68.

Devi, S., & Soni, R. 2020. Relevance of microbial diversity in implicating soil restoration and health management. In: Soil health restoration and management, Meena, R. (ed), *Springer*, Singapore, pp. 161-202.

Djiwanti, S.R., & Kaushik, S. (2019). Nanopesticide: Future application of nanomaterials in plant protection. In: Plant nanobionics, Prasad, R. (ed), *Springer*, Cham, pp. 255-298.

Doolette, C.L., Gupta, V.V., Lu, Y., Payne, J.L., Batstone, D.J., Kirby, J.K., Navarro, D.A., & McLaughlin, M.J. (2016). Quantifying the sensitivity of soil microbial communities to silver sulfide nanoparticles using metagenome sequencing. *PloS One*, 11(8), e0161979.

Duca, D., Lorv, J., Patten, C.L., Rose, D., & Glick, B.R. (2014). Indole-3-acetic acid in plant–microbe interactions. *Antonie Van Leeuwenhoek*, 106(1), 85-125.

Duhan, J.S., Kumar, R., Kumar, N., Kaur, P., Nehra, K., & Duhan, S. (2017). Nanotechnology: the new perspective in precision agriculture. *Biotechnol. Rep*, 15, 11-23.

Duke, S.O., Owens, D.K., & Dayan, F.E. (2014). The growing need for biochemical bioherbicides. In: Biopesticides: state of the art and future opportunities, Gross, A.D., Coats, J.R., Duke, S.O., Seiber, J.N. (eds), *ACS Publications*, pp. 31-43.

Eivazi, F., Afrasiabi, Z., & Elizabeth, J. (2018). Effects of silver nanoparticles on the activities of soil enzymes involved in carbon and nutrient cycling. *Pedosphere*, 28(2), 209-214.

Eleni, P., & Krokida, M.K. (2017). Other technologies for encapsulation (Air suspension coating, pan coating, and vacuum drying). In: Thermal and nonthermal encapsulation methods, Krokida, M. (ed), *CRC Press* , pp. 203-220.

Etesami, H. (2020). Plant–microbe interactions in plants and stress tolerance. In: Plant life under changing environment, Tripathi, D.K., Pratap Singh, V., Chauhan, D.K., Sharma, S., Prasad, S.M., Dubey, N. K., Ramawat, N. (eds), *Academic Press*, pp. 355-396.

Etesami, H., Jeong, B.R., & Glick, B.R. (2021). Contribution of arbuscular mycorrhizal fungi, phosphate–solubilizing bacteria, and silicon to P uptake by plant: a review. *Front. Plant Sci*, 12, 1355.

Fadiji, A.E., Mortimer, P.E., Xu, J., Ebenso, E.E., & Babalola, O.O. (2022a). Biosynthesis of nanoparticles using endophytes: a novel approach for enhancing plant growth and sustainable agriculture. *Sustainability*, 14(17), 10839.

Fadiji, A.E., Mthiyane, D.M.N., Onwudiwe, D.C., & Babalola, O.O. (2022b). Harnessing the known and unknown impact of nanotechnology on enhancing food security and reducing postharvest losses: constraints and future prospects. *Agronomy*, 12(7), 1657.

Fernandez Acero, F.J., Carbú, M., El-Akhal, M.R., Garrido, C., González-Rodríguez, V.E., & Cantoral, J.M. (2011). Development of proteomics-based fungicides: new strategies for environmentally friendly control of fungal plant diseases. *Int. J. Mol. Sci,* 12(1), 795-816.

Fisher, M.C., Henk, D.A., Briggs, C.J., Brownstein, J.S., Madoff, L.C., McCraw, S.L., & Gurr, S.J. (2012). Emerging fungal threats to animal, plant and ecosystem health. *Nature*, 484(7393), 186-194.

Forni, C., Duca, D., & Glick, B.R. (2017). Mechanisms of plant response to salt and drought stress and their alteration by rhizobacteria. *Plant Soil*, 410(1-2), 335-356.

Frankenberger Jr, W.T., & Arshad, M. (2020). Phytohormones in soils microbial production & function. *CRC Press*.

Fukami, J., Ollero, F.J., de la Osa, C., Valderrama-Fernández, R., Nogueira, M.A., Megías, M., & Hungria, M. (2018). Antioxidant activity and induction of mechanisms of resistance to stresses related to the inoculation with *Azospirillum brasilense*. *Arch. Microbiol*, 200(8), 1191-1203.

Gao, C., El-Sawah, A.M., Ali, D.F.I., Alhaj Hamoud, Y., Shaghaleh, H., & Sheteiwy, M.S. (2020). The integration of bio and organic fertilizers improve plant growth, grain yield, quality and metabolism of hybrid maize (*Zea mays* L.). *Agronomy*, 10(3), 319.

Gardea-Torresdey, J.L., Rico, C.M., & White, J.C. (2014). Trophic transfer, transformation, and impact of engineered nanomaterials in terrestrial environments. *Environ. Sci. Technol,* 48(5), 2526-2540.

Ge, Y., Schimel, J.P., & Holden, P.A. (2012). Identification of soil bacteria susceptible to TiO2 and ZnO nanoparticles. *Appl. Environ. Microbiol*, 78(18), 6749-6758.

Geetha, A. (2019). Phytotoxicity due to fungicides and herbicides and its impact in crop physiological factors. In: Advances in agricultural sciences, Naresh, A.K. (ed.), *AkiNik Publications*. New Delhi, India, pp. 29.

Gepstein, S., & Glick, B.R. (2013). Strategies to ameliorate abiotic stress-induced plant senescence. *Plant Mol. Biol*, 82(6), 623-633.

Glick, B.R. (2020). Environmental interactions. in: Beneficial plant-bacterial interactions. 2nd Ed. *Springer*, Cham, pp. 257-299.

Glick, B.R., Cheng, Z., Czarny, J., & Duan, J. (2007). Promotion of plant growth by ACC deaminase-producing soil bacteria. In: New perspectives and approaches in plant growth-promoting rhizobacteria research, Bakker, P.A.H.M., Raaijmakers, J.M., Bloemberg, G., Höfte, M., Lemanceau, P., Cooke, B.M. (eds), *Springer*, Dordrecht, pp. 329-339.

Glick, B.R., & Gamalero, E. (2021). Recent developments in the study of plant microbiomes. *Microorganisms*, 9(7), 1533.

Gouda, S., Kerry, R.G., Das, G., Paramithiotis, S., Shin, H.-S., & Patra, J.K. (2018). Revitalization of plant growth promoting rhizobacteria for sustainable development in agriculture. *Microbiol. Res*, 206, 131-140.

Gray, E., & Smith, D. (2005). Intracellular and extracellular PGPR: commonalities and distinctions in the plant–bacterium signaling processes. *Soil Biol. Biochem*, 37(3), 395-412.

Gupta, G., Parihar, S.S., Ahirwar, N.K., Snehi, S.K., & Singh, V. (2015). Plant growth promoting rhizobacteria (PGPR): current and future prospects for development of sustainable agriculture. *J. Microb. Biochem. Technol*, 7(2), 096-102.

Hartmann, A., Rothballer, M., Hense, B.A., & Schröder, P. (2014). Bacterial quorum sensing compounds are important modulators of microbe-plant interactions. *Front. Plant Sci*, 5, 131.

Hassan, R., Shaaban, M.I., Abdel Bar, F.M., El-Mahdy, A.M., & Shokralla, S. (2016). Quorum sensing inhibiting activity of *Streptomyces coelicoflavus* isolated from soil. *Front. Microbiol*, 7, 659.

Hegde, K., Brar, S.K., Verma, M., & Surampalli, R.Y. (2016). Current understandings of toxicity, risks and regulations of engineered nanoparticles with respect to environmental microorganisms. *Nanotechnol. Environ. Eng*, 1(1), 1-12.

Helman, Y., & Chernin, L. (2015). Silencing the mob: disrupting quorum sensing as a means to fight plant disease. *Mol. Plant Pathol*, 16(3), 316-329.

Hershenhorn, J., Casella, F., & Vurro, M. (2016). Weed biocontrol with fungi: past, present and future. *Biocontrol. Sci. Technol*, 26(10), 1313-1328.

Hong, K.-W., Koh, C.-L., Sam, C.-K., Yin, W.-F., & Chan, K.-G. (2012). Quorum quenching revisited—from signal decays to signalling confusion. *Sensors*, 12(4), 4661-4696.

Igiehon, N.O., & Babalola, O.O. (2018a). Below-ground-above-ground plant-microbial interactions: focusing on soybean, rhizobacteria and mycorrhizal fungi. *The Open Microbiology Journal*, 12, 261.

Igiehon, N.O., & Babalola, O.O. (2018b). Rhizosphere microbiome modulators: contributions of nitrogen fixing bacteria towards sustainable agriculture. *Int. J. Environ. Res. Public Health*, 15(4), 574.

Imran, A., Saadalla, M.J.A., Khan, S.-U., Mirza, M.S., Malik, K.A., & Hafeez, F.Y. (2014). Ochrobactrum sp. Pv2Z2 exhibits multiple traits of plant growth promotion, biodegradation and N-acyl-homoserine-lactone quorum sensing. *Ann. Microbiol*, 64(4), 1797-1806.

Ingle, A.P., Duran, N., & Rai, M. (2014). Bioactivity, mechanism of action, and cytotoxicity of copper-based nanoparticles: a review. *Appl. Microbiol. Biotechnol*, 98(3), 1001-1009.

Jaemsaeng, R., Jantasuriyarat, C., & Thamchaipenet, A. (2018). Positive role of 1-aminocyclopropane-1-carboxylate deaminase-producing endophytic Streptomyces sp. GMKU 336 on flooding resistance of mung bean. *Agric. Nat. Resour*, 52(4), 330-334.

Kamal, R.K., Athisayam, V., Gusain, Y.S., & Kumar, V. (2018). Trichoderma: a most common biofertilizer with multiple roles in agriculture. *Biomed J Sci & Tech Resl*, 4(5), MS.ID.001107.

Kandaswamy, R., Ramasamy, M.K., Palanivel, R., & Balasundaram, U. (2019). Impact of *Pseudomonas putida* RRF3 on the root transcriptome of rice plants: insights into defense response, secondary metabolism and root exudation. *J. Biosci*, 44(4), 98.

Kaushal, M., & Wani, S.P. (2017). Nanosensors: frontiers in precision agriculture. In: Nanotechnology, Prasad, R., Kumar, M., Kumar, V. (eds), *Springer*, Singapore, pp. 279-291.

Khan, M., Bhargava, P., & Goel, R. (2019). Quorum sensing molecules of rhizobacteria: a trigger for developing systemic resistance in plants. In: Plant growth promoting rhizobacteria for sustainable stress management, Sayyed, R., Arora, N., Reddy, M. (eds), *Springer*, Singapore, pp. 117-138.

Khan, N., Bano, A., Ali, S., & Babar, M.A.(2020). Crosstalk amongst phytohormones from planta and PGPR under biotic and abiotic stresses. *Plant Growth Regul*, 90, 189-203.

Kour, D., Rana, K.L., Yadav, N., Yadav, A.N., Kumar, A., Meena, V.S., Singh, B., Chauhan, V.S., Dhaliwal, H.S., & Saxena, A.K. (2019). Rhizospheric microbiomes: biodiversity, mechanisms of plant growth promotion, and biotechnological applications for sustainable agriculture. In: Plant growth promoting rhizobacteria for agricultural sustainability, Kumar, A., Meena, V. (ed), *Springer*, Singapore, pp. 19-65.

Kremer, R.J. (2019). Bioherbicides and nanotechnology: current status and future trends. In: Nano-biopesticides today and future perspectives, Koul, O. (ed), *Academic Press*, pp. 353-366.

Krishnaraj, C., Ramachandran, R., Mohan, K., & Kalaichelvan, P. (2012). Optimization for rapid synthesis of silver nanoparticles and its effect on phytopathogenic fungi. *Spectrochim. Acta A Mol. Biomol. Spectrosc*, 93, 95-99.

Kulkarni, R.A., Prabhuraj, A., Ashoka, J., Hanchinal, S., & Hiregoudar, S. (2017). Generation and evaluation of nanoparticles of supernatant of *Photorhabdus luminescens* (Thomas and Poinar) against mite and aphid pests of cotton for enhanced efficacy. *Curr. Sci,* 112, 2312-2316.

Kumar, M., Saxena, R., & Tomar, R.S. (2017). Endophytic microorganisms: promising candidate as biofertilizer. In: Microorganisms for green revolution, Panpatte, D., Jhala, Y., Vyas, R., Shelat, H. (eds), *Springer*, Singapore, pp. 77-85.

Li, Y., Gu, Y., Li, J., Xu, M., Wei, Q., & Wang, Y. (2015). Biocontrol agent *Bacillus amyloliquefaciens* LJ02 induces systemic resistance against cucurbits powdery mildew. *Front. Microbiol*, 6, 883.

Llorente, B.E., Alasia, M.A., & Larraburu, E.E. (2016). Biofertilization with *Azospirillum brasilense* improves in vitro culture of *Handroanthus ochraceus*, a forestry, ornamental and medicinal plant. *N Biotechnol*, 33(1), 32-40.

Ma, Y., Yao, Y., Yang, J., He, X., Ding, Y., Zhang, P., Zhang, J., Wang, G., Xie, C., Luo, W. (2018). Trophic transfer and transformation of CeO2 nanoparticles along a terrestrial food chain: influence of exposure routes. *Environ. Sci. Technol*, 52(14), 7921-7927.

Mącik, M., Gryta, A., & Frąc, M. (2020). Biofertilizers in agriculture: an overview on concepts, strategies and effects on soil microorganisms. *Adv. Agron*, 162, 31-87.

Maheshwari, D.K., Kumar, S., Kumar, B., & Pandey, P. (2010). Co-inoculation of urea and DAP tolerant *Sinorhizobium meliloti* and *Pseudomonas aeruginosa* as integrated approach for growth enhancement of *Brassica juncea*. *Indian J. Microbiol*, 50(4), 425-431.

Malaikozhundan, B., Vaseeharan, B., Vijayakumar, S., & Thangaraj, M.P. (2017). *Bacillus thuringiensis* coated zinc oxide nanoparticle and its biopesticidal effects on the pulse beetle, *Callosobruchus maculatus*. *J. Photochem. Photobiol. B, Biol*, 174, 306-314.

Maruyama, C., Guilger, M., Pascoli, M., Bileshy-José, N., Abhilash, P., Fraceto, L., & de Lima, R. (2016). Nanoparticles based on chitosan as carriers for the combined herbicides imazapic and imazapyr. *Sci. Rep*, 6 19768.

Mayak, S., Tirosh, T., & Glick, B.R.(2004). Plant growth-promoting bacteria confer resistance in tomato plants to salt stress. *Plant Physiol. Biochem*, 42(6), 565-572.

Mc-Carthy, U., Uysal, I., Badia-Melis, R., Mercier, S., O'Donnell, C., & Ktenioudaki, A. (2018). Global food security–Issues, challenges and technological solutions. *Trends Food Sci. Technol*, 77, 11-20.

Meybeck, A., Laval, E., Lévesque, R., & Parent, G. (2018). Food security and nutrition in the age of climate change. In: *Proceedings of the International Symposium organized by the Government of Québec in collaboration with FAO, Québec City*, pp. 132.

Meyer, S.L., Everts, K.L., Gardener, B.M., Masler, E.P., Abdelnabby, H.M., & Skantar, A.M. (2016). Assessment of DAPG-producing Pseudomonas fluorescens for management of *Meloidogyne incognita* and *Fusarium oxysporum* on watermelon. *J. Nematol,* 48(1), 43.

Mishra, S., Singh, B.R., Naqvi, A.H., & Singh, H. (2017). Potential of biosynthesized silver nanoparticles using *Stenotrophomonas* sp. BHU-S7 (MTCC 5978) for management of soil-borne and foliar phytopathogens. *Sci. Rep*, 7(1), 1-15.

Mishra, S., Singh, B.R., Singh, A., Keswani, C., Naqvi, A.H., & Singh, H. (2014). Biofabricated silver nanoparticles act as a strong fungicide against *Bipolaris sorokiniana* causing spot blotch disease in wheat. *PLoS One*, 9(5), e97881.

Misra, S., & Chauhan, P.S. (2020). ACC deaminase-producing rhizosphere competent *Bacillus* spp. mitigate salt stress and promote *Zea mays* growth by modulating ethylene metabolism. *3 Biotech*, 10(3), 1-14.

Mohanram, S., & Kumar, P. (2019). Rhizosphere microbiome: revisiting the synergy of plant-microbe interactions. *Ann. Microbiol*, 69(4), 307-320.

Moharana, P., Meena, M., & Biswas, D. (2018). Role of phosphate-solubilizing microbes in the enhancement of fertilizer value of rock phosphate through composting technology. In: Role of rhizospheric microbes in soil, Meena, V. (ed), *Springer*, Singapore, pp. 167-202.

Mukherjee, A., Maity, A., Pramanik, P., Shubha, K., Joshi, D., & Wani, S. (2019). Public perception about use of nanotechnology in agriculture. In: Advances in phytonanotechnology, Ghorbanpour, M., Wani, S. H. (ed), *Academic Press*, pp. 405-418.

Mukherjee, D. (2019). Microbial interventions in soil and plant health for improving crop efficiency. In: Microbial interventions in agriculture and environment, Singh, D., Prabha, R. (ed) *Springer*, Singapore, pp. 17-47.

Abdul Malik, N.A., Kumar, I.S., & Nadarajah, K. (2020). Elicitor and receptor molecules: orchestrators of plant defense and immunity. *Int. J. Mol. Sci*., 21(3), 963.

Nadarajah, K.K. (2017). Induction of systemic resistance for disease suppression. In: Crop improvement, Abdullah, S., Chai-Ling, H., Wagstaff, C. (eds), *Springer*, Cham, pp. 335-357.

Namasivayam, S.K.R., Tony, B., Bharani, R.A., & Raj, F.R. (2015). Herbicidal activity of soil isolate of *Fusarium oxysporum* free and chitosan nanoparticles coated metabolites against economic important weed *Ninidam theenjan*. *Asian J. Microbiol. Biotechnol. & Environ Sci*, 17, 1015-1020.

Nuruzzaman, M., Rahman, M.M., Liu, Y., & Naidu, R. (2016). Nanoencapsulation, nano-guard for pesticides: a new window for safe application. *J. Agric. Food Chem*, 64(7), 1447-1483.

Odelade, K.A., & Babalola, O.O. (2019). Bacteria, fungi and archaea domains in rhizospheric soil and their effects in enhancing agricultural productivity. *Int. J. Environ. Res. Public Health*, 16(20), 3873.

Ojha, S., Singh, D., Sett, A., Chetia, H., Kabiraj, D., & Bora, U. (2018). Nanotechnology in crop protection. In: Nanomaterials in plants, algae, and microorganisms, Tripathi, D.K., Ahmad, P., Sharma, S., Chauhan, D.K., Dubey, N.K. (eds), *Academic Press*, pp. 345-391.

Olanrewaju, O.S., Ayangbenro, A.S., Glick, B.R., & Babalola, O.O. (2019). Plant health: feedback effect of root exudates-rhizobiome interactions. *Appl. Microbiol. Biotechnol*, 103(3), 1155-1166.

Orozco-Mosqueda, M.d.C., Rocha-Granados, M.d.C., Glick, B.R., & Santoyo, G. (2018). Microbiome engineering to improve biocontrol and plant growth-promoting mechanisms. *Microbiol. Res,* 208, 25-31.

Orr, R., & Nelson, P.N. (2018). Impacts of soil abiotic attributes on *Fusarium* wilt, focusing on bananas. *Appl. Soil Ecol,* 132, 20-33.

Ortíz-Castro, R., Contreras-Cornejo, H.A., Macías-Rodríguez, L., & López-Bucio, J. (2009). The role of microbial signals in plant growth and development. *Plant Signal. Behav*, 4(8), 701-712.

Ortiz-Castro, R., & López-Bucio, J. (2019). Phytostimulation and root architectural responses to quorum-sensing signals and related molecules from rhizobacteria. *Plant Sci*, 284, 135-142.

Osman, K.T. (2018). Degraded soils. In: Management of soil problems, *Springer*, Cham, pp. 409-456.

Pallavi, Chandra, D., & Sharma, A. (2017). Commercial microbial products: exploiting beneficial plant-microbe interaction. In: Plant-microbe interactions in agro-ecological perspectives, Singh, D., Singh, H., Prabha, R. (eds), *Springer*, Singapore, pp. 607-626.

Panth, M., Hassler, S.C., & Baysal-Gurel, F. (2020). Methods for management of soilborne diseases in crop production. *Agriculture*, 10(1), 16.

Patel, J.S., Yadav, S.K., Bajpai, R., Teli, B., & Rashid, M. (2020). PGPR secondary metabolites: an active syrup for improvement of plant health. In: Molecular aspects of plant beneficial microbes in agriculture, Sharma, V., Salwan, R., Al-Ani, L.K.T (eds), *Academic Press*, pp. 195-208.

Pereira, L., Dias, N., Carvalho, J., Fernandes, S., Santos, C., & Lima, N. (2014). Synthesis, characterization and antifungal activity of chemically and fungal-produced silver nanoparticles against *Trichophyton rubrum*. *J. Appl. Microbiol*, 117(6), 1601-1613.

Pérez-de-Luque, A., & Hermosín, M.C. (2013). Nanotechnology and its use in agriculture. In: Bio-nanotechnology: a revolution in food, biomedical and health sciences, Bagchi, D., Bagchi, M., Moriyama, H., Shahidi, F. (eds), *John Wiley & Sons*, pp. 383-398.

Petit, A.-N., Fontaine, F., Vatsa, P., Clément, C., & Vaillant-Gaveau, N. (2012). Fungicide impacts on photosynthesis in crop plants. *Photosynth. Res*, 111(3), 315-326.

Prudent, M., Salon, C., Souleimanov, A., Emery, R.N., & Smith, D.L. (2015). Soybean is less impacted by water stress using *Bradyrhizobium japonicum* and thuricin-17 from *Bacillus thuringiensis*. *Agron. Sustain. Dev*, 35(2), 749-757.

Rad, F., Mohsenifar, A., Tabatabaei, M., Safarnejad, M., Shahryari, F., Safarpour, H., Foroutan, A., Mardi, M., Davoudi, D., & Fotokian, M. (2012). Detection of *Candidatus phytoplasma aurantifolia* with a quantum dots FRET-based biosensor. *Plant Pathol. J*, 94, 525-534.

Radhakrishnan, R., Alqarawi, A.A., & Abd_Allah, E.F. (2018). Bioherbicides: current knowledge on weed control mechanism. *Ecotoxicol. Environ. Saf,* 158, 131-138.

Reed, M., Glick, B.R., & Gupta, V. (2013). Applications of plant growth-promoting bacteria for plant and soil systems. Applications of microbial engineering. *Taylor and Francis*, Enfield, 181-229.

Rijavec, T., & Lapanje, A. (2016). Hydrogen cyanide in the rhizosphere: not suppressing plant pathogens, but rather regulating availability of phosphate. *Front. Microbiol*, 7, 1785.

Rodríguez, J., Martín, M.J., Ruiz, M.A., & Clares, B. (2016). Current encapsulation strategies for bioactive oils: from alimentary to pharmaceutical perspectives. *Food Res. Int*, 83, 41-59.

Rojas-Sánchez, B., Guzmán-Guzmán, P., Morales-Cedeño, L.R., Orozco-Mosqueda, M.d.C., Saucedo-Martínez, B.C., Sánchez-Yáñez, J.M., Fadiji, A.E., Babalola, O.O., Glick, B.R., & Santoyo, G. (2022). Bioencapsulation of microbial inoculants: Mechanisms, formulation types and application techniques. *Appl. Biosci*, 1(2), 198-220.

Rosier, A., Medeiros, F.H., & Bais, H.P. (2018). Defining plant growth promoting rhizobacteria molecular and biochemical networks in beneficial plant-microbe interactions. *Plant Soil*, 428(1-2), 35-55.

Rubin, R.L., van Groenigen, K.J., & Hungate, B.A. (2017). Plant growth promoting rhizobacteria are more effective under drought: a meta-analysis. *Plant Soil*, 416(1-2), 309-323.

Ruzzi, M., & Aroca, R. (2015). Plant growth-promoting rhizobacteria act as biostimulants in horticulture. *Sci. Hortic*, 196, 124-134.

Ryan, R.P., An, S.-q., Allan, J.H., McCarthy, Y., & Dow, J.M. (2015). The DSF family of cell–cell signals: an expanding class of bacterial virulence regulators. *PLoS Pathogens*, 11(7), e1004986.

Samanta, P., & Mandal, A. (2017). Effect of nanoparticles on biodiversity of soil and water microorganism community. *J. Tissue Sci. Eng*. 8, 196.

Schikora, A., Schenk, S.T., & Hartmann, A. (2016). Beneficial effects of bacteria-plant communication based on quorum sensing molecules of the N-acyl homoserine lactone group. *Plant Mol. Biol*, 90(6), 605-612.

Schütz, L., Gattinger, A., Meier, M., Müller, A., Boller, T., Mäder, P., & Mathimaran, N. (2018). Improving crop yield and nutrient use efficiency via biofertilization—a global meta-analysis. *Front. Plant Sci*, 8, 2204.

Seneviratne, G., Weerasekara, M., Kumaresan, D., & Zavahir, J. (2017). Microbial signaling in plant—microbe interactions and its role on sustainability of agroecosystems. *AgroEnviron. Sustain*, 1, 1-17.

Shabbir, R.N., Ali, H., Nawaz, F., Hussain, S., Areeb, A., Sarwar, N., & Ahmad, S. (2019). Use of biofertilizers for sustainable crop production. In: Agronomic crops, Hasanuzzaman, M. (ed), *Springer*, Singapore, pp. 149-162.

Shah, V., & Belozerova, I. (2009). Influence of metal nanoparticles on the soil microbial community and germination of lettuce seeds. *Water Air Soil Pollut*, 197(1), 143-148.

Shukla, S.K., Kumar, R., Mishra, R.K., Pandey, A., Pathak, A., Zaidi, M., Srivastava, S.K., & Dikshit, A. (2015). Prediction and validation of gold nanoparticles (GNPs) on plant growth promoting rhizobacteria (PGPR): a step toward development of nano-biofertilizers. *Nanotechnol. Rev*, 4(5), 439-448.

Simonin, M., & Richaume, A. (2015). Impact of engineered nanoparticles on the activity, abundance, and diversity of soil microbial communities: a review. *Environ. Sci. Pollut. Res*, 22(18), 13710-13723.

Singh, A., Singh, N., Hussain, I., Singh, H., & Singh, S. (2015). Plant-nanoparticle interaction: an approach to improve agricultural practices and plant productivity. *Int. J. Pharm. Sci. Invent,* 4(8), 25-40.

Singh, J., Vishwakarma, K., Ramawat, N., Rai, P., Singh, V.K., Mishra, R.K., Kumar, V., Tripathi, D.K., & Sharma, S. (2019). Nanomaterials and microbes' interactions: a contemporary overview. *3 Biotech*, 9(3), 1-14.

Singhal, B., & Rana, S. (2019). Nanosensors in food safety: current status, role, and future perspectives. In: Nanotechnology and nanomaterial applications in food, health, and biomedical sciences, Verma, D.K., Goya, M.R., Suleria, H.A.R. (eds), *Apple Academic Press*, Boca Raton, pp. 249-292.

Someya, N., Kubota, M., Takeuchi, K., Unno, Y., Sakuraoka, R., & Morohoshi, T. (2020). Diversity of antibiotic biosynthesis gene-possessing rhizospheric fluorescent *Pseudomonads* in Japan and their biocontrol efficacy. *Microbes Environ*, 35(2), ME19155.

Subrahmanyam, G., Kumar, A., Sandilya, S.P., Chutia, M., & Yadav, A.N. (2020). Diversity, plant growth promoting attributes, and agricultural applications of rhizospheric microbes. In: Plant microbiomes for sustainable agriculture, Yadav, A., Singh, J., Rastegari, A., Yadav, N. (eds), *Springer*, Cham, pp. 1-52.

Suresh, A., & Abraham, J. (2019). Harnessing the microbial interactions in rhizosphere and microbiome for sustainable agriculture. In: Microbial interventions in agriculture and environment, Singh, D., Gupta, V., Prabha, R. (eds), *Springer*, Singapore, pp. 497-515.

Tripathi, A.D., Mishra, R., Maurya, K.K., Singh, R.B., & Wilson, D.W. (2019). Estimates for world population and global food availability for global health. In: The role of functional food security in global health, Singh, R. B., Watson, R.R., Takahashi, T. (eds), *Academic Press*, pp. 3-24.

Trivedi, P., Leach, J.E., Tringe, S.G., Sa, T., & Singh, B.K. (2020). Plant–microbiome interactions: from community assembly to plant health. *Nat. Rev. Microbiol*, 18(11), 607-621.

Tsukanova, K., Meyer, J., & Bibikova, T. (2017). Effect of plant growth-promoting *Rhizobacteria* on plant hormone homeostasis. *S. Afr. J. Bot*, 113, 91-102.

Vaid, S.K., Srivastava, P.C., Pachauri, S.P., Sharma, A., Rawat, D., Shankhadhar, S.C., & Shukla, A.K. (2020). Effective zinc mobilization to rice grains using rhizobacterial consortium. *Isr. J. Plant Sci*, 1, 1-13.

Verma, P.P., Shelake, R.M., Das, S., Sharma, P., & Kim, J.-Y. (2019). Plant growth-promoting rhizobacteria (PGPR) and fungi (PGPF): potential biological control agents of diseases and pests. In: Microbial interventions in agriculture and environment, Singh, D., Gupta, V., Prabha, R. (eds), *Springer*, Singapore, pp. 281-311.

Wang, J., Li, R., Zhang, H., Wei, G., & Li, Z. (2020). Beneficial bacteria activate nutrients and promote wheat growth under conditions of reduced fertilizer application. *BMC Microbiol*, 20(1), 1-12.

Wenz, J., Davis, J.G., & Storteboom, H. (2019). Influence of light on endogenous phytohormone concentrations of a nitrogen-fixing *Anabaena* sp. cyanobacterium culture in open raceways for use as fertilizer for horticultural crops. *J. Appl. Phycol*, 31(6), 3371-3384.

Wilkinson, S.W., Magerøy, M.H., López Sánchez, A., Smith, L.M., Furci, L., Cotton, T.A., Krokene, P., & Ton, J. (2019). Surviving in a hostile world: plant strategies to resist pests and diseases. *Annu. Rev. Phytopathol,* 57, 505-529.

Win, T.T., Barone, G.D., Secundo, F., & Fu, P. (2018). Algal biofertilizers and plant growth stimulants for sustainable agriculture. *Ind. Biotechnol*, 14(4), 203-211.

Win, T.T., Bo, B., Malec, P., Fu, P. (2021). The effect of a consortium of *Penicillium* sp. and *Bacillus* spp. in suppressing banana fungal diseases caused by *Fusarium* sp. and *Alternaria* sp. *J. Appl. Microbiol*, 131(4), 1890-1908.

Yadav, A., Kon, K., Kratosova, G., Duran, N., Ingle, A.P., & Rai, M. (2015). Fungi as an efficient mycosystem for the synthesis of metal nanoparticles: progress and key aspects of research. *Biotechnol. Lett*, 37(11), 2099-2120.

Ye, L., Zhao, X., Bao, E., Li, J., Zou, Z., & Cao, K. (2020). Bio-organic fertilizer with reduced rates of chemical fertilization improves soil fertility and enhances tomato yield and quality. *Sci. Rep*, 10(1), 1-11.

Zhang, F., & Smith, D.L. (1995). Preincubation of *Bradyrhizobium japonicum* with genistein accelerates nodule development of soybean at suboptimal root zone temperatures. *Plant Physiol*, 108(3), 961-968.

Zhao, S., Zhou, N., Zhao, Z.-Y., Zhang, K., Wu, G.-H., & Tian, C.-Y. (2016). Isolation of endophytic plant growth-promoting bacteria associated with the halophyte Salicornia europaea and evaluation of their promoting activity under salt stress. *Curr. Microbiol*, 73(4), 574-581.

Zhou, C., Ma, Z., Zhu, L., Xiao, X., Xie, Y., Zhu, J., & Wang, J. (2016). Rhizobacterial strain *Bacillus megaterium* BOFC15 induces cellular polyamine changes that improve plant growth and drought resistance. *Int. J. Mol. Sci*, 17(6), 976.

Zhou, N., Zhao, S., & Tian, C.-Y. (2017). Effect of halotolerant rhizobacteria isolated from halophytes on the growth of sugar beet (*Beta vulgaris* L.) under salt stress. *FEMS Microbiol. Lett*, 364(11), fnx091.

Zhu, J., Tan, T., Shen, A., Yang, X., Yu, Y., Gao, C., Li, Z., Cheng, Y., Chen, J., & Guo, L. (2020). Biocontrol potential of Bacillus subtilis IBFCBF-4 against *Fusarium* wilt of watermelon. *Plant Pathol. J*, 102, 443-441.

Zulfiqar, F., Navarro, M., Ashraf, M., Akram, N.A., & Munné-Bosch, S. (2019). Nanofertilizer use for sustainable agriculture: advantages and limitations. *Plant Sci*, 289, 110270.

Impact of plant-based nanoparticles synthesized from *Carica papaya* and *Bryophyllum pinnatum* against selected microorganisms

Francis Aibuedefe Igiebor[1]✉, Favour Chinaza Michael[1],
Ochoyama Haruna[2], and Beckley Ikhajiagbe[3]

[1]*Department of Biological Sciences, College of Science and Computing, Wellspring University, Benin City, Nigeria;* [2]*Department of Science Laboratory Technology, Faculty of Life Sciences, University of Benin, Benin City, Nigeria;* [3]*Department of Plant Biology and Biotechnology, Faculty of Life Sciences, University of Benin, Benin City, Nigeria;*
✉**Corresponding author, E-mail: francis.igiebor@lifesci.uniben.edu.**

Abstract. Plant-based nanoparticles offer sustainable, eco-friendly alternatives to conventional methods, promising antibacterial properties in the face of antibiotic resistance and addressing global health concerns. Five urine and stool samples were collected from the Benin Medical Centre in Benin City, Edo State, and sent to the Wellspring University Research Laboratory for microbiological analysis. *Carica papaya* and *Bryophyllum pinnatum* were used for fresh utilization by washing, weighing, and crushing their leaves, then mixing them with distilled water and heating at 85 °C and 60 °C for 60 minutes. Silver and copper nanoparticles (AgNPs and CuNPs) were synthesized using standard procedures. The NPs were preliminary validated by visual detection of color changes and characterized using a UV-visible spectrophotometer at 300 nm and Fourier transform infrared. The *in vitro* antimicrobial activity of plant-mediated NPs was investigated using five isolates: *S. aureus*, *B. alvei*, *H. pylori*, *P. aeruginosa*, and *E. coli*. The *in vitro* antimicrobial activity of plant-mediated NPs was investigated using five clinical strains displaying multiple resistance to antibiotics: *S. aureus*, *B. alvei*, *H. pylori*, *P. aeruginosa*, and *E. coli*. The agar-well diffusion method showed inhibition of the isolates by plant-mediated NPs but no inhibition by the plant extract alone. The study indicates that plant-mediated NPs

exhibit promising antimicrobial activity, promoting sustainability and eco-friendliness, but further research is needed to assess their safety and efficacy in clinical settings.

Keywords: nanoparticles, resistant, antimicrobial, plant-mediated, MAR index.

Introduction

Plant-based nanoparticles are the green synthesis of nanoparticles (NPs) mediated by plant leaves, stems, soot, fruits, and roots (Ikhajiagbe *et al.*, 2021; Igiebor *et al.*, 2023). These NPs offer a sustainable and eco-friendly alternative to conventional methods of synthesis (Igiebor *et al.*, 2023). By harnessing the natural compounds present in plants, such as flavonoids, phenols, and terpenoids, researchers can create NPs with unique properties and applications (Marslin *et al.*, 2018). The versatility of these NPs is remarkable, as they can be tailored for various purposes, including drug delivery systems, water purification, catalysis, and even solar cells (Gupta and Xie, 2018; Joseph *et al.*, 2023; Yusuf *et al.*, 2023). Moreover, the abundance and diversity of plant sources make this approach highly scalable and cost-effective. With ongoing advancements in this field, plant-based nanoparticles hold great promise for revolutionizing numerous industries while minimizing environmental impact.

NPs are classified based on their physical and chemical properties. Different types of nanoparticles are carbon-based NPs, metal NPs, semi-conductor NPs, lipid-based NPs, ceramic NPs, and polymeric NPs (Troncarelli *et al.*, 2013; Igiebor *et al.*, 2023). Under the category of metal NPs, silver (Ag), copper (Cu), zinc (Zn), iron (Fe), and gold (Au) are currently used NPs with great antibacterial properties (Sánchez-López *et al.*, 2020; Skłodowski *et al.*, 2023).

According to Kuppusamy *et al.* (2016), plant-based NPs have excellent antibacterial activity against organisms that are resistant to antibiotics. The great stability and quick rate of plant-based NPs generated interest in understanding and describing the mechanisms of metal ion absorption and bioreduction by plants as a result of the biosynthesis of metal NPs. In this way, numerous investigations have supported this. As a result, a number of plant-based NPs have been successfully synthesized (Ikhajiagbe *et al.*, 2021; Igiebor *et al.*, 2023). Plants such as *Brassica juncea* (mustard greens, Brassicaceae), *Medicago sativa* (alfalfa, Fabaceae), and *Helianthus annuus* (sunflower, Asteraceae) can accumulate a significant amount of silver when it is present in the substrate (Aswini *et al.*, 2021).

The most researched plant-based NPs are silver nanoparticles (AgNPs), which have mainly been linked to the production of powerful antibacterial and antifungal capabilities. In order to synthesize silver nanoparticles (AgNPs), Malabadi *et al*. (2012) employed cell cultures from the leaves, callus, and roots of *Catharanthus roseus* (Apocynaceae). The maximum antimicrobial activity of stabilized AgNPs against all pathogens tested has been demonstrated, demonstrating the efficacy, affordability, and environmental friendliness of nanoparticles with the desired features. It has also been reported that AgNPs can be synthesized quickly, in just 5 hours, by reducing aqueous Ag$^+$ ions with *Dioscorea bulbifera* tuber extract (Dioscoreaceae). The resulting AgNPs have potent antibacterial properties against both Gram-negative and Gram-positive bacteria. Due to its distinctive phytochemistry, this plant species also has significant therapeutic potential (Ghosh *et al*., 2012).

Moreover, copper nanoparticles (CuNPs) have also shown promising antimicrobial properties. These NPs have been synthesized using various methods, including chemical reduction and green synthesis approaches. In other studies (Ali *et al*., 2021; Ahmed *et al*., 2023), CuNPs were successfully prepared using the leaf extract of *Azadirachta indica* (Neem). The synthesized CuNPs exhibited potent antibacterial activity against both Gram-positive and Gram-negative bacteria, making them a potential candidate for combating microbial infections. Also, CuNPs have been found to possess antifungal properties, as demonstrated in a study by Singh *et al*. (2020). They reported that CuNPs synthesized using the fruit extract of *Syzygium cumini* showed significant inhibition of fungal growth, highlighting their potential as an alternative treatment for fungal infections. Therefore, the development of silver and copper nanoparticles offers a promising avenue for the production of effective antimicrobial agents with broad-spectrum activity against bacteria.

Materials and methods

Sample collection

A total of five (5) samples were obtained from the Benin Medical Centre (BMC), Benin City, Edo State. The samples were immediately transported to the laboratory for microbiological analysis. Fresh leaves of *Carica papaya* and *Bryophyllum pinnatum* were obtained from the agricultural farm at Wellspring University, Benin City, Edo State.

Preparation of leaves extract

Carica papaya leaves were washed with distilled water to remove dust and dirt on the surface of the leaves and to leave no impurities. For fresh use, 20g of the leaves was weighed using the weighing balance, and thereafter transferred into mortar and pestle, the leaves were carefully crushed and transferred into a beaker containing 100 ml of distilled water. The mixture was heated in a water bath at 85 °C for 60 minutes, and then kept to cool at room temperature. The mixture was filtered using whatman filter paper.

The surface *Bryophyllum pinnatum* leaves were washed with distilled water and crushed into tiny pieces on a foil paper and was placed into the oven at 60 °C until fully dried, the dried plant leaves was grinded to fine powder using a dry electrical blender, 5 g of the plant powder was dissolved into 50 ml of distilled water and was placed in the water bath at 60 °C for 60 minutes, when it cooled to room temperature, the plant extract was filtered using whatman filter paper.

Synthesis of silver nanoparticles (AgNPs) using plant extracts

For the synthesis of silver nanoparticles, 1.7 g of $AgNO_3$ salt was dissolved in 1000 ml of distilled water to prepare 10 mM of $AgNO_3$ stock solution. Thereafter, 45 ml of precursor $AgNO_3$ solution was measured in a measuring cylinder and poured into a beaker covered in foil paper and labelled for each plant extract, 5 ml of the aqueous extract of *Carica papaya* filtrate is dropped (using dropping pipette) into the beaker containing silver nitrate ($AgNO_3$), while stirring using magnetic stirrer for an hour, during this synthesis the lights in the laboratory was switched off. There was an observation for change in colour. The same procedure was done for *Bryophyllum pinnatum* filtrate, 5 ml of the plant extract filtrate of *Bryophyllum pinnatum* was dropped into the beaker (the beaker was also wrapped in foil paper) containing 45 ml of silver nitrate, while stirring on the magnetic stirrer, during this synthesis the lights in the laboratory was also switched off, there was an observation for colour change. The formation of AgNPs was characterized with the development of colour, which was produced as a result of the reduction of silver ion by biomolecules present in the plant extract. The colour of the solute changed (Melkamu and Bitew, 2021; Asif *et al.*, 2022).

Synthesis of copper nanoparticles (CuNPs) using plant extract

The synthesis was done according to the method of Rajesh *et al.* (2018). 24.9 g of copper sulphate ($CuSO_4$) was dissolved in 1000 ml distilled water to prepare 10 Mm of $CuSO_4$ stock solution. CuNPs were produced by dropping

1 ml (using a dropping pipette) of *Bryophyllum pinnatum* extract into a beaker (the beaker was wrapped in foil paper and labelled), containing 20 ml of the precursor $CuSO_4$, while stirring using the magnetic stirrer for an hour, there was an observation for change in colour. The same procedure was done for *Carica papaya* leave extract filtrate, 1ml of the leave extract filtrate was poured into a beaker (the beaker was labelled and wrapped in foil paper) containing 20 ml of precursor $CuSO_4$, while stirring on the magnetic stirrer, an observation of colour change was expressed.

Antibacterial activity of AgNPs and CuNPs on the selected pathogens

The *in vitro* antimicrobial activity of AgNPs and CuNPs was investigated using the method of Balouiri *et al*. (2016). Filter paper disc diffusion and Agar wells methods were used to test the antibacterial capabilities of CuNPs and AgNPs, to test if silver nitrate ($AgNO_3$) and copper sulphate ($CuSO_4$) has inhibitory effects, as well as compare the nanoparticles synthesised from each plant (*Bryophyllum pinnatum* and *Carica papaya*) for their inhibition activities.

Filter paper disc diffusion test

This was carried out using the methods of Zia *et al*. (2018). A 3.8 g of Mueller Hinton agar was dissolved in 100 ml of distilled water and autoclaved at 121 °C for 25 minutes. After sterilization the medium was kept to cool, then poured into sterile Petri plates/dish (one dish for each isolate) to solidify. Sterile swab sticks were used to collect an inoculum and spread evenly on the surface of Mueller Hinton agar plates, filter papers were carefully cut to small circular pieces and soaked with CuNPs, AgNPs, plant extract, $CuSO_4$, and $AgNO_3$ separately. The filter paper discs loaded with CuNPs, AgNPs, plant extract, $CuSO_4$, and $AgNO_3$ was placed on the surface of the inoculated plates (each solute was placed according the label at the back of the plates). Before incubation, the plates were kept at room temperature for few minutes to allow the diffusion of the solutions, and then afterwards placed at 37 °C for 24 hours. The zones of inhibition was measured (diameter in mm). This procedure was done for each extract solution; this implies the nanoparticles synthesized from each plant extract followed this filter disc diffusion step.

Agar wells diffusion method

Zia *et al*. (2018) protocol was adopted with few modifications. A 9.5 g of Mueller Hinton agar to 250 ml of distilled water was prepared and sterilized using the autoclave at 121 °C. The medium was transferred to Petri plates and

allowed to solidify. A sterile swab stick was used to collect an inoculum and spread evenly on the surface of the agar plates. After some time, five wells were punched into the inoculated Mueller Hinton agar plates that was well separated using 6 mm cork borer, thereafter 10 μL (using a micropipette) of CuNPs, AgNPs, $CuSO_4$, $AgNO_3$ and plant extract solution are poured into each well, the samples were allowed to diffuse into the agar by keeping them under room temperature for few minutes, before proceeding to keep in the incubator, after 24 hours of incubation, the diameter of the zone of inhibition was evaluated and measured in mm. the inhibition zone of the different nanoparticles (CuNPs and AgNPs) that was gotten from the two plants (*Bryophyllum pinnatum* and *Carica papya*) used was compared and recorded.

Nanoparticles characterization

UV-visible characterization

UV-Visible spectroscopy analysis was carried out on a UV Visible absorption spectrophotometer. Equal amounts of the suspension were taken and analysed at room temperature. The progress of the reaction between metal ions and the leaf extract was monitored at different wavelength, between spectra ranges of 300 to 800 nm.

Fourier Transform Infrared (FT-IR) characterization

This technique is a powerful tool used to identify the chemical bonds in a molecule by producing an IR spectrum that is similar to a molecular fingerprint. FT-IR characterization was also done to analyse the functional groups of samples. About 1-2 mg of powdered leaves samples were mixed with potassium bromide, pressed into a pellet (KBr pellet) and placed in the machine. The FT-IR instrument sent infrared radiation of about 10,000 to100 cm^{-1} through the sample, with some radiation absorbed and some passed through. The absorbed radiation was converted into rotational and vibrational energy by the sample molecules. The resulting signal at the detector presents as a spectrum, typically from 4000 cm^{-1} to 400 cm^{-1}, representing a molecular fingerprint of the sample. Each molecule or chemical structure thus produces a unique spectral finger print (Wang and Weller, 2006).

Identification of the isolates collected

Isolates were identified following the procedure of Cheesbrough (2006). The colony morphology of the isolates were observed and recorded. Gram staining of the isolates was carried out. The biochemical tests used to confirm

the collected isolates were oxidase, citrate, catalase, motility, sugar fermentation, indole, urease, coagulase (Maduka *et al.*, 2022).

Antimicrobial Susceptibility Test (AST)

Antimicrobial susceptibility test was carried out on each isolate using the disc diffusion method, to evaluate the sensitivity of test organisms to various antibiotics. Mueller hinton agar was used for this medium, 3.8 g of Mueller Hinton agar was dissolved in 100 ml of distilled water, an sterilized in the autoclave at 121 ℃ for 25 minutes, the medium was poured into petri plates/dish to solidify, using a sterile swab the test organism was carefully spread on the agar plate, waited for few seconds before placing the discs, the discs was placed on the surface of the inoculated Mueller Hinton agar plate (using a sterile forceps) then placed inside the incubator 37 ℃ for 24 hrs. After incubation, diameters (measured in mm) of zones of inhibition were measured using a ruler, the results for sensitivity and resistance was evaluated using Clinical Laboratory Standard Institute (CLSI, 2020).

Multiple antibiotic resistance (MAR) index

The MAR was determined for each isolate by dividing the number of antibiotics the isolate was resistant to by the total number of antibiotics tested (Ehiaghe *et al.*, 2022).

$$MAR\ index = \frac{a}{b}$$

Key: a = the number of antibiotics which the test isolate showed resistance; b = the total number of antibiotics used in subjecting the isolates to susceptibility test.

Results

Table 1 shows the qualitative phytochemical screening of *Bryophyllum pinnatum* and *Carica papaya* leaves. The content of cardiac glycosides was very high in *Bryophyllum pinnatum* but high in *Carica papaya*. Flavonoids, tannins, saponin, steroids, phenols, alkaloids and terpenoids contents were present in both plants, whereas phlabotannins, coumarin and anthraquinone contents were absent.

Table 1. Qualitative phytochemical screening
of *Bryophyllum pinnatum* and *Carica papaya* leaves

Active ingredients	*Bryophyllum pinnatum*	*Carica papaya*
Flavonoids	++	++
Tannins	++	++
Cardiac glycosides	+++	++
Saponin	-	+
Steroids	++	+
Phenols	++	++
Phlabotannins	-	-
Coumarin	-	-
Alkaloids	+	++
Anthraquinone	-	-
Terpenoids	+	++

Key: - Negative (Absent); + Positive (Present) But low; ++ (High); +++ (Very high)

Table 2 shows the results of the antibiotics susceptibility test for Gram-positive bacteria. Two clinical isolates were tested against twelve antibiotics, *Staphylococcus aureus* was resistant to ten antibiotics and sensitive to only two antibiotucs. However, *Bacillus alvei* was resistant to all the twelve antibiotics.

Table 3 shows the results of the antibiotics susceptibility test for Gram-negative bacteria. Three clinical isolates were tested against twelve antibiotics. *Pseudomonas aeruginosa* and *Helicobacter pylori* were resistant to all the twelve antibiotics. However, *Escherichia coli* was only sentivie to only one antibiotic (ofloxacin), but resistant to eleven antibiotics.

Table 4 shows the multiple antibiotic resistance (MAR) index of the isolates. It was observed that the isolates MAR index was greater than 0.2 signified that the organisms have originated from high- risk sources of contamination, where antibiotics are often used.

Table 2. Antibiotics susceptibility test for Gram-positive bacteria

Antibiotic disks			Inhibition zone diameter (mean±standard deviation, mm)		**CLSI standard (mm)	
Test/ Report group	Antimicrobial agent	Disk content	**Staphylococcus aureus*	**Bacillus alvei*	S ≥	R ≤
Aminoglycosides	Gentamicin	10µg	R	R	15	12
Macrolides	Azithromycin	15µg	R	11.67±2.08	18	13
	Erythromycin	15µg	R	R	23	13
Quinolones & Fluoroquinolones	Ciprofloxacin	5µg	14.67±1.33	13.67±1.45	21	15
	Levofloxacin	5µg	R	R	19	15
	Ofloxacin	5µg	R	R	18	14
Carbapenems	Imipenem	5µg	20.67±1.76	11.00±0.58	19	15
β-lactam combinations	Amoxicillin-clavulanate	30µg	19.00±1.53	15.33±1.76	18	13
	Cefotaxime	25µg	R	R	26	22
Cephems (parenteral)	Ceftriaxone	45µg	11.00±0.58	R	23	19
	Cefuroxime	30µg	R	14.00±2.00	18	14
Cephems (oral)	Cefixime	5µg	R	R	19	15

*CLSI standard for *Bacillus alvei* could not be determined;

**CLSI standard for *Staphylococcus aureus*

Key: S = Sensitive; I = Intermediate; R = Resistant.

Figure 1 shows the absorbance spectrum of plant-mediated nanoparticles. It was observed that *Carica papaya*-mediated AgNPs and *Bryophyllum pinnatum*-mediated CuNPs had the highest absorbance, of 1.9 at 300 nm. *Bryophyllum pinnatum*-mediated AgNPs had absorbance of 1.6 and *Carica papaya*-mediated CuNPs had absorbance of 1.3 at 300 nm.

Table 3. Antibiotics susceptibility test for Gram-negative bacteria

Antibiotic disks			Inhibition zone diameter (mean±standard deviation, mm)			**CLSI standard (mm)	
Test/Report group	Antimicrobial agent	Disk content	**Pseudomonas aeruginosa*	*Helicobacter pylori*	**Escherichia coli*	S ≥	R ≤
Aminoglycosides	Gentamicin	10µg	13.33±1.76	12.00±1.15	12.67±1.76	15	12
Quinolones & Fluoroquinolones	Levofloxacin	5µg	14.00±2.31	14.00±2.31	16.00±2.31	22	14
	Ofloxacin	5µg	R	R	23.33±1.76	16	12
	Nalidixic acid	30µg	R	R	13.33±1.76	19	13
Carbapenems	Imipenem	10µg	R	R	R	19	15
β-lactam combinations	Amoxicillin-clavulanate	30µg	R	R	R	18	13
Cephems (parenteral)	Cefotaxime	25µg	R	R	13.33±2.40	26	22
	Ceftriaxone	45µg	11.33±1.33	14.00±1.15	R	23	19
	Cefuroxime	30µg	R	10.67±0.67	R	18	14
Cephems (oral)	Cefixime	5µg	R	12.00±1.15	14.67±2.91	18	14
Nitrofurans	Nitrofurantoin	300µg	14.00±1.15	10.00±0.00	R	17	14
Penicillins	Ampiclox	10µg	R	R	13.33±1.76	17	13

*CLSI standard for *Helicobacter pylori* could not be determined;

**CLSI standard for *Pseudomonas aeruginosa* and *Escherichia coli*

Key: S = Sensitive; I = Intermediate; R = Resistant.

Table 4. Multiple antibiotic resistance (MAR) index of the isolates

Isolates	Sample	MAR index	Standard (≤0.2)
Staphylococcus aureus	Urine	0.83	
Escherichia coli	Urine	0.92	
Pseudomonas aeruginosa	Urine	1.00	**High risk**
Helicobacter pylori	Stool	1.00	
Bacillus alvei	Stool	1.00	
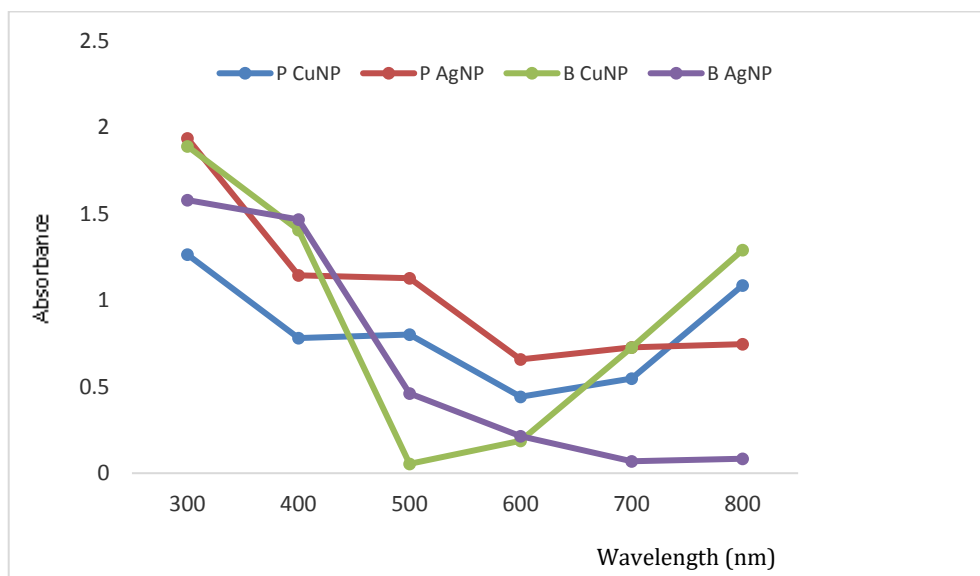
Figure 1. UV-VIS absorbance spectrum of P CuNPs (*Carica papaya* copper nanoparticles), P AgNPs (*Carica papaya* silver nanoparticles), B CuNPs (*Bryophyllum pinnatum*), B AgNPs (*Bryophyllum pinnatum* silver nanoparticles), at room temperature.

It is evident that the major peak positions (Figure 2) for *B. pinnatum*-mediated AgNPs were observed at 3,464.18 and 1,640.57 cm^{-1}, while for *B. pinnatum*-mediated CuNPs, the peaks were found at 3,437.41 and 1,643.49 cm^{-1}. Similarly, *C. papaya*-mediated AgNPs exhibited peaks at 3,439.28 and 1,643.73 cm^{-1}, whereas *C. papaya*-mediated CuNPs displayed peaks at 3,438.82 and 1,643.78 cm^{-1}.

These results demonstrate that there are slight variations in peak positions among the different plant extracts used, indicating the presence of residual plant extract as a capping agent for both AgNPs and CuNPs. The similarities observed in the spectra further support this conclusion, as they suggest a common mechanism of nanoparticle synthesis involving the plant extracts as stabilizing agents.
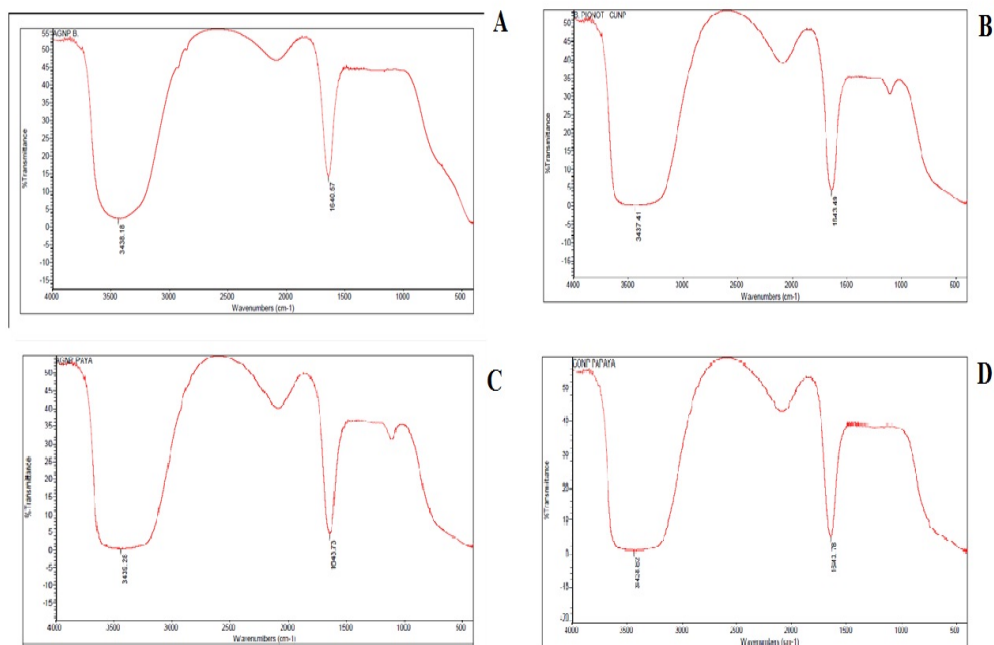
Figure 2. FT-IR spectrum of synthesized nanoparticles
(a) *B. pinnatum*-mediated AgNPs (b) *B. pinnatum*-mediated CuNPs
(c) *C. papaya*-mediated AgNPs (d) *C. papaya*-mediated CuNPs

Table 5 shows the antimicrobial activities of copper sulphate ($CuSO_4$) and silver nitrate ($AgNO_3$). The results revealed that there were high inhibitory activity of *Escherichia coli*, *Pseudomonas aeruginosa*, *Helicobacter pylori* and *Bacillus alvei* in $CuSO_4$ and $AgNO_3$ ranging from 7 – 24 mm using the filter and Agar-well diffusion methods. However, there was no activity of inhibition of *Staphylococcus aureus* by $AgNO_3$. Generally, $CuSO_4$ had a better inhibition in both filter discs and agar wells methods.

Table 6 shows the antimicrobial test using filter paper discs diffusion method. The result showed that *Carica papaya* and *Bryophyllum pinnatum*-mediated CuNPs and AgNPs inhibited the activity of the *Staphylococcus aureus*, *Escherichia coli*, *Pseudomonas aeruginosa*, *Helicobacter pylori* and *Bacillus alvei* However, *Carica papaya*-mediated AgNPs could not inhibit the activity of *Pseudomonas aeruginosa* and *Helicobacter pylori*. Similarly, the plant extracts alone could not inhibit the activity of the isolates. Interestingly, *Carica papaya*-mediated CuNPs and *Bryophyllum pinnatum*-mediated AgNPs had better inhibition levels.

Table 5. Antimicrobial activities of CuSO$_4$ and AgNO$_3$

Isolates	Filter disc Inhibition zone diameter (mean±standard deviation, mm)		Agar wells Inhibition zone diameter (mean±standard deviation, mm)	
	AgNO$_3$	CuSO$_4$	AgNO$_3$	CuSO$_4$
Staphylococcus aureus	NA	20.33±1.53	6.67±1.53	21.67±1.53
Escherichia coli	19.33±1.53	22.00±1.00	9.33±2.08	20.33±2.08
Pseudomonas aeruginosa	23.33±1.53	16.67±1.53	6.33±2.08	13.00±2.64
Helicobacter pylori	24.67±2.08	17.00±2.64	7.00±2.64	18.00±2.64
Bacillus alvei	23.00±2.64	25.33±1.53	6.33±2.08	17.67±1.53
Mean±Standard error values in triplicate				

Key: NA = No activity

Table 6. Antimicrobial activity using filter paper method

Isolates	*Carica papaya* Inhibition zone diameter (mean±standard deviation, mm)			*Bryophyllum pinnatum* Inhibition zone diameter (mean±standard deviation, mm)		
	CuNPs	AgNPs	CA extract	CuNPs	AgNPs	BP extract
S. aureus	20.67±1.53	5.67±1.53	NA	17.00±2.00	12.67±2.52	NA
E. coli	31.00±2.00	20.33±1.53	NA	13.00±2.00	19.67±3.06	NA
P. aeruginosa	26.67±1.53	NA	NA	13.67±1.53	19.67±1.53	NA
H. pylori	17.00±2.00	NA	NA	17.00±2.00	30.00±3.00	NA
B. alvei	30.00±2.00	20.00±2.00	NA	21.67±2.52	19.67±2.52	NA
Mean±Standard error values in triplicate						

Key: NA = No activity; CuNPs = copper nanoparticles; AgNPs = silver nanoparticles; CA extract = *Carica papaya*; BP extract = *Bryophyllum pinnatum*.

Table 7 shows the antimicrobial test using agar wells diffusion method. The result reveals 100 % inhibition of the isolates by *Carica papaya* and *Bryophyllum pinnatum*-mediated copper and silver nanoparticles. However, there no inhibition of isolates by the plant extract alone.

Table 7. Antimicrobial activity using agar wells diffusion method

Isolates	*Carica papaya* Inhibition zone diameter (mean±standard deviation, mm)			*Bryophyllum pinnatum* Inhibition zone diameter (mean±standard deviation, mm)		
	CuNPs	AgNPs	CA extract	CuNPs	AgNPs	BP extract
S. aureus	21.33±1.04	6.00±2.00	NA	24.00±2.00	9.83±2.25	NA
E. coli	18.33±2.52	6.00±1.00	NA	12.67±1.53	4.33±0.58	NA
P. aeruginosa	34.83±1.52	6.50±1.32	NA	11.33±1.15	18.33±0.58	NA
H. pylori	18.17±0.76	15.83±0.76	NA	14.83±1.26	15.17±0.76	NA
B. alvei	20.33±1.52	6.83±1.26	NA	17.83±1.26	19.17±0.76	NA
Mean±Standard error values in triplicate						

Key: NA = No activity; CuNPs = copper nanoparticles; AgNPs = silver nanoparticles; CA extract = *Carica papaya*; BP extract = *Bryophyllum pinnatum.*

Discussion

The impact of plant-based nanoparticles synthesized from *Carica papaya* and *Bryophyllum pinnatum* against selected microorganisms has been investigated. The time of addition of the plant extracts to the metal ion solution was considered the start of the reaction. It is well known that silver nanoparticles exhibit a yellowish-brown colour in aqueous solutions due to the excitation of surface plasmon vibrations in silver nanoparticles (Sulochana *et al*., 2012). The colour change of the solution to green after the reaction of plant extract with copper ions can be used to illustrate the synthesis of copper nanoparticles (Gebremedhn *et al*., 2019).

The phytochemical constituents of *Bryophyllum pinnatum* and Carica papaya are known for their diverse biological activities and potential health benefits. However, it is worth noting that phlabotannins, coumarin, and anthraquinone were not detected in either *Bryophyllum pinnatum* or *Carica papaya*. This information sheds light on the unique chemical profiles of these two plants and underscores their potential applications in various fields, such as medicine and nutrition. According to Ahmad *et al*. (2010), flavonoids, which were one of the phytochemicals detected in this study, contain various functional groups that

have an enhanced ability to reduce metal ions. The reactive hydrogen atom is released due to tautomeric trans-formations in flavonoids, through which the enol-form is converted into the keto-form. This process is realised by the reduction of metal ions into metal nanoparticles.

The absorbance spectrum in this study reveals that *Carica papaya*-mediated AgNPs and *Bryophyllum pinnatum*-mediated CuNPs exhibit the highest absorption at 300 nm, reaching an impressive value of 1.9. On the other hand, *Bryophyllum pinnatum*-mediated AgNPs display a slightly lower absorbance of 1.6, while *Carica papaya*-mediated CuNPs exhibit a comparatively lower absorbance of 1.3 at the same wavelength. These findings indicate that both *Carica papaya* and *Bryophyllum pinnatum* have the ability to synthesize nanoparticles with significant absorbance properties, thus making them promising candidates for various applications in fields such as medicine, catalysis, and environmental remediation.

Five clinical isolates were tested against 12 antibiotics, *B. alvei*, *P. aeruginosa* and *H. pylori* showed resistance to 12 antibiotics, whereas *E. coli* and *S. aureus* showed resistance to 11 and 10 antibiotics respectively, indicating a significant challenge in managing infections caused by these pathogens as well. The consistent presence of multidrug-resistant *P. aeruginosa* and *S. aureus* isolates reported by Ehiaghe *et al*. (2022) and *H. pylori* reported by Wang *et al.* (2019)reinforces the notion that this bacterium poses a persistent threat to patient health in Medicare facilities. The collective evidence from these studies highlights the urgent need for comprehensive infection control measures, including prudent antibiotics.

In this study, the multiple antibiotic resistances (MAR) index of all the isolates was greater than 0.2, indicating they likely originated from high-risk sources of contamination. This is similar to the study by Ayandele *et al*. (2020), Serwecińska (2020) and Ehiaghe *et al*. (2022), who also found a high MAR index in isolates from hospitals. The presence of multidrug resistance in these isolates highlights the urgent need for effective surveillance and control measures to prevent the spread of resistant bacteria. Furthermore, it emphasises the importance of prudent antibiotic use in both human and veterinary medicine to minimise the selection pressure for resistance.

This study revealed that copper sulphate ($CuSO_4$) and silver nitrate ($AgNO_3$) showed high antimicrobial activity against *E. coli*, *P. aeruginosa*, *H. pylori*, and *B. alvei* using filter and agar-well diffusion methods. However, there was no inhibitory activity against *S. aureus* by the plant extracts; this is similar to the report of Ahmed *et al*. (2016) who reported that the plant extract showed no antimicrobial activity.

Interestingly, *Carica papaya* and *Bryophyllum pinnatum*-mediated CuNPs and AgNPs effectively inhibited the activity of *S. aureus*, *E. coli*, *P. aeruginosa*, *H. pylori*, and *B. alvei*, demonstrating their broad-spectrum antimicrobial potential. These findings suggest that the combination of metal salts with plant-mediated

nanoparticles could be a promising approach for combating bacterial infections. The result of this study is in agreement with the report by Anandalakshmire *et al*. (2016) and Bhat *et al*. (2021), who reported that plant-mediated nanoparticles showed significant antimicrobial activity against a range of bacterial strains. Also, Ahmed *et al*. (2016) reported that the produced NPs displayed equal efficacy against *E. coli* and *S. aureus*, while the plant extract showed no antimicrobial activity.

The mechanisms by which AgNPs and CuNPs exert their antimicrobial effects are multifaceted and involve various mechanisms. AgNPs and CuNPs have been shown to disrupt bacterial cell membranes, leading to leakage of intracellular components and subsequent cell death (Bruna *et al*., 2021; Lai *et al*., 2022). They can interact with bacterial DNA, inhibiting replication and causing genetic damage. Furthermore, these nanoparticles can generate reactive oxygen species (ROS), which induce oxidative stress in bacteria and impair their vital cellular processes (Manke *et al*., 2013; Mammari *et al*., 2022). CuNPs have the ability to interfere with bacterial enzyme systems, disrupting crucial metabolic pathways necessary for bacterial survival (Kaur *et al*., 2023). Moreover, copper ions released from CuNPs can generate ROS within bacterial cells, causing oxidative damage and inhibiting microbial growth (Orta-Rivera *et al*., 2023). Moreover, the use of Carica papaya and Bryophyllumpinnatum as green synthesis agents offers a sustainable and eco-friendly alternative to conventional chemical methods (Ikhajiagbe *et al*., 2022).

Conclusions

The use of *Carica papaya* and *Bryophyllum pinnatum*-mediated copper and silver nanoparticles has demonstrated promising results in terms of their antimicrobial activity against various bacterial strains. This approach not only provides an effective alternative to conventional chemical methods but also promotes sustainability and eco-friendliness. It is crucial to evaluate their safety and efficacy in clinical settings to ensure their suitability for practical applications. By continuing to explore these aspects, this will help to unlock the full potential of these green synthesis agents and pave the way for a safer and more sustainable future in antimicrobial research..

References

Ahmad, N., Sharma, S., Alam, M.K., Singh, V.N., Shamsi, S.F., Mehta, B.R., & Fatma, A. (2010). Rapid synthesis of silver nanoparticles using dried medicinal plant of basil. *Coll Surf B Biointer,. 81*(1), 81–86. Doi:10.1016/j.colsurfb.2010.06.029

Ahmed, M., Marrez, D.A,, Mohamed Abdelmoeen, N., Abdelmoneem Mahmoud, E., Ali M.A., Decsi, K., & Tóth, Z. (2023). Studying the antioxidant and the antimicrobial activities of leaf successive extracts compared to the green-chemically synthesized silver nanoparticles and the crude aqueous extract from *Azadirachta indica*. *Processes 11*(6), 1644. Doi:10.3390/pr11061644

Ahmed, S., Ahmad, M., Swami, B.L., & Ikram, S. (2016). A review on plants extract mediated synthesis of silver nanoparticles for antimicrobial applications: A green expertise. *J Adv Res*, *7*(1), 17–28. Doi:10.1016/j.jare.2015.02.007

Ali, E., Islam, M.S., Hossen, M.I., Khatun, M.M., & Islam, M.A. (2021). Extract of neem (*Azadirachta indica*) leaf exhibits bactericidal effect against multidrug resistant pathogenic bacteria of poultry. *Veter Med Sci*, *7*(5), 1921–1927. Doi:10.1002/vms3.511

Anandalakshmi, K., Venugobal, J. & Ramasamy, V. (2016). Characterization of silver nanoparticles by green synthesis method using *Pedalium murex* leaf extract and their antibacterial activity. *Appl Nanosci, 6*, 399–408. Doi:10.1007/s13204-015-0449z.

Asif, M., Yasmin, R., Asif, R., Ambreen, A., Mustafa, M., & Umbreen, S. (2022). Green synthesis of silver nanoparticles (AgNPs): structural characterization, and their antibacterial potential. *Inter Horm Society*, *20*(1), 15. Doi:10.1177/15593258221088709

Aswini, R., Murugesan, S. & Kannan, K. (2021) Bio-engineered TiO$_2$ nanoparticles using *Ledebouria revoluta* extract: larvicidal, histopathological, antibacterial and anticancer activity. *Int J Environ Analyt Chem*, *101*(15), 2926-2936. Doi:10.1080/03067319.2020.1718668

Ayandele, A.A., Oladipo, E.K., Oyebisi, O., & Kaka, M. O. (2020). Prevalence of multi-antibiotic resistant *Escherichia coli* and *Klebsiella* species obtained from a tertiary medical institution in Oyo State, Nigeria. *Qatar Med J*, *2020*(1), 9. Doi:10.5339/qmj.2020.9

Balouiri, M., Sadiki, M., & Ibnsouda, S.K. (2016). Methods for in vitro evaluating antimicrobial activity: A review. *J Pharm Analy*, *6*(2), 71–79. Doi:10.1016/j.jpha.2015.11.005

Bhat, M., Chakraborty, B., Kumar, R.S., Abdulrahman, I.A., Natarajan, A., Kotresha, D., Pallavi, S.S., Dhanyakumara, S.B., Shashira., K.N. & Nayaka, S. (2021). Biogenic synthesis, characterization and antimicrobial activity of *Ixora brachypoda* (DC) leaf extract mediated silver nanoparticles. *J King Saud Univ-Sci*, *33*(2), 101296, Doi:10.1016/j.jksus.2020.101296.

Bruna, T., Maldonado-Bravo, F., Jara, P., & Caro, N. (2021). Silver nanoparticles and their antibacterial applications. *Inter J Mol Sci*, *22*(13), 7202.

Cheesbrough, M. (2006). District Laboratory Practice in Tropical Countries, Second Edition, Part 2. pp. 442.

Clinical and Laboratory Standards Institute (2020) CLSI M100-ED29: 2021 Performance Standards for Antimicrobial Susceptibility Testing, 30th Edition. Vol. 40.

Ehiaghe, J.I., Amengialue, O.O., Ehiaghe, F.A., Igiebor, F.A. and Koyonen, U. (2022) Antimicrobial susceptibility pattern and plasmid dna profiling of bacteria isolated in some selected hospital in Benin City, Nigeria. *BIU J Basic Appl Sci*, *7*(2), 155 – 165.

Gebremedhn, K., Kahsay, M.H. & Aklilu, M.J.J.O.P. (2019). Green synthesis of CuO nanoparticles using leaf extract of *Catha edulis* and its antibacterial activity. *Pharmacol*, *7*(7), 327-342. Doi:10.17265/2328-2150/2019.06.007

Ghosh, S., Patil, S., Ahire, M., Kitture, R., Kale, S., Pardesi, K., Cameotra, S.S., Bellare, J., Dhavale, D.D., Jabgunde, A., & Chopade, B.A. (2012). Synthesis of silver nanoparticles using *Dioscorea bulbifera* tuber extract and evaluation of its synergistic potential in combination with antimicrobial agents. *Int J Nanomedicine*, 7, 483–496. Doi:10.2147/IJN.S24793

Igiebor, F.A., Asia, M. & Ikhajiagbe, B. (2023). Green nanotechnology: A modern tool for sustainable agriculture – a Review. *Int J Horticult Sci Tech*, *10*(4), 269-286. Doi:10.22059/ijhst.2022.344790.571

Ikhajiagbe, B., Igiebor, F.A. & Ogwu, C. (2021).Growth and yield performances of rice (*Oryza sativa* var. nerica) after exposure to biosynthesized nanoparticles. *Bull Nat Res Centre*, *45*(62), 1-13. Doi:10.1186/s42269-021-00508-y

Joseph, T.M., Kar Mahapatra, D., Esmaeili, A., Piszczyk, Ł., Hasanin, M.S., Kattali, M., Haponiuk, J., & Thomas, S. (2023). Nanoparticles: Taking a unique position in medicine. *Nanomaterials (Basel, Switzerland)*, *13*(3), 574. Doi:10.3390/nano13030574

Kaur, R., Alayami, M.H., Saini, B., Bayan, M.F. & Chandrasekaran, B. (2023). Combating microbial infections using metal-based nanoparticles as potential therapeutic alternatives. *Antibiotics*, *12*(5), 909. Doi:10.3390/antibiotics12050909

Kuppusamy, P., Yusoff, M.M., Maniam, G.P., & Govindan, N. (2016). Biosynthesis of metallic nanoparticles using plant derivatives and their new avenues in pharmacological applications - An updated report. *Saudi Pharm J*, *24*(4), 473–484. Doi:10.1016/j.jsps.2014.11.013

Lai, M.J., Huang, Y.W., Chen, H.C., Tsao, L.I., Chang Chien, C.F., Singh, B., & Liu, B.R. (2022). Effect of size and concentration of copper nanoparticles on the antimicrobial activity in *Escherichia coli* through multiple mechanisms. *Nanomaterials (Basel, Switzerland)*, *12*(21), 3715. Doi:10.3390/nano12213715

Maduka, N., Igiebor, F.A. and Elum, O. (2022). Microbiological assessment of home-packed children's meal, antibiotic susceptibility and prevalence of intestinal parasites among pupils in selected schools in Benin City, Nigeria. *FUW Trends Sci Tech J*, *7*(3), 138 150.

Malabadi, R.B., Chalannavar, R.K., Meti, N.T., Mulgund, G.S., Nataraja, K. & Kumar, S.V. (2012). Synthesis of antimicrobial silver nanoparticles by callus cultures and *in vitro* derived plants of *Catharanthus roseus*. *Research Pharm*, *2*(6), 18-31.

Mammari, N., Lamouroux, E., Boudier, A., & Duval, R.E. (2022). Current knowledge on the oxidative-stress-mediated antimicrobial properties of metal-based nanoparticles. *Microorganisms*, *10*(2), 437. Doi:10.3390/microorganisms10020437

Manke, A., Wang, L., & Rojanasakul, Y. (2013). Mechanisms of nanoparticle-induced oxidative stress and toxicity. *BioMed Res Int, 2013*, 942916. Doi:10.1155/2013/942916

Marslin, G., Siram, K., Maqbool, Q., Selvakesavan, R.K., Kruszka, D., Kachlicki, P., & Franklin, G. (2018). Secondary metabolites in the green synthesis of metallic nanoparticles. *Materials (Basel, Switzerland)*, *11*(6), 940. Doi:10.3390/ma11060940

Melkamu, W.W., & Bitew, L.T. (2021). Green synthesis of silver nanoparticles using *Hagenia abyssinica* (Bruce) J.F. Gmel plant leaf extract and their antibacterial and anti-oxidant activities. *Heliyon, 7*(11), e08459. Doi:10.1016/j.heliyon.2021.e08459

Orta Rivera, A.M., MeléndezContés, Y., Medina Berríos, N., Gómez Cardona, A.M, Ramos Rodríguez, A., Cruz Santiago, C., González Dumeng, C., López, J., Escribano, J. & Rivera Otero, J.J, (2023). Copper-based antibiotic strategies: exploring applications in the hospital setting and the targeting of Cu regulatory pathways and current drug design trends. *Inorganics*, *11*(6), 252. Doi:10.20944/preprints202304.1124.v2

Rajesh, K.M., Ajitha, B., Ashok Kumar Reddy, Y., Suneetha, Y. & Sreedhara Reddy, P. (2018). Assisted green synthesis of copper nanoparticles using *Syzygium aromaticum* bud exract: Physical, optical and antimicrobial properties. *Optik J, 154*, 593-600. Doi:10.1016/J.IJLEO.2017.10.074

Sánchez-López, E., Gomes, D., Esteruelas, G., Bonilla, L., Lopez-Machado, A.L., Galindo, R., Cano, A., Espina, M., Ettcheto, M., Camins, A., Silva, A.M., Durazzo, A., Santini, A., Garcia, M.L., & Souto, E.B. (2020). Metal-based nanoparticles as antimicrobial agents: An overview. *Nanomaterials (Basel, Switzerland)*, *10*(2), 292. Doi:10.3390/nano10020292

Serwecińska, L. (2020). Antimicrobials and antibiotic-resistant bacteria: A risk to the environment and to public health. *Water*. *12*(12), 3313. Doi:10.3390/w12123313

Singh, A., Gautam, P.K., Verma, A., Singh, V., Shivapriya, P.M., Shivalkar, S., Sahoo, A.K., & Samanta, S.K. (2020). Green synthesis of metallic nanoparticles as effective alternatives to treat antibiotics resistant bacterial infections: A review. *Biotech Rep (Amsterdam, Netherlands)*, *25*, e00427. Doi:10.1016/j.btre.2020.e00427

Skłodowski, K., Chmielewska-Deptuła, S.J., Piktel, E., Wolak, P., Wollny, T., & Bucki, R. (2023). Metallic nanosystems in the development of antimicrobial strategies with high antimicrobial activity and high biocompatibility. *Int J Mol Sci*, *24*(3), 2104. Doi:10.3390/ijms24032104

Sulochana, S., Krishnamoorthy, P. & Sivaranjani, K. (2012). Synthesis of silver nanoparticles using leaf extract of *Andrographis paniculata*. *J Pharm Toxic*, *7*, 251-258. Doi:10.3923/jpt.2012.251.258

Troncarelli, M.Z., Brandão, H.M., Gern, J.C., Guimarães, A.S. & Langoni, H. (2013). Nanotechnology and antimicrobials in veterinary medicine. *Formatex*, 13, 543-556.

Wang, D., Guo, Q., Yuan, Y., & Gong, Y. (2019). The antibiotic resistance of *Helicobacter pylori* to five antibiotics and influencing factors in an area of China with a high risk of gastric cancer. *BMC Micro*, *19*(1), 152. https://doi.org/10.1186/s12866-019-1517-4

Wang, L. & Weller, C.L. (2006) Recent advances in extraction of nutraceuticals from plants. *Trends Food Sci Tech*, *17*, 300-312. Doi:10.1016/j.tifs.2005.12.004

Yusuf, A., Almotairy, A.R.Z., Henidi, H., Alshehri, O.Y., & Aldughaim, M.S. (2023). Nanoparticles as drug delivery systems: A review of the implication of nanoparticles' physicochemical properties on responses in biological systems. *Polymers*, *15*(7), 1596. Doi:10.3390/polym15071596

Zia, R., Riaz, M., Farooq, N., Qamar, A. & Anjum, S. (2018). Antibacterial activity of Ag and Cu nanoparticles synthesized by chemical reduction method: A comparative analysis. *Mat Res Exp*, *5*, 7. Doi:10.1088/2053-1591/aacf70

Lipid classes and fatty acid composition of *Thapsia garganica* L. seeds oil

Halima Nebeg[1✉], Fatiha El-Houiti[1], Djilali Tahri[2✉],
Chahrazed Hamia[1], Mohamed Yousfi[1]

*[1]Laboratory of Fundamental Sciences, University of Amar TELIDJI, P.O. Box: 37G,
Road of Ghardaïa, Laghouat 03000, Algeria; [2]Department of natural sciences, Ecole normale
supérieure of Laghouat, P.O. Box 4033, Road of Ghardaïa, 03000, Laghouat, Algeria;
✉**Corresponding author, E-mail:** haliman@hotmail.fr; d.tahri@lagh-univ.dz*

Abstract. This study focused on characterizing the seed oil of *Thapsia garganica* (Apiaceae), a medicinal plant native to Laghouat, Algeria, and evaluating its antioxidant properties. Various solvent systems were employed to extract and fractionate the lipid content of *T. garganica* seeds oil. Chemical indices were determined, and fatty acids methyl esters were analyzed using GC/MS. Tocopherol composition was assessed via HPLC, and antioxidant activity was evaluated using the 2,2-diphényl 1-picrylhydrazyle (DPPH) method. The GC/MS analysis revealed distinct fatty acid profiles across various fractions, highlighting a notable presence of petroselinic acid and higher-than-usual levels of pentadecanoic acid in all fractions. *T. garganica* oil exhibited richness in tocopherols, particularly with α-tocopherol being the predominant homolog. The antioxidant activity assessment of different lipid fractions indicated potent activity within polar lipids (glycolipids and phospholipids). Furthermore, *T. garganica* oil was abundant in unsaturated fatty acids, notably petroselinic acid, displaying significant radical scavenging activity in its polar fractions.

Keywords: *T. garganica*, petroselinic acid, pentadecanoic acid, tocopherols, antioxidant activity.

Introduction

The Apiaceae family distinguishes itself among plant families with its umbel inflorescence and singular-seeded fruits. Comprising species native to temperate regions, they have garnered extensive use as spices or medicines due to their abundant secondary metabolites (Heywood, 1971). Numerous plants within the Apiaceae family, particularly those belonging to the genus *Thapsia*, are recognized for their significant concentration of petroselinic acid (*cis*-6 18:1) found in their seed oil (Avato *et al.*, 2001; Ngo-Duy*et al.*, 2009). Because of the unsaturation at carbon 6, this fatty acid has potential industrial significance (Cahoon, 1992).

T. garganica L. stands as a significant medicinal plant, the subject of numerous scientific studies (Makunga *et al.*, 2003; Nebeg *et al.*, 2019). Historically, this ancient medicinal herb featured in various European remedies until 1937 (Jäger *et al.*, 1993). Widely distributed across several regions of Algeria, *T. garganica* has been traditionally employed to alleviate rheumatism (Aït Youssef, 2006). Notably, original data on the lipid fraction isolated from its seeds are lacking. Our study aims to characterize the lipid fraction of *T. garganica* seed oil, contributing to a deeper understanding and valorization of this medicinal species.

Materials and methods

Sample preparation

The fruits of *T. garganica* were collected from the Sidi Makhlouf region in Laghouat, Algeria. Professor Yousfi Mohamed identified the *T. garganica* plant, and a voucher has been deposited in the herbarium of the Laboratoire des Sciences Fondamentales at Laghouat University (voucher number: Tg-s 2022). These fruits exhibit an elliptical shape, ranging from 1 to 2 cm in length and nearly 1 cm in width, characterized by strongly winged margins. The wings, finely striated and bright yellow in color, adorn the green-hued fruit. Following collection, the fruits were air-dried at room temperature. Subsequently, the seeds were separated from the umbels and wings, then pulverized using a mortar in preparation for the extraction procedure.

Chemical reagents

All chemicals were purchased from Sigma (USA), Aldrich (Milwaukee, USA), FlukaChem (Buchs, Switzerland) and Merck (Germany).

Lipid quantification

The powdered seeds of *T. garganica* underwent maceration with petroleum ether as the extraction solvent for 24 hours, shielded from light. Following maceration, the extract underwent filtration and drying with an excess of anhydrous sodium sulfate. Subsequently, the petroleum ether extract was evaporated under reduced pressure at 40°C and then stored at 6°C.

Lipids were extracted using Folch's method (Folch *et al.*, 1957) from *T. garganica* seeds. The lipid fraction was obtained by macerating and mixing the seeds at room temperature in chloroform:methanol (2:1) for 24 hours. After extraction, the mixture underwent filtration, and the recovered solution was washed with a 9% NaCl solution. The chloroform fraction, containing the total lipids, was then filtered and dried with an excess of anhydrous sodium sulfate before being evaporated under vacuum at 40°C. The resulting oil was stored at 6°C. Subsequently, the crude *Thapsia* oil was fractionated using silica gel column chromatography (Rouser *et al.*, 1967). For this, 9 g of the lipid extract were added to the column along with 10 g of activated silica gel. Elution was carried out successively using chloroform, acetone, and methanol as eluents to separate neutral lipids, glycolipids, and phospholipids, respectively.

Determination of chemical indices

The acid value (AV), saponification value (SV), and iodine value (IV) were determined following the protocols outlined in the French norm AFNOR (1984), specifically AFNOR NFT 60-204, AFNOR NF T 60-206, and AFNOR NF T 60-203, respectively. AFNOR standards encompass a wide range of topics including analysis methods, quality standards, good manufacturing practices, and regulatory requirements. These standards play a crucial role in ensuring methodological consistency and quality control. Additionally, they establish a framework for assessing the safety, purity, and nutritional content of fats and oilseeds, thereby facilitating evidence-based research and informed decision-making across various disciplines such as nutrition, food science, agriculture, and biochemistry.

GC-MS analysis of fatty acids methyl esters

The fatty acid methyl esters (FAMEs) of total lipids, neutral lipids, glycolipids, and phospholipids were prepared using the standard boron trifluoride procedure BF3. Initially, the oil underwent hydrolysis in the presence of methanolic potassium, followed by esterification in the presence of a 10% w/v boron trifluoride-methanol complex. Subsequently, the methyl esters were recovered through liquid-liquid extraction using hexane after the addition of water. Fatty acid analysis was

conducted by Gas Chromatography/Mass Spectrometry (GC/MS) using a 1 HP 5890 Series II chromatograph. Separation was achieved using a silica gel capillary column (60 m x 0.25 mm) grafted with a DB-Wax stationary phase of 0.2 µm thickness. The analysis involved temperature programming and the use of hydrogen as the carrier gas. Identification of FAMEs was facilitated by comparing retention indices and mass spectra with reference standards.

Tocopherol content

The tocopherol composition was analyzed using a Waters HPLC system equipped with a nonpolar reversed-phase (RP18) column and a fluorescent detector. A diluted sample of twenty microliters in pentane (representing neutral lipids of *Thapsia* oil) was isocratically eluted with HPLC-grade methanol and water (92:8 v/v). Tocopherols were detected using fluorimetry, with excitation at 290 nm and emission at 330 nm. By comparing peak areas, the relative contents of tocopherols in the extract were determined using external standards for α, β, γ, and δ-tocopherol.

Antioxidant activity analysis using DPPH radical scavenging test

The antiradical activity of various lipid classes was assessed using the DPPH method (Molyneux, 2004). Different concentrations of the analyzed fraction were prepared, and each dilution (100 µL) was added to 1 mL of a 250 µM ethanolic solution of DPPH. After 30 minutes, the absorbance at 517 nm was measured. The following equation was utilized to determine the DPPH radical scavenging capacity:

Inhibition (%) = [1 - (Test sample absorbance/Control absorbance)]x 100

The EC50 value represents the concentration of substrate needed to reduce DPPH activity by 50% (Molyneux, 2004). Graphical analysis of inhibition percentage variation against concentration curves for each oil fraction was used to derive the EC50 value. This process was repeated three times for each lipid fraction, and the EC50 value was determined as the average of three repetitions.

Statistical analysis

Hierarchical Cluster analysis (HCA) of chemical data was performed with XlStat 2014.5.03. Ward's linkage method was used to determine the distance between clusters and Euclidean distance for their agglomeration. Differences between means were assessed by one-way ANOVA using Fisher's test at a level of 0.001 with Origin b9.3.226.

Results

Lipid quantification

The crude fat content extracted using petroleum ether 9.45%. Conversely, a mixture of two solvents (chloroform:methanol) extracted 22.4% of the weight of *T. garganica* seeds. Significantly divergent extraction performances were observed between petroleum ether and the solvent mixture (chloroform:methanol). This variation stems from the differing polarities of the solvents used; petroleum ether, being nonpolar, may not efficiently extract all lipids, primarily targeting neutral lipids such as triglycerides. Conversely, miscible solvents like methanol and chloroform have the capacity to extract a broader spectrum of lipids, particularly polar lipids like glycolipids and phospholipids. Additionally, differences in extraction rates may also be influenced by sample type variability. Similar to many other plant species, *T. garganica* crude oil exhibited a high proportion of neutral lipids, constituting 83.37% of the total, in contrast to minor lipids represented by modest levels of glycolipids (5.82%) and phospholipids (1.93%).

Determination of chemical indices

Assessing the quality and structural stability of the oil can be achieved through the examination of its acid value (AV), saponification value (SV), and iodine value (IV), as detailed in Table 1.

Table 1. Chemical characterization of *T. garganica* oil

AV (mg KOH/g)	SV (mg KOH/g)	IV (Wijs)
8.16±0.3	206.04 ± 0.8	87.65±0.5

AV: acid value, SV: saponification value, IV: iodine value; SD: standard deviation.

Analysis of fatty acids methyl esters

Table 2 illustrates the relative proportions of various FAMEs found in crude oil and across different lipid classes. It highlights a prevalent presence of unsaturated fatty acids with diverse profiles within these classes. Specifically, total lipids, neutral lipids, and phospholipids exhibit notable concentrations of linoleic acid (41.37%, 40.32%, and 35.353%, respectively). Conversely, the glycolipid fraction demonstrates a higher abundance of linolenic acid (73.35%) and encompasses a broad spectrum of fatty acids, including short-chain (C8:0, C14:0), as well as an unusual fatty acid, pentadecanoic acid (C15:0).

In our investigation, we observed the presence of two isomers of C18:1 in the phospholipids chromatogram, manifested as two distinct peaks with respective retention times of 46.8 and 46.9 minutes. Upon analyzing chromatograms of total lipids, neutral lipids, and glycolipids, we identified peaks at 46.8, 46.7, and 46.7 minutes, respectively, corresponding to petroselinic acid. However, in the case of phospholipids, the ratio of C18:1 acid was calculated by summing the ratios of the two peaks representing the two isomers: petroselinic (C18:1ω6) and oleic (C18:1ω9) acids.

Multivariate analysis was employed to compare the fatty acid profiles of *T. garganica* oil with those of other species within the *Thapsia* genus and certain seed oils from the Apiaceae family (Avato *et al.*, 2001; Ngo-Duy *et al.*, 2009). This analytical approach helps to simplify the graphical representation of complex multivariate data and illustrate their underlying patterns.

As depicted in Fig. 1, notable differences in fatty acid levels are evident between the studied *T. garganica* (1) and the five species within the *Thapsia* genus, including *T. garganica* (2), as reported by Avato *et al.* (2001), who noted a very similar composition among these five species. To enable a meaningful comparison of this oil with other vegetable oils, a similar statistical analysis was conducted, as depicted in Fig. 2.

Table 2. The relative proportions on various fatty acids of crude oil and the various classes of lipids

Fatty acid	Sample			
	TL	NL	GL	PL
C8:0	-	-	14.458	-
C14:0	-	-	0.695	-
C15:0	-	-	0.336	-
C16:0	19.499	18.908	18.023	27.064
C16:1	-	-	0.808	-
C18:0	5.971	5.069	1.585	2.425
C18:1	28.364	33.911	31.813	32.801
C18:2	41.368	40.315	23.893	35.353
C18:3	2.612	1.069	7.335	2.07
C20:0	1.318	0.727	0.480	0.287
C22:0	0.573	-	0.573	-
C24:0	0.294	-	-	-

TL: total lipids, NL: neutral lipids, GL: glycolipids, PL: phospholipids.
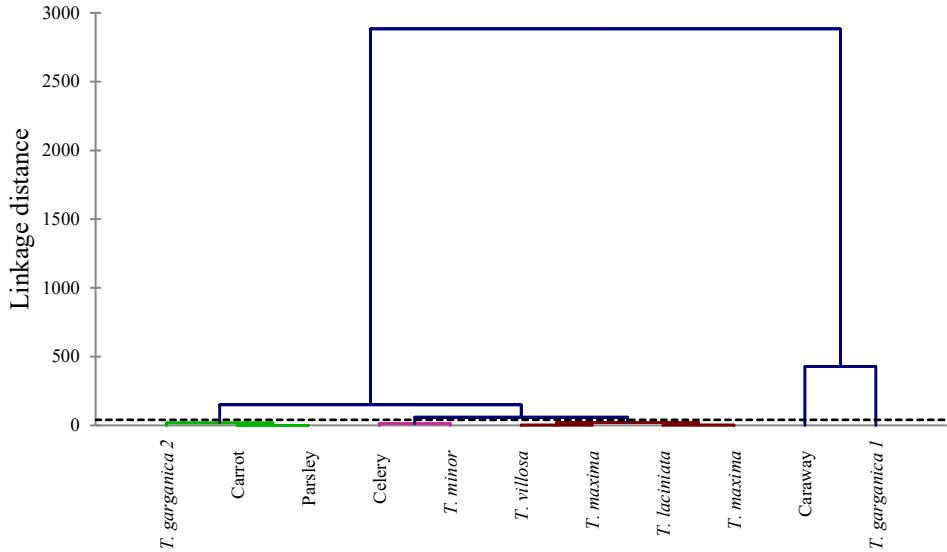
Figure 1. Cluster analysis (Ward's method) of *T. garganica* and some plants of same genus and family.
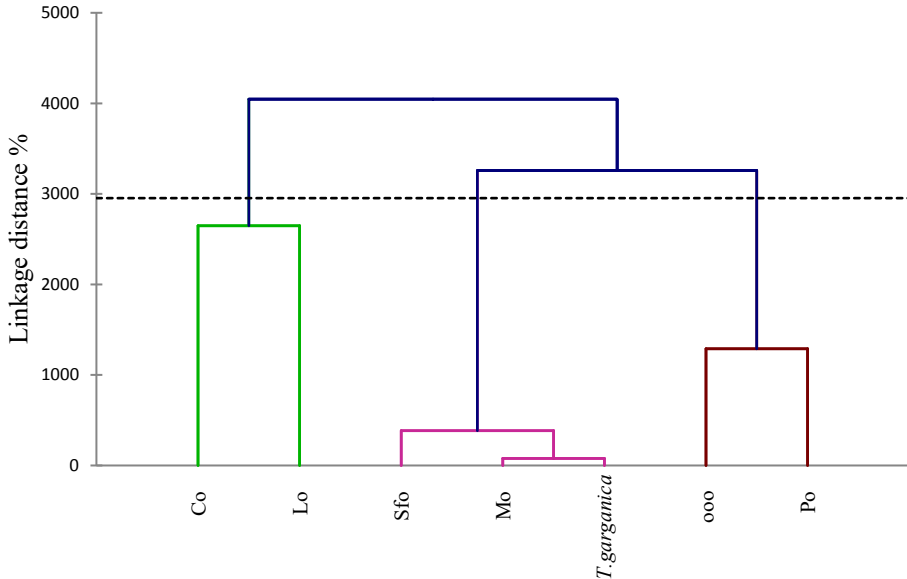
Figure 2. Cluster analysis (Ward's method) of *T. garganica* and some vegetable oils (MO, maize oil; SFO, sunflower oil; OOO, Orujo olive oil; CO, coconut oil; LO, linseed oil; PO, palm oil).

Tocopherol content

The total tocopherol content in *T. garganica* oil measured 940.62 mg/kg (Table 3). Comparatively, vitamin E-active compound levels in other plants range from 430 to 2680 mg/kg in rapeseed oil and 600 to 3370 mg/kg in soybean oil (Matthäus and Özcan, 2015). Consequently, *T. garganica* seed oil emerges as a potential source of antioxidants. The primary tocopherol compounds in *T. garganica* seed oil were α-tocopherol homologs, followed by (β+γ)-tocopherol. Notably, all obtained contents exhibited significant differences at $P \leq 0.001$. The α-tocopherol content (516.84 mg/kg), boasting the highest vitamin E concentration, aligns with ranges observed in corn (23–573 mg/kg) (Rossell and Pritchard, 1991), golden apple (514 mg/kg), starking apple (544 mg/kg), quince (496 mg/kg), and chufa (685 mg/kg) (Matthäus and Özcan, 2015).

Table 3. Tocopherol content of *T. garganica* oil (µg/g of oil)

α-tocopherol	[β+γ]-tocopherols	δ-tocopherol	Total tocopherols
516.84	394.49	29.29	940.62

Antioxidant activity

Table 4 presents the results of the DPPH test. Each lipid fraction displayed distinct inhibition potentials, with lower EC50 values indicative of higher antioxidant activity. Significantly divergent activities were observed among the lipid fractions ($P \leq 0.001$), as well as in comparison with Vit E and Vit C. Notably, the difference between the latter two was insignificant at this same significance level.

Table 4. The results of DPPH test

Lipid fractions	IC50 (g/l)[§]
NL	5.38± 0.28
TL	2.41 ± 0.042
PL	1.44 ± 0.12
GL	0.976 ± 0.1
Vit E	0.026 ±0.001
Vit C	0.008 ± 0.002

TL: total lipids, NL: neutral lipids, GL: glycolipids, PL: phospholipids, Vit-E: vitamin E, Vit-C: vitamin C. [§] The values are significantly different at P≤0.001 according to Fisher's test except for Vit-E and Vit-C which are not significantly different at this level.

Discussion

The seeds of *T. garganica* cannot be classified as oleaginous akin to peanut, olive, and sunflower seeds, which typically contain 30-40% oil (Karleskind, 1992). The elevated acidity value suggests a significant presence of free fatty acids, likely stemming from either grain maturity or inadequate oil preservation. A high iodine value may indicate a substantial quantity of unsaturated bonds (unsaturated fatty acids). According to our analysis, the saponification number (206.04 mg KOH/g) closely resembles that of date seed oil (207.8 mg KOH/g) (Boukouada *et al.*, 2014) and is relatively comparable to those of olive (184–196 mg KOH/g), corn (187–195 mg KOH/g), and cottonseed (189–198 mg KOH/g) oils (Rossell and Pritchard, 1991). Additionally, *T. garganica* oil is characterized by medium chain-length and unsaturated fatty acids, as inferred from the inverse relationship between saponification value and fatty acids weight.

In this study, a comparison was made with several other investigations focusing on oils within the Apiaceae family, revealing the abundant presence of petroselinic acid, an isomer of oleic acid, among its members (Avato *et al.*, 2001; Ngo-Duy *et al.*, 2009). Chromatographic separation of oleic and petroselinic acids indicates that these two isomers possess similar chain lengths (LCE) on a polar stationary phase, differing by approximately 0.04 to 0.06 carbon units. Theoretically, this slight difference enables some separation between the two fatty acids, although resolution largely depends on operational conditions (Wolff, 1995). Furthermore, a multivariate analysis was employed to compare the fatty acid profiles of *T. garganica* oil with those of other *Thapsia* genus species and selected seed oils within the Apiaceae family (Avato *et al.*, 2001; Ngo-Duy *et al.*, 2009).

The multivariate analysis reveals that this dissimilarity stems from variations in the percentages of C18:1 acid isomers, likely influenced by differences in sample variety and origin. Within the same cluster, *T. garganica* oil exhibits a comparable fatty acid profile to that of caraway seeds (carrot, celery, and parsley). The hierarchical cluster analysis (Fig. 2) delineates three structures, segmented into two levels. *T. garganica* is positioned at the second level, clustering with corn rather than sunflower, forming a unified class with similar fatty acid profiles (Pinzi *et al.*, 2011).

Despite its lower concentration, δ-tocopherol exhibits greater antioxidant potency in the oil compared to other tocopherols. Notably, its concentration surpasses that found in other oils such as coconut (ND-2 mg/kg), cottonseed (ND-17 mg/kg), groundnut (ND-3–22 mg/kg), and sunflower (ND–7 mg/kg) (Rossell and Pritchard, 1991). Glycolipids and phospholipids emerged as more

effective DPPH radical scavengers, representing a promising finding given their significantly lower EC50 values compared to standards (vitamin E and vitamin C). While phospholipids are recognized natural antioxidants, further research is warranted to elucidate the mechanism behind the radical scavenging activity of these two fractions from *T. garganica* oil. The antioxidant activity of total lipids exceeded that of neutral lipids, likely attributed to the presence of various molecules such as tocopherols, glycolipids, phospholipids, and other polar active compounds present in the crude oil, which are retained in the polar mixture of two solvents (chloroform/methanol).

Conclusion

Describing the seeds of *T. garganica* as oil-bearing would be inaccurate, given the relatively low oil content obtained using non-polar solvents (9.45%). However, this oil is notable for its richness in unsaturated fatty acids, particularly with a significant presence of petroselinic acid. Moreover, its tocopherol content, primarily consisting of α-tocopherol, along with the pronounced radical scavenging activity of its polar fractions (PL and Gl), positions *T. garganica* oil within the realm of other plant materials sought after for their bioactive components or pharmaceutical applications.

References

AFNOR (1984). Recueil de normes françaises des corps gras, graines oléagineuses, produits dérivés. *AFNOR* Paris.

Aït Youssef, M. (2006). Plantes médicinales de Kabylie. *Éditions Ibis press* Paris.

Avato, P., Fanizzi, F.P., & Rosito, I. (2001). The genus *Thapsia* as a source of petroselinic acid. *Lipids*, *36*(8), 845-850.

Boukouada, M., Ghiaba, Z., Gourine, N., Bombarda, I., Saidi, M., & Yousfi, M. (2014). Chemical composition and antioxidant activity of seed oil of two Algerian date palm cultivars (*Phoenix dactylifera*). *Nat Prod Commun*, *9*(12), 1777-80.

Cahoon, E.B., Shanklin, J., & Ohlrogge, J.B. (1992). Expression of a coriander desaturase results in petroselinic acid production in transgenic tobacco. *Proc Natl Acad Sci*, *89*(23), 11184-11188.

Folch, J., Lees, M., & Sloane Stanley, G.H. (1957). A simple method for the isolation and purification of total lipids from animal tissues. *J biol Chem*, *226*(1), 497-509.

Heywood, V.H. (1971). The biology and chemistry of the Umbelliferae. *Academic Press for the Linnean Society* London.

Jäger, A.K., Schottländer, B., Smitt, U.W., & Nyman, U. (1993). Somatic embryogenesis in cell cultures of *Thapsia garganica*: correlation between the state of differentiation and the content of thapsigargins. *Plant Cell Rep*, *12*, 517-520.

Karleskind, A. (1992). Manuel des corps gras. *Technique et Documentation-Lavoisier* Paris.

Makunga, N.P., Jäger, A.K., & Van Staden, J. (2003). Micropropagation of *Thapsia garganica*—a medicinal plant. *Plant Cell Rep*, *21*, 967-973.

Matthäus, B., &Özcan, M.M. (2015). Oil content, fatty acid composition and distributions of vitamin-E-active compounds of some fruit seed oils. *Antioxidants*, *4*(1), 124-133.

Molyneux, P. (2004). The use of the stable free radical diphenylpicrylhydrazyl (DPPH) for estimating antioxidant activity. *Songklanakarin J Sci Technol*, *26*(2), 211-219.

Nebeg, H., Benarous, K., Serseg, T., Lazreg, A., Hassani, H., & Yousfi, M. (2019). Seeds, leaves and roots of *Thapsia garganica* as a source of new potent lipases inhibitors: *in vitro* and *in silico* studies. *Endocr Metab Immune Disord Drug Targets*, *19*(5), 683-696.

Ngo-Duy, C.C., Destaillats, F., Keskitalo, M., Arul, J., & Angers, P. (2009). Triacylglycerols of Apiaceae seed oils: Composition and regiodistribution of fatty acids. *Eur J Lipid Sci Technol*, *111*(2), 164-169.

Pinzi, S., Gandía, L.M., Arzamendi, G., Ruiz, J.J., & Dorado, M.P. (2011). Influence of vegetable oils fatty acid composition on reaction temperature and glycerides conversion to biodiesel during transesterification. *Biores Technol*, *102*(2), 1044-1050.

Rossell, J.B., & Pritchard, J.L.R. (1991). Analysis of oilseeds, fats, and fatty foods. *Elsevier Applied Science* New York.

Rouser, G., Kritchevsky, G., & Yamamoto, A. (1967). Column chromatographic and associated procedures for separation and determination of phosphatides and glycolipids, In: *Lipid chromatographic analysis*, Marinetti G. V., Ed., Vol. 1, Marcel Dekker, New York, pp. 99-162.

Wolff, R.L. (1995). Recent applications of capillary gas-liquid chromatography to some difficult separations of positional or geometrical isomers of unsaturated fatty acids, In: *New Trends in Lipid and Lipoprotein Analyses*, Sébédio, J.-L., & Perkins, E.G., eds., AOCS Press, Champaign, pp. 147–180.

Characterization of *Celosia argentea* Linn. germplasm using ISSR markers

Odunayo Joseph Olawuyi[1✉], Haneefah Lola Misbahudeen[1],
Oluwagbade Joseph Odimayo[2], Adedayo Omotayo Faneye[2],
Olumayowa Mary Olowe[3] and Akinlolu Olalekan Akanmu[3]

[1]*Genetics and Molecular Biology Unit, Department of Botany, P.M.B 128, University of Ibadan, Ibadan, Nigeria;* [2]*Department of Virology, University Teaching Hospital (UCH), University of Ibadan, Ibadan, Nigeria;* [3]*Food Security and Safety Focus Area, Faculty of Natural and Agricultural Sciences, North-West University, Private Bag X2046, Mmabatho, South Africa.*
✉*Corresponding author, E-mail: olawuyiodunayo@yahoo.com*

Abstract. *Celosia argentea* is an annual leafy vegetable popularly known for its dietary and medicinal values. Hence, it is important to preserve and further improve this vegetable to enhance its numerous benefits. This study therefore investigated the genetic variability among different genotypes of *C. argentea* using ISSR primers. A total of 15 *C. argentea* genotypes were sourced from National Centre for Genetic Resources and Biotechnology (NACGRAB) in Ibadan, Nigeria and 10 genotypes sourced from different markets. The open field experiment was set up in a completely randomized design. Seeds of each cultivar were grown and seedlings transplanted. Fresh young apical leaves were harvested. DNA was extracted from young frozen apical leaves. Six ISSR primers were optimized and used in PCR with a touch-down procedure in a thermocycler. Agarose gel electrophoresis was performed, and bands were visualized. Molecular data was analyzed for total gene diversity, while morphological data was analyzed using ANOVA. The genotypes of NGB recorded the highest mean performance for plant height, leaf biomass and seed weight, while the A00 genotypes were observed to have higher values of leaf length, leaf area and root biomass. The principal component analysis showed that the first component accounted

for 42% of the total variation. The correlation matrix for growth, agronomic and yield characters show highly significant positive relationship among the growth characters at $P<0.05$. Primer UBC-866(CTC)$_6$ was highly polymorphic. Genotype A005 performed best for growth characters while NGB00182 performed best for yield characters. Genetic assessment and improvements in *C. argenta* germplasm play key role in future studies and improvements of vegetable crop.

Keywords: *Celosia argentea*, germplasm, genomic DNA, ISSR primers.

Introduction

Celosia argentea L. is an annual leafy vegetable of the genus *Celosia*, order Caryophyllales and family Amaranthaceae which shares features with members of the genus Amaranthus (Thorat, 2018). It is one of the leading vegetables in South-Western Nigeria, it is propagated by seed and grows up to 200 cm (6.5 feet) in height. The plant produces globular fruits, black seeds, and simple, spirally arranged leaves. It also frequently exhibits pink or white flowers (Ejoh *et al.,* 2021).

Celosia argentea is a tetraploid species (2n=36), though some varieties were found to be octaploid (Olawuyi *et al.,* 2016; Hussain *et al.*, 2024). The commonly cultivated *C. argentea* are the green broad-leaved cultivars (soko green), the broad-leaved cultivars with anthocyanin pigmentation of the leaf blades and part of the stem (soko pupa-red soko) and cultivars with deep green narrow leaves with a hard texture and early flowering (Grubben and Denton, 2004; Falodun *et al.,* 2022). The leaves and stems are prepared as soups, sauces or stew which could be consumed with food items such as maize, rice, yam and cassava (Bamigbegbin *et al.,* 2016). Medicinally, the stems and leaves are applied as poultice smeared in honey as treatment for infected sores, wounds and abscesses. Leaf concussions are used to relieve gastrointestinal disorders. Finely powdered or decocted seeds are considered antidiarrhoeal or aphrodisiac. Furthermore, the plant root is used for abdominal colic, gonorrhea and eczema while the whole plant serves as antidote for snake poison (Nahida *et al.,* 2012; Stuart, 2016).

Molecular markers are used to assess the influence of various factors on genetic diversity (Zhao *et al.*, 2023). Inter-Simple Sequence Repeats (ISSRs) are DNA fragments about 100 - 3000 bp in length which are located between flanking microsatellite regions. The ISSR technique is a PCR based technique involving the amplification of DNA segments present between two identical microsatellite regions that are oppositely oriented to each other. The technique uses single microsatellite primers ISSRs of different sizes usually 16-25 bp long amplifying

in a PCR reaction to target multiple genomic loci. Thus, fragments of several loci are generated at once, separated by gel electrophoresis and scored for presence or absence (Omondi *et al.,* 2016; Conțescu and Anton, 2023). In spite of this, there are limited information on the characterization of *C. argentea* using ISSR primers. Therefore the study was carried out to investigate the molecular characterization of *C. argentea* genotypes.

Materials and methods

Sample collection and study location

Twenty-five genotypes of *Celosia argentea* were used for this research. The *C. argentea* genotypes were sourced from National Centre for Genetic Resources and Biotechnology (NACGRAB) in Ibadan and ten (10) selected markets from ten local governments in Ibadan, Nigeria shown in Table 1. An open field experiment was conducted between June and September 2018 at the research farm of the Department of Botany, University of Ibadan, Ibadan (7.4417° N; 3.9000°E) located in the rainforest area of Southwestern Nigeria (Table 1). The molecular studies were carried out at the Department of Virology, University College Hospital, Ibadan.

Experimental design, method of planting, cultural practices and storage

A total of one hundred perforated polythene bags were each filled with 8 kg of sandy-loamy soil and arranged in a completely randomized design, with four replicates, spaced at 0.75 m within the row and column. The genotypes were raised for 2 weeks in the nursery bags before transplanting into polythene bags. The crop was raised following good agronomic practices according to standard procedures of FAO (2004). The weeds were removed manually weekly whenever it appears and watering was done on daily basis till the rainy period started. Two plants were transferred into polythene bags and thinned to a plant per bag after two weeks. Fresh young apical leaves were collected randomly for each genotype early in the morning, preserved in ice bags before being transported to the laboratory where it was stored in the refrigerator at -20°C prior to molecular studies.

Data collection

A total of 20 morphological characters comprising 15 quantitative and 5 qualitative traits were evaluated on the cultivated *C. argentea* genotypes according to the method described by IPGRI (2006). Data collection on growth characters of *C. argentea* genotypes commenced after transplanting at four weeks after planting

(WAP). This was carried out continuously every week till the 13th week after planting. Data collected were: growth habit, leaf shape, leaf color, color of flower, petiole pigmentation, plant height (cm), leaf length (cm), leaf width (cm), leaf area (cm²), petiole length (cm), number of internodes on stem, number of leaves per plant, plant height at flowering (cm), number of days to flowering, fruit length at maturity (cm), number of flowers per plant. Harvesting was done at fourteen weeks after planting and data collected on yield related characters were: leaf biomass (g), root biomass (g), seed weight (g) and shoot weight (g).

Table 1. *Celosia argentea* genotypes and their location

S/N	Genotype name	Location	Local government
1	A001	Mapo	Ibadan South East
2	A002	Agbowo	Ibadan North West
3	A003	Bodija	Ibadan North
4	A004	Iwo road	Egbeda
5	A005	New garage	Oluyole
6	A006	Apata	Ido
7	A007	Olodo	Lagelu
8	A008	Oja Oba	Ibadan South West
9	A009	Amuloko	Ona ara
10	A0010	Moniya	Akinyele
11	NGB00126	NACGRAB	Ibadan
12	NGB00128	NACGRAB	Ibadan
13	NGB00129	NACGRAB	Ibadan
14	NGB00133	NACGRAB	Ibadan
15	NGB00136	NACGRAB	Ibadan
16	NGB00137	NACGRAB	Ibadan
17	NGB00138	NACGRAB	Ibadan
18	NGB00151	NACGRAB	Ibadan
19	NGB00155	NACGRAB	Ibadan
20	NGB00170	NACGRAB	Ibadan
21	NGB00172	NACGRAB	Ibadan
22	NGB00177	NACGRAB	Ibadan
23	NGB00179	NACGRAB	Ibadan
24	NGB00182	NACGRAB	Ibadan
25	NGB00183	NACGRAB	Ibadan

DNA extraction

DNA was extracted from young frozen apical leaves of twenty-five *C. argentea* samples using the ISSR technique following the protocol outlined in the Jena Bioscience Plant DNA extraction kit. Fresh frozen tissue was macerated in a mortar and homogenized with a pestle, followed by the addition of 1 ml of phosphate buffer saline (PBS). In a 2 ml Eppendorf tube, 300 µl of cell lysis solution was added, followed by 500 µl of ground sample. The solution was then incubated at 65°C for 60 minutes, with occasional inversion during incubation, and subsequently allowed to cool at room temperature (25°C). After the addition of 100 µl of protein precipitation solution, the cell lysate was vortexed, and the solution was centrifuged at 15,000 rpm for three minutes. The DNA-containing supernatant was carefully transferred into a clean 2 ml Eppendorf tube containing 300 µl of isopropanol. The mixture was vortexed for 2 seconds and then centrifuged at 15,000 rpm for 1 minute. The supernatant was discarded, and the tube was drained on a clean absorbent paper. Subsequently, 500 µl of buffer was added, and the tube was inverted multiple times to create the DNA pellet. The solution was then centrifuged for one minute at 15,000 rpm, and the supernatant was gently discarded. The DNA pellets were air-dried at room temperature. Finally, 50-100 µl of DNA hydration solution was added to the dried pellets, and the samples were stored in the refrigerator for PCR analysis.

DNA amplification

Six Inter Simple Sequence Repeat (ISSR) primers were optimized and utilized in Polymerase Chain Reactions (PCR) (Table 2). Each locus was amplified within a 10 µl PCR cocktail reaction mixture comprising 2 µl of each primer, 1 µl of PCR buffer, 0.8 mM dNTPs, 0.4 mM MgCl2, 0.06 units of Taq polymerase, 0.8 µl of DMSO, 3 µl of PCR-grade H2O, and 2 µl of total genomic DNA. DNA amplification was conducted using a touch-down PCR procedure in a thermocycler. The PCR protocol included the initial denaturation at 95°C for 2 minutes, followed by 10 cycles of touch-down cycling comprising of denaturation at 95°C for 30 seconds, annealing starting at 65°C and decreasing by 1°C each cycle until reaching 55°C, for 30 seconds per cycle, and extension at 72°C for 1 minute. This was followed by 25 cycles of standard PCR with denaturation at 95°C for 30 seconds, annealing at 55°C for 30 seconds, and extension at 72°C for 1 minute. The final extension step lasted five minutes at 72°C, followed by indefinite maintenance at 4°C until further analysis.

Table 2. Oligonucleotide primers and their sequences

S/N	Primers	Nucleotide sequence 5'-3'
1.	UBC-866 $(CTC)_6$	CTC CTC CTC CTC CTC CTC
2.	ISSCR-2 $(CA)_8$ AG	CA CA CA CA CA CA CA CA AG
3.	ISSCR-3 $(CA)_8$ CG	CA CA CA CA CA CA CA CA CG
4.	ISSCR- 4 $(CT)_8$ TG	CA CA CA CA CA CA CA CA TG
5.	ISSCR- 5 $(CA)_8$ AC	CA CA CA CA CA CA CA CA AC
6.	ISLA- $(AGC)_4$ G	AGC AGC AGC AGC G

Agarose gel electrophoresis

Agarose gel electrophoresis was performed to detect the presence of DNA amplicons after PCR. To prepare the gel, 1 g of agarose was dissolved in 100 mL of 0.5×TBE buffer using a microwave for 3 minutes. The solution was then allowed to cool before casting the gel. Once solidified, the gel was placed in the electrophoresis tank and covered with 0.5×TBE buffer. Each DNA sample was mixed with loading dye and then loaded into the wells of the prepared gel in the electrophoresis tank. The electrophoresis was run for 30 minutes at 100 volts. A negative control, lacking a DNA template, was included. After electrophoresis, the gel was stained with SYBR Green and the separated amplified fragments were visualized under UV transilluminator light to observe the formation of bands.

Statistical analysis and data interpretation

Morphological data was subjected to Analysis of Variance (ANOVA) using SAS 9.1 software (2003 version), with differences in means determined through the Duncan Multiple Range Test (DMRT). Relationships among growth and yield characteristics were assessed using dendrograms, Pearson correlation coefficients, and Principal Component Analysis (PCA).

Molecular data was analyzed to elucidate total gene diversity using the NTSYS-pc version 2.02e package and PowerMarker version 3.25 software. Amplified fragments were scored as 1 for present and 0 for absent according to Liu and Muse (2005). These scores were then utilized to construct a dendrogram employing the Unweighted Pair Group Method with Arithmetic Average (UPGMA) cluster analysis, as outlined by Sneath and Sokal (1973), to elucidate the genetic relationships among *C. argentea* genotypes.

Results

The results obtained in this study indicate great morphological and molecular variability among the investigated genotypes. Due to the high polymorphism level detected by the primers, the study validates ISSR markers as useful tools to assess the *C. argente*ga genotypes.

Mean square effect of location and growth stages on growth characters of *C. argentea*

The analysis of variance of morphological traits (Table 3) shows that there is significant variation in all the samples of *C. argentea* for growth characters (P<0.05). The growth characters of *C. argentea* are significantly affected by the age of the plant (weeks).

Table 3. Mean square effect of genotypes and growth stages
on growth characters of *Celosia argentea*

SOV	DF	PH (cm)	LL (cm)	LW (cm)	LA (cm^2)	PL (cm)	NOI	NOLPP	PHF (cm)
Genotypes	24	1561.32**	30.35**	24.80**	7635.73**	10.62**	405.48**	2887.96**	430.20**
Weeks	9	92474.68**	275.29**	87.22**	37756.66**	132.91**	10897.30**	33312.93**	39110.86**
Replicates	3	82.13^{ns}	8.64*	6.04**	1449.31*	3.83^{ns}	103.07^{ns}	891.96*	10.06^{ns}
Error	923	129.28	2.87	0.96	391.46	1.48	42.76	174.86	107.67
Corrected total	959	996819	5835.42	2260.07	872953	2799.02	147652	527048	454761

Note: ** P<0.01 highly significant, * P<0.05 significant, ns=not significant; KEYS: SOV: sources of variation, DF: degree of freedom, PH: plant height, LL: leaf length, LW: leaf width, LA: leaf area, PL: petiole length, NOI: no. of internodes on main stem, NOLPP: no. of leaves per plant, PHF: plant height at flowering.

Mean square effect of genotypes and growth stages on yield characters of *C. argentea*

The results in Table 4 show that the agronomic and yield characters of *C. argentea* highly vary with genotypes, being significantly affected by the age of the plant (weeks), but the observed variation among replicates for these characters are not statistically significant.

Table 4. Mean square effect of genotypes and growth stages
on yield characters of *Celosia argentea*

SOV	DF	NDF	FLM (cm)	NFPP	LB (g)	RB (g)	SW (g)	SHW (g)
Genotypes	24	429.33**	3.99**	175.84**	328.72*	367.80*	43.81**	1948.20*
Weeks	9	32381.24**	205.96**	5238.92**	37807.57**	23251.55**	1075.47**	124956.35**
Replicates	3	7.62^{ns}	0.05^{ns}	19.14^{ns}	243.22^{ns}	188.10^{ns}	10.88^{ns}	203.68^{ns}
Error	923	97.78	1.08	59.17	191.43	176.19	15.29	821.77
Corrected total	959	38398.3	2889.74	104279	525531	377789	24668.1	1904906

Note: ** $P<0.01$ highly significant, * $P<0.05$ significant, ns=not significant; KEYS: SOV: sources of variation, DF: degree of freedom, NDF: no. of days to flowering, FLM: fruit length at maturity, NFPP: no. of flowers per plant, LB: leaf biomass, RB: root biomass, SW: Seed weight, SHW: shoot weight.

Mean square effect of genotypes on growth and yield of C. argentea

Plant height ranged from 35.22 cm in NGB00133 to 62.08 cm in NGB00151. The height of 50.22 cm recorded in A001 did not differ significantly from genotypes A002, A003, A010, NGB00137, NGB00155, NGB00170, NGB00172 and NGB00182, with respective heights of 46.10, 51.24, 50.12, 47.50, 47.13, 51.24, 51.68 and 49.3 cm. Similarly, genotypes NGB00126, NGB00128, NGB00138, NGB00151, NGB00177 and NGB00183 with heights 61.30, 57.85, 62.08, 56.68, 61.15 and 58.76 cm did not vary significantly from one another, but they were significantly taller than all other genotypes studied (Table 5).

The leaf parameters (leaf length, leaf width and leaf area) recorded the greatest values in A005, NGB00177 and A005 respectively, while the lowest values were recorded in NGB00151, NGB00183 and NGB00183 respectively (Table 6). Plant height at flowering, number of days to flowering and the root biomass did not differ significantly across all the genotypes, except for A001, with a value of 0.00 in each character state. Also, NGB00182 produced the highest leaf biomass. Generally, it was observed that the highest mean performance for plant height, leaf biomass and seed weight are found in the NGB genotypes while the A00 genotypes were observed to have remarkably higher values in terms of leaf length, leaf area and root biomass.

Table 5. Mean square effect of genotypes on growth and yield characters of *C. argentea*

GN	PH (cm)	LL (cm)	LW (cm)	LA(cm^2)	PL (cm)	NOI
A001	50.22^{efgh}	10.85^{efghi}	5.80^{hij}	66.08^{efg}	4.99^{cde}	16.33^{defg}
A002	46.1^{ghi}	11.85^{bc}	6.46^{cde}	79.79^{cd}	5.80^{ab}	18.67^{defgh}
A003	51.24^{defg}	11.53^{bcde}	6.40^{cdef}	75.91^{cd}	5.36^{abcd}	22.31^{abc}
A004	44.53^i	10.12^{hijk}	5.67^{hij}	60.55^{ghi}	4.66^{cde}	14.75^{lm}
A005	45.07^{hi}	12.89^a	6.85^{bc}	94.79^a	5.49^{abcd}	21.64^{bcde}
A006	54.52^{cde}	11.90^b	7.03^{ab}	84.21^{bc}	5.95^a	20.19^{cdefg}
A007	38.12^k	10.24^{ghijk}	5.83^{ghij}	63.11^{fghi}	5.51^{abc}	14.86^{klm}
A008	42.43^j	10.35^{ghijk}	5.78^{hij}	61.96^{ghi}	5.96^a	12.08^m
A009	55.06^{bede}	11.02^{cdefg}	6.35^{def}	72.81^{fe}	5.51^{abc}	18.28^{fghij}
A010	50.12^{efgh}	10.07^{ijk}	5.54^{ij}	59.46^{ghi}	4.89^{cde}	17.78^{ghijk}
NGB00126	61.30^a	12.18^b	6.60^{cd}	83.82^c	5.43^{abcd}	23.70^{ab}
NGB00128	57.85^{abc}	10.92^{defgh}	6.11^{efgh}	68.78^{efg}	5.12^{cde}	20.90^{bcdef}
NGB00129	54.85^{bcde}	9.97^{jk}	5.68^{hij}	58.73^{hi}	5.13^{cde}	15.08^{jklm}
NGB00133	35.22^k	10.49^{ghij}	5.54^j	63.64^{fgh}	5.11^{cde}	13.60^{lm}
NGB00136	52.32^{def}	10.47^{ghijk}	5.57^{ij}	61.12^{ghi}	4.97^{cde}	21.85^{abcd}
NGB00137	47.50^{fghi}	9.77^{jk}	5.55^{ij}	54.95^i	4.60^e	16.20^{ijkl}
NGB00138	62.08^a	10.69^{fghi}	5.90^{ghij}	65.64^{fg}	4.84^{de}	20.50^{bcdefg}
NGB00151	56.68^{abcd}	10.69^{efghi}	6.00^{efghi}	66.54^{efg}	5.31^{abcd}	19.23^{cdefgh}
NGB00155	47.13^{ghi}	9.57^k	5.45^j	52.81^i	4.97^{cde}	17.25^{hijk}
NGB00170	51.24^{efg}	11.02^{defg}	5.98^{fghij}	67.40^{efg}	5.46^{abcd}	17.90^{fghijk}
NGB00172	51.68^{defg}	10.33^{ghijk}	5.65^{ij}	63.03^{ghi}	5.53^{abc}	18.48^{fghi}
NGB00177	61.15^a	11.98^b	7.30^a	90.11^b	5.36^{abcd}	20.33^{cdefg}
NGB00179	56.57^{bcd}	11.37^{cdef}	6.31^{defg}	74.95^{de}	5.80^{ab}	24.28^a
NGB00182	49.32^{fgh}	11.61^{bcd}	6.16^{defgh}	73.26^{def}	5.22^{cde}	19.00^{defgh}
NGB00183	58.76^{ab}	9.60^k	3.06^k	28.85^j	5.63^f	13.40^m

Note: Mean with the same letter in the same column are not significantly different at P≥0.05 according to DMRT; KEYS: GN: genotype, PH: plant height, LL: leaf length, LW: leaf width, LA: leaf area, PL: petiole length, NOI: no. of internodes on main stem.

Table 6. Genotypic effect on agronomic and yield characters of *Celosia argentea*

GN	NOLPP	PHF (cm)	NDF	FLM (cm)	NFPP	LB (g)	RB (g)	SW (g)	SHW (g)
A001	34.86[defg]	0.00[b]	0.00[b]	0.00[d]	0.00[d]	0.00[d]	0.00[b]	0.00[c]	0.00[c]
A002	42.33[c]	7.41[a]	7.08[a]	0.54[abcd]	3.08[abcd]	4.69[bcd]	3.53[ab]	0.81[c]	11.08[bc]
A003	49.33[a]	5.72[a]	5.89[a]	0.64[abc]	4.06[abcd]	2.19[d]	3.11[ab]	1.89[bc]	7.22[bc]
A004	36.69[def]	5.75[a]	6.50[a]	0.41[bcd]	1.83[bcd]	5.92[abcd]	6.67[ab]	0.67[c]	15.14[abc]
A005	47.92[ab]	4.64[ab]	5.58[a]	0.92[a]	4.25[abcd]	3.0[cd]	3.08[ab]	2.17[abc]	9.72[bc]
A006	33.72[efgh]	4.95[ab]	7.14[a]	0.63[abc]	1.81[bcd]	7.11[abcd]	8.28[a]	0.61[c]	16.33[ab]
A007	22.50[jkl]	8.62[a]	7.34[a]	0.56[abcd]	2.69[abcd]	6.28[abcd]	8.75[a]	1.00[c]	16.92[ab]
A008	22.47[kl]	7.38[a]	7.53[a]	0.64[abc]	20.3[bcd]	3.83[bcd]	2.72[ab]	0.70[c]	9.72[bc]
A009	28.78[hijk]	7.43[a]	7.47[a]	0.44[abcd]	4.94[ab]	2.58[cd]	3.31[ab]	1.03[bc]	13.44[abc]
A010	30.97[ghi]	7.40[a]	6.75[a]	0.51[abcd]	3.97[abcd]	3.56[cd]	3.83[ab]	1.36[bc]	11.81[abc]
NGB00126	38.83[cde]	6.11[a]	5.90[a]	0.64[abc]	2.10[bcd]	2.23[cd]	1.75[b]	0.09[c]	6.95[c]
NGB00128	32.90[fghi]	8.47[a]	6.95[a]	0.84[ab]	4.78[abc]	9.91[abc]	8.16[a]	2.17[bc]	15.82[abc]
NGB00129	26.33[jk]	8.87[a]	6.30[a]	0.54[abcd]	3.93[abcd]	7.57[abc]	7.52[a]	3.07[ab]	15.52[abc]
NGB00133	22.25[l]	8.39[a]	6.75[a]	0.54[abcd]	3.90[abcd]	9.53[abc]	5.61[ab]	1.29[bc]	14.70[abc]
NGB00136	38.33[cde]	4.20[b]	5.95[a]	0.15[d]	0.48[d]	6.71[abcd]	3.13[ab]	0.11[c]	9.71[bc]
NGB00137	26.50[ijk]	7.72[a]	7.13[a]	0.54[abcd]	2.38[bcd]	8.23[abc]	8.38[a]	0.58[c]	12.70[abc]
NGB00138	37.98[cde]	6.74[a]	7.08[a]	0.28[cd]	1.43[bcd]	7.26[abcd]	4.74[ab]	0.55[c]	9.72[bc]
NGB00151	29.30[ghij]	7.46[a]	4.98[a]	0.80[ab]	6.68[a]	5.91[abcd]	3.98[ab]	4.07[a]	12.09[abc]
NGB00155	27.73[ijk]	8.33[a]	7.10[a]	0.63[abc]	2.90[abcd]	9.20[abc]	7.56[a]	0.76[c]	16.12[abc]
NGB00170	26.45[ijk]	7.96[a]	8.03[a]	0.43[abcd]	0.73[cd]	5.92[abcd]	5.49[ab]	0.26[c]	9.85[bc]
NGB00172	40.13[cd]	8.56[a]	8.18[a]	0.42[abcd]	0.60[cd]	6.32[abcd]	3.96[ab]	0.28[c]	10.23[bc]
NGB00177	38.53[cde]	7.40[a]	6.85[a]	0.46[abcd]	1.93[bcd]	7.96[abc]	5.50[ab]	1.28[bc]	15.32[abc]
NGB00179	46.58[b]	7.83[a]	5.98[a]	0.71[abc]	2.56[bcd]	10.78[ab]	8.06[a]	1.20[bc]	13.54[abc]
NGB00182	30.98[fghi]	7.55[a]	6.45[a]	0.54[abcd]	4.05[abcd]	11.74[a]	7.29[ab]	1.72[bc]	26.79[a]
NGB00183	19.53[l]	8.34[a]	8.00[a]	0.49[abcd]	1.20[bcd]	6.69[abcd]	7.33[ab]	0.56[c]	13.18[abc]

Note: Mean with the same letter in the same column are not significantly different at P≥0.05 according to DMRT; KEYS: GN: Genotype, NOLPP: no. of leaves per plant, PHF: plant height at flowering, NDF: no. of days to flowering, FLM: fruit length at maturity, NFPP: no. of flowers per plant, LB: leaf biomass, RB: root biomass, SW: Seed weight, SHW: shoot weight.

PCA of growth and yield characters of C. argentea

The result of the PCA analysis reveals that the quantitative characters of *C. argentea* are delineated into nine different principal component axes (Table 7). 78% of the total variation is explained by the first three components (prin 1, prin 2 and prin 3) with Eigen values 6.3, 3.89 and 1.49 respectively. The first component, prin 1, is a measure of the agronomic and yield characters of *C. argentea*. It captures 42% of the total variation and shows that plant height (0.37) at flowering is closely related with number of days to flowering (0.36), fruit length at maturity (0.36), number of flowers per plant (0.34), leaf biomass (0.35), root biomass (0.35), seed weight (0.31) and shoot weight (0.37). It is an indication that these eight characters vary together.

Table 7. PCA of growth and yield characters of *C. argentea*

Characters	Prin 1	Prin 2	Prin 3	Prin 4	Prin 5	Prin 6	Prin 7	Prin 8	Prin 9
PH	-0.02	0.23	0.5	0.1	0.77	0.15	0.25	0.1	0.04
LL	-0.07	0.43	-0.26	0.03	0.14	0.03	-0.25	0.19	-0.69
LW	-0.07	0.44	-0.27	0	0.1	0	-0.16	-0.21	0.64
LA	-0.06	0.46	-0.26	0.03	0.09	0.03	-0.28	-0.01	0.08
PL	-0.05	0.38	-0.22	-0.04	-0.27	0.09	0.85	0.08	-0.04
NOI	0.03	0.33	0.5	-0.11	-0.27	-0.01	-0.05	0.7	-0.2
NOLPP	-0.01	0.32	0.49	-0.13	-0.39	-0.22	-0.17	0.61	0.18
PHF	0.37	0.02	0	-0.1	0.03	0.44	-0.03	0.05	0.1
NDF	0.36	0.02	0	-0.18	-0.04	0.53	-0.08	0.05	0.03
FLM	0.36	0.05	0.03	0.17	-0.15	0.31	-0.07	0.08	-0.06
NFPP	0.34	0.06	0	0.48	-0.06	-0.16	-0.01	-0.12	-0.05
LB	0.35	0.04	-0.08	-0.35	0.12	-0.32	0.04	0.02	-0.04
RB	0.35	0.02	-0.07	-0.32	0.14	-0.32	0.08	0	0
SW	0.31	0.06	0	0.63	-0.04	-0.23	0.06	0.06	0.08
SHW	0.37	0.03	-0.06	-0.2	0.13	-0.27	0.03	-0.03	-0.03
Eigen value	6.3	3.89	1.49	0.81	0.64	0.48	0.43	0.27	0.21
Proportion	0.42	0.68	0.78	0.83	0.88	0.91	0.94	0.95	0.97

Prin 2, accounting for a little above a quarter of the total variation, gives a measure of the growth characters of *C. argentea*. It shows the closeness of leaf length (0.43), leaf width (0.44) and leaf area (0.46) and number of leaves per plant (0.49) while petiole length (0.38), number of internodes on stem (0.33) and number of leaves per plant (0.32) are related to one another. This means genotypes with large leaf length are likely to have large leaf width and leaf area while genotypes with petiole length have similar characteristics with number of internodes on main stem and number of leaves per plant. The third component shows that plants height (0.50) is similar to number of internodes on main stem (0.50). This implies that closeness of these traits could be used as a predictor for the other. Overall, the observation from the PCA analysis confirms the result of the correlation matrix which shows that the growth characters of *C. argentea* are not significantly associated its agronomic and yield characters.

Correlation matrix among growth and yield characters of C. argentea

Correlation matrix for growth, agronomic and yield characters (Table 8) show a highly significant positive relationship among the growth characters; although, no significant correlation existed between the growth characters and any of the agronomic and yield characters, it was observed that the agronomic and yield characters are well related to one another. This suggests that the variation in the growth characters does not affect the agronomic and yield characters.

Plant height had a positive correlation with leaf width (r = 0.5) and a strong positive association with leaf length (r = 0.63), leaf area (r = 0.62), petiole length (r = 0.61), number of internodes on main stem (r = 0.85), number of leaves per plant (r = 0.79) at p<0.01. Leaf length is positive and strongly related to leaf width (r = 0.86), leaf area (r = 0.94), petiole length (r = 0.77), number of internodes on main stem (r = 0.65), number of leaves per plant (r = 0.64). Likewise, leaf width is positive and strongly correlated with respect to leaf area (r = 0.95), petiole length (r = 0.77), number of internodes on main stem (r = 0.61) and number of leaves per plant (r = 0.60). A positive and strong correlation exist between leaf area and petiole length (r = 0.79), number of internodes on main stem (r = 0.66) and number of leaves per plant (r = 0.68). Petiole length has a strong positive correlation with number of internodes on main stem (r = 0.66) and number of leaves per plant (r = 0.64). A positive and strong association also exists between number of internodes on main stem and number of leaves per plant (r = 0.68). Furthermore, plant height at flowering has strong positive correlation with number of days to flowering (r = 0.97), fruit length at maturity (r = 0.90), number of flowers per plant (0.77), leaf biomass (r = 0.82), root biomass

(r = 0.81), seed weight (r = 0.69) and shoot weight (r = 0.85). A strong positive correlation was observed for number of days to flowering with fruit length at maturity (r = 0.89), number of flowers per plant (r = 0.72), leaf biomass (r = 0.88), root biomass (r = 0.81), seed weight (r = 0.63) and shoot weight (r = 0.83). Fruit length at maturity had strong and positive relationship with number of flowers per plant (r = 0.84), leaf biomass (r = 0.75), root biomass (r = 0.76), seed weight (0.78) and shoot weight (r = 0.81). Number of flowers per plant had strong and positive relationship with leaf biomass (r = 0.69), root biomass (r = 0.70), seed weight (r = 0.89) and shoot weight (r = 0.77). Leaf biomass had strong and positive correlation with root biomass (r = 0.92), seed weight (r = 0.61) and shoot weight (r = 0.93). Root biomass also had strong and positive relationship with seed weight (r = 0.62) and shoot weight (r = 0.92) while strong and positive association existed between seed weight and shoot weight (r = 0.69) (Table 8).

Frequency, diversity of alleles and PIC of C. argentea genotypes using ISSR markers

A total of six polymorphic primers of ISSR markers were used to investigate the genetic diversity and molecular relationship of *C. argentea* genotypes (Figure 1, Table 2). The percentage gene diversity recorded 80% while the polymorphism in the population was diverse at 78%. The number of allele ranges from 4.0 to 15.0 with a mean of 10.50. Major allele frequency ranges from 0.24 to 0.48, with a mean of 0.35. Gene diversity and PIC varied from 0.67 to 0.87 and 0.61 to 0.85 with means of 0.80 and 0.78 respectively. There was variation in major allele frequency, number of alleles, gene diversity and PIC. Primer ISSCR3 had the highest major allele frequency at 0.48 and primer UBC866 had the lowest major allele frequency at 0.24. Primers ISLA, ISSCR-2, ISSCR-4, and ISSCR-5 had major allele frequencies of 0.28, 0.32, 0.36 and 0.44 respectively. Primer ISSCR2 had the highest number of alleles at 15.0, primer ISSCR5 had the lowest number of alleles at 4.0, primers ISLA and ISSCR3 had the same numbers of allele at 12.0, while primers UBC866 and ISSCR4 had allele numbers of 11.0 and 9.0 respectively. Primer UBC866 had the highest value for gene diversity at 0.87, the lowest value of gene diversity was found in primer ISSCR5, primers ISSCR2 and ISLA had gene diversity values of 0.86 while primers ISSCR3 and ISSCR4 had gene diversity values of 0.74 and 0.81 respectively. PIC was highest in primers UBC866 with 85.40% followed by ISLA with 85.22% and ISSCR2 with a value 85.21%. Primer ISSCR5 had the lowest PIC value at 60.61%, while primers ISSCR4 and ISSCR3 had PIC values of 77.67 and 72.45 respectively (Table 9).

Table 8. Correlation matrix among growth and yield characters of *Celosia argentea*

Character	PH (cm)	LL (cm)	LW (cm)	LA (cm²)	PL (cm)	NOI	NOLPP	PHF (cm)	NDF	FLM (cm)	NFPP	LB (g)	RB (g)	SW (g)	SHW (g)	ACC	WK
PH																	
LL	0.63**																
LW	0.57*	0.86**															
LA	0.62**	0.94**	0.95**														
PL	0.61**	0.77**	0.77**	0.79**													
NOI	0.85**	0.65**	0.61**	0.66**	0.66**												
NOLPP	0.79**	0.64**	0.60**	0.65**	0.64**	0.88**											
PHF	0.45ns	0.22ns	0.19ns	0.23ns	0.26ns	0.45ns	0.36ns										
NDF	0.46ns	0.24ns	0.19ns	0.24ns	0.26ns	0.46ns	0.37ns	0.97**									
FLM	0.43ns	0.25ns	0.20ns	0.26ns	0.27ns	0.46ns	0.39ns	0.90**	0.89**								
NFPP	0.37ns	0.22ns	0.19ns	0.24ns	0.22ns	0.39ns	0.31ns	0.77**	0.72**	0.84**							
LB	0.38ns	0.22ns	0.19ns	0.22ns	0.23ns	0.39ns	0.31ns	0.82**	0.80**	0.75**	0.69**						
RB	0.37ns	0.19ns	0.16ns	0.19ns	0.22ns	0.37ns	0.30ns	0.81**	0.80**	0.76**	0.70**	0.92**					
SW	0.35ns	0.21ns	0.18ns	0.22ns	0.22ns	0.34ns	0.29ns	0.69**	0.63**	0.78**	0.89**	0.61**	0.62**				
SHW	0.40ns	0.22ns	0.19ns	0.22ns	0.23ns	0.39ns	0.32ns	0.85**	0.83**	0.81**	0.77**	0.93**	0.92**	0.69**			
ACC	0.08ns	-0.08ns	-0.16ns	-0.14ns	-0.08ns	0.02ns	-0.08ns	0.05ns	0.03ns	0.00ns	-0.02ns	0.08ns	0.05ns	0.01ns	0.04ns		
WK	0.92**	0.61**	0.54*	0.59*	0.62**	0.81**	0.74**	0.50*	0.51*	0.48ns	0.40ns	0.43ns	0.42ns	0.36ns	0.44ns	0.07ns	
REP	0.00ns	0.05ns	0.08ns	0.06ns	-0.04ns	-0.00ns	-0.07ns	0.01ns	-0.00ns	-0.00ns	0.01ns	-0.02ns	-0.03ns	0.00ns	-0.01ns	-0.00ns	-0.00ns

Note: * P<0.05 significant, ** P<0.01 highly significant, ns=not significant; KEYS: PH: Plant Height, LL: leaf length, LW: leaf width, LA: leaf area, PL: petiole length, NOI: no. of internodes on main stem, NOLPP: no. of leaves per plant, PHF: plant height at flowering, NDF: no. of days to flowering, FLM: fruit length at maturity, NFPP: no. of flowers per plant, LB: leaf biomass, RB: root biomass, SW: Seed weight, SHW: shoot weight, SOV: sources of variation, ACC: Genotypes, WK: Weeks, REP: Replicates.
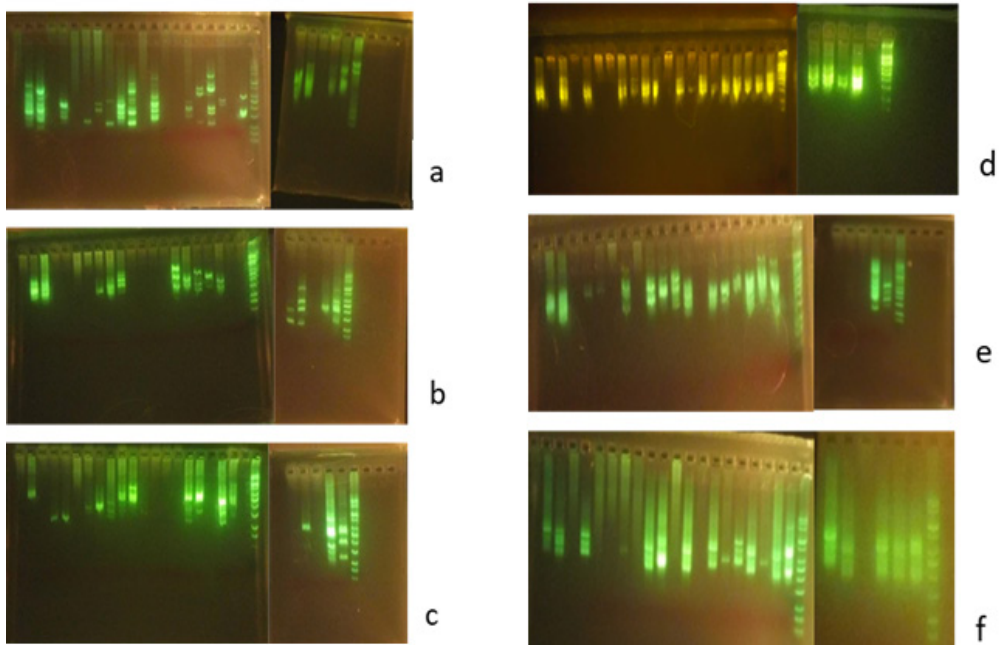
Figure 1: Gel Photograph showing 25 *Celosia argentea* genotypes with primers: a. (ISSCR-2 $(CA)_8$ AG), b. (ISSCR-3 $(CA)_8$ CG), c. (ISSCR- 4 $(CT)_8$ TG), d. (ISSCR- 5 $(CA)_8$ AC), e. (ISLA- $(AGC)_4$ G) and f. (UBC-866 $(CTC)_6$).

Note: Order of loading gel from well 1-27: NGB00129, A006, NGB00155, NGB00182, A005, NGB00128, NGB00183, NGB00179, NGB00151, NGB00138, A003, NGB00126, A002, NGB00172, A001, NGB00170, A004, A008, NGB00136, NGB00137, control, ladder, A007, A010, NGB00177, A009, NGB00133 and ladder.

Table 9. Frequency, diversity of alleles and PIC of *Celosia argentea* genotypes using ISSR markers

Marker	Major allele frequency	No. of observations	Allele No	Gene diversity	PIC (%)
UBC-866	0.24	25.00	11.00	0.87	85.40
ISSCR-2	0.32	25.00	15.00	0.86	85.21
ISLA	0.28	25.00	12.00	0.86	85.22
ISSCR-3	0.48	25.00	12.00	0.74	72.45
ISSCR-4	0.36	25.00	9.00	0.81	78.67
ISSCR-5	0.44	25.00	4.00	0.67	60.61
Mean	0.35	25.00	10.50	0.80	77.93

Dendogram showing qualitative characters of C. argentea genotypes

The result of the cluster analysis in Figure 2 shows that *C. argentea* genotypes clustered into six main groups based on their qualitative characters. Groups 1, 4 and 6 are groups comprising of single genotypes each namely NGB00128, NGB00179 and NGB00126 respectively. Group 2 composed of A010, NGB00136, A005, A006, A007, A008, NGB00183, A004, NGB00137, A001 and A003. Group 3 contains NGB00177, NGB00182, NGB00138, NGB00170, A009, NGB00172, and A002 while group 5 contains the remaining genotypes. The clustering indicates that NGB00128, NGB00179 and NGB00126 are more distantly related to each other than any of the other NGB genotypes but are more related to the market accessions.
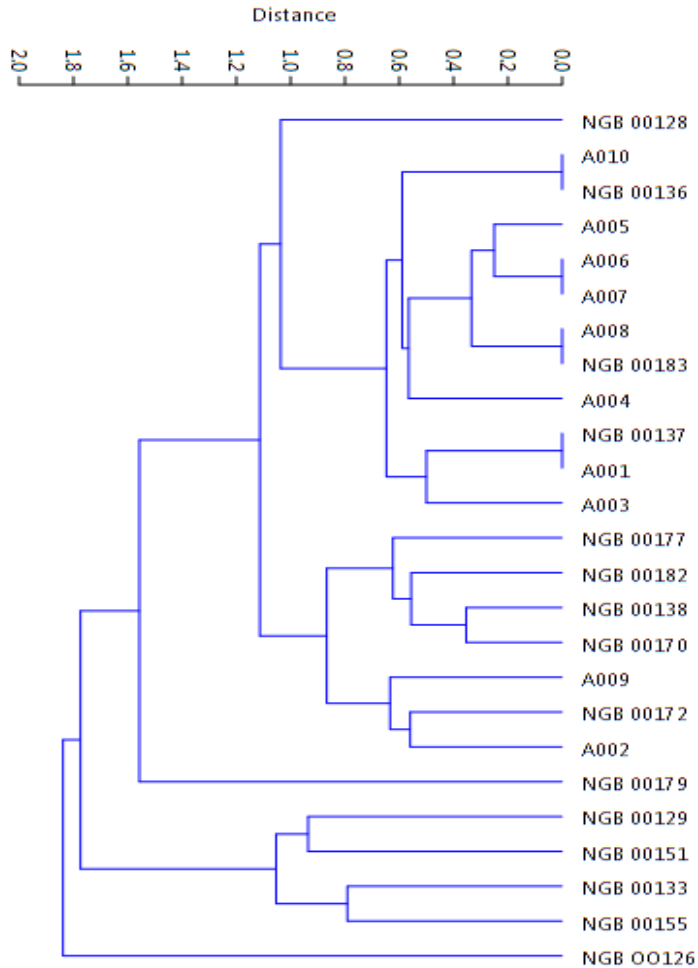
Figure 2. Dendogram showing qualitative characters of *Celosia argentea* genotypes

Dendogram showing genetic relatedness of C. argentea genotypes

The dendogram in Figure 3 consist of five clusters and two monolifolious groups (A003 and A005). Cluster 1 had the highest number of genotypes (12), while clusters 2 and 3 had each at least 2 genotypes. NGB00182 and NGB00172, as well as NGB00128 and NGB00177 are closely related. Also, NGB00126 and NGB00137 are genetically related as compared to NGB00179. Meanwhile NGB00151 and NGB00136 are related and A004 and A010 are closely related in

cluster 2 and 3. In cluster 4, A002 and NGB00156 are closely related to each other while in cluster 5, A006 and A007 are closely related to each other, and also A001 and NGB00137 (Figure 3). The result in Figure 4 depicts that the growth habit, leaf shape and leaf color are more closely related than petiole pigmentation and colour of flowers across the qualitative character studied in all twenty-five genotypes of *C. argentea.*

Figure 3. Dendogram showing genetic relatedness of *Celosia argentea* genotypes

Figure 4. Scattered diagram of qualitative characters of *Celosia argentea* genotypes

Discussion

The information on genetic variability of morphological characters is of economic importance and pre-requisite for studies on any plant species (Olawuyi and Fawole 2005; Begna and Begna, 2021), it as well enables effective conservation and utilization of crop germplasm. Variations observed in the mean performance of the growth and yield characters of *C. argentea* across the accessions are in line with the findings of Olawuyi *et al.,* (2015). The plant height among growth characters exhibited positive and significant relationship with other characters studied as similarly observed by Nwangburuka *et al.,* (2012). However, genotype A005 from Oluyole Local government performed best for growth and NGB00182 performed best for yield related characters. The findings from correlation matrix shows that plant height shows a highly significant positive relationship among the growth characters as similarly observed by Nwangburuka *et al.,* (2012) and Olawuyi *et al.,* (2014). The correlation between plant height and growth characters is an implication that selection based on

137

plant height will favour the growth characters and does not affect those of the agronomic and yield characters (Balbaa *et al.*, 2022). Likewise, plant height at flowering shows a positive and significant correlation with number of days to flowering, fruit length at maturity, number of flowers per plant, leaf biomass, root biomass, seed weight and shoot weight.

The PCA from Prin.1 which accounted for the highest variation conformed to the findings made by Olawuyi *et al.,* (2016), previously observed by Olakojo *et al.,* (2005), and Olowe *et al.,* (2013). The principal component analysis reveals the variation patterns among the assessed characters and primarily accounts for the variation within a group of entries (Aremu *et al.,* 2007). This method supplements the insights gained from cluster analysis techniques as it provides more detailed information regarding distances among major groups (Taran *et al.*, 2005). This suggests that significant characters converging in specific components, contributing to variability, tend to be associated together. This presents an opportunity for their utilization in crop improvement strategies. Overall, the observation from the PCA analysis confirms the result of the correlation matrix and shows that the growth characters of *C. argentea* are not significantly correlated to its yield characters. In this study, cluster analysis and dendrogram show that cluster groups consist of genotype from different geographical locations with diverse variability, these may be due to cultivation approach and genetic makeup of individual genotype. This agrees with the findings by Ganapathy *et al.,* (2011) who accounted that wide adaptability of different genotype has been attributed to population genetic architecture, selection history and approach under domestic cultivation and developmental traits. The relationships that exist among the genotypes in the clusters show that there were genetic similarities which were similarly reported by Bamgbegbin *et al.,* (2016). This indicates these genotypes could be useful as breeding material in the improvement of this crop.

Christopoulos *et al.* (2010) demonstrated the utility of ISSR markers across various domains including genetic diversity assessment, phylogenetic studies, gene tagging, genome mapping, and evolutionary biology in numerous plant species. Moreover, Mariana *et al.* (2012) highlighted that ISSR markers effectively delineate high genetic variation among genotypes, facilitating their unambiguous identification. In this study, ISSR markers were employed to evaluate the level and distribution of genetic diversity in 25 accessions of Celosia argentea. The markers revealed over 85% polymorphism, indicating extensive genetic variability. The substantial polymorphism observed with the utilized primers aligns with the findings of Rakoczy-Trojanowska and Bolibok (2004), who noted a similarly highly polymorphic pattern when employing microsatellite

sequence-based reaction primers in plants. Also, amplification with the ISSR primers yielded highly informative patterns supporting the reports of Basel (2011). The differences in major allele frequency, number of allele and gene diversity accounted for variations in the population. This is supported by the reports of Denton (2004), Bamigbegbin *et al.,* (2016) and Oduwaye *et al.* (2014).

Conclusion and recommendation

Genetic evaluation and enhancement of *Celosia argentea* germplasm will be pivotal in future studies and the improvement of vegetable crops. The findings indicate that certain traits, including plant height, leaf length, leaf width, leaf area, petiole length, number of internodes on the main stem, and number of leaves per plant, exhibit strong linear relationships and could serve as selection criteria for enhancing other vegetable crops. Genotype A005 displayed superior performance for growth traits, whereas NGB00182 excelled in yield-related characteristics. The primer UBC-866 $(CTC)_6$ demonstrated high polymorphism and gene diversity. Generally, all A00 market genotypes exhibited early emergence, while NGB genotypes showed elevated values for plant height, leaf biomass, and seed weight. Conversely, A00 genotypes exhibited notably higher values in terms of leaf length, leaf area, and root biomass.

References

Agbolade, J.O., Olawuyi, O.J., Bello, O.B., Oluseye, O.D., & Komolafe, R.J. (2016). Genetic diversity and correlated response to selection of grain and associated characters in maize (*Zea mays* L.), *Intl. Res. J. Appl. Basic. Sci., 13*(1), 56-61.

Aremu, C.O., Adebayo, M.A., Ariyo, O.J., & Adewale, B.B. (2007). Classification of genetic diversity and choice of parents for hybridization in cowpea *Vigna unguiculata* (L.) Walp for humid savanna ecology. *Afr. J. Biotechnol.*, *6*(20), 2333-2339. Doi: 10.4314/ajb.v6i20.58040.

Badra, T. (1993). Lagos spinach (*Celosia* sp.). In Williams, J.T. (ed.) Underutilized crops: Pulses and vegetables. Chapman and Hall, London. 131-163.

Balbaa, M.G., Osman, H.T., Kandil, E.E., Javed, T., Lamlom, S.F., Ali, H.M., Kalaji, H.M., Wróbel, J., Telesiñski, A., Brysiewicz, A., & Ghareeb, R.Y. (2022). Determination of morpho-physiological and yield traits of maize inbred lines (*Zea mays* L.) under optimal and drought stress conditions. *Front. Plant Sci.*, *13*, p.959203.

Bamigbegbin, B.J., Olawuyi, O.J., & Jonathan, S.G. (2016). Molecular variability of *Celosia argentea* using amplified fragment length polymorphism (AFLP) marker. *Mol. Plant Breed.*, *7*(26), 1-6. Doi: 10.5376/mpb.2016.07.0026.

Basel, S. (2011). Efficiency of RAPD and ISSR markers in assessing genetic variation in *Arthrocnemum macrostachyum* (Chenopodiaceae). *Braz. Arch. Biol. Technol.*, 54(5), 859-866. Doi: 10.1590/S1516-89132011000500002.

Begna, T., & Begna, T. (2021). Role and economic importance of crop genetic diversity in food security. *Int. J. Agric. Sci. Food Technol.*, *7*(1), 164-169.

Brenan, J.P. (1981). The genus *Amaranthus* in Southern Africa. *J. S. Afr. Bot.*, *47*(3), 451-492.

Chioma, L.K., Olatunde, O., Innocent, O.I., & Adefolarin, O.M. (2017). A review of the multifaceted usefulness of *Celosia argentea* Linn. *Eur. J. Pharm. Med. Res.*, *4*(10), 72-79.

Christopoulos, M.V., Rouskas, D., Tsantili, E., & Bebeli, P.J. (2010). Germplasm diversity and genetic relationships among walnut (*Juglans regia* L.) cultivars and Greek local selections revealed by inter-simple sequence repeat (ISSR) markers. *Sci. Hortic.,* *125*(4), 584-592. Doi: 10.1016/j.scientia.2010.05.006.

Conţescu, E.L., & Anton, F.G. (2023). Study of the genetic diversity of some wild sunflower species using ISSR markers. *Rom. Agric. Res.*, *40*, 2023-2116.

Denton, O.A. (2004). *Celosia argentea* L. *Plant Resour. Trop. Africa*, 2, 167-171.

Englbrecht, C.C., Freyhof, J., Nolte, A., Rassmann, K., Schliewen, U., & Tautz, D. (2000). Phylogeography of the bullhead *Cottus gobio* (Pisces: Teleostei: Cottidae) suggests a pre-Pleistocene origin of the major central European populations. *Mol. Ecol.*, *9*(6), 709–722. Doi: 10.1046/j.1365-294x.2000.00912.x.

Ejoh, S.I., Wireko-Manu, F.D., Page, D., & Renard, C.M. (2021). Traditional green leafy vegetables as underutilised sources of micronutrients in a rural farming community in south-west Nigeria I: estimation of vitamin C, carotenoids and mineral contents. *S. Afr. J. Clin. Nutr., 34*(2), 40-45.

Falodun, E.J., Akpomuaire, E., & Abidakun, O.P. (2022). The effects of organic manures and harvesting types in two seasons for yield and yield contributing agronomic traits in *Celosia* (*Celosia argentea* L.). *Agric. Conspec. Sci.*, *87*(1), 17-23.

Food and Agriculture Organization statistical database (2004): FAOSTAT website, http//faostat.fao.

Ganapathy, K.N., Gnanesh, B., Gowda, N., Byre, M., Venkatesha, S.C., Gomashe, S. S., & Mallikarjuna, V.C. (2011). AFLP analysis in pigeon pea (*Cajanus cajan*(L.) Millsp.) revealed close relationship of cultivated genotypes with some of its wild relatives. *Genet. Resour. Crop Evol.,* 58, 837-847.

Gehan, G., Asmaa, M.A., & Hoda, E.E. (2014). Induction of mutations in *Celosia argentea* using dimethyl sulphate and identification of genetic variation by inter simple sequence repeats (ISSRs) markers. *Int, J. Plt. Breed. Genet.,* 8(2), 44-56. Doi: 10.3923/ijpbg.2014.44.56.

Hussain, U., Afza, R., Gul, I., Sajad, M.A., Shah, G.M., Muhammad, Z., & Khan, S.M. (2024). Phytoremediation of heavy metals spiked soil by *Celosia argentea* L.: effect on plant growth and metal stabilization. *Environ. Sci. Pollut. Res.*, 1-9.

IPGRI. (2006). Descriptors for mango (*Mangifera indica* L.). International Plant Genetic Resources Institute, Rome, Italy.

Jabbarzadeh, Z., Khosh-Khui, M., Salehi, H., & Saberivand, A. (2010). Inter simple sequence repeat (ISSR) markers as reproducible and specific tools for genetic diversity analysis of rose species. *Afr. J. Biotechnol.*, 9(37), 6091-6095.

Liu, K., & Muse, S.V. (2005). PowerMarker: An integrated analysis environment for genetic marker analysis. *Bioinformatics,* 21(9), 2128-2129. Doi: 10.1093/bioinformatics/bti282.

Zhao Z., Zhang H., Wang P., Yang Y., Sun H., Li J., Chen X., Li J., Ji N., Feng H., & Zhao S. (2023). Development of SSR molecular markers and genetic diversity analysis of *Clematis acerifolia* from Taihang Mountains. *PLoS One*, 18(5), e0285754. Doi: 10.1371/journal.pone.0285754. PMID: 37205665; PMCID: PMC10198494.

Mariana, P.T., Martín, G., Ruth, H., & Alejandro, E. 2012. Analysis of genetic variability by ISSR markers in *Calibrachoa caesia*. *Electron. J. Biotechnol.*, 15(5), 8. Doi: 10.2225/vol15-issue5-fulltext-8.

Nahida, Ansari, S.H., & Siddiqui, A.N. (2012). *Pistacia Lentiscus*: A review on phytochemistry and pharmacological properties. *Int. J. Pharm. Pharm. Sci.,* 4, 16-20.

Nidavani, R.B., Mahalakshmi,A.M., & Mallappa, S. (2013). Towards a better understanding of an updated ethnopharmacology of *Celosia argentea* L. *Int J Pharm Pharm Sci.*, 5(3), 54-59.

Nwangburuka, C.C., Olawuyi, O.J., Kehinde, O., Kayode, O.O., Denton, O.A., Daramola, S.D.& Awotade, D. (2012). Effect of *Arburscular mycorrhizea* (AM), poultry manure (PM), NPK fertilizer and the combination of AM-PM on the growth and yield of okra (*Abelmoschus esculentus*) *Nat. Sci.*, 10(9), 35-41.

Oduwaye, O.A., Baranek, M., Cechova, J., & Raddova, J. (2014). Reliability and comparism of the polymorphism revealed in amaranth by amplified fragment length polymorphism (AFLPs) and inter simple sequence repeats (ISSRs). *J. Plant Breed. Crop Sci.,* 6(4), 48-56. Doi: 10.5897/JPBSC2013.0413.

Olakojo, S.A., Kogbe, J.O.S., Iken, J.E., & Daramola, A.M. (2005). Yield and disease evaluation of some improved maize (*Zea mays* L) varieties in Southwestern Nigeria. *Trop. Subtrop. Agroeco.*, 5, 51-55.

Olawuyi, O.J., & Fawole, I. (2005). Studies on genetic variability of some quantitative and qualitative characters in pigeon pea - *Cajanus cajan* (L.) Millsp. (Fabaceae). *Acta Satech.,* 2(1), 30-36.

Olawuyi, O.J., Bamigbegbin, B.J., & Bello, O.B. (2016). Genetic variation of morphological and yield characters of *Celosia argentea* L. Germplasm. *J. Basic Appl. Res. Int., 13*(3), 160-169.

Olawuyi, O.J., Odebode, A.C., Babalola, B.J., Afolayan, E.T., & Onu, C.P. (2014). Potentials of arbuscular mycorrhiza fungus in tolerating drought of miaze (*Zea mays* L.). *Am. J. Plant Sci., 5*(5), 779-786. Doi: 10.4236/ajps.2014.56092.

Olowe, O.A., Suman C., Peter, S., Lothar, H.W., Olufunmilola, B.M., Albert, B.O., & Muna, A. (2013). Pathotyping blaCTX-M *Escherichia coli* from Nigeria. *European J. Microbiol. Immunol., 3*(2), 120–125. Doi: 10.1556/EuJMI.3.2013.2.5.

Omondi, E.O., Thomas, D., Marcus, L., Mary, A.O., Fekadu, F.D., & Traud W. (2016). Molecular markers for genetic diversity studies in African leafy vegetables. *Adv. Biosci. Biotechnol., 7*(3), 188-197. Doi: 10.4236/abb.2016.73017.

Rakoczy-Trojanowska, M., & Bolibok, H. (2004). Characteristics and a comparison of three classes of microsatellite-based markers and their application in plants. *Cell. Mol. Biol. Lett., 9*(2), 221-238.

Rathanaswamy, R., Veeraswamy, R., Raghupathy, A., & Palaniswamy, G.A. (1973). Studies on genetic variability of certain quantitative characters in red gram. *Madras Agric. J., 63*(3), 204-206.

Stuart, Jr. G.U. (2016). Philippine medicinal plants. Family Amaranthaceae Palong-manok. Retrieved on 03/08/2018 from http://www.stuartxchange.org/Palong-manok.html 13.

Taran, B., Zhang, C., Warkentin, T., Tullu, A., & Vandenberg, A. (2005). Genetic diversity among varieties and wild species accessions of pea (*Pisum sativum* L.) based on molecular markers, and morphological and physiological characters. *Genome. 48*(2), 257-72. Doi: 10.1139/g04-114

Thorat, B.R. (2018). Review on *Celosia argentea* L. Plant. *Res. J. Pharmacogn. Phytochem., 10*(1), 109-119.

Tindall, H.D. (1983). Vegetables in the tropics. *Macmillian Press Ltd, London.* 533.

Wee, Y.C, (1992). A guide to medicinal plants, Singapore Science Centre Publication, Singapore.

Whitehead, A., Anderson, S.L., Kuivila, K.M., Roach, J.L., & May, B. (2003). Genetic variation among interconnected populations of *Catostomus occidentalis*: implications for distinguishing impacts of contaminants from biogeographical structuring. *Mol. Ecol*. *12*(10), 2817–2833. Doi: 10.1046/j.1365-294x.2003.01933.x

Zietkiewicz, E., Rafalski, A., & Labuda, D. (1994). Genome fingerprinting by simple sequence repeats (SSR)- anchored polymerase chain reaction amplification. *Genomics*, *20*(2), 176-183. Doi: 10.1006/geno.1994.1151

Sneath, P.H.A., & Sokal, R.R. (1973). Numerical taxonomy, The principle and practice of numerical classification. W. H. Freeman, San Francisco. 573.

Adaptation of the diaphonization protocol and the highlight of some significant structures development in the chicken embryo (*Gallus gallus*) skeleton

Leonard Calistru✉, Alexandru Nicolae Stermin

Babeş-Bolyai University; Str. Republicii nr. 44, Cluj-Napoca, Roumania
✉***Corresponding author, E-mail: leonard.calistru@gmail.com***

Abstract. Diaphonization is a technique used in developmental biology, anatomy, and comparative morphology to visualize and study the internal structures of small organisms. In this study, we used diaphonization to visualize the development of chicken embryos (*Gallus gallus*). Diaphonization was performed on chicken eggs at different stages of development, from 10 to 13 days of incubation, and the resulting specimens were analyzed using microscopy. The results suggest that for embryos older than 14 days, a longer storage time in 1% KOH is recommended (approximately 30% longer incubation time compared to the original protocol). In the case of more developed chicken embryos, it is also recommended to carry out evisceration. These results provide insight into the early stages of avian development and may have applications in the fields of developmental biology and anatomy.

Keywords: diaphonization protocol, chicken embryo development, skeletal visualization, developmental biology, avian skeletal adaptation.

Introduction

Diaphonization, also known as "clearing and staining", is a staining technique used to prepare wet specimens, typically animal embryos or small vertebrates (Liutenko *et al.*, 2023). The process involves making the tissues of the specimen transparent while staining cartilage and bone to make them more visible (Chitra and Sharon, 2020; Vovk *et al.,*2022).

In the past, this technique has been used primarily for anatomical studies, scientific research and educational purposes. It allows for a detailed examination of internal structures, particularly skeletal and soft tissues, aiding in the understanding of anatomical features, their development, and variations among different species (Atanasoff *et al.*, 2018). The resulting specimens can be further used for scientific purposes or as an educational tool in universities or public museums (Liutenko *et al.*, 2023). Moreover, by making internal structures visible, diaphonization aids in the comparison of anatomical features between different species, contributing to the understanding of evolutionary relationships and adaptations (Khan *et al.*, 2015; Tsandev *et al.*, 2020).

While newer imaging technologies have advanced in recent years, providing non-destructive ways to visualize internal structures, diaphonization continues to be used due to its ability to provide detailed, three-dimensional insights into anatomical structures, especially bones and cartilage, which some imaging technologies like X-ray microtomography or magnetic resonance microscopy may not capture as comprehensively. Additionally, this technique is crucial nowadays in the field of developmental biology because it allows for the visualization of embryos and their developmental stages in intricate detail (Stern, 2022). This leads to researchers being able to study how skeletal elements and organs form and change during development, identify abnormalities or variations in development and understand evolutionary relationships and adaptations across different taxa (Atanasoff *et al.*, 2018).

The diaphonization protocol used on rat embryos (see materials and methods section) was tested on chicken embryos and optimized in order to obtain viable wet specimens. The modifications were mandatory since the chicken embryo is significantly larger than the rat embryo after twelve days of incubation (Hamburger and Hamilton, 1951). The specific stage of embryonic development is an important element in adapting the diaphonization protocol. Late-stage embryos, from the 15th day of incubation, have some internal organs, such as air sacs and guts, much more developed than mid-stage embryos, from the 10th day of incubation, which need to be taken into consideration when using this technique (Chatterjee, 2015). While rat embryos follow mammalian developmental patterns, chicken embryos show avian developmental characteristics such as feathering (Sullivan *et al.*, 2017). Those feathers are a hindrance to the staining process, making them also a thing to consider when working with chicken embryos (Gofur, 2020).

In this context the main objectives of this study were to optimize the diaphonization protocol, making it viable for chicken embryos; and to highlight skeletal structures in upper limb, lower limb and tail.

Materials and methods

The diaphonization protocol was completed two times. For each attempt, 20 chicken eggs of farm origin were incubated at 37°C in a manual, still-air mini-incubator, and turned daily. The eggs were evenly taken out of incubation after 10, 11, 12 and 13 days, following this, the protocol was applied. The experiment was performed in duplicate during a two month period. During the second experiment, the eggs were removed from the incubator two days earlier compared to the first batch. Details of the experimental design are presented in Table 1.

Table 1. Steps of the diaphonization protocol performed
on chicken (*Gallus gallus*) embryos.

Day	Number of eggs sampled	Steps	Number of viable embryos
1	20	Start of incubation	-
2-11		Manual egg turning	
12	3	Embryo extraction, washing in tap water and fixation in 35mL ethanol 96%	3
13	6	Embryo extraction, washing in tap water and fixation in 35mL ethanol 96%	5
14	11	Embryo extraction, washing in tap water and fixation in 35mL ethanol 96%	3
		11 embryos were used for the rest of the experiment	
15		Staining with Alcian blue solution for 24 hours	
16		Washing twice in 35mL ethanol 96% for 5 minutes each and store in 35mL ethanol 96% for 24 hours	
17		Clarification with 35 mL KOH solution (1%) for 6 hours Staining with Alizarin red solution for 3 hours Clarification with 35 mL KOH solution (2%) for 2 days	
18		Washing in 35 mL of 80/20 solution made of KOH (2%) and glycerin for 5 hours	
19		Washing in 35 mL of 60/40 solution made of KOH (2%) and glycerin overnight	
20		Storage for unlimited time in 35 mL of 20/80 solution made of KOH (2%) and glycerin	

The experimental design was adapted after the diaphonization protocol for rat embryos (provided courtesy of Prof. Dr. Iacob Checiu, not published):

1) Fixation using 35mL of 96% ethanol for 3-5 days;
2) Staining for 24 hours. using Alcian blue (final concentration 0.15 mg/mL) dissolved in a solution consisting of 80 mL of 96% ethanol and 20 mL of glacial acetic acid;
3) Washing twice using 35mL of 96% ethanol for 5 minutes each;
4) Storage of the resulting embryos for 24 hours. in 35 mL of 96% ethanol;
5) Carification using 35 mL of KOH solution (1%) for 2-6 hours;
6) Staining for 1-3 hours. using Alizarin red (final concentration 0.05 mg/mL) dissolved in 1L of KOH solution (2%);
7) Clarification using 35mL of KOH solution (2%) for 4 hours. to 3 days;
8) Washing the embryos twice after clarification with 35 mL of KOH(2%)/ glycerin solution with a ratio of 4:1 and 3:2 for 24 hours each.
9) Storage the embryos for unlimited time in 35 mL of 1:4 solution made of KOH (2%) and glycerin.

Results and discussions

The protocol was successfully implemented for chicken embryos between 10 and 13 days of incubation. As embryos approach the late-stage of development, their bones and cartilages are much more matured and well-defined, making the 12th and 13th day embryos the most successful in terms of staining from our batch (Figure 1).
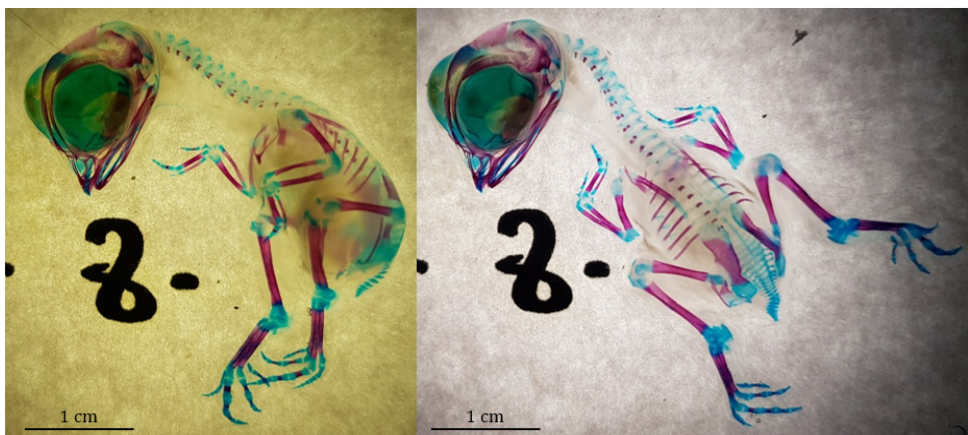
Figure 1. Chicken (*Gallus gallus*) embryos from the 12th day of incubation.

Highlighted structures

The skeleton of birds is particularly adapted to flight. Both limbs and girdles have been modified during evolution to make this type of movement more effective (Chatterjee, 2015; Gofur, 2020). These changes can be observed during the development stages of the embryos (Hamburger and Hamilton, 1951, Namba *et al.*, 2010), the most important and significant ones, captured by us are described below.

Upper limb. In the upper limb of the 10th day chicken embryo (Figure 2A) the staining observed is predominantly Alcian blue, with little to no red, due to the coloring agent's action on the polysaccharides, specifically on the glycosaminoglycans present in cartilages (Liutenko *et al.*, 2023). It allows for the differentiation of the structures constituting the wing, such as the humerus, radius, ulna, carpals, metacarpals and phalanges. Embryos from the 11th day of incubation (Figure 2B) present a more intense Alizarin red staining compared to the embryos on the 10th day. The phalanges are more clearly defined, and due to the staining, we can observe the metacarpals, which will later fuse. Fingers 3 and 4 display Alizarin red staining, while finger 2 only shows Alcian blue staining. This finger displays
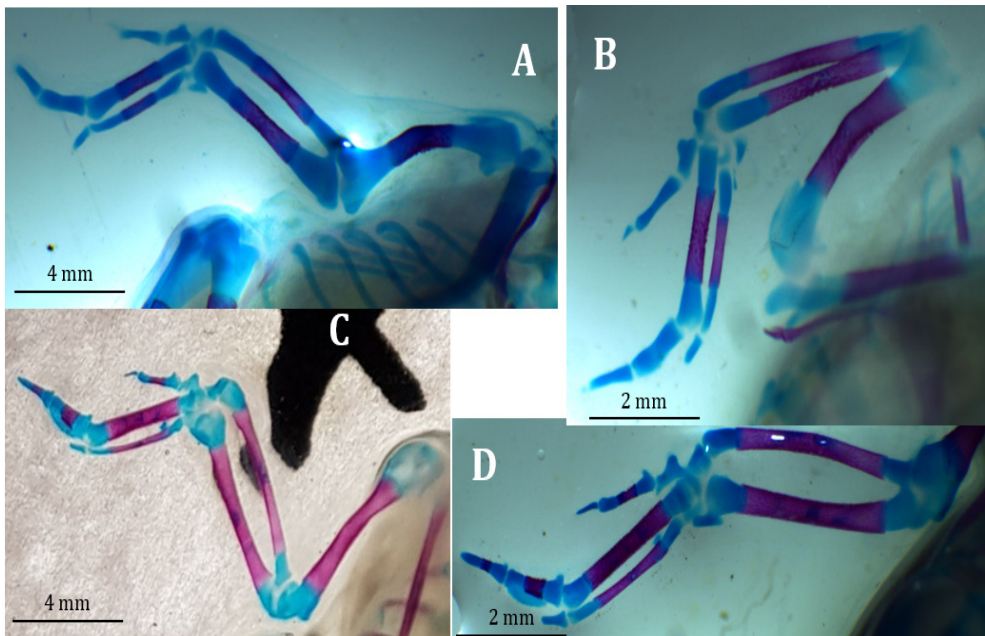
Figure 2. Upper limb of the chicken embryo from the 10th (A), 11th (B), 12th (C) and 13th (D) day of incubation.

Alizarin red staining for the first time in the specimens from the 12th day (Figure 2C), those also having the radius, ulna, and the metacarpal of finger 3 wider compared to the previous embryos. On day 13 (Figure 2D), the carpal and wrist bones are clearly visible. Additionally, the dilation of the phalange in finger 3 increases while the metacarpal of finger 4 becomes thinner.

Table 2. Summary of observations for the upper limb of chicken embryos.

Day of incubation	Observations
10th day of incubation	The structures constituting the upper limb, such as the humerus, radius, ulna, carpal bones, metacarpal bones, and phalanges, are differentiated. The predominant staining is Alcian blue.
11th day of incubation	Alizarin red staining appears in the humerus, radius, ulna, carpal bones, metacarpal bones, and phalanges, except for the phalanges of finger 2.
12th day of incubation	The more intense Alizarin red staining is due to osteogenesis, which also appears in the phalanges of finger 2. There is a dilation observed in the phalanx of finger 3. The radius, ulna, and metacarpal of finger 3 are wider.
13th day of incubation	The carpal and the wrist bones are visible. The dilation of the phalanx in finger 3 increases, while the metacarpal bone of finger 4 becomes thinner.

Lower limb. On the 10th day of incubation we observe the femur, tibia, and fibula very clearly (Figure 3). Between the tibia and the phalanges, which only have an Alcian blue staining, are the three bones that, through fusion, will form the tarsometatarsal bone. On the 11th day of incubation, the phalanges are more developed, the fibula differentiates more slowly compared to the tibia, and the Alizarin red staining is more pronounced due to the presence of osteocytes containing calcium. The embryo on the 12th day of incubation shows Alizarin red staining on the phalanges, except for the posteriorly positioned digit 1, which changes its shape by narrowing the areas where osteocytes are present. The Alcian blue staining is only found at the knee and heel levels, otherwise, Alizarin red is predominant. On the 13th day of incubation, osteocytes are present even in digit 1, evidenced by the Alizarin red staining. The three bones forming the tarsometatarsal are close but not yet fused. The claw-like shape of the distal phalanges in all digits is very distinct (Table 3).
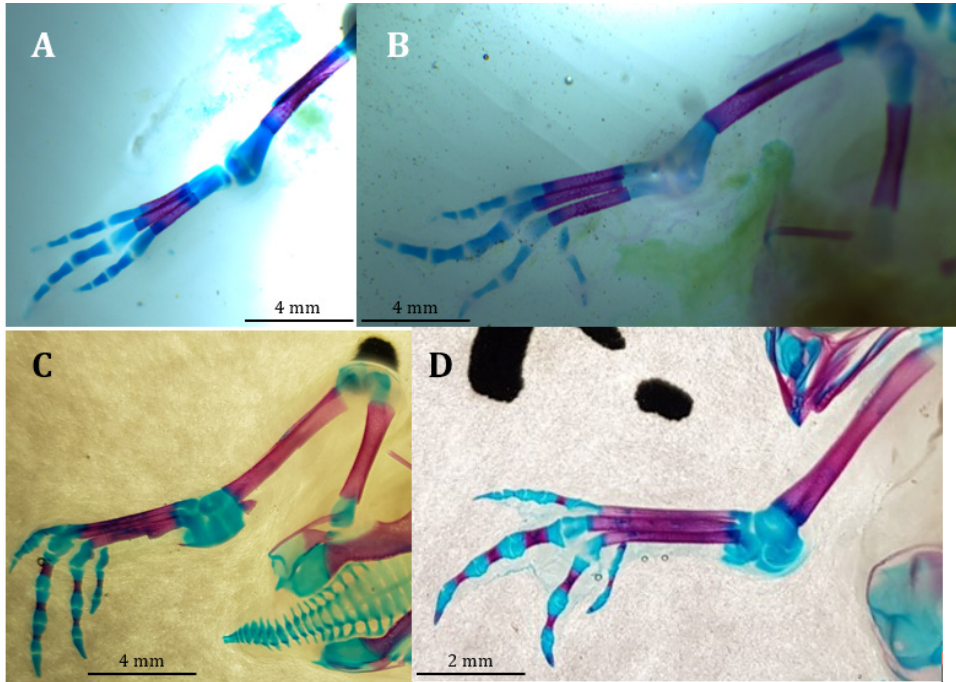
Figure 3. Lower limb of the chicken embryo from the 10th (A), 11th (B), 12th (C) and 13th (D) day of incubation.

Table 3. Summary of observations for the lower limb of chicken embryos.

Day of incubation	Observations
10th day of incubation	The femur, tibia, fibula, and the bones that will form the tarsometatarsal exhibit Alizarin red staining in addition to Alcian blue staining. The phalanges only have blue alcian staining.
11th day of incubation	The phalanges are more developed and the fibula differentiates more slowly compared to the tibia. The Alizarin red staining is more pronounced.
12th day of incubation	All phalanges, except those of digit 1, show Alizarin red staining, and the areas where it appears are narrower. Alcian blue staining is present around the phalanges only at the knee and heel level.
13th day of incubation	The phalanges of digit 1 exhibit Alizarin red staining; the three bones forming the tarsometatarsal are close but not fused. The distal phalanges of all digits have a claw-like shape.

Tail and pygostyle. The vertebrae that will contribute to the formation of the tail are spaced and decrease in length up to the last coccygeal vertebrae in the embryo on the 10th day of incubation (Figure 4). The structure is entirely Alcian blue. Condensed areas of Alcian blue staining are observed on the sides of the vertebrae in the embryo on the 11th day of incubation, and the last vertebrae are getting closer to each other. The vertebra from the embryo in the 12th day of incubation are larger and closer to each other in order to form the pygostyle. The last ones are going to partake in the process of fusion. In the 13th day of incubation, the developing pygostyle is very well observed. All vertebrae are closer and interconnected, and the coccygeal ones are partially fused or in the process of fusion. Alizarin red staining is absent in this case as well (Table 4).
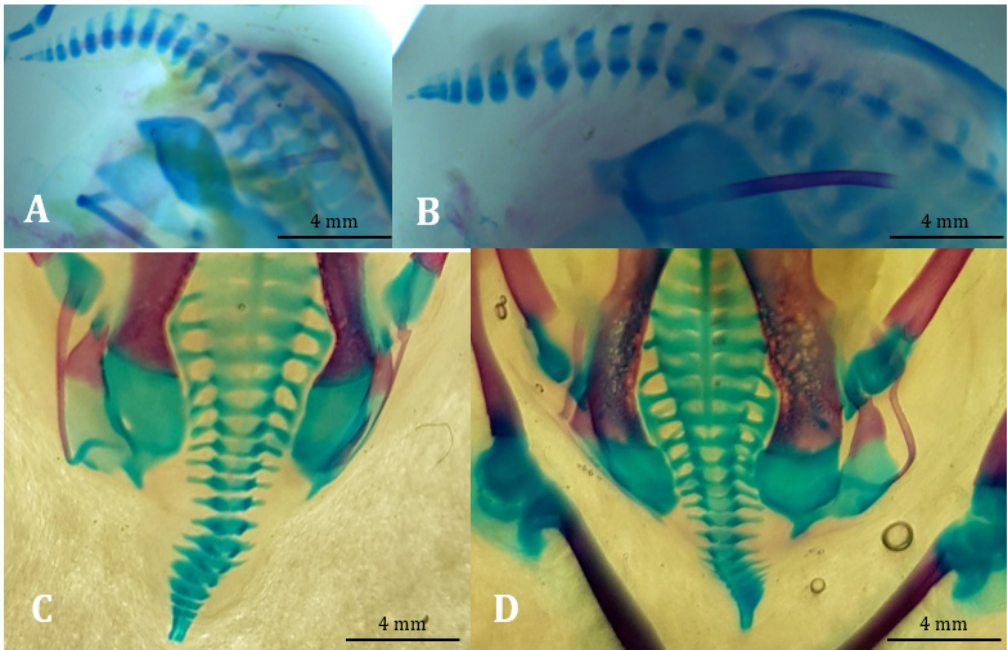
Figure 4. Tail of the chicken embryo from the 10th (A), 11th (B),
12th (C) and 13th (D) day of incubation.

These findings underscore the intricate process of skeletal development in chicken embryos, offering a detailed timeline of bone and cartilage formation. This knowledge is pivotal for developmental biology, providing a framework

for studying skeletal abnormalities and evolutionary biology. One example of evolutionary study is the tarsometatarsal bone, which in the chicken embryo is made up of three bones unfused, meaning that it has the structure closely related to that of reptiles, such as *Archaeopteryx*.

Table 4. Summary of observations for the tail of chicken embryos.

Day of incubation	Observations
10th day of incubation	The staining is entirely Alcian blue. The vertebrae are consistently spaced and naturally decrease in length.
11th day of incubation	Distinct areas of condensed Alcian blue staining are observed on the sides of the vertebrae. The last vertebrae are getting closer to each other.
12th day of incubation	The proximity of the vertebrae intensifies. They are wider and narrower, and the last ones are in the process of fusion.
13th day of incubation	The developing pygostyle can be observed. All vertebrae are close and interconnected, and the coccygeal ones are partially fused or in the process of fusion.

Protocol improvements

The improvements made to the diaphonization protocol are targeted towards embryos with darker skin pigmentation or those that have surpassed 14 days of incubation and are more developed. Since the staining shows lower efficiency and clarity in these cases, we recommend a longer storage in 1% KOH, approximately 30% more than the initially mentioned time. The clarification stage being extended by almost two hours allows the KOH to chemically break down more soft tissue. Another suggestion would be to add an evisceration step before fixation, ensuring that the stains in bones and cartilages are more distinct and clear.

Such improvements can be applied for staining other organisms as well, but further research needs to be done. The size and complexity of organs or specific features, such as feathers in our case, contribute to the list of factors needed to be taken into account for a successful staining.

Conclusions

The protocol was successfully applied for chicken embryos up to the 13th day of incubation, those being also the best specimens obtained. Due to the reduced efficiency and clarity of staining the embryos older than 14 days of incubation or with darker skin pigmentation, we propose the following modifications to the protocol: extending the clarification step and performing an evisceration. Firstly, by extending the clarification stage by 30% beyond the initial time, we allow the 1% KOH to chemically decompose more soft tissue. Secondly, through evisceration, we remove internal organs and facilitate the staining of the structures of interest.

Highlighted structures that are closely linked to phylogenetic evolution are the upper limbs, the lower limbs, and the tail and pygostyle. In embryos from days 10-13 of incubation, the upper limb undergoes significant changes at the wing tip level. Alizarin red staining appears later in the wing tip compared to the humerus, radius, or ulna. Digit 4's metacarpal thins to fuse with digit 3's metacarpal, which dilates at the penultimate phalanx. Digit 2 remains less developed, maintaining a consistent size. The lower limb shows notable changes at the terminal segment, where phalanges enlarge, thin medially, and take on a claw-like shape. The three bones forming the tarsometatarsal bone remain unfused, a trait seen in reptiles, particularly *Archaeopteryx*. In the tail, caudal vertebrae converge, with the last four fusing to form the pygostyle, and the beginning of the fusion of the first caudal vertebrae is also clearly observed to form the sacral bone. This region is entirely stained with Alcian blue, with no Alizarin red staining observed.

Further exploration with this staining technique will most likely lead to advances in the quality of the protocol for a broader range or organisms. With this development, more progress can be made in the field of developmental biology and anatomy by using diaphonization for comparative analysis between different species, embryonic studies or even for educational purposes in universities of public museums.

References

Abourachid A., & Höfling E. (2012). The legs: a key to bird evolutionary success. *J. Ornithol.*, *153*(1), 193-198. Doi: 10.1007/s10336-012-0856-9;

Atanasoff A., Tsandev N., Roydev R., Ekim O., Pavlova-Petrova E., & Uzunova K. (2018). Using the diaphonization for enhanced visualization of skeletal anomalies in juvenile Siberian sturgeon (*Acipenser baerii*). *Hydromedit. 3rd Int. Congr. Appl. Ichthyol. Aquat. Environ.*, 601-602;

Barber J., Daly J., Rutland C., Hauber M., & Cawthray A. (2018). The chicken: a natural history. Princeton University Press. p. 14-25. Doi: 10.2307/j.ctv3dnq3j.

Casinos A., & Cubo J. (2001). Avian long bones, flight and bipedalism. *Comp. Biochem. Physiol. A Mol. Integr. Physiol.*, *131*(1), 159-167. Doi: 10.1016/S1095-6433(01)00463-9;

Chatterjee S. (2015). The rise of birds: 225 million years of evolution. University Press. p. 19-72;

Chitra V., & Sharon S.E. (2020). Diaphonization of the ovariectomized laboratory animal. *Res. J. Pharm. Technol.*, *13*(5), 2228;

Gofur M. R. (2020). Aves osteology and skeletal system. Textbook of avian anatomy. Uttoran Offset Printing Press. p. 16-28;

Hamburger V., & Hamilton H.L. (1951). A series of normal stages in the development of the chick embryo. *J. Morphol.*, *88*(1), 49-92. doi:10.1002/jmor.1050880104;

Khan F.R., Rehman K., & Habib S. (2015). Diaphonization: a recipe to study teeth. *J. Contemp. Dent. Pract.*, *16*(3), 248-251;

Liutenko M.A., Hromko Y.A., & Tretiakov A.V. (2023). History of origin, advantages and disadvantages, vectors of application of the diaphonization method: current state of the problem. *Pol. Merkur. Lekarski*, *51*(6), 632-637. DOI: 10.36740/merkur202306109. PMID: 38207065;

Namba Y., Yamazaki Y., Yuguchi M., Kameoka S., Usami S., Honda K., & Isokawa K. (2010). Development of the tarsometatarsal skeleton by the lateral fusion of three cylindrical periosteal bones in the chick embryo (Gallus gallus). *Anat. Rec.*, *293*(9), 1527-1535. Doi: 10.1002/ar.21179;

Ostrom J.H. (1976). Archaeopteryx and the origin of birds. *Biol. J. Linn. Soc.*, *8*(2), 91-182. doi:10.1111/j.1095-8312.1976.tb00244.x;

Rashid D.J., Chapman S.C., & Larsson H.C. (2014). From dinosaurs to birds: a tail of evolution. *EvoDevo*, *5*(25), 1-20. Doi: 10.1186/2041-9139-5-25;

Shipman P. (1998). Taking wing: Archaeopteryx and the evolution of bird flight. Simon & Schuster p. 21-47;

Stern C.D. (2022). Reflections on the past, present and future of developmental biology. *Dev. Biol.*, *488*, 30-34. doi:10.1016/j.ydbio.2022.05.001.

Sullivan T.N., Wang B., Espinosa H.D., & Meyers M.A. (2017). Extreme lightweight structures: avian feathers and bones. *Mater. Today*, *20*(7), 377-391. Doi: 10.1016/j.mattod.2017.02.004;

Tsandev N., Vodenicharov A., & Stefanov I. (2020). Using of diaphonization for study of domestic pig's auditory tube. *Acta Morphol. Anthropol.*, *27*(3-4), 101-105;

Tsuihiji T. (2017). The atlas rib in Archaeopteryx and its evolutionary implications. *J. Vertebr. Paleontol.*, *37*(4), 1-9. Doi: 10.1080/02724634.2017.1342093;

Vovk O.Y., Ionov I., Lyutenko M., & Gromko Y. (2022). Diaphonization as a method of modern morphological research. *Clin. Anat. Oper. Surg*, *21*(4), 46–51. Doi:10.24061/1727-0847.21.4.2022.45.*;*

Wang M., Li Z., & Zhou Z. (2017). Insight into the growth pattern and bone fusion of basal birds from an early Cretaceous enantiornithine bird. *Proc. Natl. Acad. Sci. U.S.A.*, *114*(43), 11470-11475. Doi: 10.1073/pnas.1707237114.

Diversity of arthropods subservient to olive groves in arid region (Northeastern Algeria)

Hayet Mimeche [1,2], Smail Chafaa[1,2✉] and Ayache Laabassi [1,2]

¹Department of Ecology and Environment, University of Batna 2, Batna, Algeria;
²Laboratory of Physiotoxicology, Cellular pathology and Molecular -Biomolecules,
Faculty of Science of Nature and Life, University of Batna 2, Batna, Algeria;
✉Corresponding author: E-mail: s.chafaa@univ-batna2.dz

Abstract. *Olea europaea* L. 1753, is one of the oldest and most distinctive trees in the Mediterranean region. Its nutritional, social, cultural, and economic value is very important for populations in arid regions, where it is widely distributed. A sign of a sustainable environment in many agricultural regions is the existence of a wide variety and abundance of arthropod groups. The main objective of the study is to evaluate the diversity of arthropods subservientin in olive agro-systems in the arid region by using several sampling techniques, namely classic sight hunting, visual inspection, Barber pots, and yellow traps. The inventory is carried out over a period of 5 months, from February to June 2023, in three stations in M'Sila (northeastern Algeria). Three classes of arthropods were found: Insecta, Arachnida, and Malacostraca. Captures were numerically dominated by Insecta, representing 96.88% of total captures. Arachnida and Malacostraca classes represented about 2.74 and 0.38%, respectively. During this research, a total of 1861 arthropod individuals were collected and identified into 83 species, 79 genera, 53 families, and 15 orders. The most abundant orders were: Diptera (42.56%), Hymenoptera (28.11%), and Coleoptera (7.32%). However, we found a significant difference in species composition according to habitat (P < 0.01). The species were determined, and the ecological indices were calculated (Shannon Value, Evenness values and Simpson reciprocal index). The dominant functional feeding groups were phytophages (41.91 %), predators (32.94%), and polyphages (22.14%).

The arthropods included several olive pests such as *Euphyllura olivina* (Costa) (Hemiptera: Liviidae), *Bactrocera oleae* (Rossi) (Diptera: Tephritidae), *Prays oleae* (Bernard) (Lepidoptera: Praydidae), *Liothrips oleae* Costa (Thysanoptera: Phlaeothripidae), and *Oxycenus maxwelli* (Keifer) (Arachnida: Eriophyidae).

Keywords: diversity, arthropods, pests, olive grove, species richness, arid land.

Introduction

The olive tree (*Olea europaea* L. 1753) is among the most ancient and distinctive trees, holding significant historical and regional importance, particularly in the Mediterranean area. It is widely dispersed, and its nutritional, social, cultural, and economic value to the communities in this region is immense, as noted by Claridge and Walton in 1992. Olives, which are small trees belonging to the Oleaceae family, are indigenous to tropical and warm temperate zones worldwide.

Olives are grown in a variety of agroecological zones, mostly in plain and hilly areas (Gkisakis *et al.,* 2014). These agroecological zones differ in terms of elevation, biotic factors, pedoclimatic conditions, and landscape structure. In Algeria, the olive tree is a major element of the agricultural economy. The areas cultivated for olive growing in Algeria reach 450,000 hectares, with an olive number reaching 6.2 million trees and a production of 7 million quintals of olives and nearly 70,000 tons of olive oil (DSASI, 2018; Amrouni Sais *et al.*, 2021). M'Sila province occupies the most important rank in Algeria, with an established area of 11500 hectares (DSA, 2023). The irrigated areas have become widespread in the interior department due to rain deficiency and climate change. Olive production faces threats from various arthropods and pathogens that affect olive trees. Despite the hardiness and adaptability of the olive tree, enabling it to thrive and produce even in difficult ecological conditions, most olive plantations in Algeria are marked by either aging trees or a lack of proper cultural care (Chafaa, 2013).

Large populations of arthropods are present in the agroecosystem, and these populations are impacted by agronomic techniques, temperature, humidity, rainfall, and the surrounding crop (Divya Sri *et al.,* 2023). A few are harmful, such as agriculture pests and disease vectors whereas, others are beneficial, such as decomposers, seed dispersers, pollinators, and natural enemies of pests (Deghiche-Diab *et al.,* 2021). Numerous pest species cause significant harm to

the olive tree and its yield by growing on its fruit, foliage, flowers, and timber (Chafaa *et al.,* 2019a). It is noteworthy to mention that climate is the main driver that controls the distribution range of arthropods as well as the seasonal variation in their community composition (Chenchouni *et al.,* 2015; Chafaa *et al.,* 2019a). Few studies have investigated the biodiversity of arthropods subservient to olive groves under arid and semiarid conditions carried out in Algeria (Chafaa *et al.,* 2019a, Deghiche-Diab *et al.,* 2021).

The main objective of this study is to assess the diversity of arthropods subservient to the agro-systems of olive plantations grown in three arid zones in M'Sila province (north-eastern Algeria).

Materials and methods

Study area

M'Sila is located in northeastern Algeria. Overall, it is part of the region of the East Highlands and extends over an area of 18 718 km². It is composed of 47 municipalities grouped into 15 daïras. The area is characterised by a Mediterranean arid bioclimatic stage with a mild winter (Q_2 = 17.02 – 19.84, m = 3.37 to 4.10°C, M = 38.87 to 40.06°C, P = 182.94 to 201.86 mm) based in weather data from nearby meteorological stations (Zedam *et al.,* 2022). The rainy season spans from October to May, while the dry season typically persists until August. The region's Mediterranean climate is influenced by the Sahara (Mimeche and Oliva-Paterna, 2018). Hydrologically, this environment is linked to a rainfall regime marked by pronounced irregularities leading to the absence of permanent flows from most watercourses (Mimeche, 2014). Agriculture, still the primary occupation in the M'sila region, focuses on the production of vegetables, cereals (barley and corn) and olive orchard, adapting to the available water supplies. The arable land area covers an area of 50,000 ha, with 50% of it under irrigation (Abdesselam *et al.,* 2013). The majority of the groundwater in the M'Sila region is situated below 125 m.

Sample collection

The research was conducted from February to June 2023, in three pilot orchards located at different sites in M'Sila: Ouled Mansour (S1), Ouled Sidi Amor (S2) and District Ksob (S3) (Tab. 1). This period was chosen as it corresponds to the peak activity of many arthropods, and abundances exhibits the most significant differences across farming systems (Cotes *et al.,* 2011).

To prevent the edge effect, all samplings were carried out more than 30 meters from the olive grove's edge (Carpio *et al.,* 2019). It is important to combine different sample techniques since prior research has demonstrated that some sampling strategies might lead to a significant bias towards specific species. In this study, we used three sampling methods-pan traps, bait traps, and sweep nets – following the methodology outlined by Castro *et al.* in 2017.

The traps were placed above the ground and between olive trees to enhance visibility to arthropods; they were set at each study site for two weeks using different technics. We employed a combination of qualitative sampling (classical hunting) (Colas, 1974), and a quantitative sampling using different methods including trapping (colored traps, Barber pots, fly gobbles), and mowing (Benkhelil, 1991), as well as striking (Fauvel *et al.,* 1981).

The sampled species were taken to the laboratory and preserved in tubes filled with 70% alcohol. Each tube was labeled with essential information, including the date of collection, the type of traps used, and the specific site. In the laboratory, the collected insects were sorted, counted, and finally identified using specialized identification keys.

Table 1. Characteristics of studied Stations.

Site	Ouled Mansour (S1)	Ouled Sidi Amor (S2)	District KSob (S3)
Latitude	35°48'59''N	35°56'51''N	35°49'07''N
Longitude	4°27'07''E	4°22'58''E	4°33'55''E
Altitude (m)	504	828	556
Vegetation	Olive tree, pistachio tree, eggplant and chili pepper	Olive tree	Olive tree, Grenadine
Number and variety of olive tree	160 chemlal, 140 sigoise and 150 different variety	95 chemlal	105 chemlal and 50 Azeradj
Irrigation	by channel	by drip	by drip
Implantation date	2002	2009	2010
Treatments	do not benefit from phytosanitary treatments		

Statistical analysis

Diversity parameters of arthropods, diversity in each region of olive orchards were evaluated by calculating: (i) the relative frequency (RF) of each arthropod order (RF= percentage of the number of individuals of a species on

the total number N in each station); (ii) species richness (S), which represents the total number of species identified; (iii) the N/S ratio; (iv) Shannon diversity index (H): H = − Σ((ni/ N)× log2(ni N)), with ni represents the abundance of species i and N is the total number of individuals of a given sample; (v) evenness (E) with E = H/H max, where H max= log2 S (Magurran 2004); (vi) Simpson reciprocal index, SRI = (1/D), with D=Σ(ni(ni−1)/N(N−1)); and (vii) the SRI/S ratio, which varies between 0 and 1. Some diversity parameters (N, S, RF) were expressed at the level of taxonomic orders to facilitate comparisons with previous studies (Chenchouni, 2017; Chafaa *et al.,* 2019a).

We used Kruskal-Wallis to assess impacts of habitat (grouping factors) on biodiversity and species abundances. All of these analyzes were developed using PAST 4.16. 2024.

Results

Abundances and relative frequency of arthropods

A taxonomic composition analysis of the species identified in the study area revealed the presence of 83 species from 1861 individuals in 3 classes, 15 orders, 53 families, and 79 genera. In the M'Sila region, three classes of arthropods were found: Insecta, Arachnida, and Malacostraca.

Insecta accounted for 96.88% of all captures, while Arachnida and Malacostraca classes represented approximately 2.74 and 0.38%, respectively. At the Ouled Mansour station, 65 species belonged to 14 orders; Ouled Sidi Amor station had 57 species belonged to 14 orders, and in the Ksob district station, insects included 54 species in 13 orders (Tab. 2). The Kruskal-Wallis test revealed a significant variation in arthropods abundances between the three stations (χ^2= 10.28, P < 0.01).

Out of a total of 1,861 individuals collected during the sampling period in three olive grove, the most abundant species were from Diptera order; *Bactrocera oleae* (7.52%) and *Musca domestica* (6.99%). In Ouled Mansour station, the most abundant species was *Bactrocera oleae* (Diptera) (10.27%); *Musca domestica* (9.53%), *Apis mellifera* (8.39%), *Chlorops* sp, and *Halictuss cabiosae* (5.83%) in OuledSidi Amor station. In the district Ksob, the most abundant species were from Diptera order *Bactrocera oleae* (10.55%) and *Musca domestica* (8.97%), Blattodea order; *Blatta orientalis* (8.44%), and Hymenoptera order; *Aphaenogaster rupestris* (5.28%).

Arthropods families with high capture frequency included Thephritidae (18.49%), Formicidae (11.04%), and Syrphidae (7.06%) in Ouled Mansour station; in Ouled Sidi Amor Apidae (14.94%), Formicidae (13.51%), Syrphidae (9.67%), Muscidae (9.53%) and Calliphoridae (7.82%); in the district Ksob olive grove Thephritidae (13.46%), Formicidae (11.35%), Blattidae (10.82%), Syrphidae (5.54) and Myrmicinae (5.28%). The abundance of other orders was <5% in all three stations of olive groves (Tab. 3). The Kruskal-Wallis test showed a significant relationship between the abundances of arthropods families in the three stations (χ^2= 6.20, P < 0.01).

Arthropods orders with high capture frequencies were Diptera (42.88%), Hymenoptera (21.05%), Coleoptera (6.68%), and Hemiptera (5.91%) in Ouled Mansour station; in the second station Ouled Sidi Amor, Diptera (45.95%), Hymenoptera (37.98%), Coleoptera (5.83%), and Homoptera (5.12%). In the district Ksob olive grove; Diptera (35.62%), Hymenoptera (37.98%), and Blattodea (10.82). The abundance of other orders was <5% in all three olive groves (Tab. 4). Overall, there was no difference in the frequency of abundance, as indicated by the non-significant variation in abundances between stations (Kruskal-Wallis test, *P*> 0.05).

Table 2. Systematic list of the relative frequency (RF)
of arthropods and functional feeding group recorded
in olive groves at three stations in M'Sila, Algeria.

Class	Order	Family	Species	RF (%)				FFG
				S1	S2	S3	Overall	
Insecta	Orthoptera	Acrididae	*Locusta migratoria*	0.13	0.14	3.69	0.86	Phy
			Anacridium aegyptium	2.44	0.00	0.79	1.18	Phy
		Gryllidae	*Gryllus campestris*	0.00	0.28	1.32	0.38	Phy
	Homoptera	Aphididae	*Myzus* sp.	0.26	0.00	0.26	0.16	Phy
			Aphis gossypii	0.51	0.00	0.26	0.27	Phy
			Aphis fabae	0.64	0.00	0.00	0.27	Phy
		Psyllidae	*Euphyllura olivina*	1.54	4.41	2.64	2.85	Phy
		Pentatomidae	*Palomena* sp	0.13	0.71	0.00	0.32	Phy
	Coleoptera	Coccinellidae	*Coccinella algerica*	0.64	0.14	2.37	0.81	Pre
			Hippodamia variegata	0.26	0.43	0.00	0.27	Pre
		Chrysomelidae	*Longitarsus* sp	0.00	0.43	0.00	0.16	Phy
		Anobiidae	*Lasioderma* sp	0.13	0.00	0.00	0.05	Phy
		Curculionidae	*Phloeotribus scarabeoides*	0.00	0.71	0.26	0.32	Phy
		Melyridae	*Psilothrix* sp	0.39	0.00	0.00	0.16	Phy

Class	Order	Family	Species	RF (%)				FFG
				S1	S2	S3	Overall	
		Cryptophagidae	*Cryptophagus* sp	0.26	0.00	0.26	0.16	Phy
		Geotrupidae	*Geotrupes*sp	0.00	0.28	0.00	0.11	Cop
		Scarabaeidae	*Phyllognathus excavatus*	1.67	0.28	1.06	1.02	Sap
		Tenebrionidae	*Omophlus* sp	0.00	0.43	0.26	0.21	Pre
			Tenebrio molitor	0.26	0.00	0.00	0.11	Pol
		Melolonthidae	*Amphimallonsolsticialis*	0.00	0.00	2.11	0.43	Phy
		Carabidae	*Amara* sp	0.13	0.00	1.58	0.38	Pre
			Calathus fuxipes	1.41	0.28	0.00	0.70	Pre
			Chlaenius spoliatus	0.00	0.28	0.00	0.11	Pre
			Badister sp	0.00	0.00	0.79	0.16	Pre
			*Harpalus*sp	0.13	0.00	0.53	0.16	Pre
			Carabusfami ninumidus	0.00	1.56	0.00	0.59	Pre
		Staphylinidae	*Tachyporus hypnorum*	0.00	0.57	0.00	0.21	Pre
		Cleridae	*Trichodes alvearius*	1.41	0.43	2.11	1.18	Pre
	Diptera	Syrphidae	*Eupeodes corollae*	3.34	4.84	3.17	3.87	Pre
			Toxomerus marginatus	3.72	4.84	2.37	3.87	Pre
		Muscidae	*Musca domestica*	3.72	9.53	8.97	6.99	Pol
		Drosophilidae	*Drosophila melanogaster*	1.54	2.99	0.53	1.88	Sap
		Calliphoridae	*Calliphora erythrocephala*	1.54	4.84	2.37	2.96	Pol
			Calliphora vicina	2.18	1.14	1.32	1.61	Pol
			Chloroprocta sp	0.77	1.85	0.00	1.02	Pol
		Chloropidae	*Chlorops* sp	3.98	6.54	2.90	4.73	Phy
			Thaumatomyiaglabra	0.26	2.70	0.00	1.13	Pre
		Sarcophagidae	*Sarcophaga* sp	0.51	0.00	0.00	0.21	Pre
		Tephritidae	*Bactrocera oleae*	10.27	2.84	10.55	7.52	Phy
			Tephritis postica	1.80	0.28	0.00	0.86	Phy
			Tephritis praecox	1.41	0.00	0.79	0.75	Phy
			Ceratitis capitata	4.62	2.13	2.11	3.17	Pol
			Trupanea guimari	0.39	0.00	0.00	0.16	Phy
		Tachinidae	*Phryxe vulgaris*	2.82	1.42	0.53	1.83	Pol
	Hymenoptera	Formicidae	*Camponotus* sp	3.34	2.99	0.00	2.53	Pre
			Monomorium salomonis	1.54	2.28	2.11	1.93	Pre
			Cataglyphis bicolor	1.93	2.56	2.64	2.31	Pre
			Tetramorium lanuginosum	0.00	0.00	3.96	0.81	Pre
			Tapinoma melanocephalum	2.18	3.84	0.53	2.47	Pre
			Tapinoma nigerrimum	2.05	1.85	2.11	1.99	Pre

161

Class	Order	Family	Species	RF (%)				FFG
				S1	S2	S3	Overall	
		Myrmicinae	*Aphaenogaster rupestris*	0.00	0.00	5.28	1.07	Pre
		Halictidae	*Halictus scabiosae*	2.70	5.83	0.53	3.44	Phy
		Scoliidae	*Scolia* sp	0.39	0.71	0.00	0.43	Pre
		Megachilidae	*Anthidium laterale*	1.54	1.71	0.79	1.45	Phy
			Hoplitis anthocopoides	0.51	0.00	2.37	0.70	Phy
		Vespidae	*Polistes gallicus*	0.64	0.00	0.26	0.32	Pre
		Apidae	*Nomada cinnabarina*	0.00	3.84	0.26	1.50	Phy
			Andrena bicolor	0.39	1.14	1.32	0.86	Phy
			Eucera oraniensis	0.00	0.43	1.06	0.38	Phy
			Bombus terrestris	0.26	1.14	0.00	0.54	Phy
			Apis mellifera	2.70	8.39	0.53	4.41	Phy
		Braconidae	*Psyttalia concolor*	0.90	1.28	0.26	0.91	Pre
	Thysanoptera	Aeolothripidae	*Aeolothrips* sp	0.64	0.00	0.00	0.27	Pre
		Phlaeothripidae	*Liothrips oleae*	0.26	0.57	0.00	0.32	Phy
	Blattodea	Ectobiidae	*Dziriblatta stenoptera*	0.00	0.14	0.00	0.05	Phy
		Blattidae	*Periplaneta americana*	1.93	0.28	2.37	1.40	Pol
			Blatta orientalis	1.54	0.00	8.44	2.36	Phy
	Dermaptera	Forficulidae	*Forficula auricularia*	1.41	0.28	1.06	0.91	Pol
		Anisolabididae	*Anisolabis maritima*	0.00	0.71	0.00	0.27	Pol
	Neuroptera	Coniopterygidae	*Conwentzia psociformis*	1.80	0.00	1.32	1.02	Pre
		Chrysopidae	*Chrysoperla carnea*	2.82	0.28	1.06	1.50	Pre
	Lepidoptera	Noctuiidae	*Agrotis segetum*	0.39	0.00	0.26	0.21	Phy
		Praydidae	*Prays oleae*	1.16	0.57	0.00	0.70	Phy
	Hemiptera	Lyctocoridae	*Lyctocoris* sp	0.77	0.00	0.00	0.32	Pre
		Pentatomidae	*Nezara viridula*	2.82	0.43	2.64	1.88	Pol
		Lygaeidae	*Spilostethus pandurus*	2.31	0.28	0.26	1.13	Phy
	Mantodea	Mantidae	*Mantis religiosa*	0.00	0.57	0.53	0.32	Pre
Arachnida	Aranea	Agelenidae	*Lycosoides coarctata*	0.00	0.00	0.26	0.05	Pre
		Lycosidae	*Trochosa* sp	0.26	0.00	0.00	0.11	Pre
		Dysderidae	*Dysdera crocata*	1.16	0.43	0.26	0.70	Pre
	Trombidiformes	Eriophyidae	*Aculops lycopersici*	2.44	0.00	0.00	1.02	Phy
			Oxycenus maxwelli	1.16	0.14	1.58	0.86	Phy
Malacostraca	Isopoda	Agnaridae	*Hemilepistus* sp	0.90	0.00	0.00	0.38	Phy

FFG, functional feeding group; Phy, phytophagous species; Pre, predatory species; Cop, coprophagous species; Sap, saprophagous specie; Pol, polyphagous species.

Table 3. Summarisation of species richness (S) and relative frequency (RF) for arthropods family recorded in olive groves, M'Sila (Algeria).

Family	S1		S2		S3		Overall	
	S	RF (%)	S	RF (%)	S	RF (%)	S	RF (%)
Acrididae	2	2.57	1	0.14	2	4.49	2	2.04
Gryllidae	0	0.00	1	0.28	1	1.32	1	0.38
Aphididae	3	1.41	0	0.00	2	0.53	3	0.70
Psyllidae	1	1.54	1	4.41	1	2.64	1	2.85
Pentatomidae	1	0.13	1	0.71	0	0.00	1	0.32
Coccinellidae	2	0.90	2	0.57	1	2.37	2	1.07
Chrysomelidae	0	0.00	1	0.43	0	0.00	1	0.16
Anobiidae	1	0.13	0	0.00	0	0.00	1	0.05
Curculionidae	0	0.00	1	0.71	1	0.26	1	0.32
Melyridae	1	0.39	0	0.00	0	0.00	1	0.16
Cryptophagidae	1	0.26	0	0.00	1	0.26	1	0.16
Geotrupidae	0	0.00	1	0.28	0	0.00	1	0.11
Scarabaeidae	1	1.67	1	0.28	1	1.06	1	1.02
Tenebrionidae	1	0.26	1	0.43	1	0.26	2	0.32
Melolonthidae	0	0.00	0	0.00	1	2.11	1	0.43
Carabidae	3	1.67	3	2.13	3	2.90	6	2.10
Staphylinidae	0	0.00	1	0.57	0	0.00	1	0.21
Cleridae	1	1.41	1	0.43	1	2.11	1	1.18
Syrphidae	2	7.06	2	9.67	2	5.54	2	7.74
Muscidae	1	3.72	1	9.53	1	8.97	1	6.99
Drosophilidae	1	1.54	1	2.99	1	0.53	1	1.88
Calliphoridae	3	4.49	3	7.82	2	3.69	3	5.59
Chloropidae	2	4.24	2	9.25	1	2.90	2	5.86
Sarcophagidae	1	0.51	0	0.00	0	0.00	1	0.21
Tephritidae	5	18.49	3	5.26	3	13.46	5	12.47
Tachinidae	1	2.82	1	1.42	1	0.53	1	1.83
Formicidae	5	11.04	5	13.51	5	11.35	6	12.04
Myrmicinae	0	0.00	0	0.00	1	5.28	1	1.07
Halictidae	1	2.70	1	5.83	1	0.53	1	3.44
Scoliidae	1	0.39	1	0.71	0	0.00	1	0.43
Megachilidae	2	2.05	1	1.71	1	3.17	2	2.15
Vespidae	1	0.64	0	0.00	1	0.26	1	0.32
Apidae	3	3.34	5	14.94	4	3.17	5	7.68
Braconidae	1	0.90	1	1.28	1	0.26	1	0.91
Aeolothripidae	1	0.64	0	0.00	0	0.00	1	0.27
Phlaeothripidae	1	0.26	1	0.57	0	0.00	1	0.32
Ectobiidae	0	0.00	1	0.14	0	0.00	1	0.05
Blattidae	2	3.47	1	0.28	2	10.82	2	3.76
Forficulidae	1	1.41	1	0.28	1	1.06	1	0.91
Anisolabididae	0	0.00	1	0.71	0	0.00	1	0.27
Coniopterygidae	1	1.80	0	0.00	1	1.32	1	1.02
Chrysopidae	1	2.82	1	0.28	1	1.06	1	1.50
Noctuiidae	1	0.39	0	0.00	1	0.26	1	0.21

Family	S1		S2		S3		Overall	
	S	RF (%)	S	RF (%)	S	RF (%)	S	RF (%)
Praydidae	1	1.16	1	0.57	0	0.00	1	0.70
Lyctocoridae	1	0.77	0	0.00	0	0.00	1	0.32
Pentatomidae	1	2.82	1	0.43	1	2.64	1	1.88
Lygaeidae	1	2.31	1	0.28	1	0.26	1	1.13
Mantidae	0	0.00	1	0.57	1	0.53	1	0.32
Agelenidae	0	0.00	0	0.00	1	0.26	1	0.05
Lycosidae	1	0.26	0	0.00	0	0.00	1	0.11
Dysderidae	1	1.16	1	0.43	1	0.26	1	0.70
Eriophyidae	2	3.59	1	0.14	1	1.58	2	1.88
Agnaridae	1	0.90	0	0.00	0	0.00	1	0.38
Total	65	100	55	100	53	100	83	100

Table 4. Summarisation of species richness (S), relative frequency (RF) and variation of diversity indices for arthropods orders recorded in olive groves, M'Sila (Algeria).

Order	S1		S2		S3		Overall	
	S	RF (%)	S	RF (%)	S	RF (%)	S	RF (%)
Orthoptera	2	2.57	2	0.43	3	5.80	3	2.42
Homoptera	5	3.08	2	5.12	2	3.17	5	3.87
Coleoptera	11	6.68	12	5.83	10	11.35	20	7.31
Diptera	16	42.88	14	45.95	11	35.62	16	42.56
Hymenoptera	14	21.05	14	37.98	15	24.01	18	28.05
Thysanoptera	2	0.90	1	0.57	0	0	2	0.59
Blattodea	2	3.47	2	0.43	2	10.82	3	3.82
Dermaptera	1	1.41	2	1.00	1	1.06	2	1.18
Neuroptera	2	4.62	1	0.28	2	2.37	2	2.53
Lepidoptera	2	1.54	1	0.57	1	0.26	2	0.91
Hemiptera	3	5.91	2	0.71	2	2.90	3	3.33
Mantodea	0	0	1	0.57	1	0.53	1	0.32
Aranea	2	1.41	1	0.43	2	0.53	3	0.86
Trombidiformes	2	3.59	1	0.14	1	1.58	2	1.88
Isopoda	1	0.90	0	0	0	0	1	0.38
S	65		57		54		83	
N	779		703		379		1861	
Ratio N/S	11.98		12.33		7.02		22.42	
Shannon_H	3.195		2.83		3.069		3.213	
Evenness e^H/S	0.581		0.446		0.5815		0.4687	
Simpson 1-D	0.9336		0.917		0.9348		0.9396	
Ratio SRI /S	0.0144		0.0161		0.0173		0.0113	

Variation of insect diversity parameters

The variation in insect diversity parameters was evident across the olive groves, particularly between Ouled Mansour and district Ksob stations. The insects spices richness recorded in Ouled Mansour station was notably higher (65 species), compared to Ouled Sidi Amor, and district Ksob station, which recorded 57 and 54 species respectively (Tab. 4). The average number of individuals per species (ratio N/S) was higher in Ouled Sidi Amor station (12.33) compared to the other stations (11.98 in Ouled Mansour. and 7.02 in district Ksob). However, the values of Shannon diversity index and evenness were very close between Ouled Mansour and district Ksob olive groves (H′ = 3.19; E = 0.5 and H′ = 3.07; E = 0.58 respectively). Both stations showed greater diversity compared to Ouled Sidi Amor (H′ = 2.83. E = 0. 44). In addition, the values of Simpson reciprocal index (SRI) and SRI/S very close across all olive groves in M'Sila region.

Functional diversity

In all three olive groves stations, phytophagous, predators and polyphagous arthropods were the most frequently captured (Tab. 5). In terms of the number of species. phytophagous arthropods were the most abundant, totaling 36 species across the entire M'Sila region, followed by predators arthropods with 33 species. Polyphagous arthropods, on the other hand, exhibited a species richness of 11 species across all olive groves. Other functional groups displayed lower numbers and richness (Tab. 5).

Table 5. Species richness (S) and relative frequency (RF in %) for the functional feeding groups of arthropods captured in olive groves located in M'Sila (Algeria).

Trophic status	S1		S2		S3		Overall	
	S	RF (%)	S	RF (%)	S	RF (%)	S	RF (%)
Coprophages	0	0	1	0.28	0	0	1	0.11
Phytophages	30	42.49	21	40.54	23	43.27	36	41.91
Polyphages	10	22.08	10	22.62	8	21.37	11	22.14
Predators	24	32.22	21	33.29	21	33.77	33	32.94
Saprophages	2	3.21	2	3.27	2	1.58	2	2.90
Total	66	100	55	100	54	100	83	100

Discussion

Arthropods play a crucial role in the food web as herbivores, predators, parasitoids, and detritivores, thus making significant contribution to biodiversity. This study was designed to gather information about arthropod biodiversity in olive groves. Throughout all the olive groves, a diverse range of specimens from various taxa was discovered, with insects particularly dominating the captures in terms of numbers. During the present study a total of 1861arthropods belonging to 83 species were recorded from three olive groves: Ouled Mansour station, Ouled Sidi Amor, and district Ksob. Comparing these results with those of other inventories conducted in Algeria and various countries, we find that they have relatively significant importance. Chafaa *et al.* (2019a) used the same trapping technique in Batna region and reported the presence of 1325 individuals distributed among 15 species. In a study by Deghiche-Diab *et al.* (2021), 725 individuals belonging to 69 taxa of arthropods were caught in olive grove in Biskra, (Algeria). Jiménez-García *et al.* (2019) reported 2275 individuals distributed among 25 families, with species trapped belonging to the classes of Arachnida and Insecta in vineyard agroecosystems in La Rioja (Spain). The presence of some spontaneous plants adapted to the climate conditions of the region attracts more phytophagous and pollinating insects mainly during the spring (Chafaa *et al.,* 2019a; Deghiche-Diab *et al.,* 2021).

The Tephritidae family, consisting of fruit flies, was the most abundant family of the Diptera order, that was collected mainly from yellow sticky traps (Ullah *et al.,* 2023). These flies are widely recognized across the world as major pests of economically valuable fruits in gardens and orchards (Courtney *et al.,* 2017; Ullah *et al.,* 2023). Within the Diptera order, *O. europea* flowers attracted various number of different Syrphidae species (Canale and Loni, 2010). According to Santos *et al.* (2007) and *Cotes et al.* (2011), the most prevalent taxon in olive orchard soil is Formicidae. It is commonly known that Formicidae play a significant role in agricultural ecosystems. They actively contribute to soil improvement, pollination, natural control, and nutrient management (Gonçalves and Pereira, 2012).

Sampled arthropods belonged to 12 insect orders, 2 Arachnida orders, and 1 Isopoda. Diptera, Hymenoptera, and Coleoptera are the three most dominant arthropod taxa in our study region. Happe *et al.* (2019) reported, the coleopteran and dipteran were more common in organic than in integrated pest management (IPM) orchards. Hymenoptera dominated below-ground arthropod groups, as revealed by a comprehensive analysis of terrestrial arthropod populations in dry areas of southeast Spain (Piñero *et al*., 2011). Hymenoptera are important in terms of abundance in the arid area as they find ideal ecological conditions to thrive (Chafaa *et al.,* 2019a).

The Shannon diversity index, Evenness and Simpson reciprocal index offer a comprehensive overview of the diversity across all populations. These indices take into account the number of individuals from various populations, including different stand and trophic groups, in addition to the number of species (Chafaa *et al.*, 2019b).Importantly, these diversity indices provide more information than simply counting the numbers of species present (Drouai *et al.*, 2018).

The dominance of phytophagous arthropods in the studied groves in M'Sila region can be attributed to the permanent presence of water in olive orchards and the high specific diversity of herbaceous plants in the olive grove understory, which provides abundant food resources (Chafaa *et al.,* 2019a). According to Haddad *et al.,* (2009), the low plant diversity can lead to a decrease in arthropod diversity and a shift in trophic structure. Phytophagous insects exhibit a high degree of selectivity for plant species that they prefer (Chafaa *et al.,* 2019b). The phytophagous species represented by pollinators from bees (*Apis mellifera*; *Bombus terrestris*; *Halictus scabiosae*) and ants (three species of *Tapinoma*), are related to the flowering period of olive trees and the presence of weeds in and around field (Deghiche-Diab *et al.,* 2021). Nectar from flowers likely serves as a significant food source for species within the *Tapinoma* genera (Seifert, 2016). We have recorded five phytophagous arthropods considered serious pests in olive cultivation. These includes four species belonging to the insect class: *Euphyllura olivina* (Homoptera), *Bactrocera oleae* (Diptera), *Liothrips oleae* (Thysanoptera), *Prays oleae* (Lepidoptera), as well as one species in the arachnida class: *Oxycenus maxwelli* (Arachnida). Several studies have mentioned the presence of certain olive tree pests in Algeria, *E. olivina* (Chafaa *et al.,* 2019a; Chabaane *et al.,* 2023), *B oleae* and *L. oleae* (Chafaa *et al.,* 2019a; Deghiche-Diab *et al.,* 2021), *P.oleae* (Nichane and Khelil, 2015; Ilias *et al.,* 2017), and olive bud mite *Oxycenus maxwelli* (Arachnida) (Smith Meyer, 1990). The abundance of phytophagous arthropods has a positive impact on the evolution of natural predators, as arthropods serve as a food source for predators (Susanti *et al.,* 2022).

In the study region, predators constitute the second most diverse group after phytophagous arthropods. Predators play a vital role in agroecosystems by controlling the populations of arthropod pests (Chafaa *et al.,* 2019a). In fact, the three stations do not undergo any phytosanitary treatment. The four most important predators identified are: *Psyttalia concolor*, *Chrysoper lacarnea*, *Coccinella algerica,* and *Hippodamia variegata*. This predatory parasite complex contribute to the regulation of olive tree. The polyphagous are the third group. Numerous polyphagous species reside in plants, and these species can act as alternate hosts or prey for many entomophagous species. Due to their polyphagous nature, entomophagous species interact with phytophagous species specifically linked to olive trees (González-Ruiz *et al.,* 2023).

167

Conclusions

In conclusion, our results reveal that the dominant arthropods in our olives groves belong to the following orders and families: Diptera (Tephritidae, Muscidae, Syrphidae, and Chloropidae), Hymenoptera (Formicidae and Apidae), Coleoptera (Carabidae, Cleridae, Coccinellidae, and Scarabaeidae). The dominant functional feeding groups were phytophagous and predators. We recorded five phytophagous arthropods, identified as serious pests in the olive grove of M'Sila (*Euphyllura olivina*, *Bactrocera oleae*, *Liothrips oleae*, *Prays oleae* and *Oxycenus maxwelli)*. Many natural enemies were supported by pest populations as a source of food. These results provide a fundamental tool for directing prevention and control efforts against the primary pests of olive trees.

References

Abdesselam, S., Halitim, A., Jan, A., Trolard, F., & Bourrié, G. (2013). Anthropogenic contamination of groundwater with nitrate in arid region: case study of southern Hodna (Algeria). *Environ. Earth. Sci*, *70*, 2129-2141. Doi: 10.1007/s12665-012-1834-5.

Amrouni Sais, A., Fethallah, R., & Fahas, M. (2021). Les exploitations oléicolesenAlgérie; quelle performance économique?. *Recherche Agronomique*, *19* (1), 65-76.

Benkhelil, M.L. 1991. Les techniques de récolte et de piégeage utilisées en entomologie terrestre. [in French]. ED.OPU, Algiers (Algeria).

Canale, A., & Loni, A. (2010). Insects visiting olive flowers (*Olea europaea* L.) in a Tuscan olive grove. *Redia*, *92*, 95-98.

Carpio, A.J., Castro, J., & Tortosa, F.S. (2019). Arthropod biodiversity in olive groves under two soil management systems: presence versus absence of herbaceous cover crop. *Agric. For. Entomol*, *21*(1), 58-68. Doi: 10.1111/afe.12303.

Castro, J., Tortosa, F.S., Jimenez, J., & Carpio, A.J. (2017). Spring evaluation of three sampling methods to estimate family richness and abundance of arthropods in olive groves. *Anim. Biodivers. Conserv, 40*(2),193-210. Doi: 10.32800/abc.2017.40.0193.

Chaabane, N., Chafaa, S., Naama, F., Nouidjem, Y., & Mimeche, F. (2023). Population dynamics of *Euphyllura olivina* Costa, 1857 (Psyllidae: Hemiptera) in olive trees in the semi-arid region of Djelfa (Algeria). *Studia UBB Biologia,68* (2), 185-195.
Doi: 10.24193/subbbiol.2023.2.01.

Chafaa, S. (2013). Contribution to the study of the entomofauna of olive tree, *Olea europaea* and the population dynamics of the purple scale *Parlatoria oleae* Colvée, 1880 (Homoptera: Diaspididae) in the region of Batna. Dissertation Doctorat. National Superior School of Agronomy,El Harrach- Algiers.

Chafaa, S., Mimeche, F., & Chenchouni, H. (2019a). Diversity of insects associated with olive (Oleaceae) groves across a dryland climate gradient in Algeria. *Can. Entomo*, *151*(5), 629-647- *ERRATUM. Can. Entomo*, *151*(5), 684-684.
Doi: 10.4039/tce.2019.35.

Chafaa, S., Belkhadria, S., & Mimeche, F. (2019b). Entomofauna investigations in the apricot orchards, *Prunus armeniaca* L. (*Rosales Rosaceae*), in Ouled Si Slimane, Batna, North East Algeria. *Biodiversity journal*, *10*(2), 95-100. Doi: 10.31396/Biodiv.Jour.2019.10.2.95.100.

Chenchouni, H., Menasria, T., Neffar, S., Chafaa, S., Bradai, L., Chaibi, R., ... & Bachir, A.S. (2015). Spatiotemporal diversity, structure and trophic guilds of insect assemblages in a semi-arid Sabkha ecosystem. *PeerJ*, *3*, e860. Doi: 10.7717/peerj.860

Chenchouni, H. (2017). Variation in White Stork (*Ciconia ciconia*) diet along a climatic gradient and across rural-to-urban landscapes in North Africa. *Int. J. Biometeorol*, *61*(3), 549-564. Doi: 10.1007/s00484-016-1232-x.

Claridge, M.F., & Walton, M. (1992). The European olive and its pests-management strategies. Monographs-British Crop Protection Council, 3-3.

Colas, G. (1974). Guide de l'entomologiste. Boubée, Paris.

Cotes, B., Campos. M., García. P.A., Pascual,F. & Ruano, F. (2011). Testing the suitability of insect orders as indicators for olive farming systems. *Agric. For. Entomol, 13,* 357–364. Doi: 10.1111/j.1461-9563.2011.00526.x.

Courtney, G.W., Pape, T., Skevington, J.H., & Sinclair, B.J. (2017). Biodiversity of Diptera. Insect Biodiversity: Science and Society, John Wiley & Sons: Chichester, UK.

Deghiche-Diab, N., Deghiche, L., & Belhamra, Y.I. (2021). New record of *Phloeotribus scarabaeoides* (Bernard, 1788) on introduced olive trees in Biskra region–Algeria. *Mun. Ent. Zool*, *16*(2), 1093-1102.

Divya Sri, S., Ratna Kumari, B., Koteswara Rao, S.R., & Varaprasada Rao, C. (2023). Diversity and abundance of foliar arthropods in different crop ecosystems. *The Andhra Agricultural Journal, 70*(1), 084-092. Doi: 10.61657/aaj.2023.13.

Drouai, H., Belhamra, M., & Mimeche, F. (2018) Inventory and distribution of the rodents in Aurès Mountains and Ziban oasis (Northeast of Algeria), *An. Biol, 40*, 47-55. Doi: 10.6018/analesbio.40.06.

DSASI. (2018). Series B, agricultural statistics and information systems department. Ministry of Agriculture and Rural Development of Algeria.

DSA, (2023). Directorate of Agricultural Services: Agricultural statistics for the wilaya of M'Sila. Digital data provided by the Agricultural Statistics Bureau, M'Sila.

Fauvel, G., Rambier, A., & Balduque-Martin, R. (1981). La technique du battage pour la surveillance des ravageursen cultures fruitière et florale. I.-Comparaison des résultats obtenus en verger de pommiers avec des entonnoirsrigides de taille moyenne et avec des entonnoirsen toile. Étude de l'influence de quelquesfacteurs sur l'efficacité du battage. [in French]. *Agronomie*, *1*(2), 105-111.

Gkisakis, V.D., Kollaros, D., & Kabourakis, E.M. (2014). Soil arthropod biodiversity in plain and hilly olive orchard agroecosystems, in Crete, Greece. *Entomol. Hell*, *23*(1), 18-28. Doi: 10.12681/eh.11531.

Gonçalves, M.F., & Pereira, J.A. (2012). Abundance and diversity of soil arthropods in the olive grove ecosystem. *J. Insect. Sci*, 12(1), 20. Doi: 10.1673/031.012.2001.

González-Ruiz, R., Gómez-Guzmán, J.A., Martínez-Rojas, M., García-Fuentes, A., Cordovilla, M.D.P., Sainz-Pérez, M., Sánchez-Solana, A.M., Carlos-Hervás, J., Rodríguez-Lizana, A. (2023). The influence of mixed green covers, a new trend in organic olive growing, on the efficiency of predatory insects. *Agriculture*, *13*(4), 785. Doi: 10.3390/agriculture13040785.

Haddad, N.M., Crutsinger, G.M., Gross, K., Haarstad, J., Knops, J.M., & Tilman, D. (2009). Plant species loss decreases arthropod diversity and shifts trophic structure. *Ecol. Lett*, *12*(10), 1029-1039. Doi: 10.1111/j.1461-0248.2009.01356.x.

Happe, A.K., Alins, G., Blüthgen, N., Boreux, N., Bosch, J., García, D., Hambäck, P.A., Klein, A.M., Martínez-Sastro, R., Miñarro, M., Müller, A.K., Porcel, M., Rodrigo, A., Roquer-Beni, L., Samnegård, U., Tasin, M., & Mody, K. (2019). Predatory arthropods in apple orchards across Europe: Responses to agricultural management, adjacent habitat, landscape composition and country. *Agric. Ecosyst. Environ, 273*,141-150. Doi: 10.1016/j.agee.2018.12.012.

Ilias, F., Medjdoub, K., & Gaouar, N. (2017). Phenolics compounds of olive and olive leaves identified in the resistence to *Praysoleae* (Bernard). *Plant. Arch*, *17*(2), 1761-1764.

Jiménez-García, L., García-Martínez, Y.G., Marco-Mancebón, V., Pérez-Moreno, I., & Jiménez-García, D. (2019). Biodiversity analysis of natural arthropods enemies in vineyard agroecosystems in La Rioja, Spain. *J. Asia-Pac. Entomol, 22*(1), 308-315. Doi: 10.1016/j.aspen.2019.01.008.

Magurran, A.E. 2004. Measuring biological diversity. Wiley-Blackwell, Oxford, United Kingdom.

Mimeche, F. (2014). Ecology of Algerian barbel. *Luciobarbuscallensis* (Valenciennes, 1842) (Pisces: Cyprinidae) in the EL K'sob dam (M'sila). Doctoral thesis. National Higher School of Agronomy. El-Harrach-Algiers.

Mimeche, F., & Oliva-Paterna, F.J. (2018). Temporal variations in abundance and biomass of fish species inhabiting the K'sob reservoir (Eastern of Algeria). *Studia UBB Biologia*, *63*(2), 131-138. Doi: 10.24193/subbbiol.2018.2.10.

Nichane, M., & Khelil, A.M. (2015) Health status of the olive tree (*Olea europaea* l) in the mountains of western traras (Tlemcen–Algeria). *BEST* : *IJHAMS*, *3*(3), 45-52.

Piñero, F.S., Tinaut, A., Aguirre-Segura, A., Miñano, J., Lencina, J.L., Ortiz-Sánchez, F.J., & Pérez-López, F.J. (2011). Terrestrial arthropod fauna of arid areas of SE Spain: Diversity, biogeography, and conservation. *J. Arid Environ.*, *75*(12), 1321-1332. Doi: 10.1016/j.jaridenv.2011.06.014.

Santos, S., Cabanas, J., & Pereira, J. (2007). Abundance and diversity of soil arthropods in olive grove ecosystem (Portugal): Effect of pitfall trap type. *Eur. J. Soil Biol*, *43*, 77–83. Doi: 10.1016/j.ejsobi.2006.10.001.

Seifert, B. (2016). Clypeal excision in Tapinoma Förster, 1850 ants is adaptive (Hymenoptera: Formicidae). *Contrib. Entomo*, *66* (1), 125-129.
Doi: 10.21248/contrib.entomol.66.1.125-129.

Smith Meyer, M.K.P. (1990). African Eriophyoidea: on some related genera: Neooxycenus Abou-Awad, Oxycenus Keifer, Neotegonotus Newkirk & Keifer, Tegonotus Nalepa and Tegolophus Keifer (Acari: Eriophyidae). *Phytophylactica*, *22*(4), 371-386.

Susanti, A., Zulfikar, Z., Yuliana, A.I., Faizah, M., & Nasirudin, M. (2022). Keragaman Serangga Hama Dan Predator Pada Dua SistemPertanian Di Pertanaman Kedelai. *Exact Papers in Compilation*, *4*(2), 565-570.

Ullah, M.I., Arshad, M., Abdullah, A., Altaf, N., Zahid, S.M.A., & Afzal, M. (2023). Diversity of arthropods in citrus orchards of Sargodha, Pakistan: Use of different trapping techniques. *Int. J. Trop. Insect. Sci*, *43*(5), 1797-1809. Doi: 10.1007/s42690-023-01086-4.

Zedam, A., Khoudour, D., & Mimeche, F. (2022). A Ramsar wetland's endemic flora inventory and conservation of Chott ElHodna's plants (northeastern Algeria). *Pak. J. Bot*, *54*(3), 1025-1032. Doi: 10.30848/PJB2022-3(13).

MATN1 gene variant (rs1065755) and malocclusion risk: Evidence from Romanian population analysis

Adina Maria Topârcean[1], Arina Acatrinei[2,3], Ioana Rusu[2,4✉],
Cristina Mircea[2,4], Dana Feştilă[5], Ondine Patricia Lucaciu[1],
Radu Septimiu Câmpian[1], Odette Bodo[6], Iulia Lupan[2,4],
Beatrice Kelemen[2,4], Mircea Constantin Dinu Ghergie[5]

[1] *Oral Rehabilitation Department, "Iuliu Haţieganu" University of Medicine and Pharmacy Cluj-Napoca, Romania;* [2] *Molecular Biology Center, Interdisciplinary Research Institute on Bio-Nano-Sciences, Babeş-Bolyai University, Cluj-Napoca, Romania;* [3] *Doctoral School of Agricultural Engineering Sciences, University of Agricultural Sciences and Veterinary Medicine, Calea Mănăştur 3-5 street, Cluj-Napoca, Romania;* [4] *Department of Molecular Biology and Biotechnology, Faculty of Biology and Geology, Babeş-Bolyai University, Cluj-Napoca, Romania;* [5] *Department of Conservative Odontology, "Iuliu Haţieganu" University of Medicine and Pharmacy Cluj-Napoca, Romania;* [6] *Dentalexpert Dentistry Practice, Cluj-Napoca, Romania*
✉*Corresponding author: ioana.rusu@ubbcluj.ro*

Abstract. Malocclusion, characterized by its diverse phenotypic expression, significantly impacts patients' quality of life. Over recent years, extensive attention has been directed towards the genetic basis of this condition, particularly focusing on various polymorphisms of the *MATN1* gene. Among these, the rs1065755 polymorphism has emerged as particularly relevant, associated with an elevated risk of mandibular prognathism. In this study, employing DNA sequencing, we investigated the extent of association between the rs1065755 SNP and malocclusion risk within the Romanian population. Our approach concentrated on assessing continuous phenotypic variation through four cephalometric measurements, aiming for a comprehensive understanding beyond categorical phenotypes. The findings shed light on the relationship between the *MATN1* rs1065755 SNP and the investigated dentofacial disorder, revealing a positive association between TT homozygous individuals and Class II skeletal malocclusion.

However, further investigations employing larger sample sizes are necessary to validate these findings conclusively.

Introduction

Malocclusion represents a multifaceted oro-facial anomaly, exhibiting complexity both in its phenotypic expression and genetic underpinnings. It manifests as a disharmony in growth between the maxillary and mandibular structures, resulting in an improper relationship between the two dental arches (Nishio and Huynh, 2016, Weaver *et al.*, 2017). The growth and development of the mandible are influenced by a combination of environmental factors and genetically predetermined intrinsic factors. According to Angle's classification system, based on the relative position of the Maxillary First Molar, malocclusion is categorized into three classes: Class I, Class II, and Class III (Yadav *et al.*, 2014).

Class I malocclusions represent one of the most common conditions in the daily clinical practice, being more common than normal occlusion. Individuals exhibiting Class I malocclusion typically demonstrate normal molar relationships, yet their teeth are misaligned within the occlusal line due to malpositioned teeth, rotations, spacing, overbites, open bites, posterior crossbites, or anterior crossbites (Buschang, 2014). When the patient exhibits a phenotype characterized by a maxilla protruding relative to the mandible (or a mandible retruded), accompanied by a convex facial profile, the condition is classified as Class II. Conversely, Class III malocclusion is characterized by a protruded mandible relative to the maxilla (or a maxilla retruded), resulting in a concave facial profile. Class III encompasses a wide spectrum of phenotypic variations, with mandibular prognathism being the most well-known (Liu *et al.*, 2009, Li *et al.*, 2010, Hardy *et al.*, 2012, Doraczynska-Kowalik *et al.*, 2017).

These latter two types of malocclusions (II and III) are frequently encountered among orthodontic patients and significantly impact both their masticatory functions and aesthetic appearance, as well as their mental well-being, leading to a diminished quality of life (Graber *et al.*, 2017, Ma *et al.*, 2019, Liu *et al.*, 2009). Hence, a comprehensive understanding of the genetic factors underlying this complex trait is imperative to facilitate accurate diagnosis and effective treatment by orthodontists (Zabrina *et al.*, 2021, Weaver *et al.*, 2017).

Among the candidate genes implicated in malocclusion, the *MATN1* (*matrilin-1*) gene situated on chromosome 1p35.2 (GRCh38.p14; NCBI accession number: NC_000001.11) is of particular interest in this study. *MATN1* encodes a cartilage extracellular matrix protein pivotal in enhancing and sustaining the chondrogenesis process upon stimulation by *TGFb1* (Moreno Uribe and Miller, 2015, Pei *et al.*, 2008). Notably, *MATN1* is markedly upregulated during chondrogenesis (Stokes *et al.*, 2002). Given the correlation of multiple single nucleotide polymorphisms (SNPs) with malocclusion, this paper focuses on the rs1065755 polymorphism (8572 C>T), which has been associated with an elevated risk of mandibular prognathism in Korean population (Jang *et al.*, 2010). Other studies address the potential genetic predisposition linked to the *MATN1* gene in various dental conditions across populations primarily from India (Rathod *et al.*, 2023, Balkhande *et al.*, 2018), Korea (Yamaguchi *et al.*, 2005), and Indonesia (Laviana *et al.*, 2021), leaving the European space a less explored territory.

In this frame, this research work aims to identify the connection between mutation in gene encoding *MATRILIN-1* (rs1065755) and the risk of various malocclusion types in the Romanian population, with specific consideration to continuous phenotypic variation as demonstrated by four different cephalometric measurements.

Materials and methods

The experimental sample comprises a total of 78 Romanian patients of both genders (50 females and 28 males) with an average age of 21.8 years. The sample set originated from the records of a private clinic and were included in this study only after an informed consent was obtained from the patients who volunteered for the study. Exclusion criteria involved instances of growth disturbances, syndromes, cleft lip and palate, missing teeth, inadequate quality of radiographic records, unsigned consent forms, and trauma. The patients were categorized into study (skeletal class II and III) and control groups based on the cephalometric morphology. The studied cephalometric measurements included ANB (Point A-Nasion-Point B), SNA (Sella-Nasion-Point A), SNB (Sella-Nasion-Point B) angles, as well as the Wits appraisal (AoBo). The SNA angle denotes the maxillary position, where values exceeding the mean (82°) indicate maxillary prognathism, while values below the mean suggest maxillary retrognathism. The SNB angle assesses mandibular position relative to the cranial base, with values surpassing the mean (80°) indicating mandibular prognathism and values lower than the mean suggesting mandibular retrognathism.

A.M. TOPÂRCEAN, A. ACATRINEI, I. RUSU, C. MIRCEA, D. FEŞTILĂ, O. P. LUCACIU,
R.S. CÂMPIAN, O. BODO, I. LUPAN, B. KELEMEN, M.C. D. GHERGIE

Jaw disparity is evaluated through ANB (mean of 0-2°) and AoBo (mean of 0-2 mm) angles. Elevated values relative to the mean signify a Class II tendency, while values below the mean indicate a Class III trend (Ghergie *et al.*, 2013a). Based on these parameters, the analyzed sample set consists of 37 patients classified under class II anomalies, 25 categorized with class III malocclusion, and 16 belonging to the control group.

Buccal swabs were obtained from all patients for molecular investigations and promptly transported on ice to the genetic laboratory for DNA isolations and amplification. Genomic DNA was extracted from oral mucosa cells using the Animal and Fungi DNA Preparation (Jena Bioscience, Germany) following the manufacturer's guidelines. After the quality and quantity of genomic DNA was evaluated using NanoDrop 1000 Spectrophotometer (ThermoFischer Scientific, US), the gene fragment containing the target SNP (rs1065755) was amplified. A 330 bp segment of *MATN1* gene was amplified using the forward 5'-CACCTTCTGGTTCTGCCAACT-3' and reverse 5'-CATCCCCATGTCCAGCCTTAC-3' primers (Jang *et al.*, 2010). The PCR reaction was optimized and consistent results were obtained when using the following reaction mixture: 1x Reaction Buffer, 2.5 mM $MgCl_2$, 0.2 mM each dNTP, 0.5 μM of each primer, 1.25 units/reaction of MangoTaq polymerase (Bioline, Meridian Bioscience, USA), and 1 μl of DNA template. The standard amplification conditions were initial denaturation at 95°C for 5 minutes, followed by 35 cycles of 95°C for 30 seconds (denaturation), 62°C for 30 seconds (annealing), 72°C for 30 seconds (extension), and a final extension of 72°C for 5 minutes. The PCR products were visualized on a 1.5% agarose electrophoresis gel (Cleaver Scientific Ltd, Warwickshire, United Kingdom). The expected amplicons were purified from the agarose gel using FavorPrep GEL/ PCR Purification Kit (Favorgen Biotech Corp., Pingtung, Taiwan), and subjected to Sanger sequencing at Macrogen Europe (The Netherlands). To screen for the rs1065755 C>T *MATN1* polymorphism the obtained sequences were aligned in BioEdit Sequence Alignment Editor v. 7.2.5.0 (Hall, 1999) along with the reference sequence deposited in NCBI (NC_000001.11).

Frequencies of alleles and genotypes between malocclusion cases and control individuals were analyzed. To assess the associations between *MATN1* gene polymorphisms and mandibular prognathism, the Pearson Chi-square test was performed, and the standardized residuals were visualized using the *corrplot* package, available with R 4.1.1 (R Core, 2020). A p -value of less than 0.05 was considered statistically significant ($p < 0.05$). Furthermore, to evaluate the relationship between the cephalometric parameters and the genetic variability at the investigated locus a principal component analysis (PCA) was computed using the *prcomp* function of R and visualized in a two-dimensional space using *ggplot2 package.*

Results

Of the total number of selected individuals, the SNP of *MATN1* gene (rs1065755) was successfully genotyped in 75 instances. Overall, the wildtype allele (C) exhibited a frequency of 64.67%, while the alternate variant (T) appeared with a frequency of 35.33%. Remarkably, the observed allele frequencies within the Romanian population closely align with global frequencies, with a minor difference of 1.87. This discrepancy becomes even more negligible when comparing allele frequencies with those of the European population, reveled by the ALFA project (Phan *et al.*, 2020). The heterozygous were dominant (54.67%), followed by wildtype homozygous (37.33%), and a smaller proportion of homozygous for the mutant allele (8%).

While there is only a slight variation in terms of allelic frequency among the investigated categories (mandibular retrognathism, prognathism and controls having orthognathic mandible) (Fig. 1a), there is a sizeable difference exists in genotypic composition among malocclusion types (Fig. 1b). The highest frequency of mutant homozygous (TT) is observed in Class II individuals (11.76%), it decreases to 8.33% in Class III and it is completely absent from the control group, in which the T allele is exclusively present in heterozygous individuals, constituting the most frequent genotype (64.71%).
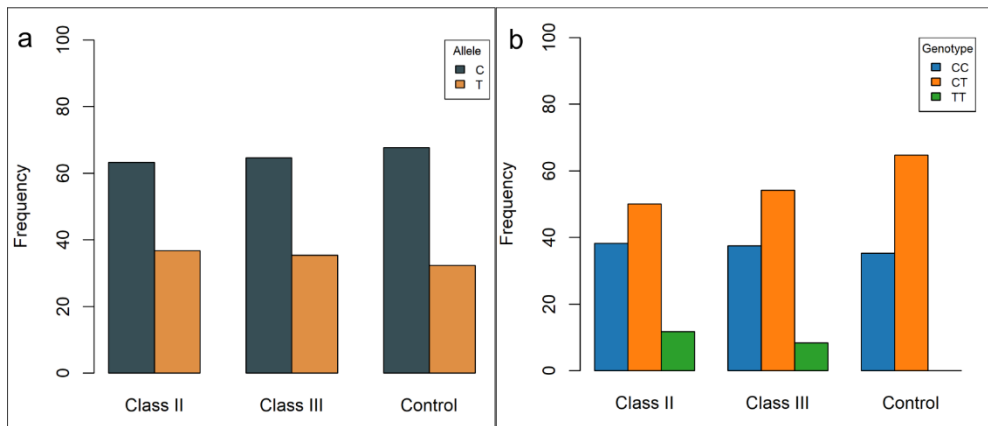
Figure 1. Allelic (**a**) and genotypic (**b**) frequencies
in the investigated malocclusion types.

Moreover, the Pearson's Chi-squared test for each allele in a category of individuals (chi-squared = 0.45, p-value = 0.7984) indicated that there is not enough evidence to suggest an association between allele type and a class of orthodontic deformity. On the other hand, the correlation plot for the Pearson's

chi squared test residuals for each genotype in a class (chi-squared = 13.056, p-value = 0.01082) showed a positive association between TT homozygotes and Class II malocclusion, as well as a negative correlation between this genotype and the control group (Fig. 2). At the same time, the heterozygotes show an opposite pattern.
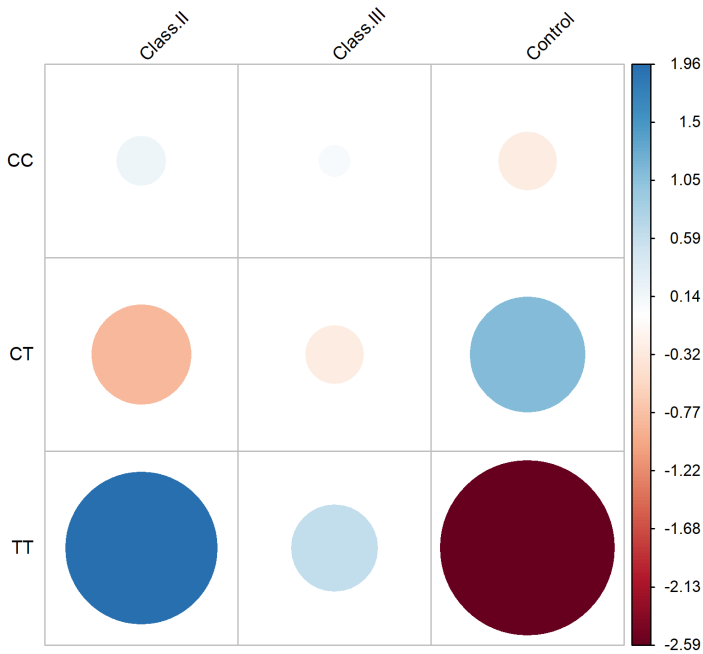
Figure 2. Correlation plot for the Pearson's chi squared test residuals
for each genotype in a class (*p-value* = 0.01082).

The PCA performed based on four cephalometric measurements (Fig. 3) shows a clear division between the Class II malocclusion and Class III cases along the PC1 and PC2 components, capturing 80.57% of the variance is displayed. Samples from the control group are dispersed along a diagonal between these categories, except for one outlier (the farthest heterozygous on the PC1 component). However, there is no evident clustering of the samples based on the identified genotype. The PCA analysis was performed exclusively on individuals with complete records, encompassing a total of 47 samples with both genetic and cephalometric measurements available.
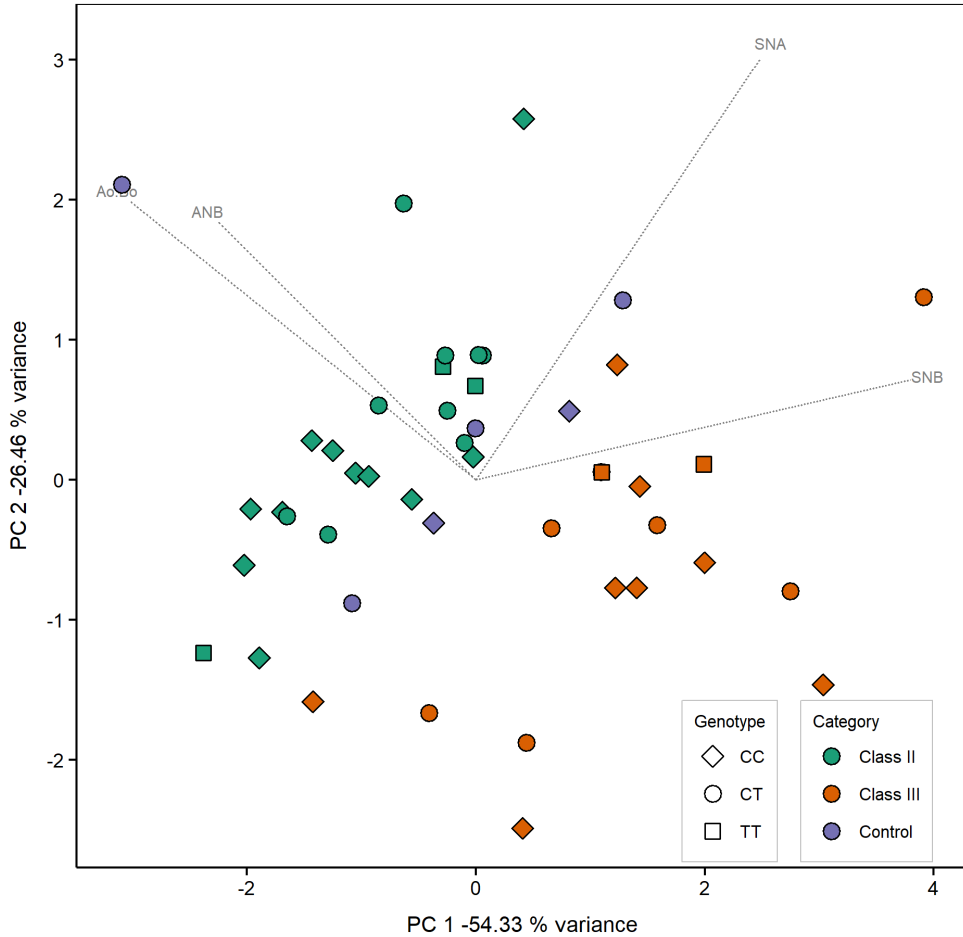
Figure 3. Principal Component Analysis (PCA) performed based on four cephalometric measurements.

Discussion

Class II and III malocclusion are recognized as complex dentofacial anomalies, with varied prevalence across ethnic groups and geographic areas, and as such a comprehensive understanding of the genetic basis is crucial for the development of innovative, personalized therapies, as well as more effective preventive strategies (Dehesa-Santos *et al.*, 2021, Moreno Uribe and Miller, 2015). Research into hereditary factors as the root cause of mandibular deformities such as mandibular

177

prognathism and advancements in genetics highlight the quest for gene candidates associated with mandibular prognathism (Zohud *et al.*, 2023). It has been suggested that genetic investigations concerning Class II and I malocclusion are scarce and characterized by small sample sizes, uncertainty regarding the generalizability of findings to populations of diverse ancestries, and narrow trait definitions that overlook the intricate phenotypic spectrum of malocclusion (George *et al.*, 2021). Previous studies have identified several gene candidates as genetic contributors to skeletal malocclusion class II and III (some reviewed in: (Subono *et al.*, 2021, Doraczynska-Kowalik *et al.*, 2017, Mokhtar *et al.*, 2020)). Across various ethnicities, studies have suggested that genes correlated with mandibular prognathism are situated in different loci.

The *MATN1* gene, located on chromosome 1p35.2, is involved in the regulation of matrilin-1 synthesis in endochondral skeletal growth and has been identified as a candidate gene that could serve as a biological marker in mandibular prognathism (Jang *et al.*, 2010). The majority of studies examining the association between *matrilin-1* gene polymorphisms and craniofacial issues have concentrated on East Asian populations. This is likely due to the higher prevalence of dental malocclusion in this region compared to other ethnicities (Lone *et al.*, 2023). Through the examination of three *MATN1* polymorphisms (-158 T>C, 7987 G>A, 8572 C>T) in the Korean population, Jang *et al.* (2010) demonstrated that the 8572 C>T polymorphism is associated with an elevated risk of mandibular prognathism, whereas the 7987 G>A polymorphism exhibits a protective effect. Although demonstrating comparable minor allele frequencies of rs1065755 C>T between Koreans and Indians, the latter population did not exhibit a significant association with mandibular retrognathism at either the genotype or allele level (Balkhande *et al.*, 2018). In contrast, the frequencies observed in the Romanian population differ and the TT genotypes are positively correlated with Class II malocclusion (Fig. 2). In a different study (Kulkarni *et al.*, 2020), albeit somewhat constrained by a small sample size, rs20566 and frameshift variants at rs1065755 exhibited notably higher frequencies in 35 skeletal Class III patients with mandibular prognathism compared to 30 control individuals from an Indian population. By studying the *MATN1* gene's association with mandibular prognathism in the Deutero-Malay race in Indonesian subjects, Laviana *et al.* (2021) indicate that polymorphism of exon 5 regions of the *MATN1* gene, 354 T>C (rs20566) CC genotype, is the risk factor of such craniofacial disorder. In this case no CC genotype was identified in the control group. Similarly, our study reveals an absence of TT genotype at rs1065755 in the control group.

This preliminary study sheds light on the influence of *MATN1* polymorphism depicted by sequence variation at rs1065755 on skeletal malocclusion class II and III in Romanian population. For this ethnic group, only a limited number of

genes including *MYO1H* (Ghergie *et al.*, 2013a), *VDR* (Ghergie *et al.*, 2013b), and *COL1a1* (Topârcean *et al.*, 2021) have been investigated for their role in dental anomalies.

Conclusions

Overall, our study contributes to understanding the genetic basis of skeletal malocclusion Class II and III, particularly within the Romanian population. Our findings underscore the potential role of *MATN1* polymorphisms, specifically rs1065755, as a genetic marker for mandibular prognathism. However, further research with larger sample sizes is warranted to validate these findings and explore additional genetic factors contributing to malocclusion.

References

Balkhande, P.B., Lakkakula, B.V.K.S. & Chitharanjan, A.B. (2018). Relationship between matrilin-1 gene polymorphisms and mandibular retrognathism. *Am J Orthod Dentofacial Orthop. 153*, 2, 255-261 e1, Doi: 10.1016/j.ajodo.2017.06.023.

Buschang, P.H. (2014). Class I malocclusions—The development and etiology of mandibular malalignments. *Seminars in Orthodontics. 20*, 1, 3-15, Doi: 10.1053/j.sodo.2013.12.002.

Dehesa-Santos, A., Iber-Diaz, P. & Iglesias-Linares, A. (2021). Genetic factors contributing to skeletal class III malocclusion: a systematic review and meta-analysis. *Clin Oral Investig. 25*, 4, 1587-1612, Doi: 10.1007/s00784-020-03731-5.

Doraczynska-Kowalik, A., Nelke, K.H., Pawlak, W., Sasiadek, M.M. & Gerber, H. (2017). Genetic factors involved in mandibular prognathism. *J Craniofac Surg. 28*, 5, e422-e431, Doi: 10.1097/SCS.0000000000003627.

George, A.M., Felicita, A.S., Milling Tania, S.D. & Priyadharsini, J.V. (2021). Systematic review on the genetic factors associated with skeletal Class II malocclusion. *Indian J Dent Res. 32*, 3, 399-406, Doi: 10.4103/ijdr.IJDR_59_20.

Ghergie, M., Festila, D., Kelemen, B. & Lupan, I. (2013a). Myo1H gene single nucleotide polymorphism rs10850110 and the risk of malocclusion in the romanian population. *Acta Medica Transilvanica. 2*, 4, 281-284.

Ghergie, M., Feştila, D., Lupan, I., Popescu, O. & Kelemen, B.S. (2013b). Testing the association between orthodonthic classes I, II, III and SNPs (rs731236, rs8004560, rs731236) in a Romanian clinical sample. *Ann Romanian Soc Cell Biol. 18*, 2, 43-51.

Graber, L., Rl, J., Vanarsdall, Kwl, V. & Gj., H. (2017). Orthodontics: current principles and techniques. 6th Ed. *Elsevier* St. Louis, Missouri, pp. 928.

Hall, T. BioEdit: a user-friendly biological sequence alignment editor and analysis program for Windows 95/98/NT. *Nucleic Acids Symp. Ser.*, 1999. 95-98.

Hardy, D.K., Cubas, Y.P. & Orellana, M.F. (2012). Prevalence of angle class III malocclusion: A systematic review and meta-analysis. *Open J. Epidemiol. 2*, 4, 75-82, Doi: 10.4236/ojepi.2012.24012.

Jang, J.Y., Park, E.K., Ryoo, H.M., Shin, H.I., Kim, T.H., Jang, J.S., Park, H.S., Choi, J.Y. & Kwon, T.G. (2010). Polymorphisms in the Matrilin-1 gene and risk of mandibular prognathism in Koreans. *J Dent Res. 89*, 11, 1203-7, Doi: 10.1177/0022034510375962.

Kulkarni, S.D., Bhad, W.A. & Doshi, U.H. (2020). Association between mandibular Prognathism and MATRILIN-1 gene in Central India population: A cross-sectional study. *J Indian Orthod Soc. 55*, 1, 28-32, Doi: 10.1177/0301574220956421.

Laviana, A., Thahar, B., Melani, A., Mardiati, E., Putri, L. & Zakyah, A.D. (2021). Role of matrilin-1 (MATN1) polymorphism in class III skeletal malocclusion with mandibular prognathism in Deutero-Malay race: a case-control study. *Egyptian J Med Human. 22*, 1, Doi: 10.1186/s43042-021-00131-6.

Li, Q., Zhang, F., Li, X. & Chen, F. (2010). Genome scan for locus involved in mandibular prognathism in pedigrees from China. *PloS one. 5*, 9, 1-4, Doi: 10.1371/journal.pone.0012678.

Liu, Z., Mcgrath, C. & Hagg, U. (2009). The impact of malocclusion/orthodontic treatment need on the quality of life. A systematic review. *Angle Orthod. 79*, 3, 585-91, Doi: 10.2319/042108-224.1.

Lone, I.M., Zohud, O., Nashef, A., Kirschneck, C., Proff, P., Watted, N. & Iraqi, F.A. (2023). Dissecting the complexity of skeletal-malocclusion-associated phenotypes: mouse for the rescue. *Int J Mol Sci. 24*, 3, Doi: 10.3390/ijms24032570.

Ma, J., Huang, J. & Jiang, J.H. (2019). Morphological analysis of the alveolar bone of the anterior teeth in severe high-angle skeletal Class II and Class III malocclusions assessed with cone-beam computed tomography. *PloS one. 14*, 3, e0210461, Doi: 10.1371/journal.pone.0210461.

Mokhtar, K.I., Abu Bakar, N. & Md Ali Tahir, A.H. (2020). Genetics of malocclusion: A review. *IIUM Journal of Orofacial and Health Sciences. 1*, 1, 1-6, Doi: 10.31436/ijohs.v1i1.2.

Moreno Uribe, L.M. & Miller, S.F. (2015). Genetics of the dentofacial variation in human malocclusion. *Orthod Craniofac Res. 18 Suppl 1*, 01, 91-99, Doi: 10.1111/ocr.12083.

Nishio, C. & Huynh, N. (2016). Skeletal malocclusion and genetic expression: An evidence-based review. *J dent Sleep. 3*, 2, 57-63, Doi: 10.15331/jdsm.5720.

Pei, M., Luo, J. & Chen, Q. (2008). Enhancing and maintaining chondrogenesis of synovial fibroblasts by cartilage extracellular matrix protein matrilins. *Osteoarthritis Cartilage. 16*, 9, 1110-7, Doi: 10.1016/j.joca.2007.12.011.

Phan, L., Jin, Y., Zhang, H., Qiang, W., Shekhtman, E., Shao, D., Revoe, D., Villamarin, R., Ivanchenko, E. & Kimura, M. (2020). ALFA: allele frequency aggregator. *National Center for Biotechnology Information, US National Library of Medicine. 10*.

R Core, T. 2020. R: A language and environment for statistical computing. Vienna, Austria: R Foundation for Statistical Computing.

Rathod, N., Patel, P., Shah, H.T. & Thakar, M. (2023). Association between mandibular prognathism and MATRILIN-1 gene. *NeuroQuantology. 21*, 3, 300-306, Doi: 10.48047/NQ.2023.21.3.NQ33032.

Stokes, D.G., Liu, G., Coimbra, I.B., Piera-Velazquez, S., Crowl, R.M. & Jimenez, S.A. (2002). Assessment of the gene expression profile of differentiated and dedifferentiated human fetal chondrocytes by microarray analysis. *Arthritis Rheum. 46*, 2, 404-19, Doi: 10.1002/art.10106.

Subono, M., Alima, I.R.N. & Auerkari, E.I. (2021). Genetics and epigenetics of class II and class III malocclusions. *J Phys Conf Ser 1943*, 1, 012091, Doi: 10.1088/1742-6596/1943/1/012091.

Topârcean, A.M., Acatrinei, A., Rusu, I., Mircea, C., Feştilă, D.G., Lucaciu, O.P., Câmpian, R.S., Bodo, O., Kelemen, B.S. & Ghergie, M. (2021). Preliminary data regarding the influence of the COL1a1 rs2249492 polymorphism on the risk of malocclusion in the Romanian population. *Stud Univ Babeş-Bolyai Biol. 66*, 2, 45-51, Doi: 10.24193/subbbiol.2021.2.03.

Weaver, C.A., Miller, S.F., Da Fontoura, C.S., Wehby, G.L., Amendt, B.A., Holton, N.E., Allareddy, V., Southard, T.E. & Moreno Uribe, L.M. (2017). Candidate gene analyses of 3-dimensional dentoalveolar phenotypes in subjects with malocclusion. *Am J Orthod Dentofacial Orthop. 151*, 3, 539-558, Doi: 10.1016/j.ajodo.2016.08.027.

Yadav, D., Rani, M., Shailaja, A., Anand, D., Sood, N. & Gothi, R. (2014). Angle's molar classification revisited. *J Indian Orthod Soc. 48*, 4_suppl2, 382-387, Doi: 10.5005/jp-journals-10021-1282.

Yamaguchi, T., Park, S.B., Narita, A., Maki, K. & Inoue, I. (2005). Genome-wide linkage analysis of mandibular prognathism in Korean and Japanese patients. *J Dent Res. 84*, 3, 255-9, Doi: 10.1177/154405910508400309.

Zabrina, S., Ramadhanti, Jazaldi, F., Gultom, F.P. & Auerkari, E.I. (2021). Genetic and epigenetic aspects of class III malocclusion with mandibular prognathism phenotypes. *AIP Conf. Proc. 2344*, 1, 10-16, Doi: 10.1063/5.0047282.

Zohud, O., Lone, I.M., Midlej, K., Obaida, A., Masarwa, S., Schroder, A., Kuchler, E.C., Nashef, A., Kassem, F., Reiser, V., Chaushu, G., Mott, R., Krohn, S., Kirschneck, C., Proff, P., Watted, N. & Iraqi, F.A. (2023). Towards genetic dissection of skeletal class III malocclusion: a review of genetic variations underlying the phenotype in humans and future directions. *J Clin Med. 12*, 9, 3212, Doi: 10.3390/jcm12093212.

Characterization and biocontrol potential of some rhizobacteria against fungal pathogens causing foliar diseases in maize

Akinlolu Olalekan Akanmu and Olubukola Oluranti Babalola[✉]

Food Security and Safety Focus Area, Faculty of Natural and Agricultural Sciences, North-West University, Private Mail Bag X2046, Mmabatho 2735, South Africa
https://orcid.org/0000-0003-2816-9820 and https://orcid.org/0000-0003-4344-1909
[✉]***Corresponding author, E-mail:*** *olubukola.babalola@nwu.ac.za*

Abstract. Maize is one of the most consumed cereal crops worldwide, and it is a strategic crop to the attainment of SDG 2 of Zero hunger. Despite its importance, the cultivation of maize has been significantly impaired by fungal pathogens causing foliar diseases. The occurrence of this disease in maize plantations at the Research Farm of the North-West University, Molelwane, Mafikeng, South Africa prompted this investigation. Samples of diseased maize rhizosphere soil were aseptically collected. Bacteria species associated with the rhizosphere were isolated and characterized as *Bacillus siamensis, Enterobacter asburiae, Enterobacter chengduensis, Priestia aryabhattai, Burkholderia* sp., *Priestia megaterium* strain AOA6 and *Priestia megaterium* strain AOA7. The anti-fungicidal potentials of the bacterial species were evaluated against pathogenic fungal species, *Nigrospora sphaerica, Alternaria alternata* and *Fusarium equiseti* in-vitro. The percentage mycelia growths were calculated and the data were subjected to ANOVA using SAS version 9.8. All the seven bacteria isolates tested positive to ammonia production, phosphate solubilization, siderophore production and ACC deaminase tests. The percentage mycelia inhibition showed *Nigrospora sphaerica* (36.29%), *A. alternata* (26.19%) and *F. equiseti* (20.63%) as the order of fungal inhibition by the bacteria species. Furthermore, *E. asburiae > P. megatarium* strain AOA7 *> B. siamensis > P. aryabhattai > E. chengduensis > Bulkholderia* sp. were the order of antifungal efficacy of the bacteria species evaluated. In conclusion, the efficacy of the bacteria especially *E. asburiae, P. megatarium* strain AOA7 and *B. siamensis* over various fungal pathogens.

The result obtained, therefore, justifies the further investigation, formulation and deployment of the bacteria species as biofungicide in the management of foliar diseases of maize.

Keywords: antifungicidal potential, biofungicide, microbial formulations, rhizosphere, zero hunger.

Introduction

Maize (*Zea mays* L.) is of immense importance to ensuring food sustainability worldwide. It is an essential crop that plays a strategic role in actualizing the second United Nations Sustainable Development Goal (SDG 2) of attaining zero hunger (Akanmu *et al.*, 2023a; Ngoune Tandzi & Mutengwa, 2019). This is a result of the nutritional benefits derived from maize by millions of people across the world who depend on it as a staple food (Dlamini *et al.*, 2023a). In addition, the relatively high yield potential of maize and the ability to grow in diverse kind of environments ensures its stability in food supply both to human and the livestock (Poole *et al.*, 2021). Furthermore, the crop has been reported for its climate resilience which is a unique attribute that makes maize an important crop in regions prone to floods, drought and other weather-related challenges (Agunbiade & Babalola, 2023; Prasanna *et al.*, 2021).

Despite its resilience, the growth and yield of maize are adversely affected by pests and diseases caused by fungi, viruses, nematodes and bacteria (Akanmu *et al.*, 2023b; Dlamini *et al.*, 2023b; Gadag *et al.*, 2021). The infection of pathogenic organisms has been found to often result in significant yield losses (Akanmu *et al.*, 2020; Dlamini *et al.*, 2023b; Imade & Babalola, 2021), and fungi constitute an important domain of microorganisms infecting the cultivated maize (Babalola *et al.*, 2022). Fungi causing the foliar diseases of maize have been reported across the world including grey leaf spot caused by *Cercospora* spp., common rust (*Puccinia sorghi*), leaf spot disease (*Phoma herbarum*), brown spot (*Physoderma maydis*), *Phaeosphaeria* leaf spot (*Phaeosphaeria maydis*), downy mildew (*Peronosclerospora sorghi*), *Bipolaris zeicola* (*Helminthosporium* leaf spot) and a range of foliar and root diseases caused by *Fusarium verticillioides* (Babalola *et al.*, 2022; Belisário *et al.*, 2022; Korsman *et al.*, 2012; Liu *et al.*, 2021). The effects of these diseases have been reported to occur from mild to severe cases that are capable of causing an entire yield loss in the field.

Varying management techniques have been employed to salvage maize from fungal diseases. The most commonly employed method among maize growers

is chemical-based fungicides (Padrilah *et al.*, 2024). However, the further use of this chemical has been widely discouraged because of its possible contamination of the environment and the associated health risks to humans, which mostly result from inadequate or prolonged chemical usage. Although, some cultural approaches such as crop rotation and minimum tillage practices had yielded progressive results (Degani *et al.*, 2022; Sharma *et al.*, 2022), but had in most instances, not satisfactorily curtailed the deleterious effect of these fungal pathogens alone. Hence, there is a need to further channel investigation into a sustainable means of fungal disease control, which mimics the natural disease management model, by the use of bioagents with bioprotectant and antagonistic properties (Akanmu *et al.*, 2023a; Scortichini, 2022; Wahid *et al.*, 2020).

Some biochemical mechanisms including ACC deaminase, phosphate solubilization, ammonium and siderophore production have been linked to the reduction of both plant pathogenic fungi and deleterious rhizobacteria by Plant Growth-Promoting Rhizobacteria (PGPR) (Enebe and Babalola, 2018; Etesami & Maheshwari, 2018). Therefore PGPR has been reported for its potential to offer alternative and sustainable methods of plant disease management (Benaissa, 2024; Jiao *et al.*, 2021). The association of PGPR with the plant roots has been documented to promote plant growth through enhanced mineral nutrition, trigger the production of plant hormones or other molecules that stimulate plant growth and strengthen plant defenses against both biotic and abiotic stresses. The rhizobacteria also protect plants by regulating the abundance and activities of pathogenic microbes (Fadiji *et al.*, 2023; Gupta & Pandey, 2023; Lyu *et al.*, 2019). As a result of the suitability of the use of PGPR in the same and sustainable agricultural production, this study set out to investigate the potentials of some rhizobacteria associated with maize rhizosphere in the management of fungal diseases in maize.

Materials and methods

Source of the fungal species. The fungal pathogens used in this study were obtained from the culture collections of the Microbial Biotechnology Laboratory, North West University, South Africa. The consensus nucleotide sequence of the fungal isolates had been earlier deposited in GenBank with accession numbers OP536174, OP536183 and OP536186.

Sample collection and isolation of bacteria. The experimental samples were collected from the rhizosphere region of maize plants at the Teaching and Research Farm of the North-West University, Molelwane (25°47′26.4″ S 25°37′01.6″ E)

in March 2022. A total of eight diseased maize plants were randomly selected and uprooted. The soils that were tightly bound to the plant roots were scraped from each of the collected samples. The samples were transferred to the laboratory in an ice cooler box (-4°C). The soil samples were subjected to serial dilution and plated on Nutrient Agar (NA). The plates were incubated at 30°C for 24 hours. The colonies obtained were further subcultures on NA to obtain pure cultures. The isolates were then categorized for morphological characterization using the Bergey's Manual of Determinative Bacteriology (Holt *et al.*, 1994).

Screening for plant-growth promoting rhizobacteria (PGPR) properties. The following screening was conducted to determine the suitability of the bacteria isolates as PGPR candidates and their potential to inhibit the pathogenic effects of the foliar fungal pathogens of maize.

Ammonia production. The assessment of ammonia production by bacterial isolates was in line with the method described by Islam *et al.* (2009). In each test tube, 10 μl of freshly prepared bacterial cultures with an optical density of 0.2 were introduced into 10 ml of peptone water. After inoculation, the test tubes underwent a seven-day incubation period at 34°C. Post-incubation, 1 ml of Nessler's reagent was introduced into each test tube, and any observable changes in color were documented. A positive outcome, indicating ammonia production, was denoted by a shift in the medium color to brown or yellow. The experimental procedure was replicated three times to ensure reliability and consistency.

Phosphate solubilization. The methodology outlined by Islam *et al.* (2009) was employed to assess the phosphorus solubilization potentials of the seven bacterial isolates. Specifically, 10 μl of freshly prepared culture was spot-inoculated onto Pikovskaya agar plates containing 2% tri-calcium phosphate. Subsequently, these inoculated plates were incubated for 7 days at 37°C, during which the development of a clear zone surrounding the bacterial colonies was monitored. Following the procedure detailed by Farooq and Bano (2013), the solubility index was then determined.

$$Phosphatase\ index = \frac{Clear\ zone\ diameter - Colony\ diameter}{Colony\ diameter}$$

Siderophore production. The investigation of siderophore production by bacteria isolates involved testing their ability to utilize Chrome Azurol S (CAS) dye (CAS from Merck, SA) as an indicator. Initially, 60.5 mg of CAS was dissolved in 50 ml of distilled water and mixed with 10 ml of iron (III) solution

(1 mM FeCl3. 6H20 in 10 mM HCl). This mixture was gradually added to 72.9 mg of hexadecyltrimethylammonium (HDTMA, Merck, SA) bromide that had been previously dissolved in 40 ml of distilled water, with continuous stirring. The resulting solution was autoclaved for 15 minutes at 121°C. To prepare the Petri plates, 900 ml of sterilized LB broth, pH-adjusted to 6.8, was poured, and 100 ml of the autoclaved mixture was added while stirring. Once solidified, freshly prepared bacterial cultures were spot-inoculated onto Petri plates and incubated for 7 days at 25°C. Successful siderophore production was confirmed by the presence of a yellowish-orange halo surrounding bacterial colonies.

ACC deaminase activity. The investigation into ACC deaminase activity among the recovered bacterial isolates was conducted according to the method described by Ali *et al*. (2014). All bacterial isolates were cultured in 5 milliliters of tryptone-soy broth (TSB, rich medium, Merck, SA) at room temperature for 48 hours. Subsequently, bacterial cells were centrifuged at 5000 g for 5 minutes, washed twice with sterile 0.1 M Tris-HCl (pH 7.5), and then resuspended in 1 ml of the same solution. The cleaned bacterial cells were spot-inoculated on Petri plates containing modified Dworkin and Foster salts minimum media (Dworkin and Foster, 1958). The exclusive nitrogen source in the minimal media utilized for this investigation was 3 mM ACC. Negative control plates comprised Petri dishes with DF minimal salt medium without ACC, while positive control plates contained DF minimal salt medium supplemented with 0.2% (w/v) $(NH_4)_2SO_4$. The inoculated plates were incubated at 30°C for 7 days. The growth of bacteria on DF minimum plates, utilizing ACC as the solitary nitrogen source, was compared to both positive and negative controls. The experiment was replicated three times, and the evaluation of cultured Petri plates was predicated on the growth of bacteria that relied exclusively on ACC for nitrogen (Penrose & Glick, 2003).

Molecular characterization of the bacteria isolates. The Quick-DNA Fungal/Bacterial Miniprep Kit (Zymo Research, Irvine, CA, USA) was employed to extract DNA from each bacterial isolate, following the manufacturer's provided instructions. A PCR was carried out to amplify the 16S rRNA gene in the genomic DNA of the extracted bacteria, utilizing the primers 1492R (CGGTTACCTTGTTACGACTT) and 27F (AGAGTTTGATCMTGGCTCAG). The PCR reaction was conducted using a Thermocycler Bio-Rad T100. The reaction mixture consisted of 12.5 µl of 1×NEB OneTaq 2x MasterMix with Standard buffer (Catalogue No. M0482S), 1 µl (10 µM) of each primer, 2 µl of the DNA template, and 9.5 µl of nuclease-free water in a 25 µl reaction volume. The PCR protocol included an initial denaturation stage at 94 °C for 5 minutes, followed by 35 cycles of 30 s at 94 °C, 30 s at 50 °C, and 1 min at 68 °C, with a final 10-minute elongation step at 68 °C.

Subsequent to PCR, ExoSAP-IT from Applied Biosystems, Foster City, CA, USA, was employed for the purification of the resulting PCR products according to the manufacturer's instructions. The separated DNA molecules were visualized through gel electrophoresis using the ChemidocTM imaging system (BIO-RAD Laboratories, Hercules, CA, USA). The sequencing of the amplified and purified DNA was carried out by Inqaba Biotechnology Pty in Pretoria, South Africa.

   Phylogenetic analysis. Pairwise comparisons and multiple alignments were carried out using BioEdit software version 7.0.5, which made it easier to evaluate nucleotide variants and similarities. Pairwise affinity values were computed and the maximum likelihood approach was then applied to create phylogenetic trees. For this approach, the Tamura–Nei parameter was used as a substitute model (Tamura & Nei, 1993). MEGA X (v 10.1.7) was used for the implementation (Kumar *et al.*, 2018). The bootstrap approach with 1000 repetitions was used to evaluate the internal branches' reliability (Felsenstein, 1985). All the consensus nucleotide sequences in used in this investigation have been deposited in GenBank under the accession numbers OR044417–OR044423 (Tab. 1).

Table 1. 16s rRNA gene sequence-based identification of the isolates
and their accession numbers

Code	Isolate name	Accession number	Blasting, closest relative	Relative accession	Similarity %	E value
B1	*Bacillus siamensis* strain AOA1	OR044417	*Bacillus siamensis*	OP904261	99.85	0.00
B2	*Enterobacter asburiae* strain AOA2	OR044418	*Enterobacter asburiae*	OP986762	99.18	0.00
B3	*Enterobacter chengduensis* strain AOA3	OR044419	*Enterobacter chengduensis*	OP811866	84.60	0.00
B4	*Priestia aryabhattai* strain AOA4	OR044420	*Bacillus aryabhattai*	MT453993	100.00	0.00
B5	*Burkholderia* sp. strain AOA5	OR044421	*Burkholderia* sp.	MW930845	99.75	0.00
B6	*Priestia megaterium* strain AOA6	OR044422	*Bacillus megaterium*	MT827122	99.30	0.00
B7	*Priestia megaterium* strain AOA7	OR044423	*Priestia megaterium*	OQ931927	99.74	0.00

Evaluation of the antifungal potentials of bacteria species. A line of bacteria culture was streaked on the solidified Potato Dextrose Agar (PDA) at 3 cm from the edge of 9 cm diameter Petri-dishes. A point inoculation of fungi was made at a distance of 4 cm away from the streaked bacteria (Fig. 1).
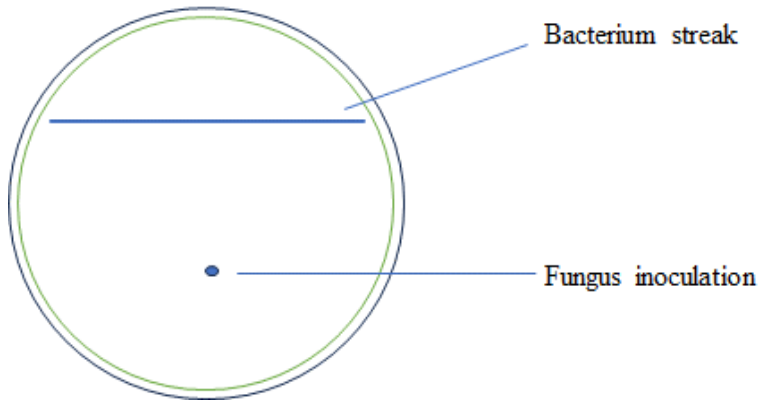
Figure 1. Bacteria streak and fungal inoculation on a PDA plate

A total of 7 bacterial isolates were assessed against 3 pathogenic fungal species, with fungal plates serving as the control. The experiment was replicated 3 times and incubated at 25 ± 2 °C for 7 days. The radius of mycelia growths was measured at two days intervals. The percentage rate of mycelia inhibition was calculated as:

$$\% \, Growth = \frac{Rc - Rt}{Rc} \, x \, 100$$

R_t = radius of the fungi when inoculated in a plate with bacteria
R_c = radius of the fungi when inoculated alone (control).

Statistical analysis. The data collected from each replicate were subjected to Analysis of Variance (ANOVA) using Statistical Analysis Software (version 9.8). Post hoc analysis was performed using Duncan's Multiple Range Test to separate mean values. All statistical analyses were executed at a significance level of 5% (p ≤ 0.05).

Results

The isolated bacteria species were categorized into seven distinct groups based on their morphological characterization i.e. color, shape and growth patterns. All seven bacteria isolates tested positive for ammonia, phosphate siderophore and ACC (1-aminocyclopropane-1-carboxylate) deaminase tests. Isolate B5 demonstrated higher phosphatase potentials compared to other isolates. More so, isolate B1 showed no growths with $(NH_4)_2SO_4$ treatments in the ACC deaminase test (Tab. 2).

Table 2. PGPR screening of bacteria isolates

Isolate	Ammonia production (mg/L)	Phosphate solubilization (mg/L)	Siderophore production (µg/mL)	ACC deaminase test		
				ACC (µmol/min / mg protein)	$(NH_4)_2SO_4$ (mg/L)	Control
B1	+	++	+	+	-	+
B2	+	++	+	+	+	+
B3	+	++	+	+	+	+
B4	+	++	+	+	+	+
B5	+	+++	+	+	+	+
B6	+	++	+	+	+	+
B7	+	++	+	+	+	+

Note: For phosphate solubilization and siderophore production, the clear zones were: (+) = 0.10 to 0.50 cm; (++) = 0.60 to 1.00 cm; (+++) = 1.10 to 1.50 cm.

Sequences of the isolated bacteria strains were aligned with those earlier documented on the NCBI platform. The phylogenetic relationship tree of the isolates revealed B1, B4, B6 and B7 clustered into a distinct, well-supported clade with *Bacillus siamensis* OP904261, *Priestia arybhattai* OQ519933, *Preistia megatarium* OM033601, and *Priestia megaterium* MT827122 (Fig. 2a). Similarly, the phylogenetic relationship between B2 and B3 was observed in their cluster to a distinct clade with *Enterobacter asburiae* OP986762 and *Enterobacter chengduensis* OP811866 (Fig. 2b), while a separate phylogenetic tree, B5 clustered with *Burkholderia* sp. MW930845 (Fig. 2c).
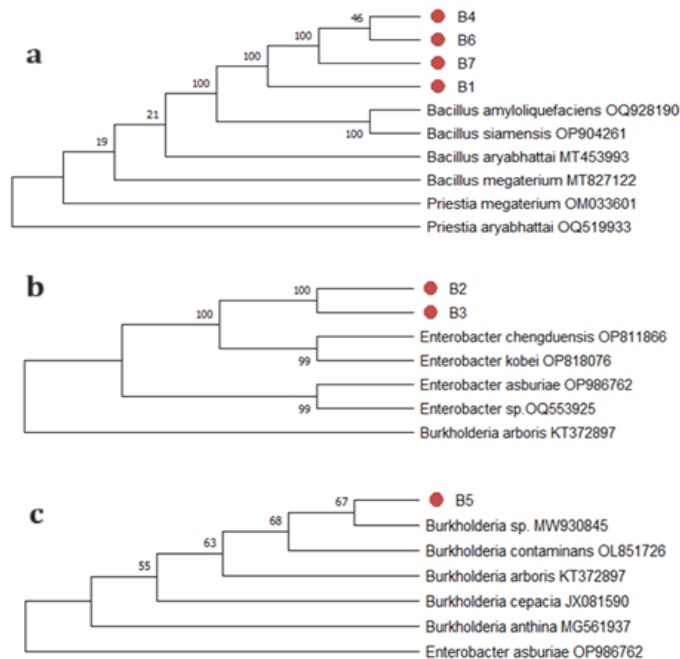
Figure 2. The phylogenetic relationships between the bacteria species and selected database relatives on the NCBI generated through transcribed spacer 16s rRNA genes, analyzed via Kimura's two-parameter models. Bootstrap support values higher than 50% from 1000 replicates are shown at the nodes. *Priestia aryabhattai* (OQ519933) (a) *Burkholderia arboris* (KT372897) (b) and *Enterobacter asburiae* OP986762 (c) were used as the out-group.

The morphological overview of the experimental set-up on day 4 showed varying rates of bacteria inhibition of the fungi mycelia growth, as compared to the control was demonstrated in Fig. 3. The evaluation of the antagonistic potentials of seven bacteria species against the fungal pathogens associated with foliar diseases of maize showed no significant (p>0.05) difference in their individual effects on mycelial inhibition of *Enterobacter chengduensis, Priestia aryabhattai, Burkholderia* sp, *Priestia megaterium* strain AOA6 and *Priestia megaterium* strain AOA7 against the fungi; *Nigrospora sphaerica, Alternaria alternata* and *Fusarium equiseti*, as observed at the 3rd, 5th and 7th days of observation. However, *Bacillus siamensis* showed the most significant inhibition of the mycelia growth of *A. alternata* on the 3rd day. In contrast, no significant difference was recorded across the fungal species on the 5th and 7th days. Similarly, *Enterobacter asburiae* recorded a similar level of significance across the fungal species at the 3rd day of evaluation. At the same time, it only showed significant (p<0.05) influence on *N. sphaerica* on the 5th and 7th days (Tab. 3).

191

Figure 3. Culture plates of three fungi species challenged with seven bacteria species taken at day 4 of the experiment
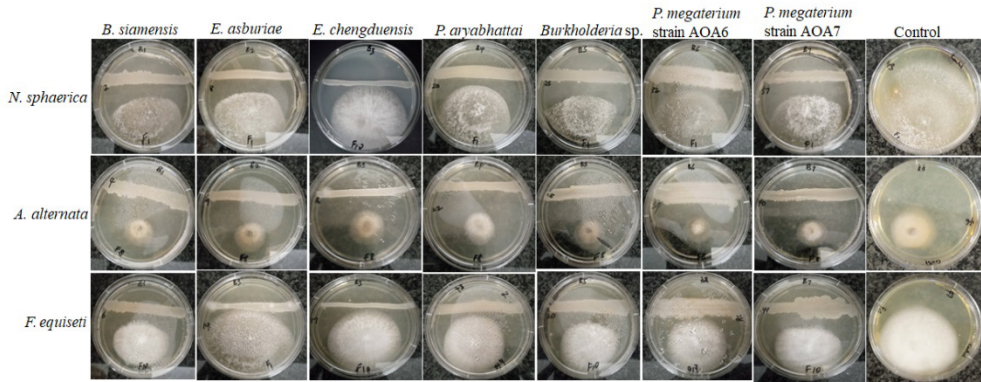
Table 3. Antagonistic potentials of bacteria against
Nigrospora sphaerica, *Alternaria alternata* and *Fusarium equiseti*

Bacterial isolates	Days	*Nigrospora sphaerica*	*Alternaria alternata*	*Fusarium equiseti*	LSD
	3	4.90b ± 3.98	25.44a ± 4.29	13.97b ± 2.42	10.18
Bacillus siamensis	5	51.08a ± 18.51	25.74a ± 7.01	32.01a ± 9.46	51.58
	7	66.02a ± 15.78	57.53a ± 12.29	45.30 a± 11.44	29.54
Enterobacter asburiae	3	16.78a ± 5.28	3.57a ± 2.06	9.86a ± 1.76	13.65
	5	62.20a ± 17.09	16.53b ± 8.21	19.60b ± 3.65	39.18
	7	67.56a ± 14.71	46.31ab ± 3.87	29.61ab ± 9.97	31.66
Enterobacter chengduensis	3	3.79a ± 3.79	5.63a ± 3.66	6.19a ± 3.07	13.16
	5	14.92a ± 5.85	5.09a ± 2.25	2.59a ± 0.49	12.05
	7	24.30a ± 8.22	34.06a ± 16.41	1.10a ± 0.73	33.44
Priestia aryabhattai	3	21.26a ± 3.39	14.72a ± 7.78	11.92a ± 1.95	18.26
	5	26.00a ± 15.79	18.00a ± 4.64	10.75a ± 2.47	37.03
	7	30.94a ± 7.71	26.64a ± 7.31	10.09a ± 3.00	21.74
Burkholderia sp.	3	7.65a ± 7.65	12.94a ± 8.61	8.51a ± 4.17	21.81
	5	46.64a ± 14.72	23.93a ± 10.99	31.92a ± 2.99	26.28
	7	56.47a ± 11.82	63.58a ± 12.66	47.55a ± 6.86	33.02
Priestia megaterium strain AOA6	3	11.93a ± 3.61	18.13a ± 4.31	15.12a ± 2.87	14.8
	5	30.02a ± 12.11	33.22a ± 4.53	16.15a ± 1.11	23.43
	7	38.34a ± 12.12	55.88a ± 10.48	28.01a ± 4.66	33.72
Priestia megaterium strain AOA7	3	17.78a ± 6.22	0.22a ± 2.74	13.35a ± 5.43	19.71
	5	63.40a ± 19.58	20.99a ± 7.55	28.50a ± 7.47	42.05
	7	100.00a ± 39.99	43.73a ± 5.53	51.24a ± 11.67	69.40

Note: Each value represents the mean of four replicates ± standard error. Means with different letters across the row are significantly (p<0.05) different.

The antagonistic effect of the bacteria species on the fungi *Nigrospora sphaerica*, *Alternaria alternata* and *Fusarium equiseti* showed similar significance levels at the 3rd day of observation. The mycelial growth of *N. sphaerica* (42.04%, 54.82%) was the most significantly inhibited on the 5th day, and together with *A. alternata* (46.53%) on the 7th day recorded a similar level of significance, while *F. equiseti* (30.41%) was the least inhibited (Fig. 4). However, the pooled effects of days of observation revealed *N. sphaerica* (36.29%) as the most significantly inhibited, followed by *A. alternata* (26.19%) and *F. equiseti* (20.63%) (Fig. 5).

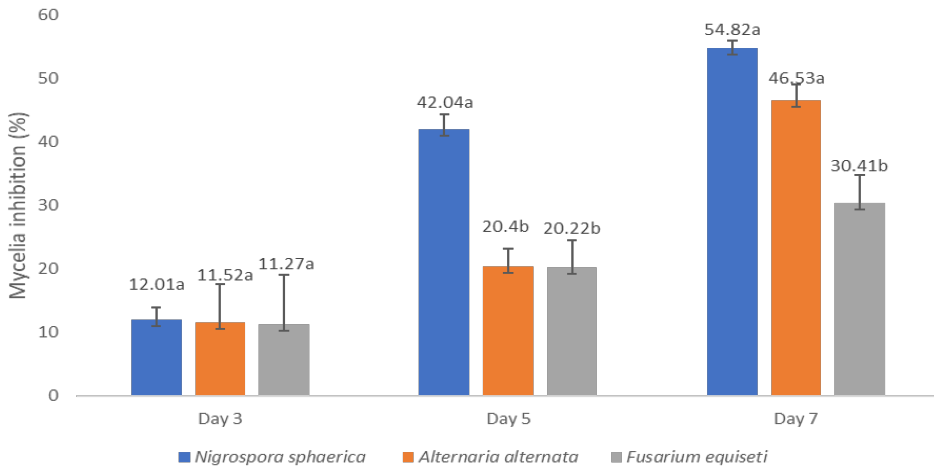

Figure 4. The percentage mycelia inhibition across different fungal species. Each value represents the mean of four replicates ± standard deviation
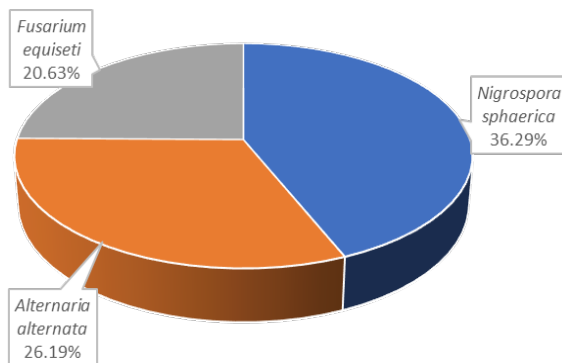

Figure 5. The pooled effects of days on the mycelia inhibition by the bacteria species

Bacillus siamensis (14.77%)*, Priestia aryabhattai* (15.97%) and *Priestia megaterium* strain AOA6 (15.06%), which showed a similar level of significance at p<0.05 expressed the mostly inhibition of the fungal species at day 3 of the observation. On the 5th day, *B. siamensis* (36.28%) and *P. megatarium* strain AOA7 (37.63%) showed the most significant inhibition, with *P. megatarium* strain AOA7 (65.02%) consistency as the most significant on the 7th day of observation. However, *Enterobacter chengduensis* (5.20%, 7.53% and 19.82%) recorded the least inhibition on days 3, 5, and 7 of the observation, respectively (Tab. 4). The antagonistic effects of bacteria against the pooled fungal species showed *E. asburiae* (35.96%) and *P. megatarium* strain AOA7 (34.65%), as causing the most significant inhibition of fungal mycelia growth. This result was followed by *B. siamensis* (30.60%), *P. aryabhattai* (27.35%), *E. chengduensis* (23.01%), and *Bulkholderia* sp. (21.23%), while *P. megaterium* strain AOA6 (21.13%) showed the least mycelia inhibition (Fig. 6).

Table 4. Pooled percentage mycelia inhibition by each bacteria species

Bacteria	Day 3	Day 5	Day 7
Bacillus siamensis	14.77a ± 3.17	36.28a ± 7.37	56.28ab ± 7.41
Enterobacter asburiae	10.07ab ± 2.42	32.78ab ± 8.57	47.83ab ± 7.21
Enterobacter chengduensis	5.20b ± 1.86	7.53c ± 2.49	19.82d ± 6.93
Priestia aryabhattai	15.97a ± 2.90	18.25bc ± 5.36	21.87cd ± 4.25
Burkholderia sp.	9.68ab ± 3.12	34.16ab ± 6.29	55.87ab ± 5.96
Priestia megaterium strain AOA6	15.06a ± 2.05	26.46ab ± 4.51	40.74bc ± 6.11
Priestia megaterium strain AOA7	10.45ab ± 3.45	37.63a ± 8.73	65.02a ± 14.74
LSD	7.80	15.43	19.71

Note: Each value represents the mean of four replicates ± standard error. Means with the different letters across the column are significantly (p<0.05) different.
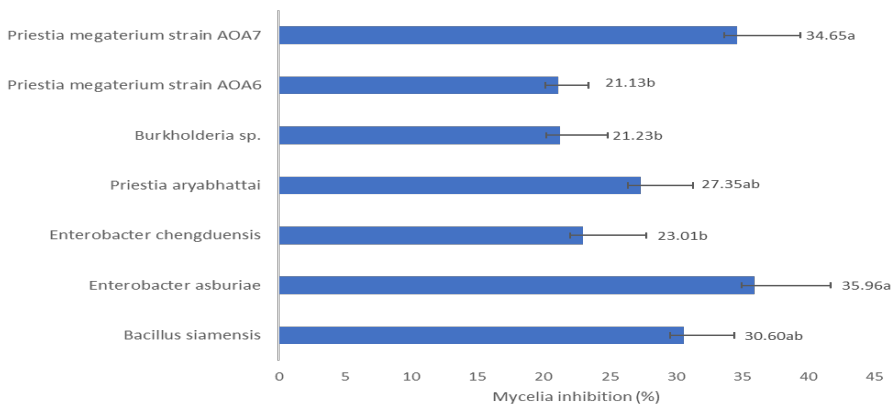

Figure 6. The antagonistic potentials of each bacterium against the mycelia growth of fungal species (LSD = 10.23)

Discussion

The positive tests of the seven bacteria isolates in this study to ammonium, ACC deaminase, phosphate and siderophore production indicate the capability of each of the isolates to suppress the soilborne fungal pathogens of maize. The isolates demonstrated the potential to sequestrate iron thereby limiting the nutrient availability to fungal pathogens as revealed by the siderophore production (Tripathi *et al.*, 2020). Bacteria species that solubilize phosphate also produces secondary metabolites with antifungal properties, thereby enhancing plant defense responses (Fasusi *et al.*, 2021; Wei *et al.*, 2024). Also, the ACC results indicated the potential of bacteria in ethylene modulation which aids in the suppression of fungal pathogenicity (Jha *et al.*, 2021). Furthermore, the ammonium production recorded revealed the potential of the bacteria to compete for nitrogen sources in the surrounding environment, and limiting its availability to fungal pathogens (Lau *et al.*, 2020).

The BLAST search on the NCBI based on the seven bacteria species found associated with diseased maize rhizosphere and characterized in this study using 16S rRNA gene, revealed the organisms as *Bacillus siamensis* strain AOA1 (B1), *Enterobacter asburiae* strain AOA2 (B2), *Enterobacter chengduensis* strain AOA3 (B3), *Priestia aryabhattai* strain AOA4 (B4), *Burkholderia* sp. strain AOA5 (B5), *Priestia megaterium* strain AOA6 (B6) and *Priestia megaterium* strain AOA7 (B7). This validates the earlier claim that bacteria are major microbiome domain that is commonly associated with plant rhizosphere (Babalola, 2010; Saqib *et al.*, 2020). Bacteria species have been reported to perform varying roles, especially in plant–microbe relationships, where they aid in plant growth promotions, health, stress and drought management, as well as phytoremediation (Dlamini *et al.*, 2022; Fadiji *et al.*, 2022b; Kabeer *et al.*, 2022), among many others. *Bacillus siamensis,* is a gram-positive bacterium in the phylum Firmicutes and class Bacilli. It is commonly isolated from soil, especially in the tropical regions. The organism has been found to produce enzymes such as amylases, proteases, and lipases, which contribute to its ability to degrade complex organic compounds. Furthermore, as a result of the antimicrobial compounds it secretes, it has been found effective against plant pathogens, as evident in its significant inhibition of mycelia growths of some pathogenic fungi i.e. *Rhizoctonia solani* and *Botrytis cinerea* (Jeong *et al.*, 2012). It has also been reported as effective against the brown spot disease of tobacco caused by *Alternaria alternata* (Xie *et al.*, 2021), *Pestalotiopsis versicolour* causing bayberry twig blight of sweet potato (Ali *et al.*, 2020) and soybean root rot disease (He *et al.*, 2023) among many studies.

Two strains of *Prestia megaterium,* which is a new separate genus from *Bacillus,* previously known as *Bacillus megaterium* (Liu *et al.*, 2023). This ubiquitous environmental bacterium was initially identified by Anton De Bary in 1884. It has been reported as important in biotechnology for the synthesis of enzymes, recombinant proteins, and vitamins as well as for bioremediation activities (Vary *et al.*, 2007). Its role from simple soil bacterium to industrial protein production host has been further enumerated (Biedendieck *et al.*, 2021; Vary *et al.*, 2007). Also, *P. megaterium* has been isolated from different plants, including pepper, cucumber, wheat, Alfalfa, carrot, black, clover etc. (Rajan *et al.*, 2021). *P. megaterium* is categorized as a potential biocontrol agent for plant diseases due to its antimicrobial activities (Jayakumar *et al.*, 2021). As indicated in previous investigations, three main mechanisms by which *P. megaterium* promotes plant growth include the secretion of organic acids which provides the template for phosphate solubilization. The organisms also cause variations in the concentration of phytohormone and other plant growth regulators, while they also can function as a biocontrol or biopesticide agent (Liu *et al.*, 2023). However, *Priestia aryabhattai,* which is another *Priestia* specie isolated in this study, has earlier been described as a stress-tolerant bacterium with the capability of enhancing salt tolerance in wheat (Shahid *et al.*, 2022), the organisms similarly showed the potential of degrading aromatic compounds, and as well antagonized both the fungal and bacterial phytopathogens (Esikova *et al.*, 2021).

In addition, the isolated *Enterobacter* species are Gram-negative bacteria in the family *Enterobacteriaceae.* Some genera within the family *Enterobacteriaceae*, such as *Enterobacter, Pantoea, Serratia* and certain species of *Klebsiella,* have been classified as Plant Growth Promoting Bacteria (PGPB). However, some of the genera have also been found to contain species, which are plant pathogens causing varying diseases of crops such as wilting, galls, necrosis and soft rot diseases (Walterson & Stavrinides, 2015). *Enterobacter asburiae* and *Enterobacter chengduensis* were isolated from diseased maize rhizosphere in this study, while earlier research had isolated a strain of *E. chengduensis* from blood in China (Wu *et al.*, 2019), indicating the diverse host of this member, as including plants, animals, humans and water (Fadiji *et al.*, 2022a). Furthermore, *E. asburiae* has been implicated with rice bacterial blight disease in China (Xue *et al.*, 2021), while another strain of *E. asburiae* was reported as a plant growth-promoting rhizobacteria in the study conducted by Saikia *et al.* (2023). Similarly to *Enterobacter*, *Burkholderia* are also versatile microorganisms that have been recovered from a wide range of ecological niches. Many of the species have been effective in plant growth promotion, biocontrol of plant pathogens and bioremediation purposes (Coenye & Vandamme, 2003). However, some *Burkholderia* species demonstrate

a twist of activities, such as the case of *Burkholderia cepacia*, which is a known plant pathogen and multiresistant pathogen in patients suffering from cystic fibrosis, yet this organism is still an efficient biological fertilizer and pesticide of a range of plant pathogens, including bacteria, fungi, and nematodes (Govan *et al.*, 1996; Parke and Gurian-Sherman, 2001; Vandamme *et al.*, 2003).

The fungi species; *Nigrospora sphaerica, Alternaria alternata,* and *Fusarium equiseti* are some of the commonly reported pathogens of maize (Akanmu *et al.*, 2023b; Aveling *et al.*, 2020). This study revealed *N. sphaerica* (36.29%) as the most inhibited by the antagonist bacteria species, followed by *A. alternata* (26.19%) and *F. equiseti* (20.63%). Thereby validating the earlier report on the antifungal potentials of bacteria species in the management of fungal diseases of maize as earlier reported (Fasusi *et al.*, 2021; Orole *et al.*, 2023; Tagele *et al.*, 2019). Furthermore, *E. asburiae > P. megatarium* strain AOA7 *> B. siamensis > P. aryabhattai > E. chengduensis > Bulkholderia* sp. were the order of the antifungal efficacy of the bacteria species evaluated. This result is consistent with the earlier characteristics of each of the isolates discussed. Thus, the presence of bacteria with biocontrol potentials in the rhizosphere soil of maize plants examined in this study signifies the natural potential of plant root architecture and exudation to modulate the rhizosphere microbiome, as to function based on the plant's requirement (Dlamini *et al.*, 2023a; Marco *et al.*, 2022).

Conclusion

In conclusion, *F. equiseti* (20.63%), *A. alternata* (26.19%) and *N. sphaerica* (36.29%) were the order of susceptibility of the pathogenic fungi to the biocontrol potentials of the bacteria evaluated. More so, the efficacy of *E. asburiae, P. megatarium* strain AOA7, and *B. siamensis* over a range of fungal pathogens justifies their further investigation, formulation and deployment as biofungicide in the management of foliar diseases of maize.

Conflict of interest statement: The authors declare no conflict of interests.

References

Agunbiade, V.F., & Babalola, O.O. (2023). Endophytic and rhizobacteria functionalities in alleviating drought stress in maize plants. *Plant Prot. Sci., 59*(1), 1–18.

Akanmu, A.O., Akol, A.M., Ndolo, D.O., Kutu, F.R., & Babalola, O.O. (2023a). Agroecological techniques: Adoption of safe and sustainable agricultural practices among the smallholder farmers in Africa. *Front. Sustain. Food Syst., 7*, 310.

Akanmu, A.O., Ajiboye, T.O., Seleke, M., Mhlanga, S.D., Onwudiwe, D.C., & Babalola, O.O. (2023b). The potency of graphitic carbon nitride (gC3N4) and bismuth sulphide nanoparticles (Bi2S3) in the management of foliar fungal pathogens of maize. *Appl. Sci., 13*(6), 3731.

Akanmu, A.O., Sobowale, A.A., Abiala, M.A., Olawuyi, O.J., & Odebode, A.C. (2020). Efficacy of biochar in the management of *Fusarium verticillioides* Sacc. causing ear rot in *Zea mays* L. *Biotechnol. Rep., 26*, e00474. doi:https://doi.org/10.1016/j.btre.2020.e00474

Ali, M.A., Ren, H., Ahmed, T., Luo, J., An, Q., Qi, X., & Li, B. (2020). Antifungal effects of rhizospheric *Bacillus* species against bayberry twig blight pathogen Pestalotiopsis versicolor. *Agronomy, 10*(11), 1811.

Ali, S., Charles, T.C., & Glick, B.R. (2014). Amelioration of high salinity stress damage by plant growth-promoting bacterial endophytes that contain ACC deaminase. *Plant Physiol. Biochem., 80*, 160-167.

Aveling, T.A., De Ridder, K., Olivier, N.A., & Berger, D.K. (2020). Seasonal variation in mycoflora associated with asymptomatic maize grain from small-holder farms in two provinces of South Africa. *J. Agric. Rural Dev. Trop. Subtrop. (JARTS), 121*(2), 265-275.

Babalola, O.O. (2010). Beneficial bacteria of agricultural importance. *Biotechnol. Lett., 32*, 1559-1570.

Babalola, O.O., Dlamini, S.P., & Akanmu, A.O. (2022). Shotgun metagenomic survey of the diseased and healthy maize (*Zea mays* L.) rhizobiomes. *Microbiol. Resour. Announc., 11*(10), e00498-00422.

Belisário, R., Robertson, A.E., & Vaillancourt, L.J. (2022). Maize anthracnose stalk rot in the genomic era. *Plant Dis., 106*(9), 2281-2298.

Benaissa, A. (2024). Rhizosphere: Role of bacteria to manage plant diseases and sustainable agriculture—A review. *J. Basic Microbiol., 64*(3), 2300361.

Holt J.G., Krieg N.R., Sneath P.H.A., Staley J.T., & Williams S.T. (1994) Bergey's manual of determinative bacteriology, 9th edn. Williams and Wikins co, Baltimore, USA, p 566.

Biedendieck, R., Knuuti, T., Moore, S.J., & Jahn, D. (2021). The "beauty in the beast"—the multiple uses of Priestia megaterium in biotechnology. *Appl. Microbiol. Biotechnol., 105*, 5719-5737.

Coenye, T., & Vandamme, P. (2003). Diversity and significance of *Burkholderia* species occupying diverse ecological niches. *Environ. Microbiol., 5*(9), 719-729.

Degani, O., Gordani, A., Becher, P., Chen, A., & Rabinovitz, O. (2022). Crop rotation and minimal tillage selectively affect maize growth promotion under late wilt disease stress. *J. Fungi, 8*(6), 586.

Dlamini, S.P., Akanmu, A.O., & Babalola, O.O. (2022). Rhizospheric microorganisms: The gateway to a sustainable plant health. *Front. Sustain. Food Syst., 6*, 925802.

Dlamini, S.P., Akanmu, A.O., & Babalola, O.O. (2023a). Variations in the functional diversity of rhizosphere microbiome of healthy and Northern corn leaf blight infected maize (*Zea mays* L.). *Span. J. Soil Sci., 13*, 10964.

Dlamini, S.P., Akanmu, A.O., Fadiji, A.E., & Babalola, O.O. (2023b). Maize rhizosphere modulates the microbiome diversity and community structure to enhance plant health. *Saudi J. Biol. Sci., 30*(1), 103499.

Dworkin, M., & Foster, J. (1958). Experiments with some microorganisms which utilize ethane and hydrogen. *J. Bacteriol., 75*(5), 592-603.

Enebe, M.C., & Babalola, O.O. (2018). The influence of plant growth-promoting rhizobacteria in plant tolerance to abiotic stress: a survival strategy. *Appl. Microbiol. Biotechnol., 102*, 7821-7835.

Esikova, T.Z., Anokhina, T.O., Abashina, T.N., Suzina, N.E., & Solyanikova, I.P. (2021). Characterization of soil bacteria with potential to degrade benzoate and antagonistic to fungal and bacterial phytopathogens. *Microorganisms, 9*(4), 755.

Etesami, H., & Maheshwari, D.K. (2018). Use of plant growth promoting rhizobacteria (PGPRs) with multiple plant growth promoting traits in stress agriculture: Action mechanisms and future prospects. *Ecotoxicol. Environ. Saf., 156*, 225-246.

Fadiji, A.E., Ayangbenro, A.S., Akanmu, A.O., & Babalola, O.O. (2022). Draft genome sequence of *Enterobacter mori* AYS9, a potential plant growth-promoting rhizobacterium. *Microbiol. Resour. Announc., 11*(12), e01008-01022.

Fadiji, A.E., Ayangbenro, A.S., & Babalola, O.O. (2023). Genomic assessment of *Enterobacter mori* AYS9: A potential plant growth-promoting drought-resistant rhizobacteria. *Span. J. Soil Sci., 13*, 11302.

Fadiji, A.E., Santoyo, G., Yadav, A.N., & Babalola, O.O. (2022). Efforts towards overcoming drought stress in crops: Revisiting the mechanisms employed by plant growth-promoting bacteria. *Front. Microbiol., 13*.

Farooq, U., & Bano, A. (2013). Screening of indigenous bacteria from rhizosphere of maize (*Zea mays* L.) for their plant growth promotion ability and antagonism against fungal and bacterial pathogens. *J. Anim. Plant Sci, 23*(6), 1642-1652.

Fasusi, O.A., Amoo, A.E., & Babalola, O.O. (2021). Characterization of plant growth-promoting rhizobacterial isolates associated with food plants in South Africa. *Antonie van Leeuwenhoek, 114*(10), 1683-1708.

Felsenstein, J. (1985). Confidence limits on phylogenies: an approach using the bootstrap. *Evolution, 39*(4), 783-791.

Gadag, R.N., Bhat, J.S., Mukri, G., Gogoi, R., Suby, S.B., Das, A.K., Yadav, S., Yadava, P., Nithyashree, M.L., Naidu, G.K., Yadav, S.K., & Shilpa, K. (2021). Chapter 3: Resistance to biotic stress: Theory and applications in maize breeding. In C. Kole (Ed.), Genomic designing for biotic stress resistant cereal crops (pp. 129-175). Springer Nature Switzerland AG. DOI: 10.1007/978-3-030-75879-0_3.

Govan, J., Hughes, J.E., & Vandamme, P. (1996). *Burkholderia cepacia*: medical, taxonomic and ecological issues. *J. Med. Microbiol., 45*(6), 395-407.

Gupta, S. & Pandey, S. (2023). Plant growth promoting rhizobacteria to mitigate biotic and abiotic stress in plants. In: Singh, N., Chattopadhyay, A., Lichtfouse, E. (eds) Sustainable agriculture reviews, vol. 60. Springer, Cham. https://doi.org/10.1007/978-3-031-24181-9_3.

He, H., Zhai, Q., Tang, Y., Gu, X., Pan, H., & Zhang, H. (2023). Effective biocontrol of soybean root rot by a novel bacterial strain *Bacillus siamensis* HT1. *Physiol. Mol. Plant Pathol., 125*, 101984.

Imade, E.E., & Babalola, O.O. (2021). Biotechnological utilization: the role of *Zea mays* rhizospheric bacteria in ecosystem sustainability. *Appl. Microbiol. Biotechnol., 105*(11), 4487-4500.

Islam, M.R., Madhaiyan, M., Deka Boruah, H.P., Yim, W., Lee, G., Saravanan, V., ... Sa, T. (2009). Characterization of plant growth-promoting traits of free-living diazotrophic bacteria and their inoculation effects on growth and nitrogen uptake of crop plants. *J. Microbiol. Biotechnol., 19*(10), 1213-1222.

Jayakumar, A., Nair, I.C., & Radhakrishnan, E. (2021). Environmental adaptations of an extremely plant beneficial *Bacillus subtilis* Dcl1 identified through the genomic and metabolomic analysis. *Microb. Ecol., 81*, 687-702.

Jeong, H., Jeong, D.-E., Kim, S.H., Song, G.C., Park, S.-Y., Ryu, C.-M., ... Choi, S.-K. (2012). Draft genome sequence of the plant growth-promoting bacterium *Bacillus siamensis* KCTC 13613. *J. Bacteriol., 194*(15), 4148-4149. doi:10.1128/jb.00805-12.

Jha, C.K., Sharma, P., Shukla, A., Parmar, P., Patel, R., Goswami, D., & Saraf, M. (2021). Microbial enzyme, 1-aminocyclopropane-1-carboxylic acid (ACC) deaminase: an elixir for plant under stress. *Physiol. Mol. Plant Pathol., 115*, 101664.

Jiao, X., Takishita, Y., Zhou, G., & Smith, D.L. (2021). Plant associated rhizobacteria for biocontrol and plant growth enhancement. *Front. Plant Sci., 12*, 634796.

Kabeer, R., Sylas V.P., Praveen Kumar, C.S., Thomas, A.P., Shanthiprabha, V., Radhakrishnan, E.K., & Baiju, K.R. (2022). Role of heavy metal tolerant rhizosphere bacteria in the phytoremediation of Cu and Pb using *Eichhornia crassipes* (Mart.) Solms. *Int. J. Phytorem., 24*(11), 1120-1132.

Korsman, J., Meisel, B., Kloppers, F.J., Crampton, B.G., & Berger, D.K. (2012). Quantitative phenotyping of grey leaf spot disease in maize using real-time PCR. *Eur. J. Plant Pathol., 133*, 461-471.

Kumar, S., Stecher, G., Li, M., Knyaz, C., & Tamura, K. (2018). MEGA X: molecular evolutionary genetics analysis across computing platforms. *Mol. Biol. Evol., 35*(6), 1547.

Lau, E.T., Tani, A., Khew, C.Y., Chua, Y.Q., & San Hwang, S. (2020). Plant growth-promoting bacteria as potential bio-inoculants and biocontrol agents to promote black pepper plant cultivation. *Microbiol. Res, 240*, 126549.

Liu, J.-M., Liang, Y.-T., Wang, S.-S., Jin, N., Sun, J., Lu, C., ... Wang, F.-Z. (2023). Antimicrobial activity and comparative metabolomic analysis of *Priestia megaterium* strains derived from potato and dendrobium. *Sci. Rep., 13*(1), 5272.

Liu, S., Guo, N., Ma, H., Sun, H., Zheng, X., & Shi, J. (2021). First report of root rot caused by *Bipolaris zeicola* on maize in Hebei Province. *Plant Dis., 105*(8), 2247.

Lyu, D., Backer, R., Robinson, W.G., & Smith, D.L. (2019). Plant growth-promoting rhizobacteria for cannabis production: yield, cannabinoid profile and disease resistance. *Front. Microbiol.*, 1761.

Marco, S., Loredana, M., Riccardo, V., Raffaella, B., Walter, C., & Luca, N. (2022). Microbe-assisted crop improvement: a sustainable weapon to restore holobiont functionality and resilience. *Hort. Res., 9*, uhac160.

Ngoune Tandzi, L., & Mutengwa, C.S. (2019). Estimation of maize (*Zea mays* L.) yield per harvest area: Appropriate methods. *Agron., 10*(1), 29.

Orole, O.O., Adejumo, T.O., Link, T., & Voegele, R.T. (2023). Molecular identification of endophytes from maize roots and their biocontrol potential against toxigenic fungi of Nigerian maize. *Sci. Prog., 106*(3), 00368504231186514.

Padrilah, S.N., Samsudin, N.I.P., Shukor, M.Y.A., & Masdor, N.A. (2024). Nanoemulsion strategies in controlling fungal contamination and toxin production on grain corn using essential oils. *Green Chem. Lett. Rev., 17*(1), 2315138.

Parke, J.L., & Gurian-Sherman, D. (2001). Diversity of the *Burkholderia cepacia* complex and implications for risk assessment of biological control strains. *Annu. Rev. Phytopathol., 39*(1), 225-258.

Penrose, D.M., & Glick, B.R. (2003). Methods for isolating and characterizing ACC deaminase-containing plant growth-promoting rhizobacteria. *Physiol. Plant., 118*(1), 10-15.

Poole, N., Donovan, J., & Erenstein, O. (2021). Agri-nutrition research: revisiting the contribution of maize and wheat to human nutrition and health. *Food Policy, 100*, 101976.

Prasanna, B.M., Cairns, J.E., Zaidi, P., Beyene, Y., Makumbi, D., Gowda, M., ... Das, A. (2021). Beat the stress: breeding for climate resilience in maize for the tropical rainfed environments. *Theor. Appl. Genet., 134*(6), 1729-1752.

Rajan, L., Chakraborty, K., & Chakraborty, R.D. (2021). Pharmacological properties of some mangrove sediment-associated *Bacillus* isolates. *Arch. Microbiol., 203*, 67-76.

Saikia, J., Kotoky, R., Debnath, R., Kumar, N., Gogoi, P., Yadav, A., & Saikia, R. (2023). De novo genomic analysis of *Enterobacter asburiae* EBRJ12, a plant growth-promoting rhizobacteria isolated from the rhizosphere of *Phaseolus vulgaris* L. *J. Appl. Microbiol., 134*(2), lxac090.

Saqib, S., Uddin, S., Zaman, W., Ullah, F., Ayaz, A., Asghar, M., ... Chaudhary, H.J. (2020). Characterization and phytostimulatory activity of bacteria isolated from tomato (*Lycopersicon esculentum* Mill.) rhizosphere. *Microb. Pathogenesis, 140*, 103966.

Scortichini, M. (2022). Sustainable management of diseases in horticulture: Conventional and new options. *Horticulturae, 8*(6), 517.

Shahid, M., Zeyad, M.T., Syed, A., Singh, U.B., Mohamed, A., Bahkali, A.H., ... Pichtel, J. (2022). Stress-tolerant endophytic isolate *Priestia aryabhattai* BPR-9 modulates physio-biochemical mechanisms in wheat (*Triticum aestivum* L.) for enhanced salt tolerance. *Int. J. Environ. Res. Public Health, 19*(17), 10883.

Sharma, A., Abrahamian, P., Carvalho, R., Choudhary, M., Paret, M.L., Vallad, G.E., & Jones, J.B. (2022). Future of bacterial disease management in crop production. *Annu. Rev. Phytopathol., 60*, 259-282.

Tagele, S.B., Kim, S.W., Lee, H.G., & Lee, Y.S. (2019). Potential of novel sequence type of *Burkholderia cenocepacia* for biological control of root rot of maize (*Zea mays* L.) caused by *Fusarium temperatum*. *Int. J. Mol. Sci., 20*(5), 1005.

Tamura, K., & Nei, M. (1993). Estimation of the number of nucleotide substitutions in the control region of mitochondrial DNA in humans and chimpanzees. *Mol. Biol. Evol., 10*(3), 512-526.

Tripathi, K., Kumar, N., Singh, M., & Singh, R.K. (2020). Fungal siderophore: Biosynthesis, transport, regulation, and potential applications. In S.K. Sharma, U.B. Singh, P.K. Sahu, H.V. Singh, & P.K. Sharma (Eds.), (Series Ed. N.K. Arora), Microorganisms for sustainability. Springer Nature Singapore Pte Ltd., Vol. 23, pp. 387-408.

Vandamme, P., Holmes, B., Coenye, T., Goris, J., Mahenthiralingam, E., LiPuma, J.J., & Govan, J.R. (2003). *Burkholderia cenocepacia* sp. nov.—a new twist to an old story. *Res. Microbiol., 154*(2), 91-96.

Vary, P.S., Biedendieck, R., Fuerch, T., Meinhardt, F., Rohde, M., Deckwer, W.-D., & Jahn, D. (2007). *Bacillus megaterium*—from simple soil bacterium to industrial protein production host. *Appl. Microbiol. Biotechnol., 76*, 957-967.

Wahid, F., Fahad, S., Danish, S., Adnan, M., Yue, Z., Saud, S., ... Datta, R. (2020). Sustainable management with mycorrhizae and phosphate solubilizing bacteria for enhanced phosphorus uptake in calcareous soils. *Agriculture, 10*(8), 334.

Walterson, A.M., & Stavrinides, J. (2015). *Pantoea*: Insights into a highly versatile and diverse genus within the Enterobacteriaceae. *FEMS Microbiol. Rev., 39*(6), 968-984.

Wei, X., Xie, B., Wan, C., Song, R., Zhong, W., Xin, S., & Song, K. (2024). Enhancing soil health and plant growth through microbial fertilizers: Mechanisms, benefits, and sustainable agricultural practices. *Agronomy, 14*(3), 609.

Wu, W., Feng, Y., & Zong, Z. (2019). Characterization of a strain representing a new *Enterobacter* species, *Enterobacter chengduensis* sp. nov. *Antonie Van Leeuwenhoek, 112*, 491-500.

Xie, Z., Li, M., Wang, D., Wang, F., Shen, H., Sun, G., ... Sun, X. (2021). Biocontrol efficacy of *Bacillus siamensis* LZ88 against brown spot disease of tobacco caused by *Alternaria alternata*. *Biol. Control., 154*, 104508.

Xue, Y., Hu, M., Chen, S., Hu, A., Li, S., Han, H., ... Zhou, J. (2021*). Enterobacter asburiae* and *Pantoea ananatis* causing rice bacterial blight in China. *Plant Dis., 105*(8), 2078-2088.

Composition of the stonefly (Plecoptera) fauna of the Balkans and the Carpathians

Dávid Murányi[✉]

Department of Zoology, Institute of Biology, Eszterházy Károly Catholic University, Eger, Hungary
[✉]**Corresponding author, E-mail: muranyi.david@uni-eszterhazy.hu**

The stoneflies are well known as a neopteran insect order adopted to cold running waters. Due to their strict habitat demands and ancient origin, often used as a model group in zoogeography, both in wide and narrow scales. In the West Palaearctic, peaks of their diversity connected to Pleistocene refugee areas. In regards of this phenomenon, the composition and diversity of the Carpathians and the Balkans are rather different: the Carpathians have 134 described species with only 19 endemic or subendemic taxa, while the Balkans have 204 described species with nearly half of them are endemics. The Carpathian endemics are rarely narrow endemics, while many Balkan taxa are restricted to small areas, and their distribution outlines Illyrian, Moesian and Attikan centres. The Balkan-Carpathian species are mostly restricted to the Moesian ranges in the Balkans while widespread in the Carpathians. Alpine-Carpathian species are mostly restricted to the North Carpathians, while Alpine-Balkanian species are restricted to the Dinarids. The few Balkano-Anatolian species are restricted to the Aegean Isles or having a disjunct Balkanian area. Widespread (European or Central-South European) species are common in the whole Carpathians and most of the Balkans, but generally lacking from the southern extremes and from the isles. Hotspots of endemicity and/or diversity considered are the Oaş-Ţibleş range in the Eastern, and the high ranges of the Southern Carpathians, the central Balkanian high ranges (Prokletije, Korab, Ríla, Pirin, Lakmos), Balkanian hills with special climate (Epirus, SE Macedonia, Strandzha) and the Aegean Isles.

Keywords: distribution, endemic taxa, hotspots, Pleistocene.

In vivo assessment of a doxorubicin chemoresistance profile in melanoma

Valentin-Florian Rauca[1], Giorgiana Negrea[1], Marta-Szilvia Meszaros[1],
Ştefan Drăgan[1], Laura Pătraş[1,] Emilia Licărete[1], Bogdan Dume[1],
Manuela Banciu[1], Alina Sesărman[1]

[1]*Department of Molecular Biology and Biotechnology, and Center of Systems Biology, Biodiversity and Bioresources, Faculty of Biology and Geology, Babes-Bolyai University, Cluj-Napoca, Romania*

Recent international guidelines recommend the development of technologies that contribute to the reduction, refinement, and replacement of animals for experiments (3Rs) [1]. Thus, the aim of our project was to develop and validate *in vitro* 3D biomimetic platforms composed of multicellular spheroids to replicate melanoma microenvironment chemoresistance. Doxorubicin (DOX), a well-known anthracycline antibiotic commonly used in cancer chemotherapy, to which melanoma cells are known to develop chemoresistance, was used to obtain our model's chemoresistance profile. DOX encapsulated in extracellular vesicles purified from B16.F10 melanoma cells, grown under metabolic stress (PEG-EV-DOX) was used to restore chemosensitivity based of the superior targeting capacity of this nanoformulation [2]. We investigated the molecular mechanisms of DOX chemoresistance profile by qPCR, protein array, WB, HPLC, spectrophotometry and ELISA. Our main findings suggest a DOX chemoresistance pro-angiogenic profile sustained by strong upregulation of IGF-II, IL-1α, IL-9, MCP1, TPO, TIMP1 and PF4 proteins. In addition, resistance to apoptosis was mediated by upregulation of anti-apoptotic factor FasL, while PEG-EV-DOX treatment restored the pro-apoptotic status via upregulation of Bax and Casp3 pro-apoptotic factors. While subtherapeutic dose of free DOX induced no significant changes in redox status, DOX induced gene expression upregulation of tumor cell survival factors HIF-1α and Akt, and an increase in invasion marker MMP-2 on both gene and protein levels. Regarding epigenetic changes, global methylation increased in DOX chemoresistant group compared to Control and PEG-EV-DOX-treated groups. Our data suggested that several features of chemoresistance were met by our model, regarding angiogenesis, apoptosis, survival, and epigenetic regulation. Further mechanistic studies and RNAseq are needed to elucidate more aspects of the model, as well as *in vivo* studies on mice inoculated with resistant tumor cells, required to compare the outcome with data from the present study.

[1] Chen CS. 3D Biomimetic Cultures: The Next Platform for Cell Biology. Trends Cell Biol. 2016 Nov; 26(11):798-800. doi: 10.1016/j.tcb.2016.08.008. Epub 2016 Sep 13. PMID: 27637342; PMCID: PMC5184827.
[2] Licarete E, Rauca VF, Luput L, Drotar D, Stejerean I, Patras L, Dume B, Toma VA, Porfire A, Gherman C, Sesarman A, Banciu M. Overcoming Intrinsic Doxorubicin Resistance in Melanoma by Anti-Angiogenic and Anti-Metastatic Effects of Liposomal Prednisolone Phosphate on Tumor Microenvironment. Int J Mol Sci. 2020 Apr 23; 21(8):2968. doi: 10.3390/ijms21082968. PMID: 32340166; PMCID: PMC7215436.

Unlocking the past: Exploring the biocultural landscape of a pre-modern necropolis in Southeastern Romania

Ioana (Rusu) Drăghici[1,2]✉

1 Molecular Biology Centre, Interdisciplinary Research Institute on Bio-Nano-Sciences, Babeş-Bolyai University, Cluj-Napoca, Romania; 2 Department of Molecular Biology and Biotechnology, Faculty of Biology and Geology, Babes-Bolyai University, Cluj-Napoca, Romania
✉**Corresponding author, E-mail: ioana.rusu@ubbcluj.ro.**

Human skeletal remains from archaeological sites offer valuable insights into various aspects of ancient life, death, and social dynamics. Advances in ancient biomolecule analysis have enhanced our understanding of the past, yet new discoveries continually enrich the narrative as more unique osteological collections are studied. This study seeks to reconstruct the biological profile of a historical population discovered within a sprawling, multi-phase archaeological site in southeastern Romania (Mireasa necropolis, T38) by integrating multiple lines of evidence. A key aspect of this investigation involves the reconstruction of complete mitogenomes from human archaeological remains, employing Next-Generation Sequencing (NGS) technology, which has emerged as the gold standard in ancient DNA (aDNA) research. The preliminary results regarding maternal line genetic signatures of historical individuals from Mireasa indicated the presence of a mixture of mitochondrial haplogroups of West Eurasian origin and variants less closely associated with European regions. This observation may possibly reflect the demographic shifts within the historical province of Dobruja during the 15th-16th centuries AD.

Keywords: pre-modern necropolis, ancient mitogenome, NGS, radiocarbon dating

The transcriptional landscape of cancer stem-like cell functionality in breast cancer

Oana Baldasici[1], Olga Soritau[1], Andrei Roman[2], Carmen Lisencu[2],
Simona Vişan[1], Daniel Cruceriu[3], Laura Maja[4], Bogdan Pop[4], Bogdan Fetica[4],
Andrei Cismaru[5], Laurian Vlase[6], Loredana Bălăcescu[1], Ovidiu Bălăcescu[1],
Aman Russom[7], Oana Tudoran[1]✉

*[1]The Oncology Institute "Prof. Dr. Ion Chiricuţă", Department of Genetics, Genomics and
Experimental Pathology, Cluj-Napoca Romania; [2]Department of Radiology, The Oncology Institute
"Prof. Dr. Ion Chiricuţă", Cluj-Napoca, Romania; [3]Department of Molecular Biology and
Biotechnology, Babes-Bolyai University, Cluj-Napoca, Romania; [4]Department of Pathology,
The Oncology Institute "Prof. Dr. Ion Chiricuţă", Cluj-Napoca, Romania; [5]Research Center for
Functional Genomics, Biomedicine and Translational Medicine, University of Medicine and
Pharmacy "Iuliu Hatieganu" Cluj-Napoca, Romania; [6]The University of Medicine and Pharmacy,
Department of Pharmaceutical Technology and Biopharmaceutics, Cluj-Napoca, Romania;
[7]KTH Royal Institute of Technology in Stockholm, Stockholm, Sweden*
✉**Corresponding author, E-mail: oana.tudoran@iocn.ro.**

Background: Cancer stem-like cells (CSCs) have been extensively researched as the primary drivers of therapy resistance and tumor relapse in patients with breast cancer. However, due to lack of specific molecular markers, increased phenotypic plasticity and no clear clinicopathological features, the assessment of CSCs presence and functionality in solid tumors is challenging. While several potential markers, such as CD24/CD44, have been proposed, the extent to which they truly represent the stem cell potential of tumors or merely provide static snapshots is still a subject of controversy. Recent studies have highlighted the crucial role of the tumor microenvironment (TME) in influencing the CSC phenotype in breast cancer cells. The interplay between the tumor and TME induces significant changes in the cancer cell phenotype, leading to the acquisition of CSC characteristics, therapeutic resistance, and metastatic spread. Simultaneously, CSCs actively shape their microenvironment by evading immune surveillance and attracting stromal cells that support tumor progression. Methods: In this study, we associated in vitro mammosphere formation assays with bulk tumor microarray profiling and deconvolution algorithms to map CSC functionality and the microenvironmental landscape in a large cohort of 125 breast tumors. Results: We found that the TME score was a significant factor associated with CSC functionality. CSC-rich tumors were characterized by an immune-suppressed TME, while tumors devoid of CSC potential exhibited high immune infiltration and activation of pathways involved in the immune response. Gene expression

analysis revealed IFNG, CXCR5, CD40LG, TBX21 and IL2RG to be associated with the CSC phenotype and also displayed prognostic value for patients with breast cancer. Conclusion: These results suggest that the characterization of CSCs content and functionality in tumors can be used as an attractive strategy to fine-tune treatments and guide clinical decisions to improve patients therapy response.

Keywords: breast cancer, cancer stem cells, tumor microenvironment

Mycoremediation of mercury and metal resistance strategies of a micromycete

Cristina L. Văcar[1,2], Karen Viacava[3], Adrien Mestrot[3],
Marcel Pârvu[2,4], and Dorina Podar[2,5✉]

[1] *Doctoral School of Integrative Biology, Babeş-Bolyai University, Cluj-Napoca, Romania;* [2] *Centre for Systems Biology, Biodiversity and Bioresources (3B), Babeş-Bolyai University, Cluj-Napoca, Romania;* [3] *Institute of Geography, University of Bern, Bern, Switzerland;* [4] *Department of Taxonomy and Ecology, Babeş-Bolyai University, Cluj-Napoca, Romania;* [5] *Department of Molecular Biology and Biotechnology, Babeş-Bolyai University, Cluj-Napoca, Romania*
✉*Corresponding author, E-mail: dorina.podar@ubbcluj.ro.*

Metal contaminants threaten environmental stability and human health, while their remediation is a challenging task. Mycoremediation, which employs fungi to mitigate metal toxicity, holds promise due to fungi's characteristics like significant biomass production, branched growth facilitating soil matrix penetration, and high surface area with cation binding properties. However, the progress of mycoremediation technologies for metal contaminants is hindered by a limited understanding of the underlying mechanisms. Terricolous micromycetes isolated from a mercury (Hg) contaminated environment, adapted to extreme metal toxicity, showed significant Hg removal efficacies (47-97%) and biosorption capacities (33.8-54.9 mg Hg g^{-1} dry weight) during 48 h exposure to 100 mg L^{-1} Hg^{2+} in aqueous solution. The highly resistant *Fusarium oxysporum* P2.7 isolate (GenBank ID: MT913528) was studied for its resistance strategies against toxic concentrations (mg L^{-1}) of Cu (250), Hg (10 and 100), and Zn (150) in liquid culture medium. Avoidance strategies against Cu and Zn stress were indicated by important proportions of these elements associated with extracellular fractions. Resistance strategies against Hg were, 14.55-47.57% extracellular immobilization, 30.4-48.93% intracellular accumulation, and 5.29-36.51% possible biovolatilization, depending on culture conditions. Removal efficacies were 6.84% for Cu, 90.67-93.73% and 81.53-83.09% for initial 10 and 100 mg L^{-1} Hg, respectively, and 4.67% for Zn. Biosorption capacities were (mg metal g^{-1} dry weight) 13.2 for Cu, 0.29-2.51 and 4.75-9.66 for 10 and 100 mg L^{-1} Hg, respectively, and 2.87 for Zn. A putative mercuric reductase protein sequence, from the genome of *F. oxysporum*, is likely the homologue for the well-described bacterial Hg^{2+}-reducing enzyme. Bioinformatic analyses suggested a possible early common origin of this enzyme for Cyanobacteria and Fungi phyla, and a distinct mechanism of Hg^{2+} reduction

compared to bacteria. Research of metal-resistant micromycetes holds implications for the development of remediation applications and contributes to understanding their role in metal speciation in the environment.

Keywords: biosorption, bioaccumulation, biovolatilization, *Fusarium oxysporum*, metals

Insights into Plant Colonization in Mercury-Contaminated Sites: Trace Metals and Rhizosphere Microbiome Interactions

Emanuela D. Tiodar[1,2], Cecilia M. Chiriac[3], Filip Pošćić[4], Cristina L. Văcar[1,2], Zoltán R. Balázs[1,2,7], Cristian Coman[5], David C. Weindorf[6], Manuela Banciu[2,7], Ute Krämer[8], Dorina Podar[2,7]

[1] Doctoral School of Integrative Biology, Babeş-Bolyai University, Cluj-Napoca, Romania; [2] Centre for Systems Biology, Biodiversity and Bioresources (3B), Babeş-Bolyai University, Cluj-Napoca, Romania; [3] Institute of Hydrobiology, Biology Centre CAS, České Budějovice, Czech Republic; [4] Freelance researcher, Tucson, USA; [5] NIRDBS, Institute of Biological Research, Cluj-Napoca, Romania; [6] School of Earth, Environment, and Sustainability, Georgia Southern University, Statesboro, GA, USA; [7] Department of Molecular Biology and Biotechnology, Babeş-Bolyai University, Cluj-Napoca, Romania; [8] Department of Molecular Genetics and Physiology of Plants, Ruhr University Bochum, 44801 Bochum, Germany

Mercury soil pollution is a great threat to ecosystem and human health due to its acute toxicity and biomagnification processes. At the site of a decommissioned chlor-alkali plant where Hg cathodes were used for more than 30 years of activity, we conducted a trace metals site assessment, a floristic survey of the pioneer native flora and determined the taxonomical and functional diversity of the microbial communities in the rhizosphere of the dominant plant species. The aim of the study was to explore the plant metal accumulation potential of local populations that would be of use for an *in situ* remediation strategy of the site. Presently, the median rhizosphere Hg concentration at the site was 962 mg kg^{-1}, and the highest concentrations of Hg accumulated in plant tissues were 10869 mg Hg kg^{-1} dry weight in roots and 1070 mg kg^{-1} in shoots, by the legume plant *Lotus tenuis*. *Diplotaxis muralis* was the most abundant plant at the site and the associated microbial communities from its rhizosphere did not exhibit an alpha diversity decrease with the soil Hg concentration gradient. The most abundant bacterial phyla were Pseudomonadata, Actinomycetota, and Acidobacteriota. Moreover, most rhizosphere communities tested positive for the presence of *merA* in the total soil DNA. For these latter communities, an inferration-based PICRUSt2 analysis revealed an abundance of ABC transporters. All in all, the five rhizosphere soil trace metals investigated in this study explained 35% of the total variance observed at the site for plant population distribution and plant metal accumulation profile, and Hg was the main community driver. Based on

the Hg accumulation pattern, *L. tenuis* and *D. muralis* are Hg indicator species of potential interest for future soil Hg phytomanagement approaches due to their abilities of immobilizing Hg at the root level.

Keywords: tolerance, phytoremediation, *Diplotaxis muralis*, *Lotus tenuis*, *mercuric reductase* (MerA)

An *in vivo* pilot study on the effects of a combined immunotherapy on murine melanoma

Marta-Szilvia Meszaros[1], Giorgiana-Gabriela Negrea[2],
Stefan Mihai Dragan[2], Vlad-Alexandru Toma[1,3], Emilia Licarete[1],
Laura Patras[1], Valentin Florian Rauca[1],
Manuela Banciu[1], Alina Sesarman[1]✉

[1] *Department of Molecular Biology and Biotechnology, Center of Systems Biology, Biodiversity and Bioresources, Faculty of Biology and Geology, "Babes-Bolyai" University, Cluj-Napoca, Romania;*
[2] *Doctoral School in Integrative Biology, Faculty of Biology and Geology, "Babes-Bolyai" University, Cluj-Napoca, Romania;* [3] *Department of Experimental Biology and Biochemistry, Institute of Biological Research, Branch of NIRDBS Bucharest, Cluj-Napoca, Romania*
✉**Corresponding author, E-mail: alina.sesarman@ubbcluj.ro**

Over the past two decades, immunotherapies have gained a major interest as treatments for many types of cancers, showing promising results. One type of cancer that has been shown to be responsive to such treatments is melanoma, one of the most aggressive skin cancers. Melanoma is known to be highly immunogenic due to the elevated tumor mutational burden, hence the effectiveness of immunotherapies based on immune checkpoint inhibitors, targeting specific proteins present in the tumor microenvironment. Nonetheless, the heterogeneity found in patients still causes diminished results, proving that further optimization of therapies is needed. To address this, combinations of various treatments are tested, while considering the desired immunomodulatory effect to improve results. This study aimed to test a combined immunotherapy based on anti-PD-L1 antibodies and curcumin-loaded extracellular vesicles, derived from stressed and peptide-pulsed dendritic cells. This immunotherapy strategy was based on past published results of the anti-PD-L1-based therapy, the immunomodulatory effect of curcumin, and the specific targeting of the tumor microenvironment with extracellular vesicles.

To test this combined immunotherapy, a pilot *in vivo* study was conducted on B16.F10 tumor-bearing C57BL/6 mice. Throughout the investigation, tumors were measured and the mice were weighed. After the treatment administration, tumors were collected, measured, and analyzed through a set of molecular methods such as western blotting, protein array, and gelatin zymography.

Our results show an overall reduction of the expression of cytokines involved in angiogenesis in the combined therapy group, compared to the anti-PD-L1 treatment group. Proteins involved in the inflammatory pathways or immune regulation

such as pNF-κB and iNOS also showed different expression patterns in the two treatment cohorts.

This combined immunotherapy presents potential that can be further improved through adjusting administration time points and dosages.

Keywords: melanoma, immunotherapy, inflammation

References:

Huang, A. C., & Zappasodi, R. (2022). A decade of checkpoint blockade immunotherapy in melanoma: understanding the molecular basis for immune sensitivity and resistance. *Nature immunology*, 23(5), 660-670.

Shakeri, F., & Boskabady, M. H. (2017). Anti-inflammatory, antioxidant, and immuno-modulatory effects of curcumin in ovalbumin-sensitized rat. *BioFactors*, 43(4), 567-576.

Negrea, G., Rauca, V. F., Meszaros, M. S., Patras, L., Luput, L., Licarete, E., Banciu, M. (2022). Active tumor-targeting nano-formulations containing simvastatin and doxorubicin inhibit melanoma growth and angiogenesis. *Frontiers in pharmacology* 5; 13:870347

Advancing the identification of novel direct gene targets of NODULE INCEPTION, a critical transcriptional regulator in legume-rhizobia symbiosis

Mihaela Gălean[1,2] ✉, Lisa Frances[2], Anais Delers[2], Fernanda de-Carvalho-Niebel[2]

[1]*Doctoral School of Integrative Biology, Departament of Molecular Biology and Biotechnology, Babeş-Bolyai University, 1 Kogalniceanu St., 400084 Cluj-Napoca, Romania; [2]Laboratoire des Interactions Plantes Microorganismes, CNRS-INRA, Castanet-Tolosan, France*
✉ *Corresponding author, E-mail: mihaela.galean@ubbcluj.ro.*

Plants form beneficial associations with microorganisms to enhance nutrient uptake essential for their growth. Legumes, particularly in nitrogen-depleted soils, establish symbiotic relationships with rhizobia, resulting in new root organs, called nodules. At this level, atmospheric nitrogen is converted by endosymbionts into ammonia, the latter being exchanged for plant-derived photosynthates. Nodule development involves intricate transcriptional reprogramming, orchestrated by major plant transcription factors, with one example being NIN (NODULE INCEPTION). While NIN Binding Site (NBS) *cis*-promoter motifs have been identified on NIN target promoters, further exploration is needed to understand their conservation among other potential NIN targets. Within this framework, the aim of the present study was to determine if two rhizobia-induced genes of *Medicago truncatula*, namely *MtSOKL* and *MtAnn1,* whose expression is regulated and dependent on NIN, could represent new direct targets of NIN. To this end, we combined *in silico cis*-motif search and transcription assays in *Nicotiana benthamiana* with mutated promoter *cis*-motifs, to identify and functionally validate motifs that would mediate NIN regulatory activity. Consequently, *in silico* analyses revealed several putative NIN binding sites (NBS) on promoters of the two genes (8 in the case of *MtAnn1*, and 6 for *MtSOKL*), consistent with the hypothesis that they may represent direct NIN targets. Furthermore, in the case of *pMtSOKL*, we identified a promising NBS, called NBS3, which when mutated, strongly affects the NIN activation of *pMtSOKL* transcription. This suggests that NBS3 represents a key *cis*-motif for NIN DNA transcriptional regulatory activity. Upcoming studies employing promoter deletion, gain-of-function assays, and DNA binding examination are warranted to consolidate the role of NBS3 in NIN-mediated transcriptional regulation.

Keywords: *MtAnn1, MtSOKL*, *Medicago truncatula*, NIN-binding site, NIN transcription factor, nodule development.

Challenges in molecular barcoding analyses – case study of *Austropotamobius bihariensis*

Andreea-Monika Lamoly[1,2]✉, David Livadariu[1,2], Andrei Ştefan[3],
Oana Popa[3], Elena Iorgu[3], Lucian Pârvulescu[1,2]

[1] Department of Biology-Chemistry, Faculty of Chemistry, Biology, Geography, West University of Timisoara, Timisoara, Romania; [2] Crayfish Research Centre, Institute for Advanced Environmental Research, West University of Timisoara, Oituz 4, Timisoara, Romania; [3] "Grigore Antipa" National Museum of Natural History, Bucharest 011341, Romania
✉ ***Corresponding author, E-mail: andreea.lamoly02@e-uvt.ro***

Austropotamobius bihariensis is a crayfish species discovered in Romania's Apuseni Mountains. Its origin is debated due to its phylogenetic link to *Austropotamobius torrentium* from Croatia's Dinaric Mountains. To hypothesize about *A. bihariensis's* origin, we focused on its ecological spread tendencies, whether cosmopolitan or endemic. This study aimed to create a time-calibrated phylogenetic tree for the three *Austropotamobius* species in Europe (*A. bihariensis, A. torrentium, A. pallipes*). By examining genetic variations of these species, we aimed to uncover evolutionary patterns and understand the factors behind their divergent distribution and ecological traits. The phylogenetic tree was built using mitochondrial cytochrome c oxidase subunit I (MT-CO1) gene sequences, obtained through sequencing for *A. bihariensis* and from GenBank for *A. torrentium* and *A. pallipes*. The tree was time-calibrated based on the divergence between the haplogroup from the Zeleni Vir Mountains, Croatia and *A. bihariensis*, an event from 15 million years ago. This analysis showed a reduced, spatially concentrated diversity for *A. bihariensis* and the Dinaric haplogroups, indicating endemism. Conversely, haplogroups from Central and South Europe and the Southern Balkans, as well as three haplogroups from *A. pallipes*, showed high haplotype diversity over a short period, suggesting cosmopolitan tendencies. In conclusion, this study supports the endemism of *A. bihariensis* and, on a larger scale, offers valuable insights for the conservation and management of *Austropotamobius* species.

Keywords: molecular phylogenetics, population genetics, endemictendencies, cosmopolitan tendencies

Drug resistance in bacterial and fungal diversity in smokers and non-smokers

Alexandra-Georgiana Hirişcău[1]✉, Cristina Mircea[2]

[1] Faculty of Biology and Geology, Babeş-Bolyai University, Cluj-Napoca, Romania;
[2] Department of Molecular Biology and Biotechnology, Faculty of Biology and Geology,
Babeş-Bolyai University, Cluj-Napoca, Romania
✉**Corresponding author, E-mail: hiriscauada@gmail.com**

The oral microbiome plays a crucial role in maintaining oral health, while oral dysbiosis is associated with numerous systemic diseases. Cigarette smoking is a notorious risk factor for a multitude of oral conditions like periodontal disease, tooth decay, and oral cancers, and exerts a significant influence on the oral microbiome. A profound understanding of the repercussions of smoking on the resident communities of oral bacteria and fungi is significant for elucidating the connection between smoking-induced oral conditions and their systemic implications. This study aims to investigate the changes in the oral microbiome caused by cigarette smoking and their correlation with individual dietary and oral hygiene habits. Moreover, the study shows that smoking affects the antidrug resistance in both bacteria and fungi. Ten participants, comprising five smokers with a minimum of one-year smoking history and five non-smokers, were recruited. Each subject self-collected oral samples using sterile cotton swabs, which were inoculated on LB and Czapek culture media to quantify bacteria and fungi. Morphologically distinct isolates were selected for DNA extraction, followed by the amplification of the 16S rRNA gene (for bacteria) and the ITS region (for fungi). The obtained PCR fragments were sequenced and used for species identification. Results revealed quantitative differences between the microbiome of smokers and non-smokers. Generally, the smokers presented higher bacterial and fungal colonies than the non-smokers. In addition, smoking was associated with an increase in the antibiotic resistance of oral bacteria against ampicillin and an increase in the antifungal resistance of oral fungi against naftifine hydrochloride. This paper emphasizes the impact of smoking on oral microorganisms, demonstrating quantitative changes between the two groups of subjects and its correlation with the lifestyle of each participant. Therefore, understanding the modifications found in this study may serve as a starting point for developing therapies that can reduce the effects of smoking on oral health and also for the elaboration of targeted treatment strategies.

Keywords: drug resistance, oral microbiome, cigarette smoking, ITS and 16S rRNA amplification, culture-based methods**.**

Cultivable microbial diversity associated with three Anuran species from Romania.

Naomi Bărbosu[1], Adorján Cristea[1]✉, Cristina Mircea[2],
Horia Leonard Banciu[2] and Alin David[1]

[1]Babeş-Bolyai University, Faculty of Biology and Geology, Departament of Taxonomy and Ecology, 5-7 Clinicilor Street, Cluj-Napoca, Romania; [2]Babeş-Bolyai University, Faculty of Biology and Geology, Departament of Molecular Biology and Biotechnology, 5-7 Clinicilor Street, Cluj-Napoca, Romania
✉**Corresponding author, E-mail: adorjan.cristea@ubbcluj.ro**

The skin microbiome of Anura plays an important role in maintaining host health through its capacity to protect against fungal pathogens and viruses. By culture-dependent methods it has been shown that bacterial strains belonging to *Pseudomonas* sp., and *Janthinobacterium* sp., are colonizing the amphibian skin and are involved in the protection against chytridiomycosis. The aim of this study was to investigate the cultivable diversity of bacterial and fungal species inhabiting the skin of three Anuran species. The selected species were *Bufo bufo*, *Bufotes viridis*, and *Bombina variegata*. For each species, swab samples were collected, suspended in sterile phosphate-buffered saline (PBS), mixed thoroughly, and serially diluted before inoculation onto tryptic soy agar (TSA), Reasoner's 2A agar (R2A), Actinomycete isolation agar (AIA), whereas Sabouraud medium was used for fungal isolation. The plates were incubated at 22°C. From pure cultures genomic DNA was extracted and the 16S rRNA gene for bacteria and ITS for fungi was amplified by PCR followed by Sanger sequencing. FASTA sequences were trimmed with MEGA 11 and strain identification was performed with BLASTn. *Pseudomonas* sp. was the most abundant bacteria across all three amphibian species. Notably, *B. bufo* additionally harbored *Janthinobacterium sp.*, *Flavobacterium* sp., and *Kocuria* sp., *B. viridis* displayed *Chryseobacterium* sp and *B. variegata* only *Pseudomonas* sp. Diverse skin-associated fungal strains were isolated including *Neocucurbitaria* and *Trichoderma* spp. from *B. bufo*; *Penicillium*, *Didymella*, and *Cadophora* spp. from *B. viridis* and *Hypocrea,* and *Beauveria* spp. from *B. variegata*, respectively. This study revealed the prevalence of *Pseudomonas* sp. among bacteria isolated from the skin of selected Anuran species and the apparent absence of skin-associated fungal pathogens. However future investigations are needed to understand the function of the microbiome in the studied amphibian species.

Keywords: *Anura***,** amphibian, culturable diversity, *Pseudomonas* sp.

Iron oxide nanoparticles: How does the size and coating affect the interaction with cancer cells?

Raul-Andrei Gurgu[1], Anett Janosi[1], Izabell Craciunescu[2], Alexandra Ciorîță[1,2]

[1]*Facultatea de Biologie si Geologie, Universitatea Babes-Bolyai, 5-7 Clinicilor Street, 400005, Cluj Napoca, Romania;* [2]*National Institute for Research and Development of Isotopic and Molecular Technologies, 67-103 Donat Str., 400293, Cluj-Napoca, Romania*

Nanotoxicology research is paramount to nanoparticles research as their types and applications continue to increase, especially in biomedicine. To better understand their effect on human cells, the nanotoxicity of iron oxide nanoparticles (IONPs) functionalized with polyethylene glycol (PEG), polyethylene glycol-silica oxide (PEGSiO2) and (3- Aminopropyl) triethoxysilane (APTES) were investigated. As consulted in the literature IONPs functionalization improves the cytotoxic effects compared to bare IONPs. This could also result in higher nanoparticle-uptake in cells. Investigating the *in vitro* effects of IONPs formulations for future use in experiments. The investigations were carried out on A549 (lung adenocarcinoma epithelial cells) and A375 (melanoma cells), using the MTT viability assay. The cells were cultured on supplemented culture media for 24 h in 96 well plates. The treatment was applied for 24 h as well, and the results were investigated spectrophotometrically. Ten different concentrations were tested. IONPs-PEG80 formulation showed significant cytotoxicity on A549 cells but not on A375 cells, while PEG80SiO2 had milder toxicity on A549 cells, and IONP-APTES had no cytotoxic effect on A375 cells. The results are all reported at 1 mg/mL nanoparticle concentration. IONPs-PEG80 has a toxic effect depending on the type of cell used, not having a toxic effect on A375s while being very toxic on A549, raising questions about the cellular factors that may be in play. PEG80SiO2 and APTES formulations have lower toxicity and thus may need to be loaded with a cytotoxic drug to achieve the same effects. All results are preliminary and further investigations are required.

Snapless wonders: Unravelling the molecular milestones behind the Venus flytrap's snap closure mechanism

Anda Iosip[1,2], Jörg Schultz[2], Ines Kreuzer[1], Rainer Hedrich[2]

[1]*Julius-von-Sachs Institute of Biosciences, University of Würzburg, Germany;*
[2]*Center for Computational and Theoretical Biology, University of Würzburg, Germany*

Within the plant kingdom, few species have evolved fast movement upon touch. One such exception is the charismatic Venus flytrap (*Dionaea muscipula*), a carnivorous plant which relies on a millisecond-range snap-trapping mechanism to catch its prey. The special tactile abilities are given by the trigger hairs, found on the trap surface, which upon bending elicit an action potential. In contrast to a functional Venus flytrap, which snaps upon the induction of two action potentials, the so-called 'ERROR' mutant – a cultivated variety of the Venus flytrap – is unable to snap its traps. To get a better understanding of the essential molecular milestones necessary for a successful trap closure, the transcriptome of the 'ERROR' phenotype was compared to the functional Venus flytrap phenotype before and after the application of mechanostimulation. The results show, for the first time, the importance of a special cell wall architecture that might confer the mechanical properties together with a certain geometry that assures a ready-to-snap configuration of the trap before stimulation. This might be crucial for a functional buckling system to amplify the speed of the trap closure, which is essential for a successful carnivorous lifestyle among green hunters.

New contributions to vegetation knowledge of Danube Delta

Oprea A.[1]✉, Sîrbu C.[2], Doroftei M.[3], Covaliov S.[3]

[1]*University "Alexandru Ioan Cuza", Botanic Garden "Anastasie Fătu", Iaşi;*
[2]*University of Life Sciences "Ion Ionescu de la Brad", Faculty of Agriculture, Iaşi;*
[3]*Institute of Research-Development „Delta Dunării", Tulcea*
✉**Corresponding author, E-mail: a_aoprea@yahoo.co.uk**

New investigations on the flora, vegetation and natural habitats of the Danube Delta (Romania) were recently carried out. Thus, more than 1200 vascular plants species were inventoried, phytocoenoses of 254 plant communities were recorded on the ground, and 32 Natura 2000 habitats were recorded, all of them mapped on a large scale. Among these, the following phyto- and coenotaxa were registered as novelties:

- a newly identified taxon for the vascular flora of Romania: *Paspalum distichum* subsp. *Paucispicatum; and*

- two new phytocoenotaxa for science are proposed here, namely: 1) Ass. *Periploco graecae-Alnetum glutinosae* ass. nova, and 2) Ass. *Cypero flavescenti-Paspaletum distichi* Horv. 1954 subass. *paspaletosum paucispicati* subass. nova.

The Natura 2000 habitats in the Danube Delta that include the new coenotaxa proposed above are: 91E0* Alluvial forests with *Alnus glutinosa* and *Fraxinus excelsior* (*Alno-Padion*, *Alnion incanae*, *Salicion albae*); 3160 Natural dystrophic lakes and ponds; 3270 Rivers with muddy banks, with vegetation of *Chenopodion rubri* p. p. and *Bidention* p. p.

Deciphering above-treeline vegetation greenness trends: Insights from the Carpathian Mountains

Pavel-Dan Turtureanu[1], Arthur Bayle[2], Mihai Puşcaş[1], Philippe Choler[2]

[1]*A. Borza Botanic Garden, Babeş-Bolyai University, Cluj-Napoca, Romania; *[2]*CNRS, Laboratoire d'Ecologie Alpine, LECA, Univ. Grenoble Alpes, Univ. Savoie Mont Blanc, Grenoble, France*

The long-term increase in vegetation greenness is a topic of considerable interest in ecology. This study aims at deciphering the spatial distribution patterns of greening and their relationships to land cover in the above-treeline ecosystems of the Carpathian Mountains, a range that has been understudied so far in greening studies. We calculated the greenness trends using Landsat imagery dating back to 1984 and employed a large training dataset for high-resolution land cover classification. The land cover types included screes, grasslands, low shrublands (mainly composed of Ericaceae and Juniperus communis), tall shrubs (composed of Pinus mugo) and woodlands dominated by Picea abies. Our analysis revealed widespread greening and high spatial variability associated with land cover types. Overall, the most pronounced greening signal was detected within Ericaceae-rich shrublands, with varying intensity observed across different mountain ranges and other land cover types. Our findings highlight that high-resolution distribution models of land cover types are pivotal to unravel the complexity of greening in mountains. In perspective, our research aims to integrate remote sensing imagery with dendroecology, with a specific focus on Pinus mugo (as part of the MUGO project) and Ericaceae species, to further elucidate the greening phenomenon in the Carpathian Mountains.

Acclimation ability, life history, and behavioral traits of an endemic copepod species from an Italian karst system

Agostina Tabilio Di Camillo[1,2✉], Diana Maria Paola Galassi[1],
Tiziana Di Lorenzo[2,3,4]

[1] Department of Life, Health and Environmental Sciences, University of L'Aquila, L'Aquila, Italy;
[2] Research Institute on Terrestrial Ecosystems of the National Research Council of Italy (IRET CNR), Florence, Italy; [3] "Emil Racovita" Institute of Speleology, Cluj-Napoca, Romania; [4] NBFC (National Biodiversity Future Center), Palermo, Italy
✉ Corresponding author, E-mail: agostina.tabiliodicamillo@iret.cnr.it.

Despite their prevalence in groundwater ecosystems, the functional ecology of groundwater-obligate copepods remains relatively understudied. In 2016, we embarked on a comprehensive investigation focusing on the life history and functional traits of *Moraria* sp., an endemic harpacticoid species inhabiting Antro del Corchia, a karst cave in the Apuan Alps (north-central Italy). We assessed the oxygen consumption rates of twenty adult females of *Moraria* sp. as a proxy of metabolic changes in a climate scenario with temperatures ranging from 8.0 °C (mean annual temperature of the Antro del Corchia cave) to 12.5 °C (maximum temperature of the cave according to climate change scenarios in 2100). In detail, we measured oxygen consumption after a 30-day acclimation period to varying temperatures to assess the species' ability to adjust its metabolic rates back to baseline levels. Our results highlighted the low metabolic activity of this species and its limited thermal adaptation ability, indicative of stenothermy. In particular, even minimal temperature variations (i.e., +1.5 °C) significantly influenced the metabolic rate of *Moraria* sp. over the long period, indicating its potential vulnerability to thermal fluctuations induced by global change. Furthermore, we assessed the life history and locomotion behavior of this species at its optimal temperature of 8.0 °C and compared them with its surface water counterpart *Bryocamptus zschokkei*. We found out that the low metabolic rates of *Moraria* sp. correlate with its longevity and low reproductive and locomotion rates, which seem to highly diverge from its epigean counterpart. These findings illuminate the ecological peculiarities of *Moraria* sp., enhancing our understanding of groundwater copepod ecology and highlighting the critical need for conservation strategies. This study emphasizes the importance of safeguarding subterranean biodiversity against the backdrop of global environmental change.

Insights into crustacean adaptations in the sulfidic mesothermal aquifer from Mangalia (Southern Dobrogea, Romania)

Maria Mirabela Pop[1,✉], Filip Paul Boancă[2], Alexandru Sonica[3], Vlad Alexandru Toma[4,5], Rozalia Magda Motoc[6], Tiziana Di Lorenzo[1,7], Radu Silaghi-Dumitrescu[3], Sanda Iepure[1,8]

[1] Emil Racoviţă" Institute of Speleology, Cluj-Napoca, Romania; [2] Doctoral school of Ecology and Evolution, Limnology Department, University of Vienna, Vienna, Austria; [3] Department of Chemistry and Chemical Engineering, Babes-Bolyai University, Cluj-Napoca, Romania; [4] Department of Molecular Biology and Biotechnology, Faculty of Biology and Geology, Babes-Bolyai University, Cluj-Napoca, Romania; [5] Department of Experimental Biology and Biochemistry, Institute of Biological Research, Branch of NIRDBS Bucharest, Cluj-Napoca, Romania; [6] National Museum of Natural History "Grigore Antipa", Bucharest, Romania; [7] Research Institute on Terrestrial Ecosystems of the National Research Council of Italy (IRET CNR), Florence, Italy; [8] Department of Taxonomy and Ecology, Babes-Bolyai University, Cluj-Napoca, Romania
✉ Corresponding author, E-mail: mariamirabelapop0@gmail.com.

Aquifers are crucial geological formations that store large quantities of groundwater and serve as vital habitats for diverse organisms like stygofauna, subterranean aquatic fauna. They also provide essential services such as water purification, biodegradation of pollutants, pathogen removal, and flood mitigation, highlighting their significance for both human well-being and biodiversity. In South-East Romania on the Black Sea coast, the presence of sulfide-rich overlapping aquifers hides an intriguing and complex biological community. The aquifers provide a high diversity of microhabitats for crustaceans (in their sulfidic vs. sulfide-free parts) and abundant food sources, enabling the coexistence of species with similar morphological and/or ecological adaptive traits. Here, the primary production is supplemented through chemosynthesis, supposedly supported by chemoautotrophic bacteria that derive their energy from chemical reactions with inorganic molecules. This study explores the most upper Sarmatian aquifer, which is accessible through the old hand-dug wells and the Movile Cave. These sites provide a suitable habitat for a diverse community of crustaceans, including cyclopoids, ostracods, harpacticoids, amphipods, and isopods, that face survival challenges due to environmental conditions. Apart from nutrient and energy limitations, darkness, oxygen scarcity, and geochemically variable conditions, that usually characterize groundwater ecosystems, sulfidic-rich groundwater poses additional pressure to these organisms, including elevated temperature (cca. 21 °C), and increased concentrations of H_2S, CH_4, NH_4, and other ions (e.g., heavy metals, arsenic). In this study, we will discuss some of the

adaptations that the crustaceans have developed to cope with these challenging extreme conditions. This includes the presence of symbiosis with sulfur-oxidizing filamentous bacteria of the genus *Thiothrix* in the case of some microcrustacean species and the epibiotic ciliates of the genus *Lagenophrys*. Such associations have been previously identified in ecosystems with similar conditions, highlighting the versatility of such associations in sulfidic groundwaters. Additionally, we will discuss the presence of respiratory pigments that can contribute to the efficient utilization of oxygen in this hypoxic environment. Sulfidic groundwater communities are recognized as an example of "life at extremes". Investigating this particular ecosystem will enhance our knowledge of life forms, establish life's limits, and help us understand the capacity of life to withstand and adapt to change.

Keywords: crustaceans, sulfidic aquifer, adaptations, symbiosis, respiratory pigments

Monitoring of groundwater fauna from Vârtop Cave (Apuseni Natural Park, Romania).

Alexandru Orest Sambor[1,✉], Bianca Şarcani[1], Aurel Perşoiu[2,3], Constantin Marin[4], Ana Isabel Camacho[5], Karina Paula Battes[1], Mirela Cîmpean[1], Alin Tudorache[4], Sanda Iepure[1,2]

[1] *Department of Taxonomy and Ecology, Faculty of Biology and Geology, Babeş-Bolyai University, Clinicilor 5-7, Cluj-Napoca, 400006, Romania;* [2] *"Emil Racoviţă" Institute of Speleology, Clinicilor 5, Cluj-Napoca, 400006, Romania;* [3] *Ştefan cel Mare University, Universităţii 13, Suceava, 720229, Romania;* [4] *Emil Racoviţă Institute of Speleology, Frumoasă 31, Bucharest, 010986, Romania;* [5] *Department of Biodiversity and Evolutive Biology, National Museum of Natural History, C/ José Gutiérrez Abascal 2, Madrid, 28006, Spain*
✉ *Corresponding author, E-mail: orestus745@gmail.com*

Ice caves host a distinctive type of subterranean ecosystems with year-round negative temperatures, spanning a wide range of latitudes and latitudes across the Northern Hemisphere. These caves offer habitats for both localy-adapted species and glacial relics that depend on the specific cold microclimate for their survival. This study explores the influence of environmental parameters on the subterranean fauna inhabiting Gheţarul de la Vârtop Cave, a small (300 m long) ice cave located in Romania's Apuseni Natural Park. The cave was selected for monitoring of groundwater fauna due to the presence of temporary ice formation near its entrance, persisting until spring, which could indicate the presence of cold-adapted fauna, as well. Our research aims to shed light on the relationship between temperature conditions within the cave and their effects on the subterranean fauna seasonal and spatial fluctuations. The monitoring has been performed between February 2022 until March 2023, from gours and percolating waters. Field measurements indicate a mean water temperature of 3.9°C (3.93°C for gour water and 3.92°C for percolation water). The lowest recorded temperature, 1.6°C, was observed at a percolation site near the entrance of the cave in early spring (April 2022). In contrast, the highest recorded temperature, 5.8°C, occurred at both gour and percolation sites in early summer (May and June, respectively). Our study indicates that the percolation water within the cave, along with its associated gours, contain diverse communities of aquatic invertebrates that shows a spatial distribution along the cave with slight seasonal fluctuations. These communities include nematodes, oligochaetes, and crustaceans, with the most prevalent groups belonging to the orders Harpacticoida and Bathynellacea (*Bathynella* cf. *motrensis* Serban, 1971). Additionally, Cyclopoida

(*Acanthocyclops reductus* Chappuis, 1925) and Oligocheta are also present, mostly found in the middle portion of the cave. Studying aquatic fauna in these caves with temporary ice formations can provide valuable insights into the understanding of the ecological dynamics of the subterranean fauna and further to establish the physiological mechanisms adaptation to low temperature.

Keywords: karst, stygofauna, percolating water, ice caves.

Morphological examination of green sea turtle (*Chelonia mydas*) hatchlings from original and relocated nests

Beatrix Takács✉, Csaba Kiss

Department of Zoology, Institute of Biology, Eszterházy Károly Catholic University, Eger, Hungary
✉**Corresponding author, E-mail: takacsbea02@gmail.com**

The protection of endangered marine species is essential nowadays due to global warming, sea level rise and unethical fishing. Green sea turtles (*Chelonia mydas*) are also suffering the consequences of anthropogenic effects. Relocation of nests is commonly used in conservation biology, and it occurs when the nests are too close to the tide line and there is a potential risk of flooding. Even if the parameters of the new nests are similar to the original, the morphological characteristics of the hatchlings can be affected during the process and by the environmental background variables. I dedicated three months to conducting comprehensive research on green sea turtle nest relocation effects in Northern Cyprus. I measured 380 individuals using a TRESNA 300 mm digital caliper from a total of 12 nests. In R statistical environment, the ANOSIM and NMDS methods showed significant differences in both morphological characteristics and environmental background variables between original and relocated hatchlings. Unfortunately, there are no other publications using the NMDS method for this species, which is why I think it is important to present my results. This research can provide information for future morphological studies and crucial insights into green sea turtle nest relocation. Additionally, it plays a pivotal role in raising awareness about the conservation of endangered species.

Keywords: *Chelonia mydas,* endangered, digital caliper, hatchling morphology

The reproduction and early development of *Mnemiopsis leidyi* (Ctenophora) in the Adriatic Sea

Krisztián Papp[1]✉, Tjaša Kogovšek[2]

[1]Department of Zoology, Institute of Biology, Eszterházy Károly Catholic University, Eger, Hungary;
[2]Center for Marine Research, Ruđer Bošković Institute, Rovinj, Croatia
✉***Corresponding author, E-mail:*** *kriszpapp02@gmail.com*

Mnemiopsis leidyi is the only species in the genus Mnemiopsis. They are successful generalists to the point where they were misidentified as three different species, whereas they simply adapted to their environment by changing their morphology. Presumably, these ctenophores reached the Adriatic Sea by ballast waters and effortlessly earned their spot on the world's 100 most invasive species list. With practically no natural predators and no commercial value, this species has a negative effect on the local fishermen in addition to being an active threat against diversity. In order to have a better grasp of why they are strong competitors, we studied their reproductive rate and their early ontogenesis.

Keywords: Ctenophora, invasive species, reproductive rate, early ontogenesis

Patterns of habitat use by the brown bear *Ursus arctos* in the Southern Carpathians revealed by occupancy modelling

Adelina Elena Petruţa[1⊠], Gabriele Retez[2]

¹Babeş-Bolyai University, Cluj-Napoca, România; ²WWF România
⊠**Corresponding author, E-mail: adelinapetruta511@gmail.com**

We live amid a global wave of anthropogenically driven biodiversity loss, especially targeting species from megafauna. Understanding the dynamics of large mammal species and their interaction with human activities is crucial for effective conservation efforts. Occupancy modeling provides an efficient framework for studying species distributions and habitat use. In this study, we employed a dynamic occupancy modeling approach to investigate the presence of brown bears *(Ursus arctos)* in the Ţarcu Mountains, located in the south-western region of Romania. The study area, encompassing the Natura 2000 site ROSCI0126, is characterized by diverse habitats, including forests, meadows, rocky areas and river systems supporting a rich assemblage of large mammals. We conducted systematic surveys using randomly selected transects covering a grid of 270 km². These transects were traversed monthly over two seasons from September 2022 to September 2023, recording signs of brown bear presence using GPS devices. Additionally, we extracted land cover data from the Pan-European land cover map of 2015 and assessed forest disturbance levels using the European forest disturbance map. Presence-absence data were analyzed at the grid cell level, with variables such as ruggedness and elevation also considered. Our analysis revealed insights into brown bear occupancy patterns, habitat preferences, and seasonal variations in detection probabilities. The results provide valuable information for conservation management strategies in the Ţarcu Mountains, emphasizing the importance of maintaining habitat connectivity and minimizing human-wildlife conflicts. This study underscores the utility of dynamic occupancy modeling coupled with spatial analysis techniques in informing biodiversity conservation efforts in complex landscapes.

Autum bird migration on Chituc Spit: the first ten years

Attila Marton[1,2]✉

[1] Evolutionary Ecology Group, Hungarian Department of Biology and Ecology, Babeș-Bolyai University, Cluj-Napoca, Romania; [2] Milvus Group Bird and Nature Protection Association, Târgu Mureș, Romania
✉ Corresponding author, E-mail: martonattila2010@gmail.com

Bird migration remains one of the main study topics of ornithology. Although the study of this phenomenon is experiencing a renaissance in part due to the technological advance in the field of telemetry, traditional study methods still have a strong contribution in less studied areas. Birds cross Europe on three main migratory flyways, Romania being located on the least studied route: the Eastern Flyway, used by birds from West Asia and North-East Europe. During each Autumn in the past ten years, Milvus Group organized a ringing camp on Chituc Spit, to study the migratory phenology of birds crossing Europe on this latitude. We marked 145,000 individuals belonging to 190 species in the past ten years, thus collecting data both about the migration of common species and the presence of species rarely observed in Romania. The most abundant species marked are the red-breasted flycatcher (*Ficedula parva*, 13.704 individuals), the blue tit (*Cyanistes caeruleus*, 13592 ind.), the robin (*Erithacus rubecula*, 13.245 ind.), and the sedge warbler (*Acrocephalus schoenobaenus*, 12.696 ind.). This long-term dataset contributes to the identification of migration phenology of some species, and the permits the long-term monitoring of migratory- and breeding population dynamics of the species crossing this study site.

Keywords: bird migration, migratory phenology, Easter Flyway

The hidden world of wasp galls: Insights from wild rose research

Zoltán László[1,3][✉], Constantin-Teodor Iordache[2], Bálint Szilágyi[1],
Borbála Macalik[1], Mátyás Biró[1], Marco Nicula[2], Dorina Podar[2,3,4]

[1]*Hungarian Department of Biology and Ecology, Faculty of Biology and Geology, Babeş-Bolyai University, Cluj-Napoca, Romania; [2]Department of Molecular Biology and Biotechnology, Faculty of Biology and Geology, Babeş-Bolyai University, Cluj-Napoca, Romania; [3] Centre 3B, Faculty of Biology and Geology, Babeş-Bolyai University, Cluj-Napoca, Romania; [4]Emil G. Racoviţă Institute, Babeş-Bolyai University, Cluj-Napoca, Romania*
[✉]***Corresponding author, E-mail: zoltan.laszlo@ubbcluj.ro.***

A wide range of organisms, including nematodes, arthropods, fungi, and bacteria, can produce characteristic growths on plants known as plant galls. These gall inducers force plants to develop new tissues and organs, which serve as food sources for the larvae of the inducers. Plant galls have long captivated ecologists and taxonomists, despite the fact that their formation mechanisms are still unknown. Since their discovery, the main objective of gall scholars has been to better understand the induction mechanisms. Advancements in genetic and molecular techniques now allow for a thorough investigation of the molecular mechanisms underlying gall formation. The different evolutionary origins of gall formation across the animal kingdom suggest different mechanisms in different groups, making it challenging to uncover these mechanisms. Although molecular techniques have advanced, finding appropriate plant and gall inducer models is still essential for this type of research.

Our research aimed to establish a sustainable laboratory ecosystem comprising wild roses (*Rosa* sp.) and gall-inducing insects, specifically rose gall wasps of the genus *Diplolepis*. We optimized controlled indoor conditions to facilitate plant growth. Following transplantation, the wild roses were subjected to exposure from gall inducers and underwent systematic monitoring. Our research has successfully established a new laboratory community to advance the study of gall formation mechanisms.

Keywords: plant gall induction, wild roses, mossy rose gall, plant vigor, *Diplolepis*

Interspecific interactions in water birds

Ana-Teodora Ştefan[1][✉], Alexandru Nicolae Stermin[1]

[1] *Babeş-Bolyai University, Faculty of Biology and Geology, Cluj-Napoca, Cluj, Romania*
[✉]**Corresponding author, E-mail: anastefan.2002@gmail.com.**

Analyzing the behavior of birds offers an insight into the conservation of biodiversity, a heavily discussed subject in the fields of ecology, as well as ornithology. Therefore, this study aims to explore the dynamic of interspecific interactions between water birds in the Afon Peţa portion of the Crişul Repede river in Bihor, Romania. We collected data over the course of 8 months, from October 2022 to May 2023, summing 51 field observations. While there have been changes related to season regarding the behavior of the studies species, no correlation between the number of species and interactions has been found in birds with a constant presence in the study area. The results obtained through this study will help broaden the knowledge about common aquatic bird species in the area, as well as the dynamic of behaviors over the course of three seasons.

Keywords: Crişul Repede river, interspecific behavior, water birds, aggression, cooperation.

Comparative phylogenetic analyses of phosphofructokinase and hexokinase evolution in several Neognathae avian species

Andreea Horghidan[1], Adorján Cristea[1✉], Alin David [1]

[1]*Department of Taxonomy and Ecology, Faculty of Biology and Geology, Babeş-Bolyai University, Cluj-Napoca, Romania*
✉**Corresponding author, E-mail: adorjan.cristea@ubbcluj.ro**

Evolutionary insights soar thanks to phylogenetic analyses, shedding light on the origins and diversification of many vertebrates, including birds. Birds possess unique metabolic features, with high circulating glucose levels compared to other animals of similar size. However, despite this fact, the evolution and diversity of the key enzymes involved in glucose catabolism among birds remains elusive. Through these analyses we aimed to examine, compare and phylogenetically investigate the evolution of phosphofructokinase (PFK) and hexokinase (HK) among Neognathae avian species. The amino acid (aa) sequences from 50 bird species were collected from NCBI Genome database. A total of 208 sequences for HK and 322 for PFK were analysed. Sequences were currated manually for isoformes and aligned by MAFFT. Maximum Likelihood (ML) phylogenetic trees were constructed using IQ-TREE with the automatic model selection, ultrafast bootstrap for 1000 replicates and SH-aLRT branch test. We identified two different enzymes annotated as hexokinase (HK) which formed a distinct clade compared to the second enzyme the HK-domain containing protein 1 (HKDC1). A clear segregation between the two enzyme groups was observed and supported by robust statistical backing (99% for HK, 97% for HKDC1). In the case of PFK, the platelet-derived aa sequences are considerably more heterogeneous, and their clustering was not accurate as the statistical support was low. The trees reconstructed from the PFK aa sequences from muscle and liver, revealed that a clear cluster is formed by the Galloanseres (*Galliformes* and *Anseriformes)* with strong support (100% in both cases). Another cluster is formed by *Passeriformes* (95-99%) and between these two clusters, there is a highly diverse grouping of other avian members like *Strigiformes*, *Accipitriformes*, *Pelecaniformes* and *Falconiformes* among others. These findings indicate the presence of at least two classes of HK in birds, and a tissue-specific distribution of PFK. Moreover, it strongly supports the genome-scale family tree of modern birds.

Keywords: hexokinase, phosphofructokinase, genome comparison, sequence analysis, phylogenetic tree.

Immune cell concentrations and cancer mortality risk in mammals

Orsolya Vincze[1,2], Csongor I. Vágási[3], Péter László Pap[3], Ágnes Szőcs[3], Nándor Erős[1,3 ✉]

[1]Wetland Ecology Research Group, HUN-REN Centre for Ecological Research, Institute of Aquatic Ecology, Debrecen, Hungary; [2]ImmunoConcEpT, CNRS UMR 5164, University of Bordeaux, Bordeaux, France; [3]Evolutionary Ecology Group, Hungarian Department of Biology and Ecology, Babeş-Bolyai University, Cluj-Napoca, Romania
✉Corresponding author, E-mail: erosnandi@gmail.com

One of the current challenges in evolutionary biology is to answer why species differ in the incidence of cancer mortality. Some species appear to be resistant to tumours, while others are more susceptible to die from tumours. According to the immune surveillance hypothesis, the immune system plays a crucial role in shaping this variation. Moreover, it posits that cancer might have been a primary selective factor in the evolution of the immune system as immune cells prevent the uncontrolled cell proliferation in tumours. This contrasts with the immunopathology hypothesis, stating that elimination of intruding pathogens and parasites by the immune system comes at a cost, as chronically activated innate immunity contributes to the formation of tumours. However, these hypotheses have never been tested by cross-species comparisons. To this end, we estimated age-controlled cancer mortality risk (immunopathology hypothesis) for 249 mammalian species and we calculated a species-specific parameter expressing inherent cancer resistance in function of body mass and longevity (immune surveillance hypothesis) and using data provided by zoos. The association of both parameters with total and specific white blood cell concentrations was analysed using phylogenetic regressions. Our results indicate that cancer is more likely to be detected in species with low monocyte and neutrophil concentrations but high eosinophil concentrations. Cancer mortality risk is unrelated to both total or specific white blood cell concentrations. Inherent cancer resistance increases with higher monocyte and neutrophil concentrations. The results suggest that certain white blood cell types might play important roles in cancer protection and evolution might have shaped their abundance in parallel with the augmenting risk of tumours with the evolution of large body sizes and extended longevities.

House sparrows on time-restricted diet: effects on body condition, blood glucose and ketone levels

Attila Marton[1✉], Zonga Bíró[1], Attila Fülöp[1], Roland Kaizer[1], Gabriella Jákó[1], Andrea Paula Pál[1], Péter L. Pap[1], Csongor I. Vágási[1]

[1] Evolutionary Ecology Group, Hungarian Department of Biology and Ecology, Babeş-Bolyai University, Cluj-Napoca, Romania
✉**Corresponding author, E-mail:** *martonattila2010@gmail.com*

Time-restricted feeding is a dietary regimen in which access to food is limited by time and it is followed by a prolonged period of fasting. Previous studies have shown that time-restricted feeding has beneficial effects on various physiological parameters, it can postpone ageing and it can reduce the risk of pathologies linked to old age. However, like most dietary restriction studies conducted so far, the effects of time-restricted feeding were tested only on laboratory model organisms artificially selected and often inbreed, while its beneficial effects are yet to be tested on wild-living organism. We conducted an experiment in which house sparrows (*Passer domesticus*) were subjected to a time-restricted feeding regimen of 8 hr/day (i.e., 16 hr of fasting/day), while control birds had *ad libitum* access to food throughout the day. We sampled the birds prior to the treatment and 50 and 120 days after starting the treatment, and collected data regarding their body condition, body temperature, blood glucose and ketone levels. Elevated ketone levels in the experimental group show that the treatment has its proposed effects (i.e., being higher in the food-restricted group), however, we found no differences between the groups regarding body condition, body temperature and blood glucose levels. Future laboratory analyses will test if time-restricted feeding managed to alleviate telomere attrition rates and oxidative stress in experimental birds, compared to controls.

Keywords: time-restricted feeding, fasting, glucose, ketone

Redescription of the larva of *Eurythyrea aurata* (Pallas, 1776) using microphotography and SEM technics

Adrian Ruicănescu[1✉], Maximilian Teodorescu[2], Cristian Sitar[3], Lucian Barbu-Tudoran[4]

[1]Naţional Institute of Research and Development for Biological Sciences, branch of Cluj-Napoca, Romania; [2]National Institute for Laser, Plasma and Radiation Physics, Măgurele, Romania; [3]Babeş Bolyai University of Cluj-Napoca, Museum of Zoology, Romania; [4]Babeş Bolyai University of Cluj-Napoca, Faculty of Biology, Romania
✉***Corresponding author, E-mail: adrian.ruicanescu@icbcluj.ro***

The larval stage of *Eurythyrea aurata* was initially described by M. G. Volkovitsh in 1975, documented in the Russian language, primarily for comparative purposes vis-à-vis the larval form of *E. quercus*. This scholarly endeavor was supplemented with meticulously crafted illustrations of exemplary quality.

A comprehensive redescription of the mature larva of *Eurythyrea aurata* is presented herein, employing microphotography and scanning electron microscopy (SEM) images as demonstrative exemples. Furthermore, endeavors were made to establish correlations between these morphological attributes and the larval biology.

3D in vitro model development to mimick DOX-chemoresistant melanoma microenvironment

Giorgiana Gabriela Negrea[1]✉, Szilvia Meszaros[1], Stefan Drăgan[2],
Vlad-Alexandru Toma[2,3], Bogdan-Răzvan Dume[1], Valentin-Florian Rauca[2],
Laura Pătraş[2], Emilia Licărete[2], Manuela Banciu[2], Alina Sesărman[2]

[1]Doctoral School in Integrative Biology, Faculty of Biology and Geology, Babes-Bolyai University, Cluj-Napoca, Romania; [2]Department of Molecular Biology and Biotechnology, Center of Systems Biology, Biodiversity and Bioresources, Faculty of Biology and Geology, Babes-Bolyai University, Cluj-Napoca, Romania; [3]Department of Experimental Biology and Biochemistry, Institute of Biological Research, Branch of NIRDBS Bucharest, Cluj-Napoca, Romania
✉*Corresponding author, E-mail:* **giorgiana.negrea@ubbcluj.ro**

Advances in immunological oncology emphasize tumor microenvironment (TME) as the primary source of drug resistance, proving the importance of 3D tumor models, which better reflect the TME, and reduce animal experimentation. Our objective was to develop a 3D-spheroid model containing B16.F10 murine melanoma cells, macrophages, endothelial cells, and fibroblasts to simulate the chemoresistant TME. We aimed to validate this model using doxorubicin (DOX), a frequently used chemotherapy drug; notably, patients with melanoma typically do not respond to DOX, which is precisely why it was selected in our investigation. To create the spheroids, B16.F10 cells were seeded in 1% commercial extracellular matrix, along with 2H11 endothelial cells, primary fibroblasts and macrophages at a ratio of 1:1:1:4 ratio, in ultra-low attachment plates. The viability of cells within spheroids was assessed by measuring acid phosphatase activity. DOX at concentration corresponding to IC30 was applied to induce DOX-chemoresitance in spheroids. The emergence of chemoresistance was assessed by various markers, such as of apoptotic proteins: Bid, Bax (western blot), of oxidative stress: total antioxidant capacity (TAC) and catalase activity (measured *via* spectrophotometry), malondialdehyde levels (HPLC technique) and of metastatic potential: matrix metalloproteinase activity (*via* zymography). Our model showed similar levels of oxidative stress markers, such as MDA, TAC and catalase post-DOX treatment compared to control group. The activity of matrix metalloproteinase-9 significantly increased in DOX-treated group, while similar expression degree was observed in the case of apoptotic proteins Bid and Bad between groups. Therefore, as an overall view, our model in which we incorporated a variety of cell types from TME showed some traits of DOX-chemoresistance demonstrated by higher invasion capabilities compared to control and similar oxidative stress levels.

This model serves as a valuable tool for investigation of TME induced drug resistance.

Keywords: 3D model; fibroblasts; endothelial cells; chemoresistance.

Ancient biomolecules reveal the past of premodern individuals from southeastern Romania

Diana Ilie[1✉], Ioana Drăghici[1,2]

[1]Faculty of Biology and Geology, Babeş-Bolyai University, Cluj-Napoca, Romania; [2]Interdisciplinary Research Institute on Bio-Nano-Sciences, Babeş-Bolyai University, Cluj-Napoca, Romania
✉**Corresponding author, E-mail: diana.ilie1@stud.ubbcluj.ro**

Ancient DNA is a valuable repository of information that enables scientists to reveal the past of different populations or individuals. Oftentimes, its study is complemented by those based on isotopes, providing further insights into the lifestyles of those analysed. This multidisciplinary approach can be of great help, especially when the lack of funerary inventory and historical context limits the classic archaeological analyses. The aim of this research is to determine the geographical origin and dietary habits of individuals discovered in a necropolis located near Mireasa village (Constanţa, Romania), using ancient mitochondrial DNA, stable and radioactive isotope analyses. The methods followed in this study consisted in the extraction of genomic DNA from tooth samples, PCR amplification of the hypervariable regions of the human mitogenome, Sanger sequencing and haplogroup assignments, followed by computational analyses intended to discover the biogeographical origin of the subjects. The major components of the diet and the sample dating were subsequently determined based on the analysis of carbon and nitrogen isotopes. The results revealed the presence of both Asiatic and European mitochondrial DNA haplogroups within the population and a diet based possibly on a combination of plants and marine food. Regarding the time period of their existence, the resulting data indicated the individuals lived in the premodern era. These results complement the little information known so far about the populations of Dobruja in the 17th century, highlighting how dynamic the human migrations and interactions were in that region at that time.

Keywords: ancient mitochondrial DNA, isotope analysis, Dobruja.

Comparative analysis of the *in vitro* effects of resveratrol and genistein on non-small cell lung cancer (NSCLC) cell line A549

Andrada Ioviță[1]✉, Cristina Ştirbu[2], Ekaterina Isachesku[1], Lajos Raduly[1], Oana Zănoagă[1], Andreea Nuțu[1], Ioana Berindan-Neagoe[1], Daniel Cruceriu[3,4]

[1]*Research Center for Functional Genomics, Biomedicine and Translational Medicine, UMFIH, Cluj-Napoca, Romania;* [2]*Medical Military Institute, UMFCD, Bucureşti, Romania;* [3]*Department of Molecular Biology and Biotechnology, Babes-Bolyai University, Cluj-Napoca, Romania;* [4]*Department of Genetics, Genomics and Experimental Pathology, The Oncology Institute "Prof. Dr. Ion Chiricuta", Cluj-Napoca, Romania.*
✉**Corresponding author, E-mail:** *andrada.iovita@gmail.com*

Non-small cell lung cancer (NSCLC) is the leading cause of cancer mortality in men and the second cause of mortality in women. Exploring treatments is imperative for patient survival. We investigated how resveratrol/genistein affects a NSCLC cell line as a treatment option. The NSCLC cell line chosen was A549. To evaluate the resveratrol/genistein cytotoxic effects, we employed the MTT assay. We performed both an apoptosis assay and a cell cycle analysis to assess the treatments' ability to induce cell death or cell cycle arrest, using the Nexcelom's Celigo. The clonogenic assay was performed and scanned with the same Nexcelom's Celigo, while the scratch assay was used to investigate whether the treatments have a cell migration inhibitory effect. IC50s of 169,6 µM for resveratrol and 112,6 µM for genistein were obtained. Both compounds induced cell death by apoptosis in the A549 cell line. Resveratrol exhibited more promising effects than genistein– 15% of apoptotic cells compared to 12,5%, when cells were treated with the IC25 concentrations. Resveratrol-treated cells also exhibited a higher rate of cell cycle redistribution from G_2/M phase to G_0/G_1 compared to genistein-treated cells: 55% for resveratrol compared to 45% for genistein. The colony formation ability of the resveratrol-treated category was statistically the same as in the genistein-treated category: <300 colony count in untreated cells to 150 colony count for resveratrol and <300 to 140 colony count for genistein. Genistein seemed to show no effect on the migration rate of A549 cells; in this case, resveratrol exhibited a reduction of cell migration area by 35,15 % after 48h of treatment. This study underscores the potential of resveratrol as a promising alternative to conventional chemotherapy agents for NSCLC.

Dopaminergic striatal system lesioned with MPTP: Michaelis-Menten profile on oxidative stress and validation of kinetic data in mice.

A.R. Jurca[1], C.A. Moldoveanu[1,2], S. Drăgan[1], V.A. Toma[1,2]

[1]*Department of Molecular Biology and Biotechnology, Faculty of Biology and Geology, Babes-Bolyai University, Cluj-Napoca, Romania;* [2]*Institute of Biological Research, Department of Biochemistry and Experimental Biology, Cluj-Napoca, 400015, Romania, Cluj-Napoca, Romania*
✉*Corresponding author, Email: vlad.toma@ubbcluj.ro*

This study explores how exogenous antioxidants affect endogenous peroxidase activity. Using both in vitro and in vivo approaches, we simulated cellular conditions in a spectrophotometer cuvette with a citrate-phosphate buffer, hydrogen peroxide, and o-dianisidine, initiating the reaction with peroxidase (**EC 1.11.1.7**). Initial kinetics studies revealed enhanced enzyme affinity at 40 µM Fe^{2+}. Exposure to these conditions for 10 minutes increased peroxidase activity, with a 5-minute interaction with 40 µM Fe^{2+} notably boosting enzyme affinity. Similar effects were observed with Fe^{3+}. Free dopamine (DA 100 nM) decreased peroxidase activity, while ascorbate's effects varied based on concentration and iron redox state. Moving to *in vivo* analysis, we induced a Parkinson's disease model in male CD21 mice using MPTP, confirming pathology through elevated α-synuclein and decreased dopamine levels. The Turnbull staining correlated focal brain ferroptosis and peroxidase activity, illustrating dopamine's role in the Haber-Weiss reaction. Dopamine acted as a noncompetitive peroxidase inhibitor, decreasing K_{MM} and V_{max}. *In vivo*, peroxidase activity decreased with dopamine variations.

In summary, our study highlights complex interactions between exogenous antioxidants, endogenous enzymes, and dopamine. These findings offer insights into potential therapeutic strategies for managing oxidative damage in Parkinson's disease.

Enhancing melanoma immune status: Utilizing extracellular vesicles loaded with curcumin in 3D models

Stefan Mihai Drăgan[2]✉, Marta-Szilvia Meszaros[1], Giorgiana-Gabriela Negrea[2],
Vlad-Alexandru Toma[1,3], Emilia Licărete[1]; Laura Pătraş[1],
Valentin Florian Rauca[1], Manuela Banciu[1]; Alina Sesărman[1]

[1] Department of Molecular Biology and Biotechnology, Center of Systems Biology, Biodiversity and Bioresources, Faculty of Biology and Geology, "Babes-Bolyai" University, Cluj-Napoca, Romania; [2] Doctoral School in Integrative Biology, Faculty of Biology and Geology, "Babes-Bolyai" University, Cluj-Napoca, Romania; [3] Department of Experimental Biology and Biochemistry, Institute of Biological Research, Branch of NIRDBS Bucharest, Cluj-Napoca, Romania
✉*Corresponding author, E-mail: stefan.dragan@ubbcluj.ro*

Immune checkpoint inhibitors (anti-PD-1/PD-L1antibodies and CTLA-4) have revolutionized cancer therapy. However, advanced melanoma has often been associated with immunotherapy resistance. To improve immunotherapy efficiency in melanoma, we aimed to develop an adjuvant immunomodulatory approach based on using extracellular vesicles derived from activated dendritic cells, loaded with curcumin and delivered into a three-dimensional model for melanoma, to mimic the *in vivo* immune status. For this, we cultured murine melanoma B16.F10, dendritic cells 2.4 and CD8+ lymphocytes in a ratio of 1:1:5, in low-adherent plates to create spheroids, that were exposed to the curcumin-loaded extracellular vesicles purified from dendritic cells activated with CpG and pulsed with TRP-2 peptide. Spheroids were characterized based on size, morphology and presence of dendritic cells and lymphocytes, using histochemical and immunofluorescence techniques. Moreover, the effects of 48h treatment of free curcumin compared to extravesicular curcumin on the viability of spheroids was determined using acid phosphatase assay, and the differences in curcumin uptake were assessed after 2h of incubation of spheroids with the two therapies tested.

Our results showed that the treatment with EVs loaded with curcumin has a higher efficiency compared to the free administered curcumin with an IC_{50} of 23 µM compared to 77 µM, inhibiting the cell viability by two-fold (p<0.001), compromising the spheroid integrity and it's tumoral landscape. When compared to the free form, the loaded curcumin had a significant increase in uptake in the three-dimensional model (p=0.0144), which may account for the effect. In

summary, this innovative formulation of extracellular vesicles containing curcumin may serve as a viable immunomodulatory therapy for concurrent administration with established immune checkpoint inhibitors, potentially enhancing their efficacy.

Expression of cytochrome P450 (CYP2A13) fused to MBP and SKIK

Sebastian Florin Oana[1], Oana-Raluca Koblicska[2], Iulia Lupan[1,2]

[1]*Babeş-Bolyai University, Faculty of Biology and Geology, Department of Molecular Biology and Biotechnology, Cluj-Napoca, Romania; [2]Institute for Interdisciplinary Research in Bio-Nano-Sciences, Molecular Biology Center, Babeş Bolyai-University, Cluj-Napoca, Romania*

The production of soluble recombinant proteins can often be challenging and require significant additional resources. Recombinant DNA technology techniques (fusion with solubilization tags, co-expression with protein chaperon) and modification of culture conditions (lowering temperature, changing inducer concentration, adding cofactors) are most commonly used to optimize expression of recombinant proteins in soluble form. Maltose binding protein (MBP) is frequently used to increase the solubility of recombinant proteins expressed in bacterial cells such as *Escherichia coli*. Meanwhile, human cytochrome P450 2A13 (CYP2A13) is an enzyme involved in the metabolism of some tobacco compounds, resulting in reactive metabolites with a carcinogenic effect. Recombinant CYP2A13 is expressed insoluble in *E. coli* cells, making its study challenging. The aim of this study was to illustrate and compare the efficiency of various methods (fusion with MBP and SKIK, lowering culture temperature) in producing a soluble CYP2A13 protein in *E. coli*. In this work, the CYP2A13 gene was fused separately at the N-terminus with MBP and SKIK tag, and with His6 affinity tag at the C-terminus by cloning them into the pET28a expression vector. The recombinant proteins (MBP-P450-His6 and SKIK-P450-His6) were expressed in *E. coli* BL21(DE3) cells. Analysis of recombinant gene expression was performed by denaturing polyacrylamide gel electrophoresis. Thus, it was found that both recombinant proteins are overexpressed, but a large part is soluble only when it is fused with MBP. SoluProt tool was also used for predicting the soluble expression by using the protein sequences of CYP2A13, MBP and of the recombinant proteins. In conclusion, recombinant cytochrome P450 2A13 protein can be expressed in soluble form by fusion with MBP at the N-terminus without other modifications that are commonly used to solubilize recombinant proteins.

Keywords: MBP, His6, SKIK, *E. coli*, CYP2A13.

Halloysite and Aerosil: The impact on melanoma cell cultures

Andrei Violet[1✉], Alexandra Ciorîță[1,2], Anca-Daniela Stoica[1,2], Zina Vuluga[3], Ioan Turcu[2]

[1]Facultatea de Biologie si Geologie, Universitatea Babes-Bolyai, 5-7 Clinicilor Street, 400005, Cluj Napoca, Romania; [2]National Institute for Research and Development of Isotopic and Molecular Technologies, 67-103 Donat Str., 400293, Cluj-Napoca, Romania; [3]National Institute for R&D in Chemistry and Petrochemistry, 202 Spl. Independentei 06002, Bucharest, Romania
✉**Corresponding author, E-mail andrei.violet@stud.ubbcluj.ro**

Halloysite and Aerosil are two types of Si-based nanoparticles and are usually used as precursors for bio-polymer nanocomposites. For their in vitro cytotoxic effects, the nanoparticles were left to interact for 24 hours with cancerous cells (A375 skin melanoma). The viability and membrane integrity were assayed through biochemical methods and the morphology was determined by light microscopy. Based on these results, the nanoparticles with higher biodisponibility (Halloysite) were functionalized with keratin extracted from chicken feathers. Two formulations were obtained (A and B) and tested again on the same cell line. The results showed that Halloysite has a medium cytotoxic effect at 195.34 µg/mL, while the IC50 for formulation A is 58.91 µg/mL, and 14.4 µg/mL for formulation B respectively. This indicates that a lower dose of nanoparticles is requested to induce cytotoxic effects in the A375 cell line. This could be associated with a higher nanoparticle uptake, however, further investigations are required to demonstrate this supposition.

Keywords: Halloysite, Aerosil, chicken-feathers keratin, skin melanoma

Halloysite vs. fibroblasts: Is keratin a good functionalising agent?

Andreea Ureche[1✉], Alexandra Ciorîţă[1,2], Anca-Daniela Stoica[1,2],
Zina Vuluga[3], Ioan Turcu[2]

[1]Faculty of Biology and Geology, Babes-Bolyai University, 5-7 Clinicilor Street, 400005, Cluj Napoca, Romania; [2]National Institute for Research and Development of Isotopic and Molecular Technologies, 67-103 Donat Str., 400293, Cluj-Napoca, Romania; [3]National Institute for R&D in Chemistry and Petrochemistry, 202 Spl. Independentei 06002, Bucharest, Romania
✉*Corresponding author, E-mail: andreea.ureche@stud.ubbcluj.ro*

One kind of silicon-based nanoparticle used as a precursor for bio-polymer nanocomposites is called Halloysite. These nanoparticles were incubated for 24 hours on normal human fibroblast (BJ) cell lines in order to evaluate their in vitro cytotoxic effects. The nanoparticles were functionalized with keratin derived from chicken feathers and retested on the same cell lines following an assessment of cell viability and membrane integrity. Two formulations were produced as a result: A and B. The results showed that at 173.07 µg/mL, halloysite had a medium level of cytotoxicity. For formulation A, the IC50 values were 166.81 µg/mL, while for formulation B, they were 103.18 µg/mL. The results imply that, probably as a consequence of higher nanoparticle uptake from the organic functionalization, lower doses of the functionalized nanoparticles are required to impact BJ cell lines. Additional research is required to validate this hypothesis.

Keywords: Halloysite, chicken-feathers keratin, fibroblasts

In vitro evaluation of oxidative stress induced by halloysite nanotubes in human lung cells line A549

Larisa-Marta Cighi[1], Maria Drejoi[1], Paula Ghiorghiasa[1], Alexandra Ciorîță[1,2], Zina Vuluga[3], Ioan Turcu[1], Anca Daniela Stoica[1,2]✉

[1] Babes-Bolyai University, Faculty of Biology and Geology, Clinicilor 5-7, 400006, Cluj-Napoca, Romania; [2] National Institute for Research and Development of Isotopic and Molecular Technologies, 67-103 Donat, 400293 Cluj-Napoca, Romania; [3]National Institute for Research and Development in Chemistry and Petrochemictry, 202 Splaiul Independenței, 060021, Bucharest, Romania
✉**Corresponding author**: Anca D. Stoica , anca.stoica@ubbcluj.ro

Halloysite nanotubes (NP) have been increasingly used in many industrial and biomedical fields. Therefore, assessing the risks and consequences of halloysite nanotubes exposure is crucial for improving human safety measures. In this study, we investegated the possible cytotoxic effects. 48,29 µl NP were left to interact for 24 hours with human lung adenocarcinoma A549 cell line. The morphology was investigated through light microscopy, while the stress oxidative was performed using two strategies: the enzymatic (CAT, SOD) determinations and the non-enzymatic pathways regarding the concentrations of TAC, TOS and oxidative stress index estimation. Therefore, the results showed that CAT activities decreased, presenting significant changes, and SOD activities increase. There were no significant changes in oxidative stress index level compared with control. A549 cells were resistant and did not present any particular changes in the oxidative status after exposure to NPs. This study demonstrates that nanoparticles do not induce significant toxic effects.

Keywords: halloysite nanotubes, oxidative stress, cytotoxicity, A549 cells.

Investigating the phytoremediation potential of an indicator plant species in mercury-contaminated soils

Maria-Anastasia Abrudan[1], Csaba Timár[1], Mihaela Gălean[1,2], Dorina Podar[1,✉]

[1] Department of Molecular Biology and Biotechnology and Centre for Systems Biology, Biodiversity and Bioresources (3B), Faculty of Biology and Geology, Babeş-Bolyai University, 1 Kogălniceanu St., 400084 Cluj-Napoca, Romania; [2] Doctoral School of Integrative Biology, Babeş-Bolyai University, 1 Kogălniceanu St., 400084 Cluj-Napoca, Romania
✉ *Corresponding author, E-mail: dorina.podar@ubbcluj.ro*

Mercury (Hg) contamination represents a significant hazard to both ecosystems and human health, given its elevated toxicity, current widespread presence in soils, and tendency to biomagnify within the food chain. Phytoremediation, an eco-friendly technology that makes use of plants and of microorganisms to reclaim environmental pollutants, has been shown promising in removing heavy-metals from soils. In this context, the present lab-scale experiment aimed to assess *Diplotaxis muralis* plants' resistance to various Hg concentrations, along with different bacterial and fungal inoculation treatments, for their potential phytoremediation usage. Plants were grown for 8 weeks in soils either artificially or naturally contaminated with Hg, with microorganism inoculation performed at 2 and 6 weeks using a non-pathogenic bacterium (*Pseudomonas chlororaphis)*, a fungus (*Sarocladium kiliense),* or their consortium. The concentrations of Hg in soil and plant samples were analyzed via ICP-OES (Inductively Coupled Plasma – Optical Emission Spectrometry). concentrations of chlorophyll, carotenoids, and ROS-scavenging enzymes, as well as enzyme activity, were determined using UV-VIS spectroscopy. Plants cultivated in artificially contaminated soils (22 ppm and 55 ppm $HgCl_2$, respectively) exhibited proportionally higher biomass compared to control plants. Upon replicating the experiment using naturally contaminated soil (with concentrations of 285 ppm and 759 ppm Hg), plant growth persisted but was reduced compared to the control group, obviously due to the particularly high Hg concentrations. These findings may suggest a notable Hg resistance of this indicator *Brassicaceae* plant species. Further, there was a significant reduction in both chlorophyll and carotenoid concentrations with increasing soil Hg levels, effect partially alleviated by the fungal inoculation. The activities of catalase (CAT), ascorbate peroxidase (APX), and glutathione reductase (GR) exhibited a decline in the presence of microorganisms for plants cultivated in Hg-contaminated soils compared to the control group, indicating potential

mechanisms aiding in the mitigation of Hg toxicity. Taken together, these outcomes indicate that *Diplotaxis muralis* inoculated with the aforementioned microorganisms may be used in phytoremediation to reduce soil Hg concentrations.

Keywords: mercury resistance, microorganisms, heavy-metals, phytoremediation, antioxidant enzymes.

Macrophage/neutrophil dialogue in the presence of TNF-α affects the endothelium

Sergiu-Marian Vatamanu[1]✉, Monica Ţucureanu[2], Andreea Mihăilă[2], Elena Butoi[2]

[1] *Faculty of Biology and Geology, University Babeş-Bolyai;* [2] *Medical and Pharmaceutical Bionanotechnologies Laboratory, Institute of Cellular Biology and Pathology Nicolae Simionescu, Bucharest, Romania*
✉ ***Corresponding author***, *E-mail: sorinmarian2002@yahoo.com*

The innate inflammatory response, controlled by immune cells and with effects on the vasculature, is a fundamental process involved in various pathologies, including cardiovascular diseases and inflammatory disorders. Macrophages, particularly the M1 subtype, play critical roles in the initiation and maintenance of inflammation. Of particular interest is the impact of TNF-α concentration on the dialogue between macrophages and neutrophils, which are critical regulators of innate immunity. When activated by inflammatory mediators, endothelial cells promote leukocyte adhesion and vascular permeability by up-regulation of adhesion molecules, key events in tissue damage associated with inflammation. We hypothesize that soluble factors derived from macrophage-neutrophil interactions, particularly under conditions of TNF-α stimulation, will induce changes in endothelial cell adhesion promoting leukocyte-endothelial cell interactions and inflammatory cell recruitment. This study aimed to investigate the impact of macrophage-neutrophil interactions, under varying concentrations of TNF-α, on the secretion of soluble factors that modulate endothelial cell activation. Specifically, we aimed to characterize the effects of soluble mediators released during macrophage-neutrophil cross-talk on endothelial cell activation and barrier function.

To evaluate the effects of TNF-α on the macrophage-neutrophil dialogue, we used a co-culture system where we seeded macrophages obtained by treating monocytes with phorbol 12-myristate 13-acetate for 72h, on the basolateral side, subsequently neutrophils were seeded in the lumenal side of the porus trans-well. The cells interacted for 24h in the presence or absence of different concentrations of TNF-α. At the end of the incubation period, cultured media resulting from macrophage-neutrophil co-cultures was collected to further investigate the effects of the secreted soluble factors on endothelial cell monolayers.

Our results showed that SAPK/JNK presented a dose-dependent response specifically for the p56 isoform, while the p46 isoform did not exhibit the same pattern of activation. ERK2 demonstrated a dose-dependent relationship, whereas ERK1 did not. NFκB levels were elevated in macrophages co-cultured with neutrophils in the absence of TNF-alpha. Endothelial ICAM expression did not show significant changes under the experimental conditions tested, suggesting potential differences in responsiveness compared to other markers like VCAM and integrins, but we also noticed that endothelial cells treated with CM from the experimental groups exposed to high levels of TNF-alfa enter apoptosis via a mechanism involving caspase-3 activation.

In conclusion, the dialogue between macrophages and neutrophils can activate both cell types, in the presence or absence of TNF-alfa by downstream signaling and activation of NFkB, SAPK/JNK, and ERK, upon this interaction macrophages transition towards a pro-inflammatory phenotype characterized by elevated levels of iNOS, IL-1β and TNF-alfa. These soluble factors released after the dialogue between the two cell types present profound effects on endothelial cells by up-regulation of adhesion proteins like VCAM-1 and ITGA5. Conditioned media from TNF-alfa exposed leukocytes induced apoptosis in endothelial cells.

Keywords: macrophage, neutrophil, TNF-α, inflammation, endothelium

MMP-9 as a candidate prediagnostic parker in Parkinson's disease

Claudia-Andreea Moldoveanu[1,2], Alia Colniţă[3], Alexandru Jurca[1,2], Ioana Roman[2], Bogdan Sevastre[4], Alexandra Sevastre-Berghian[5], Vlad-Alexandru Toma[1,2]✉

[1] *Department of Molecular Biology and Biotechnology, Babes-Bolyai University, Cluj-Napoca, RO;* [2] *Institute of Biological Research, the branch of NIRDBS Bucharest, RO;* [3] *NIRD for Isotopic and Molecular Technologies, Cluj-Napoca, RO;* [4] *Faculty of Veterinary Medicine, University of Agricultural Sciences and Veterinary Medicine, Cluj-Napoca, RO;* [5] *University of Medicine and Pharmacy "Iuliu Hatieganu", Cluj-Napoca, RO*
✉*Corresponding author, Email: vlad.toma@ubbcluj.ro*

In searching for a new prediagnostic blood marker for Parkinson's disease we investigated this pathology using an MPTP dopaminergic lesion (25 mg/kg b.w. i.p.) in male CD21 mice (n=10). Subsequently, the whole brain was dissected, and cortical and striatal areas were prepared for immunohistochemistry (α-synuclein, GFAP) and cytokine analyses (IL-1α, IL-1β, IL-6, IL-10 and PGE2). Additionally, blood was collected for serum MMP analyses. The study revealed a functional relationship between cytokines and serum matrix metalloproteinases (MMP-2 and MMP-9).

The data showed that IL-10, which was increased in striatum after the MPTP exposure, acted as a blood MMP-9 inhibitor, while IL-6, IL-1β and PGE2 were identified as MMPs activators. IL-1β, IL-10 and PGE2 levels decreased in the cortical area, while IL-1α decreased in both cortical and striatal areas. In turn, IL-6, a canonical pro-inflammatory cyotokine, increased in cortical, as well as, striatal brain regions.

Overall, the clinically silent pathology induced at the cellular level was related to serum MMP-9 decreasing, suggesting its potential as a candidate blood marker for prediagnosis of Parkinson's disease.

Revealing biogeochemical microbial actors in hypersaline, meromictic Fără Fund Lake by meta-omics

Michalis D. Lazăr✉, Ionuț M. Gridan, Adrian V. Zety, Horia L. Banciu

Faculty of Biology and Geology, Babeș-Bolyai University, Cluj-Napoca, Romania
✉**Corresponding author, Email: michalis.lazar@stud.ubbcluj.ro**

Currently, the biogeochemical cycles in hypersaline and permanently stratified lakes are underexplored, mainly due to the uncultivability of the vast majority of prokaryotes. Fast advances in sequencing technologies and data analysis strategies allowed for high-resolution prediction of diversity, interactions, and ecological roles of cultivated and uncultivated members of microbial communities in a broad range of environments. We sought to unveil the main microbial actors involved in the cycling of main elements along the water column and sediments in the hypersaline (190 to 320 g/L total salts) and permanently stratified (meromictic) Fără Fund Lake in Central Romania. Metagenomics and metatranscriptomics were jointly employed to predict the spatial distribution of microbial communities inhabiting physico-chemically distinct water strata alongside their potential metabolic traits mediating the biogeochemical cycles of main elements (C, N, S), metals (Fe, Mn), and metalloids (As, Se). The taxonomic diversity of metagenome-assembled genomes (MAGs) increased with depth, with the large majority (>90%) having no cultured representatives. By scrutinizing transcript abundance of functional marker genes, active methylotrophy, anaerobic carbon fixation by the Wood-Ljungdahl pathway, thiosulfate disproportionation, Mn-oxidation, Fe reduction/oxidation, and As and Se-utilization were detected throughout different water strata. In conclusion, the studied hypersaline, meromictic lake seems inhabited by niche-partitioned microbial communities mostly consisting of uncultured representatives of Bacteria and Archaea. These findings underscore the significance of studying stratified aquatic ecosystems to gain insights into how biogeochemical cycles are driven, distributed, and interconnected across different physico-chemical gradients.

Keywords: Biogeochemical cycles, hypersaline, MAGs, meta-omics, microbial communities

Vascular response to sheep poly-Hb in hemorrhagic conditions. The big loser: Dextran 40.

S. Oană[1], M. Lehene[2], B. Sevastre[3], I. Roman[4], S. Dandea[3], C. Moldoveanu[1,4], M. Muntean[5], R. Silaghi-Dumitrescu[2], V. Toma[1,4]✉

[1]*Department of Molecular Biology and Biotechnology, Faculty of Biology and Geology, Babes-Bolyai University, Cluj-Napoca, Romania,* [2]*Faculty of Chemistry and Chemical Engineering, Babes-Bolyai University, Cluj-Napoca, Romania,* [3]*University of Agricultural Sciences and Veterinary Medicine Cluj-Napoca, Cluj-Napoca, Romania,* [4]*Institute of Biological Research, Department of Biochemistry and Experimental Biology, Cluj-Napoca, 400015, Romania, Cluj-Napoca, Romania,* [5]*„Iuliu Hatieganu" University of Medicine and Pharmacy, Faculty of Medicine, Cluj-Napoca, Romania*
✉*Corresponding author, vlad.toma@ubbcluj.ro*

The study investigated the impact of poly-Hb on vascular homeostasis through an in vivo experiment using Wistar rats divided into three groups: Hemorrhage, Hemorrhage + Dextran 40, and Hemorrhage + sheep poly-Hb (8 rats per group). Exposure to sheep poly-Hb and Dextran 40 was limited to 24 hours. Subsequently, cervical dislocation was performed, and abdominal aorta and blood serum were sampled. The aorta underwent electron microscopy and iNOS immunohistochemistry, and inflammation status was assessed via prostaglandin E2, IL-1 alpha, IL-1 beta, IL-6, and IL-10. Catalase and peroxidase activities were measured kinetically, while colorimetric methods estimated levels of reduced and oxidized iron. Gelatin zymography was used to evaluate the serum MMP 1, 2, and 9.

Poly-Hb exposure resulted in a significant increase in oxidative stress, but ultrastructural examinations showed only superficial endothelial damage in the hemorrhage group. Both Dextran and poly-Hb had minimal detrimental effects on the vascular endothelium. Poly-Hb exposure led to decreased levels of proinflammatory cytokines and matrix metalloproteinases and an increase in IL-10, while Dextran 40 increased cytokine and MMPs levels compared to the control and poly-Hb groups.

In conclusion, poly-Hb demonstrated superiority over Dextran 40, a commonly used hemodynamic substitute in humans.

2D GMM comparison of scute shape changes in green sea turtle (*Chelonia mydas*) hatchlings from original and relocated nests

Alexandra Kamilla Adilov[1]✉, Csaba Kiss[1]

[1] Department of Zoology, Institute of Biology, Eszterházy Károly Catholic University, Eger, Hungary
✉***Corresponding author, E-mail: alexandraadilov@gmail.com***

In recent decades, there has been a notable decrease in sea turtle populations, largely due to habitat destruction, including the conversion of nesting beaches for human use. Additionally, factors such as high predation rates on juveniles, illegal harvesting of eggs and adults, pollution, and unsustainable fishing methods have also played a significant role in the population decline. Conservation efforts for green sea turtles often involve relocating endangered nests, though this approach carries risks for the embryonic development and post-hatching characteristics of the hatchlings, prompting extensive research in this area. I studied the 2D GMM (Geometric Morphometric Methods) scute morphology of green sea turtle in Northern Cyprus. I performed Principal Component Analysis (PCA) to determine which environmental background variables explain the greatest effect on the nests and which traits explain the greatest proportion of the total phenotypic variance. By performing a Procrustes ANOVA test on the shape and size changes of the carapace showed statistically significant results between groups (relocated and non-relocated nests) for shape. For the data deriving from landmarks, we have created a Thin Plate figure for better understanding on the scute and carapace dimorphisms between the two groups. Based on our results, we got an explanation of the significant differences of scute and carapace morphology between the specimens from relocated and the original nests.

Keywords: green sea turtle, endangered species, hatchling, scute morphology, 2D GMM

Aquatic invertebrate diversity in the Ţiganilor Rivulet from the "Alexandru Borza" Botanical Garden, Cluj-Napoca

Sabrina Runcan[1], Mirela Cîmpean[1,2✉], Adrian Flavian Vrabii[1], Karina Battes[1,2]

[1] Department of Taxonomy and Ecology, Faculty of Biology and Geology, Babes-Bolyai University, 5-7 Clinicilor Str., 400006 Cluj-Napoca, Romania; [2] Centre for Systems Biology, Biodiversity and Bioresources "3B", Advanced Hydrobiology and Biomonitoring Laboratory (LabHAB), Babes, -Bolyai University, 5-7 Clinicilor Str., 400006 Cluj-Napoca, Romania
✉Corresponding author, E-mail: mirela.cimpean@ubbcluj.ro

The present study aims to describe the benthic invertebrate communities found in the Ţiganilor Rivulet from the "Alexandru Borza" Botanical Garden, Cluj-Napoca, and to assess the water quality based on the presence of 16 systematic units. The three sites sampled in October 2023 were located within the botanical garden, in an area with relatively low human impacts. The samples were processed using standard methods for benthic invertebrates. Organisms belonging to phyla Nematoda, Annelida, Mollusca and Arthropoda were identified, to different taxonomic levels. Oligochaetes and chironomids dominated the benthic communities in all three samples. The water quality was assessed using the Extended Biotic Index (EBI), which converts the indicative values of the benthic groups into five classes of water quality (high, good, moderate, poor and bad). Because tolerant taxa were dominant in the Ţiganilor Rivulet, the EBI depicted moderate and poor water quality in the three sampling points selected for the present study.

Conserving hidden plant treasures:
the living plant collections in "Alexandru Borza" Botanic Garden (Cluj Napoca, Romania)

Oana Roşca-Casian[1✉], Liliana Jarda[1], Raluca Câţoiu[1], Mihai Puşcaş[1,2]

[1]*A. Borza Botanic Garden, Babeş-Bolyai University, 42 Republicii Street, 400015 Cluj-Napoca, Romania;*
[2]*Faculty of Biology and Geology, Babeş-Bolyai University, 44 Republicii Street, 400015 Cluj-Napoca, Romania*
✉**Corresponding author, E-mail: oana.rosca@ubbcluj.ro**

The preservation of plant diversity, encompassing all its aspects, has been one of the most important activities at "Alexandru Borza" Botanic Garden for quite a long time. On this basis, a special area has been designated to protect some of the rare or endangered plants found in Romanian flora. Although such plants are sheltered in different sections of the garden, a rockery was constructed to showcase rare plants from Romanian flora specifically. This rockery is located in the ornamental section of the garden, near the rose collection.

Plants that dwell in the rare plants rockery in "Alexandru Borza" Botanic Garden were obtained from seeds received through plant material exchanges with similar institutions worldwide, or collected from different habitats. The seeds were requested based on the seed catalogues issued annually by these institutions. The seeds underwent two procedures: 1) they were sown in a mixture of soil, sand and peat - according to the plants' specific needs - in small pots, watered and kept under observation; 2) they were germinated by *in vitro* culture. All the pots were labeled with the name of the plant species, the sowing date and the origin of the seeds. After germination, the seedlings were divided and transferred to larger pots. This repotting procedure was repeated several times. Once robust plants were achieved, they were transplanted into the specially designed area of the garden. These plants were monitored for at least one year, and if the acclimatization was successful, they would be marked with a standard label used for identifying plants in the botanic garden.

Following the above-mentioned procedures, several plant species were obtained. Thus, 53 plant species listed in different national red lists, with varying conservation status, are found in the rockery specifically designated for rare plants of Romanian flora. Among these, 41 plant species are considered rare (according to the Red list of plants from Romania – Oltean et al., 1994), such as: *Allium coloratum* Spreng., *A. obliquum* L., *Alyssoides utriculata* (L.) Medik., *Anchusa leptophylla* Roem. & Schult., *Delphinium simonkaianum* Pawl., *Draba*

aizoides L., *Dracocephalum austriacum* L., *Phyteuma spicatum* L., *Scutellaria alpina* L., *Silene saxifraga* L., *Veronica fruticans* Jacq. etc. Also, 12 species are threatened, such as: *Achillea ptarmica* L., *Centaurea kotschyana* Heuff., *Dianthus nardiformis* Janka, *Sedum dasyphyllum* L. The section of the rare plants from Romanian flora also shelters some endemic and/or subendemic plant species, such as: *Dianthus callizonus* Schott & Kotschy, *D. giganteus* subsp. *banaticus* (Heuff.) Tutin, *D. henteri* Heuff. ex Griseb. & Schenk, *D. serotinus* Waldst. & Kit., *Silene dinarica* Spreng., *S. nivalis* (Kit.) Rohrb., *S. zawadzkii* Herbich, *Thymus comosus* Heuff. ex Griseb. & Schenk, *Viola jooi* Janka.

One of the multiple roles of botanic gardens is to conserve *ex situ* plant species that undergo any kind of threatening. Therefore, "Alexandru Borza" Botanic Garden implements several strategies of *ex situ* plants conservation. Living plant collections are a viable way of conserving important plant species from Romanian flora, in addition to *in vitro* plants collections and seed collections.

Differential effects of neutral genetic variation, temperature and drought on the transcriptome of *Lobaria pulmonaria* Hoffm (1796)

Ioana Ardelean[1✉], Mihai Miclăuş[2,3], Christoph Scheidegger[4]

[1] *Biological Research Center, "Babeş-Bolyai" University, Jibou, Romania;* [2] *NIRDBS, Institute of Biological Research, Cluj-Napoca, Romania;* [3] *STAR-UBB, "Babeş-Bolyai" University, Cluj-Napoca, Romania;* [4] *Swiss Federal Research Institute WSL, Zürcherstrasse 111, 8903 Birmensdorf, Switzerland*
✉**Corresponding author, E-mail: ioana.v.ardelean@gmail.com**

Biodiversity comprises the variety of ecosystems, species and genes; it is crucial to ecosystem services being a measure of prosperity. However, climate change and human activities threaten global biodiversity, necessitating the understanding of species' responses. *Lobaria pulmonaria*, an epiphytic lichen, serves as a model organism for studying climate adaptation. We aimeed to elucidate its transcriptomic response to changing climates to unravel resilience mechanisms against climatic shifts. We conducted gene expression analyses using RNA-seq. Raw RNA-seq data underwent a standardized bioinformatic pipeline, including quality control (using FastQC and fastp), mapping to reference genome (utilizing HiSat2), counting reads per gene (with FeatureCount), testing for differential gene expression (using DESeq2), and visualization of results. The reference genome for Lobaria pulmonaria was obtained from the Joint Genome Institute (JGI). *L. pulmonaria* demonstrated resilience to high temperatures, both in a continuously wet state and when alternating between wet and desiccated states. The ascomycete symbiotic partner, *L. pulmonaria*, was categorized into two genepools: Continental and Mediterranean. The impact of climatic region on *L. pulmonaria* varied depending on the genepool. Temperature fluctuations exerted a stronger influence on the number of differentially expressed genes (DEGs) compared to humidity variations. Populations from the Mediterranean genepool exhibited fewer DEGs in response to temperature stress. For the Continental genepool, significant differences in DEGs were observed among populations under different treatments, indicating complex responses. This highlights the vulnerability of the continental gene pool to rising temperatures, emphasizing the urgent need to prioritize the protection of habitats that harbor it. Conversely, for the Mediterranean genepool, consistent differences in DEGs were observed between populations across treatments, suggesting a stable response regardless of climatic conditions.

Epizoic diatoms found on turtles from different freshwater ecosystems

Iulia-Maria Brătian[1], Anca-Mihaela Ciorca Şuteu[1,2]✉

[1]Doctoral School of Integrative Biology, "Babeş-Bolyai" University, Cluj-Napoca, Romania; [2]Faculty of Biology and Geology, "Babeş-Bolyai" University, Cluj-Napoca, Romania
✉ **Corresponding author, Email: anca.ciorca@ubbcluj.ro**

Diatoms are living in various aquatic ecosystems to which several cellular adaptions help them thrive. Macrophytes, stones, sand, sea shells or even the upper shell of turtles become the best microhabitats for the diatom species which prefer living attached to a surface. The aim of this study is to investigate epizoic freshwater diatoms on the turtle carapaces from three different anthropic aquatic habitats: a small pool, an anthropic pond from "Alexandru Borza" Botanic Garden and a greenhouse pool from "Vasile Fati" Botanic Garden. By scraping the entire surface of the turtle shells, samples were taken from a total of ten individuals living in these water bodies. A total number of 79 taxa were identified belonging to 30 genera. While 78% of these taxa were found in the three epizoic samples from the outside anthropic pond, the six samples from the greenhouse reached lower numbers of taxa. Moreover, at each sampling site a diatom bloom was observed: *Craticula subminuscula* (small pool), *Achnanthidium affine* (on the three turtles from the anthropic pond) and *Nitzschia inconspicua* (on almost all individuals from the greenhouse pool). A higher α-diversity and equitability was identified in the habitat found outside, thus the natural light, the higher organic and nutrient input have influenced the composition of the epizoic diatom community. The Jaccard similarity indices separates the natural environment from the controlled one in two distinct groups, with a higher similarity value observed in the greenhouse samples (0.55). Finally, the results indicate that an ecosystems diversity is indirectly proportional to the anthropic contribution to it.

First record of *Atypophthalmus umbratus* (de Meijere, 1911) (Diptera, Limoniidae) from Central Europe, a species introduced accidentally throughout global trade of exotic plants

Boróka-Zsuzsánna Jancsó[1,2], Marcell Kárpáti[3✉],
Anna Dénes[1,2], Lujza Keresztes[1]

[1] *Centre 3B, Laboratory of Advance Hydrobiology and Biomonitoring, Babeş-Bolyai University, Clinicilor 5–7, Cluj-Napoca 400006, Romania;* [2] *Doctoral School of Integrative Biology, Babeş-Bolyai University, Republicii 44, Cluj-Napoca 400015, Romania;* [3] *Hungarian Department of Biology and Ecology, Faculty of Biology and Geology, Babeş-Bolyai University, Clinicilor 5–7, Cluj-Napoca 400006, Romania*
✉***Corresponding author, Email: marcell.karpati@stud.ubbcluj.ro***

Here we report the first data of the exotic *Atypophthalmus umbratus* (de Meijere, 1911) from two Central European countries, Romania and Hungary. This is the first time that the presence of an introduced exotic species of Limoniidae (Diptera) has been reported in the area. The above-mentioned species was first observed in Cluj, Romania, on tropical plant specimens (e.g. *Alocasia x mortfontanensis* 'Polly'), which we bought from a large store selling tropical plants, from which both male and female specimens were collected. After that, checking some citizen science platforms of entomological interest, we also noticed record of the species in Hungary, based on their conspicuous wing pattern and general habitus. The presence of this accidentally introduced species far from its native tropical environment highlights the growing intensity of the global exotic plant market and the importance of citizen science in early warning systems for biological invasions.

Imaginal feeding of twenty-two Japanese endemic winter stoneflies (Plecoptera: Capniidae)

Kristóf Földi[1✉], Manuel Jesús López Rodríguez[2],
José Manuel Tierno de Figueroa[2], Dávid Murányi[1]

[1]*Department of Zoology, Institute of Biology, Eszterházy Károly Catholic University, Eger, Hungary;*
[2]*Department of Ecology, University of Granada, Granada, Spain*
✉***Corresponding author, E-mail: foldikristof2002@gmail.com***

The winter stonefly genera *Apteroperla* Matsumura, 1931 and *Eocapnia* Kawai, 1955 are restricted to Honshu and Hokkaido of Japan. They are well known for their aptery and association with habitats having thick snow cover during the whole cold season. Recently, the taxonomy of both genera is under revision, and several new species will be added to the currently distinguished three *Eocapnia* Kawai, 1955 and six *Apteroperla* Matsumura, 1931 species. In the present study, we investigated the feeding of the adults of 16 *Apteroperla* and five *Eocapnia* species, by means of dissection and analysis of their gut content. *Takagripopteryx nigra* Okamoto, 1922, an additional Japanese winter stonefly was also studied, to compare the feeding of the small sized and apterous taxa with a cohabiting larger, winged species. Contrary to most other stonefly imagoes, the studied species proved to be actively feed. Their guts contained various pollen, plants and fungi, as well animal remnants. The diet of each species seems to be different, but differences probably refer on the food supply of different habitats, and these stoneflies are most probably opportunistic feeders.

Keywords: *Apteroperla*, *Eocapnia,* gut content, *Takagripopteryx*.

On the tracks of crayfish evolution: A multidisciplinary approach

Antonio Laza[1]✉, David Livadariu[1], Lucian Pârvulescu[1]

[1] Department of Biology-Chemistry, Faculty of Chemistry, Biology, Geography, West University of Timişoara, Timişoara, Romania
✉**Correspongind author, E-mail: antonio.laza01@e-uvt.ro**

Aquatic environments pose unique challenges for organisms due to fluctuating oxygen levels. Crayfish were generally considered freshwater dwellers, often encountering hypoxic or anoxic conditions, particularly in aquatic burrow habitats due to low oxygen diffusion in water but there are some species which dig galleries in soil, away from any water sources, living in aerated burrows. This divergence in specialization prompts questions about the evolution and transmission of anoxia tolerance mechanisms among crayfish populations. To survive in such environments, crayfish rely on various physiological and behavioral adaptations, including increased ventilation, cardiovascular adjustments, and metabolic rate modulation. These responses, likely inherited from their lobster ancestors, are crucial for maintaining oxygen consumption and cellular function in hypoxic conditions. However, the presence of aerated burrows in certain crayfish species challenges the necessity of anoxic mechanisms. Advanced burrow structures optimize airflow, potentially reducing the reliance on these mechanisms by ensuring adequate oxygen supply. Recent discoveries of independent losses of HIF pathway components in certain crustacean groups further complicate our understanding of anoxia tolerance mechanisms in crayfish. This underscores the importance of considering evolutionary history in shaping an organism's ability to survive in oxygen-depleted environments. Future research should focus on elucidating the molecular and physiological mechanisms underlying anoxia endurance in crayfish, as well as exploring the adaptive significance of fossorial behavior and the evolutionary context of oxygen sensing pathways in crustaceans.

Keywords: anoxia, evolution, burrow, oxygen.

Possibilities of using herbaria, digital herbaria, and plant databases in botany and biodiversity teaching at Eszterházy Károly Catholic University

Andrea Sass-Gyarmati[1]✉, Marianna Marschall[1], Laura Szurofka[1]

[1] Department of Botany and Plant Physiology, Institute of Biology,
Eszterházy Károly Catholic University, Eger, Hungary
✉***Corresponding author, E-mail: sass.gyarmati.andrea@uni-eszterhazy.hu***

In the past herbaria were almost exclusively visited by researchers and only a small percentage of those interested had insights into collections. Digitization opened up completely new perspectives on the collection's visibility. Nowadays herbaria could have an active role in the education of botany, biodiversity, and bioconservation especially in several secondary and higher educational institutions. The Herbarium of Eszterházy Károly Catholic University (EGR) has been involved in student education for many years. The combination of studying „real" and virtual herbaria together can be a much more interesting educational approach in botany. The digital collections can bring students as well as the public closer to the world of scientific research and help preserve herbaria for the next generation. Besides the traditional utilization of herbaria, a huge possibility is using virtual plant collections as well. The main target is to highlight more important Hungarian and worldwide-used plant online resources suitable for botany teaching to the students as well as the wide public at Herbarium of Eszterházy Károly Catholic University, Eger (EGR).

Keywords: herbarium, online resources, systematics.

Preliminary results in the reassessment of *Orchidaceae* L. family within the Iron Gates Natural Park

Rareş-Ciprian Românu[1]✉, Adrian Sinitean[1]

[1]Department of Biology - Chemistry, West University of Timişoara, Romania
✉***Corresponding author, Email:*** *rares.romanu01@e-uvt.ro*

According to previous research, 28 species of orchids have been documented within the Iron Gates Natural Park. This study aims to reassess and incorporate recent changes in the orchid flora of the park. Field surveys were conducted in the spring of 2024, relying largely on maps where these species had been confirmed. Determination and individual counting were performed *in situ*, while geographic coordinates were collected using GPS. The surveyed areas included the southern slopes near Divici and Coronini and the Baziaş and Cracul Găioara nature reserves. Four species have been identified: *Neotinea tridentata* (Scop.) R.M.Bateman, Pridgeon & M.W.Chase (1997), *Orchis simia* Lam., 1779, *Cephalanthera damasonium* (Mill.) Druce (1906), and *Limodorum abortivum* (L.) Sw. (1799). It is noteworthy that the high temperatures during the spring growing season of 2024 hastened the flowering process of these orchids by several weeks compared to literature records.
New discoveries include the confirmation of *Limodorum abortivum* in the Cracul Găioara region and *Orchis simia* on a slope near Coronini. The study will persist throughout the entire vegetation period of orchids.

Keywords: Iron Gates Natural Park, orchids, biodiversity

Preserving biodiversity: The role of museum collections. A case study on moths from the Marg Wladimir Manoliu Lepidoptera collection at the Zoological Museum of Babeş-Bolyai University

Daniela Jîtcă[1], Geanina Sitar[2], Cristian Sitar[3,4]

[1] Faculty of Biology and Geology, Babes-Bolyai University, Clinicilor 5-7, 400006 Cluj-Napoca, Romania; [2] Doctoral School "Education, Reflection, Development", Faculty of Psychology and Sciences of Education, Babes-Bolyai University, 400006 Cluj-Napoca, Romania; [3] Zoological Museum, Babes-Bolyai University, Clinicilor 5-7, 400006 Cluj-Napoca, Romania; [4] Department of Cluj, Emil Racovita Institute of Speleology, Clinicilor 5, 400006 Cluj-Napoca, Romania

Our study presents an overview of the Marg - Wladimir Manoliu moth collection, currently archived at the Zoological Museum of Babeş-Bolyai University in Cluj-Napoca, Romania. M. W. Manoliu, born in 1940 in Solca, Suceava County, initiated his moth collecting pursuits in 1951, with his most prolific period spanning from 1980 to 2008. The assemblage encompasses 4858 specimens representing 464 distinct species, predominantly sourced from Cluj Napoca and Solca, supplemented by specimens acquired through exchanges or expeditions to other locales.

In Solca, specimens were procured from both local courtyards and a nearby water treatment station, utilizing a 400W mercury vapor lamp for attraction. In Cluj Napoca, collection efforts were concentrated on the balcony of Manoliu's third-floor apartment, where he deployed light traps equipped with mercury vapor lamps of varying wattages. Additionally, a 400W light trap was positioned at the Institute of Plant Protection in Cluj.

Despite its modest size and localized focus, Manoliu's collection holds significant value for biodiversity documentation and research. It offers valuable insights into species distribution and dynamics, thereby contributing to biodiversity conservation efforts. The meticulous documentation accompanying Manoliu's collection provides researchers with concrete data on species occurrences and trends, emphasizing the pivotal role of individual contributions in advancing scientific knowledge and promoting conservation endeavors.

Recent advances in the taxonomic revision of the *Dendrobaena alpina* (Rosa, 1884) species group (Oligochaeta, Lumbricidae)

Tímea Szederjesi[1✉], Csaba Csuzdi[1]

[1] Department of Zoology, Institute of Biology, Eszterházy Károly Catholic University, Eger, Hungary
✉Corresponding author, E-mail: szederjesi.timea@uni-eszterhazy.hu

The *Dendrobaena alpina* species group, as originally defined, contained some fifteen nominal species characterized by a clitellar position on segments 26, 27–33, 34, tubercles around 30–32. It was thought that a characteristic synapomorphy of this group was the reduction of the number of hearts with the last pair in segment 10 or 11 and lacking extraoesophageals in 12, and the presence of calciferous diverticula in 11–12. On the other hand, these species show a great variability in the case of several other characteristics e.g., the number of vesicles, position of the spermathecal openings, pigmentation. In order to reveal the relationships and patterns within this species group, we applied an integrative taxonomic approach. Thorough morphological examinations were carried out on several specimens collected from the Alps, Carpathians, Balkans and Anatolia. In addition, our specimens were implemented in a wider context of the genus *Dendrobaena*, and a molecular phylogenetic reconstruction was performed using COI, 16S rDNA and ITS2 sequences. Our results revealed the presence of two well-separated clades, an Alpine-Carpathian-Balkan and a Balkan-Anatolian-Levantine group. The deeply pigmented *D. alpina alpina* from the Alps formed the first clade together with the also pigmented Northeastern Carpathian *D. alpina alteclitellata*, the Dacian *D. clujensis* and a *D. alpina* ssp. from North Macedonia. However, our study pointed out that the original *D. alpina* species group was polyphyletic, because the unpigmented Bulgarian *D. alpina* specimens joined the Anatolian and Levantine species such as *D. orientalis*, *D. pentheri*, *D. orientaloides* and *D. semitica*. Consequently, the unpigmented population from Bulgaria was described as a new species, *Dendrobaena misirlioglui*. Two slightly pigmented specimens collected in the Retezat Mts, the Southern Carpathians, Romania, identified as *D. alpina alpina* in a former study, together with the Balkan-Southern Carpathian *D. alpina popi* joined the Balkan-Anatolian-Levantine clade of *Dendrobaena* as well. The genetic and morphological characteristics support the description of these Retezat specimens as a new species. The study also revealed that the subspecies *D. alpina armeniaca* and *D. alpina popi* have no connection with *D. alpina*, thus their elevation to species rank is suggested.

Keywords: Balkans, Carpathians, earthworms, new species, Retezat Mts.

Skin-associated microbiome of the yellow-bellied toad (*Bombina variegata*) in a population from Transylvania

Luciana-Paula Botezatu[1], Adorján Cristea[1✉],
Horia Leonard Banciu[2], Alin David[1]

*[1]Babeş-Bolyai University, Faculty of Biology and Geology, Departament of Taxonomy and Ecology,
5-7 Clinicilor Street, Cluj-Napoca, Romania; [2]Babeş-Bolyai University, Faculty of Biology and Geology,
Departament of Molecular Biology and Biotechnology, 5-7 Clinicilor Street, Cluj-Napoca, Romania*
✉**Corresponding author, E-mail: adorjan.cristea@ubbcluj.ro**

Microbial symbionts play a vital role in host health. The amphibian skin crucial for ion, gas and water exchange harbors a diverse microbiome studied mainly using short-read amplicon sequencing. Here we propose to explore the diversity of skin microbiome in *Bombina variegata* by using ONT long-read sequencing technology followed by taxonomic identification by One Codex platform. The toads (n=5) were captured in small ponds located near Miceşti (Cluj), Romania, then swabed on the dorsal, ventral, and lateral sides. From the swab samples (n=10), DNA was extracted using the Quick-DNA Faecal/Soil Microbe MiniPrep kit (ZR, USA). For long-read sequencing, libraries were prepared using Rapid Barcoding 24 V14 kit (ONT, UK) and the sequencing was performed using R10.4.1 chemistry flow cells and a MinION Mk1B sequencer from Oxford Nanopore Technologies. The sequences were analised using One Codex. A total of 9308 reads were generated from the samples. The analysis in the One Codex revealed that *Pseudomonadota* (64.44%), *Actinomycetota* (14.5%), *Bacteroidota* (3.53%) and *Cyanomicrobiota* (1,89%) are the most abundant phyla associated with the skin microbiome of the yellow-bellied toad. The analyses also indicated that the sample was contaminated with host-specific DNA (59%). While host DNA contamination highlights the need for method optimization, this study demonstrates the potential of long-read sequencing combined with the easy-to-use One Codex platform, for comprehensive characterization of amphibian skin microbiomes.

Keywords: *Bombina variegata*, long-read sequencing, microbiome.

Snapshot on large and medium-sized mammals in Ceahlău National Park

Gligor Alexandra[1], Cristea Adorjan[1✉], Alin David[1]

[1]*Babeş-Bolyai University, Faculty of Biology and Geology, Departament of Taxonomy and Ecology, 5-7 Clinicilor Street, Cluj-Napoca, Romania*
✉**Corresponding author, E-mail: adorjan.cristea@ubbcluj.ro.**

Knowledge of the diversity, relative abundance and activity pattern of large and medium-sized mammal species is of major importance for management planning. With an area of 8,396 ha, Ceahlău National Park is the third smallest park in Romania, the entire area having the status of a Natura 2000 site. Until now, no qualitative and quantitative information has been published regarding large and medium-sized mammals in the park. Therefor, the aim of this study was to evaluate the diversity of large and medium-sized mammal species, their relative abundance and the circadian pattern of activity. The study was carried out between October 2022 and November 2023, using a number of 16 Moultrie and Bushnell camera traps. No scent lure or another attractant was applied. Since activation, the camera traps have been in the working mode throughout the research period. During the 1-year period, 3460 trap nights were processed, 557 images with large and medium-sized mammal were obtained and 14 mammal species were recorded, five of them being herbivores and nine carnivores. The herbivore species identified were *Cervus elaphus, Capreolus capreolus, Sus scrofa, Rupicapra rupicapra* and *Lepus europaeus*, and the carnivorous species were *Canis lupus, Felis silvestris, Lynx lynx, Martes foina, Martes martes, Meles meles, Mustela putorius, Ursus arctos* and *Vulpes vulpes*. With 243 records, *Capreolus capreolus* was the most abundant species, followed by *Cervus elaphus* with 92 records. Out of a total of 24 records, the combined share of photos featuring large carnivores like wolves, lynxes, and bears amounts to just 4.31% of the overall count. Most likely, for the large carnivores, which inhabit large territories, of the order of tens of square kilometers, the surface of the Ceahlău National Park is relatively small, so they cross National Park boundaries, expanding outside the park, while for herbivores the habitat is optimal. Our findings provide the first qualitative and quantitative data on the fauna of large and medium-sized mammals in Ceahlău National Park.

Keywords: camera traps, carnivores, herbivores, large mammals.

Spatial occupancy estimation and modeling of grey wolf (*Canis lupus*) of the Bükk Mountain in Hungary

Csaba Kiss[1,3✉], Tamás Cserkész[2,3]

[1]Department of Zoology, Institute of Biology; Eszterházy Károly Catholic University, Eger, Hungary;
[2]Hungarian Natural History Museum, Budapest, Hungary; [3]Bükk Mammalogical Society, Eger, Hungary
✉***Corresponding author, E-mail: kiss.csaba@uni-eszterhazy.hu***

The wolves inhabiting the Bükk Mountain in Hungary play a vital role in maintaining the region's biodiversity and ecosystem balance. Understanding their behaviour and ecology is crucial for developing effective conservation strategies that ensure their long-term survival in the Bükk mountain landscape. As apex predators, they help regulate the population of herbivores like deer, roe deer and boars, thereby prevents forest vegetation from overgrazing. Despite facing various challenges such as habitat loss and human-wildlife conflicts, efforts are being made to study and conserve the Bükk mountain wolf population. The utilization of camera traps in studying the wolves of the Bükk Mountain in Hungary has renewed: revolutionized our understanding of these elusive predators. In the present study, we employed network of camera traps to observe the key mammal species in the area, to assess their occupancy and detection probabilities and their interactions with wolves. Our results reveal the dominant territorial presence of wolves compared to other species. Remarkably, wolves demonstrate resilience in the face of primary roads and forest trails but exhibit avoidance behaviour towards populated settlements and open areas. By harnessing the capabilities of a camera trap network conservation efforts can be enhanced by monitoring wolf populations, identifying threats, and developing targeted protection strategies to ensure the long-term viability of these majestic species in the Bükk mountain ecosystem.

Keywords: *Canis lupus*, Bükk Mountain, occupancy models.

Study of the spiders (Arachnida: Araneae) in the Cheile Baciului Reservation

Damian Flavius Ciprian[1], István Urák[2], Teodor Lucian Alexandru[1]

[1]Babeş-Bolyai University, Faculty of Biology and Geology, Cluj-Napoca, Romania; [2]Sapientia Hungarian University Of Transylvania, Faculty of Life Sciences and Sports, Department of Life Sciences, Sfântu Gheorghe, Romania

Cheile Baciului is a geological reservation, situated North-West of the Hoia Forest, close to Cluj-Napoca, comprising of habitats with clear anthropogenic influence. The area is lacking in information on the present arachno-fauna thus this study aims to expand and contribute to the knowledge of Romania's spider fauna, with Cheile Baciului as a target by realizing a list of species. The spiders were collected through different methods, excluding traps*, from the 10th of May 2023 to the 14th of August 2023. The study area was split into 7 points of collecting based on the differences in habitat vegetation composition. The specimens have been conserved in 75% isopropyl alcohol and identified in the laboratory, using a stereoscopic microscope and various identification keys and lists. Juveniles, males and females have been collected, numbering to a total of 80 species from 18 families. A remarkable diversity considering these habitats are clearly affected by human activity. Some dominant species of note are *Mangora acalypha, Neriene radiata, Synema globosum and Evarcha falcata*. Some rare species also have been identified as well as species present on red lists of other countries of the European Union, such as *Nematogmus sanguinolentus, Leptorchestes berolinensis* and *Uloborus walckenaerius*. These results show a rich diversity of spiders in this reservation. This could prompt the upgrading of this area into a mixed natural reservation on top of its geological status, with the conservation of the arachno-fauna in mind. Moreover, the rare species could be added to the red list of Romania's spiders. This would be a useful first move for conservation efforts concerning spiders, something that is lacking in Romania. If possible, a more comprehensive faunistic study should follow, to have an even more complete image of the ensemble of Araneae from Cheile Baciului. **Collecting inside Cheile Baciului was realized with access from the reservation overseers. Only manual collecting was done, no traps were used.*

Keywords: spider, conservation, biodiversity, habitat, rare species.

The effect of different light treatments of chamomile (*Matricaria chamomilla* L.)

Annabella Jakab✉, Erika Pénzesné Kónya

Department of Botany and Plant Physiology, Institute of Biology,
Eszterházy Károly Catholic University, Eger, Hungary
✉**Corresponding author, E-mail jakabanna02@gmail.com**

Chamomile occurs naturally in Hungary and also it is a cultivated medicinal plant species. The seeds germinate in direct light, and we do not know the limits of environmental conditions of the early period of germination. The basic research question was whether the early short light treatments of chamomile seeds and seedlings have further effect on the development of the plant individuals. Previous experiments showed that seeds can germinate well in distilled water without soil. Climate chamber experiments were elaborated with two different light spectra and continuous light exposition with parallel control observations with chamomile seeds. The treated individuals have been observed in the greenhouse and roof garden until they reached their maximal vegetative size. The results show that the early light treatments have effect on the further development stages of plant individuals. It is also a new result that all the groups successfully germinated and grew in distilled water for two weeks with low mortality rate.

Keywords: chamomile, light treatment, seedling observation, germination

The egg collection of the Zoological Museum of Babeş-Bolyai University

Helga Toth-Pál[1], Zsolt Kovács[1], Edgár Papp[2], Melinda Zsoldos[1], Janka Pénzes[1,3], Gergely Osváth[1,3]✉

[1]Faculty of Biology and Geology, Babeş-Bolyai University, Cluj-Napoca, Romania; [2]Milvus Group Bird and Nature Protection Association, Târgu Mureş, Romania; [3]Museum of Zoology, Academic Cultural Heritage Department, Babeş-Bolyai University, Cluj-Napoca, Romania
✉Corresponding author, E-mail: osvathgergely@gmail.com; gergely.osvath@ubbcluj.ro

An important oological collection is held in the Zoological Museum of Babeş-Bolyai University, which is unique in many ways: it covers a long-time span, it contains a variety of species belonging to different families and orders of both invertebrates and vertebrates, and it is composed of the work of several naturalists. It is one of the oldest collections of the museum. To date, however, no research has been conducted on this collection. The specimens had only been partially catalogued and no updates or revision had been carried out. Hence, our aim was to systematically check the egg specimens in the oological collection in order to identify the species to which they belong, thus providing a catalogue of these specimens.

Up to date, we identified a total of 2801 eggs, attributed to 170 species, 48 families and 19 orders. A significant proportion of the egg collection comes from Romania, mainly from the region of Cluj, but there are also collections from other areas of Transylvania. In addition, many specimens were collected in Hungary, Macedonia, Greece, Italy and the United Kingdom. The egg collection held by the Zoological Museum of the BBU spans the period between 1848 and 1960.

Considering its historical background and the presence of rare species, this collection can be viewed as one of the most valuable oological collections of Eastern-Europe, which could serve as good basis for further studies. In addition, the maps that we created represent 'hotspots' of faunistic information concerning the distribution of different species in the Carpathian Basin from the 19th and 20th century.

The revision of the ornithological collection of the Zoological Museum of Babeş-Bolyai University, Cluj-Napoca, Romania

Zsolt Kovács[1], Edgár Papp[2], Janka Pénzes[1,3], Zoltán Benkő[1,4], Gergely Osváth[1,3]✉

[1]Evolutionary Ecology Group, Hungarian Department of Biology and Ecology, Faculty of Biology and Geology, Babeş-Bolyai University, Cluj-Napoca, Romania; [2]Milvus Group Bird and Nature Protection Association, Târgu Mureş, Romania; [3]Museum of Zoology, Academic Cultural Heritage Department, Babeş-Bolyai University, Cluj-Napoca, Romania; [4]Romanian Ornithological Society/ BirdLife Romania, Cluj-Napoca, Romania
✉**Corresponding author, E-mail: osvathgergely@gmail.com; gergely.osvath@ubbcluj.ro**

The collections at the Zoological Museum of Babeş-Bolyai University, Cluj-Napoca, Romania are among the oldest, most diverse, and historically most interesting natural history collections. The museum houses a large ornithological collection consisting of skins, full taxidermic mounts of birds, eggs, nests and birds' skeletons, which have never been revisited. Here we present the catalogue of the skins and taxidermic mounts of birds deposited or exhibited at the Zoological Museum of Babeş-Bolyai University, Cluj-Napoca, Romania. We identified 2876 specimens, belonging to 489 species from 105 families and 32 orders. The collection includes numerous local and exotic rarities. The information held in this collection can be used as a basis for many valuable ornithological studies. This collection also represents a source of information for the status of the avifauna of the Carpathian basin in the 19th and 20th centuries.